ENERGY-BASED EARTHQUAKE RESPONSE ANALYSIS AND DESIGN OF REINFORCED CONCRETE SDOF COLUMNS

by

Ahmet Anıl Dindar

B.S., Civil Engineering, Yıldız Technical University, 1999

M.S. Civil Engineering, İstanbul Technical University, 2002

Submitted to the Institute of Graduate Studies in
Science and Engineering in partial fulfillment of
the requirements for the degree of
Doctor of Philosophy

Graduate Program in Civil Engineering

Boğaziçi University

2009

ACKNOWLEDGEMENTS

I would like to express my sincere gratitude to Assoc.Prof.Dr. Cem Yalçın for his invaluable guidance and help during the preparation of this dissertation. I would like to mention his patience, giving me inspiration and hope when I was stuck dead-ends.

I would like to thank Assist. Prof. Dr. Ercan Yüksel for his help, encouragement, infinite efforts on me. This study would not have been completed without his never-ending support.

Assist. Prof.Dr. Erdal Coşkun is the one I should deeply be grateful due to our helpful friendly talks at the

Prof.Dr. Oral Büyüköztürk initiated the main concept of this study three years ago. I am indebted to him for his innovative and encouraging advices throughout my thesis period.

Prof.Dr. Zeki Hasgür kindly listened me several times and gave valuable advices about the selection of the ground motion records in the development of the energy spectra.

I also owe thanks to my friends Hasan Özkaynak and Melih Sürmeli. Their support is invaluable for me.

I would like to express my deepest gratitude to my parents for their infinite encouragement.

Finally, nothing would be as it is without her, my wife, Emine Banu, was incredible tolerant in my long hour studies far from home. I must mention one more person, my son Umut Kaan. He was born in the middle of this study and he was my main motivation during this study.

ABSTRACT

ENERGY-BASED EARTHQUAKE RESPONSE ANALYSIS AND DESIGN OF REINFORCED CONCRETE SDOF COLUMNS

Earthquakes have claimed much more life and caused enormous financial damage in Turkey. It is the researchers' motivation to understand the characteristic of the earthquakes and to find out how to build the structures those resist the earthquakes' destructiveness.

This study aims to develop two algorithms, (i) energy-based seismic analysis of the structures and (ii) determination of the energy dissipation capacities of the reinforced concrete columns.

The seismic analysis of the structures was utilized by seismic input and plastic energy spectra. The energy spectra were directly derived from energy formulations. The energy demand spectra were established in terms of 4 different ductility level, 4 different site condition and 5 different intensity values.

The energy dissipation capacities of the reinforced concrete members were determined by using constant amplitude reversed cyclic displacements. While assessing the amplitude levels, the member and the section performance limits were also cared. The computed energy dissipation values were also related to the cumulative damage occurrence of the critical section of the reinforced concrete member.

The developed algorithms were combined in a proposed methodology for the earthquake resistant design of reinforced concrete precast buildings. The results of the energy-based design methodology were compared with the force- and displacement-based design methods and they were found satisfactory.

ÖZET

ENERJİ ESASLI YÖNTEMLERLE DEPREM ANALİZİ VE TEK SERBESTLİK DERECELİ BETONARME KOLONLARIN TASARIMI

Depremler Türkiye'de çok fazla can ve mal kaybına sebep olmuştur. Depremlerin karakteristikleri ve depremlerin yıkıcılığına dayanan yapıların yapılması konusu arştırmacıların motivasyonlarındna olmuştur.

Bu çalışmanın amacı yapıların enerji esaslı sismik analizi ve betonarme elemanların enerji yutma kapasitelerini belirleyecek iki çözüm yöntemi çıkartmaktır. Yapıların sismik analizi depremlerin giriş ve plastik enerji istem spektraları aracılığıyla yapılmaktadır. Enerji spektraları direk olarak enerji formülasyonlarından elde edilmektedir. Enerji istem spektraları 4 farklı süneklik, 4 farklı zemin koşulu ve 5 farklı sismik şiddet için elde edilmiştir.

Betonarme elemanların enerji yutma kapasitelerinin belirlenmesinde ise düşük-çevrimli yorulma analizne dayanan sabit genlikte çevrimsel yüklemeler kullanılmıştır. Genlik değerlerini belirlerken eleman ve kesitteki performans değerleri göz önüne alınmıştır. Elde edilen enerji yutma değerleri elemanın kritik kesitinde oluşan yığışımlı hasar bağlı olarak sınıflandırılmıştır.

Geliştirilen çözüm yöntemleri, betonarme prekast yapıların depreme dayanıklı tasarımı için bir araya getirilmiştir. Enerji esaslı yöntemle elde edilen sonuçlar kuvvet ve yer değiştirme esaslı tasarım yöntemlerinin sonuçları ile karşılaştırılmış ve tatminkar bulunmuştur.

TABLE OF CONTENTS

LIST OF FIGURES

LIST OF TABLES

LIST OF SYMBOL

EI	Input Energy
EK	Kinetic Energy
ES	Strain Energy
ED	Damping Energy
EH	Plastic Energy
SA	SAFE performance Level of Section
MN	MINIMUM performance Level of Section
CO	Collapse Performance Level Of Section
IO	Immediate Occupancy Performance Level Of System
LS	Life Safety performance Level of System
CP	Collapse Prevention performance Level of System
FA	Failure of the section
P	Axial Load
P_0	Axial Load Capacity
μ	Ductility
ξ	Damping Ratio

1. INTRODUCTION

1.1. General

Earthquake is a natural disaster that is not possible to predict with the current scientific knowledge. Therefore, it is needed to develop rational guidelines and procedures in the evaluation of the existing buildings and more important to design the new structures. By now, there were several approaches to establish reliable procedure for earthquake resistant design, however only two of them, force-based and dispslacement-based approaches have found a ground in the design codes. A design procedure should be not only rational but also must be applicable by the practicing engineers. Any evaluation or design principle far from the practice may not be a worthy effort unless it has potential of being implemented into any code of practice.

This study aims to employ the energy concept in the seismic analysis of the structures and also proposes an alternative design methodology for the single story reinforced concrete precast buildings in terms of energy dissipation.

1.2. Current Design Approaches

1.2.1. Force-Based Approach

The force-based method has been widely accepted in the modern design codes, such as FEMA 1997, UBC 2000 and ABYYHY 2007 etc. This method has been refined over the decades to consider the dynamic response characteristics as well as interaction of the soil underlying the structure. Even though this method provides very reasonable results for building and bridge type structures, there are certain shortcomings in its core assumptions. The performance of the building has not been included into the formulation of dynamic based action force on the structure and for the sake of determining the extreme action

force, the absolute maximum response values of the structures are taken into the account. This approach is not rational for a dynamic characterized problem, even though it is very simple and easy for practicing engineer to use in the earthquake resistant analysis and consequently design of structures. This method relies on the use of elastic design response spectrum (acceleration or velocity) which are the function of critical damping ratio, seismicity and the soil type. The response spectrum curves are calculated for the Single Degree of Freedom Systems (SDOF) having a range of natural periods. By calculating the appropriate period of any structural system (by either initial or secant stiffness), it is possible to calculate the elastic earthquake demand in terms of acceleration which is the ordinate of the spectrum curve.

The most irrational feature of using the elastic design spectrum in the analysis of the structures those go into the inelastic range is the assumption of Force Reduction Factor (R) that is correlated with the ductility and period of the system. Numerous researchers have been developed relationships between the Force Reduction Factor (R) and the ductility (μ) and period (T_n) of the system (Newmark and Hall, 1982; Uang, 1990; Nassar and Krawinkler, 1991; Vidic et al., 1994; Dimova and Negro, 2004). The common of the recommended relations is that the Force Reduction Factor (R) is the function of the ductility (μ) and the period (T_n) of the system.

When an engineer designs a new structure according to force-based procedure, she/he would follow an iterative procedure while assessing the period of the structure that is correlated to the size of the members. A preliminary design of the structural members is performed by the experience of the engineer and then he/she estimates the seismic lateral forces at each story levels by using the response spectrum curve and the force reduction factors. After static analysis is performed, the inter story drift ratios are checked for the given tolerance limits in the codes. If a good agreement is satisfied then the members are detailed under the member forces occurred by the estimated lateral seismic load. If the drift ratios do not satisfy the tolerance limits, the design engineer should resize the structural members until all inter story drift ratios are bounded in the tolerance limits.

Eventough its simplicity, the cumulative damage on the progressed during the earthquake is ignored since this approach considers only the maximum response which is a great drawback of the procedure (Chopra, 1995).

Another deficiency of the force-based seismic design is the selection of the member stiffness that plays a significant role in the distribution of the lateral forces (Priestley et al., 1996 and 2007). Once the size of the member is modified from the preliminary design, the re-calculation of the design forces is theoretically required.

1.2.2. Displacement-Based Approach

The performance of a structure should be defined with respect to the deformation capability of its members subjected to seismic forces. Therefore, the deformation of the member and, as a result, the displacement of the structural system has taken into the account in the development of a new design approach. Priestly and Calvi recommended such a method in 1997 (Calvi and Priestley, 1997). Their method, alike to force-based procedure, starts with a preliminary design and follows of push-over analysis which gives out the yield and ultimate displacement of the system. Beside the derivation of capacity curve, an elastic acceleration spectrum is formed. And finally the ordinates of the capacity curve and abscissa of the response spectrum is converted to acceleration and spectral displacement units, respectively, in order to overlay these two different plots to determine the target displacement. There is a phenomenal case in the determination of the target displacement due to the elastically obtained seismic demand plot and the inelastically calculated capacity curve (Celep, 2007). ATC40 recommends reducing the elastic demand spectrum, Figure 1.1a, while ABYYHY (2008) recommends converting the inelastic capacity curve to elastic by using initial slope and then using equal-displacement principle, the elastic target displacement is converted to inelastic target displacement, Figure 1.1b.

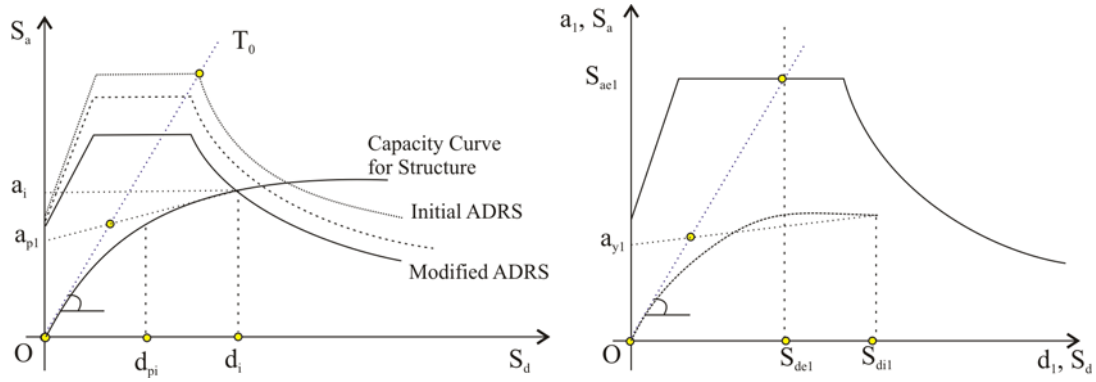

Figure 1.1. Determination of target displacement (ATC 40 and Celep, 2007)

The size of the members may be re-arranged according to the yield and target displacements those practically give the ductility ratio. For the estimated ductility ratio and damping value, the engineer intersects the capacity curve with the elastic response spectrum in order to get the secant stiffness of the system. Hereafter, the design seismic load is the product of the secant stiffness and the target displacement.

The advantage of using displacement-based method rather than force-based method is that it is the designer's ability to select the performance level of the system more realistically than using a tabulated force reduction reference table conformed to the structural configuration of the system.

On the other hand, this method may be again short-handed in the design of the members under the seismic action loads. Because the duration and the frequency content of the ground motions are the main reasons of the accumulated damage occurred in the members and the same damage occurrence is not obtained from capacity curve that is plotted for the top displacement versus base shear which is actually nonlinearly increased lateral force in one direction. Also, the seismic demand is once again calculated from the elastic response spectrum that is subjected to discussion of how much reliable in the reflection of the ground motions.

1.3. Energy-Based Approach

It is well known that the structures should endure the seismic forces by their strength capacity and also should remain under the certain deformation (or displacement) limits that classified as the performance levels (Krawinkler and Nassar, 1992; Priestley et al., 1996). However, there is also the fact that the structures should have enough energy dissipation capacity in terms of plastic deformations and viscous damping. The conventional design approaches, summarized in the preceding chapters, have either totally ignored or assumed that the energy dissipation capacity of a member is one way or another satisfied.

However, this may not be true all the time. The two identical structure having equal yield and displacement capacity may not have same energy dissipation capacity due to the constitutive behavior as in Figure 1.2. Even though, the yield and ultimate deformation of the two systems are identical (which makes them equal in the displacement-based design), the closed area of the loading and unloading force-displacement curves, those are defined as the plastic energy dissipation value of the member (Chopra, 1995), are relatively different meaning that these two structures absorb same amount of energy, while the structure 1 dissipates more energy then structure 2. This is obvious as the closed areas are compared in Figure 1.2.

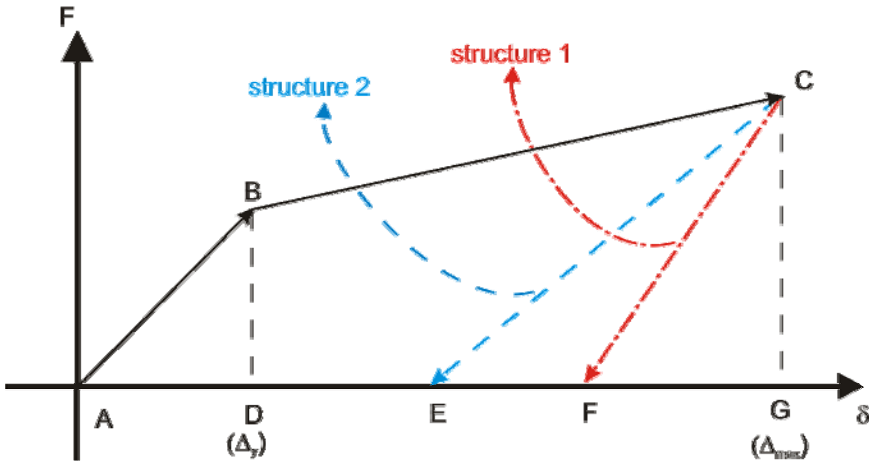

Figure 1.2. Two identical structures with different energy dissipation capacity

It is a known fact that the damage occurred in the member is directly related to the plastic energy dissipated in the member (Park and Ang, 1985). Therefore, a method that

includes not only the force and deformation capacity but also the energy dissipation capacity in its formulations would be covering all the relevant aspects of the seismic analysis and eventually the earthquake resistant design of existing or new buildings.

Such a method was first proposed in a paper submitted to the 1st World Conference Earthquake Engineering by Housner in 1956. In his paper, Housner proposed a design method for the water tanks. By nature of the energy balance equation, the cumulative damage of the member is correlated to the duration of the earthquake and its frequency content. Housner developed a formulation for the energy absorbed by an elastic system as;

$$E_a = \frac{1}{2}(m \times PGA) \times S_d^2 \tag{1.1}$$

where m is the mass of the system, S_d is the displacement spectral value and PGA is the Peak Ground Acceleration. This formulation also expressed in the form of equivalent velocity as;

$$V_e = \sqrt{\frac{2 \times E_a}{m}} = V \tag{1.2}$$

This future promising methodology has not been popular in the following years except limited studies (Veletsos and Newmark, 1960).

In 1980's three important studies were conducted, Zahrah (1981, 1984) and Akiyama (1985). Zahrah recommended that the destructiveness of any earthquake was characterized by its peak acceleration. However, this characterization does not correlate the damage patterns observed in the previous studies. Zahrah recommended that the correlation between the damage of the member and the severity of the earthquake is clearly found in the energy balance formulations. He also prepared the input energy spectra for a SDOF system that has elasto-perfectly plastic constitutive relation. This was the first attempt to rationalize the energy values as a design tool.

Akiyama (1985) published a book which uses the energy formulations for the Multi Degree of Freedom systems (MDOF) as analysis and simple design tool. He employed the shear type steel moment resisting frame structures. The most important contribution of the book is that Akiyama applied the formulation given by Housner in inelastic cases except for systems in short periods. Akiyama was the first who proposed the empirical values for the V_e values those are function of the initial period of the structure and predominant period of the soil as

$$\begin{aligned} V_e &= 2.5 \times T_n \quad \text{for } T_n \le T_g \\ V_e &= 2.5 \times T_g \quad \text{for } T_n \ge T_g \end{aligned} \tag{1.3}$$

where the T_g is the predominant period of the ground motion as a function of soil type. The values of T_g are 0.4, 0.6 ,0.8 and 1.0 for soil types I (bed rock), II, III and IV (softest soil), respectively.

Kuwamura and Galambos (1989) studied that the energy-based velocity spectrum is very similar to the smoothed Fourier Amplitude Spectrum of the input acceleration and recommended an improved version of the equation 1.2 as,

$$\begin{aligned} V_e &= \frac{1}{2} \times \sqrt{\frac{I_E}{T_g}} \times T_n \quad \text{for } T_n \le T_g \\ V_e &= \frac{1}{2} \times \sqrt{I_E \times T_g} \quad \text{for } T_n \ge T_g \end{aligned} \tag{1.4}$$

where the I_E is the integral of the square of the ground acceleration for the total duration as,

$$I_E = \int_0^t \ddot{u}_g^{\,2} dt \tag{1.5}$$

Fajfar et al (1989) employed 40 earthquake records and computed a formulation of input energy value for the intermediate-regions (constant-velocity region) with 5 per cent

damping and strength ratios of 0.5-1.0 which is the ratio of the yield force to the mass times PGA of the record, as ,

$$\frac{E_I}{m} = 2.2 \times t_D{}^{0.5} \times PGV^2 \tag{1.6}$$

in which the t_D is the duration defined by Trifunac and Brady (1975) and PGV is the Peak Ground Velocity.

With the beginning of 1990's, more researchers found the energy principles popular and employed in their studies. Uang and Bertero (1990) compared the difference between the energy formulations derived from the absolute and relative structural responses, respectively, as,

$$\frac{E_{Ia}}{m} = \int_0^t \ddot{u}_t \dot{u}_g d\tau \tag{1.7}$$

$$\frac{E_{Ir}}{m} = -\int_0^t \ddot{u}_g u d\tau \tag{1.8}$$

where $\ddot{u}_t = \ddot{u}_g + \ddot{u}$ denotes the total acceleration.

Bertero and Teran-Gilmore (1994) discussed the design energy principles in the context of performance based methods and proposed that the energy concept should be the basis for the next generation design codes.

Akbaş (1996) used the energy principles in the design of moment resisting multi story steel frames. He described the distribution of the absorbed energy through the height of the building and after through the column and beam joints at each floor level. The distribution of the energy among the joints at the same floor level is started from the top floor and based on the principle of "weak beam-strong column". Since the steel members are fabricated with little initial imperfection, it is possible to tabulate the energy dissipation

values under certain test protocols. Akbas used these energy dissipation capacity tables in his recommended design methodology.

Decanini and Mollaioli (1998 and 2001) recommended elastic and inelastic input energy spectra for the design of the buildings. The inelastic spectra which were based on the certain hysteretic models those had been widely used in the literature were so normalized that the different soil types and focal distances were included as the design parameters. The proposed elastic and inelastic energy spectra were in terms of the mass normalized input energy and the ratio of the hysteretic energy to input energy for inelastic systems. However, almost every study on the input energy spectra has been termed as the equivalent velocity since Housner (1956).

It is noticeable that the most of the researchers used energy principles studied very simple hysteretic models like elasto-plastic models with and without hardening that reflects the behavior of the steel structures. However, all the efforts on the development of the energy spectra should also cover the other material types, such as Reinforced Concrete (RC). By using reasonable constitutive models, it is possible to enlarge the energy spectra to the stiffness and strength degrading materials, even structures having some sever slip at the critical sections.

Leelataviwat et al (2002) described a yield mechanism for the multi story steel systems and developed a design methodology that cares the Interstory Drift Ratios (IDR) those are found in UBC 97.

Chou and Uang (2003) recommended a seismic energy demand method for the framed MDOF steel structures by using constant-ductility response spectra derived from three earthquake records for the SDOF systems with five per cent Rayleigh damping. The distribution of the input energy through the height of the building was formulated by the help of the first two mode shapes of the five, seven and nine stories steel frames those were preliminarily designed according to the NEHRP provisions.

Chai and Kunnath (2004) tried to develop another type of demand spectrum by benefiting from the energy balance formulation while caring the close relation between the

damage and the energy dissipated at that section. The spectra they proposed were based on the use of equivalent cycle number that has the same destructiveness with the any random characterized cyclic demand action. They illustrated their design method which is using the proposed spectra for a bridge column that was designed in accordance with ACI318.

Chai (2005) recognized the duration of the ground motion while developing an inelastic design spectra. In his study, the classical low-cycle fatigue model was used in the assessment of the cumulated damage with respect to the normalized plastic strain energies. He also intends to scrutinize the difference of the short- and long-duration ground motion that is practically not encountered in the current design methods.

Ghosh and Collins (2006) merged the energy-based design criteria for a specific site. This was an interesting study because it was the first time that an energy-based hazard mitigation work was conducted deterministically even though similar mitigation works are entirely probabilistic. A similar energy-based hazard mitigation work was performed in this thesis and results were presented in the 14th World Conference on Earthquake Engineering (Dindar et al 2008)

Surahman (2007) evaluated the test results of the different member and connections conducted in ITB Structure Laboratory in Indonesia and formulated an empirical energy dissipation formulation. The design methodology proposed in his study shows similar approach to this study, whereas seismic demand was summarized from the available literature and the energy dissipation capacity of the structural components was taken from different load patterns which makes complicated the relation between the dissipated energy and deformation path.

The evaluation of the laboratory test results have been gained interest in many researchers and among them the group from Ljubljana University in Slovenia performed a statistical study on the relation of hysteretic energy dissipation capacity and the drift ratio of reinforced concrete (RC) columns (Poljansek et al,. 2008). The results of the 156 and 757 specimens from the databases of University of Washington and University of Patras, respectively, were evaluated to determine the relation between the energy-dissipation and the drift ratio of the RC columns. This extensive study focuses on the flexural failure mode

of the RC columns those were subjected to different test protocols. In order to clarify the first order flexural affects, the P-Delta were eliminated from the selected results. The result of the study produces that the energy dissipation of the columns are proportional to the drift capacity under the reversed cyclic loading. The simplest damage index of drift should be assumed a reliable performance limit indicator for the RC structural components.

Recently, Leelataviwat et al. (2009) brought a design procedure that is similar to the displacement-based methodology. Based on the energy balance of the dynamic action of the systems, they propose to create a energy demand spectra derived from the displacement response spectra and congest it with the energy-displacement curve calculated from the capacity curve. By this way, the seismic displacement demand is determined while the energy terms are taken into the seismic analysis. The reformulation of the displacement spectra to energy demand spectra inherently carries the shortcomings of the elastic spectra calculation even if the conversion is very simple. On the other side, the energy-displacement capacity curve again based on the push-over analysis which do not include cumulative damage occurrences.

All studies summarized above try to implement the energy terms in the seismic analysis and design of the structures. Therefore, it is important to emphasize that the use of the energy in the formulations may extend the limits of the structural engineers from the simple calculations to more complicated solutions which are more reliable. The following paragraphs explain such a complex analysis method.

The basic principle in Earthquake Resisting Design (EQ-RD) is simply formulated as

$$Demand \leq Capacity \tag{1.9}$$

The recent seismic design codes use this principle in terms of their design parameters such as the force-based design aims to find the force acting on the structural member due to the lateral static loads calculated from the multiplication of the weight of the system by the seismic coefficients and finally the ordinate of the response spectrum. If the inelastic behavior is desired than the loads found above is divided by the Load Reduction Factor

(*R*). On the other hand, the displacement-based design aims to keep the target displacement of the structure within the limits of the so-called “capacity curve”.

As given in the previous paragraph, The Earthquake Resisting Design principle (equation 1.9) has been valid for the vectors, force and displacement. However, it is a well-known fact that the structures should also have not only enough deformation and strength capacity but also energy dissipation capacity during the earthquake. This third capacity requirement has always been credited as satisfied somehow in either method. This study aims to give a better understanding in the design of structural elements by including the energy terms in a new proposed methodology.

The energy as a design parameter should be very inconvincible regarding its hard-to-visualize physical meaning. Since the energy values are calculated by the multiplication of the force and the displacement, it may not be easy to evaluate the deformation or resisting rate of the member. In order to overcome this phenomenon, the relation between the force due to the dynamic actions and the created deformation on the member must be studied very well. The aim of learning the relation between these two physical concepts has been the main topic of the tests in laboratories and in numerous numerical studies. The tests in laboratories are to simulate the physical events and obtain the data in order to develop the mathematical models those reflecting with high accuracy. One of the test protocols developed in the laboratories is based on the concept of fatigue.

One of the well established tests on the fatigue analysis was made by Kunnath et al. in 1997. The purpose of the tests was to deal with the relation between the load path and the inelastic damage induced in RC member. Kunnath and his team accomplished reverse cyclic quasi-static tests on one-quarter scaled bridge footing designed according to American Association of State Highway and Transportation Officials (AASHTO) under three sets of lateral displacement amplitudes (constant, varying and arbitrary due to seismic action). 12 samples were divided into four groups, one for monotonic pushover test (capacity test), one for saw-teeth test (standard displacement pattern), four for constant amplitude test and six for arbitrary amplitude test. The results of the test were interesting from the view of damage and load path. They found out that the confining spirals will fail prior the low-cycle fatigue failure of the longitudinal reinforcement under the sequence of

low amplitude cycles. Conversely, the bridge under the high amplitude inelastic cycles, the reinforcing bars will rupture before the confinement failure occurs. And, another interesting finding from the tests is that the arbitrary displacement histories are actually harmony of the 5 different time-histories. The sequences of these five time-histories were different for the all samples in last group. And the energy dissipation trends of the samples in the last group show that there's a strong relation between the load histories.

Another experimental study based on fatigue concept was conducted by Erberik in 2001. Different from the Kunnath et al.'s tests, the 17 RC members were appointed as beam elements and their flexural and shear configurations arranged according to Turkish Standards (TS500-1985). The test samples were separated into three sets; one for monotonic loading, 12 for constant amplitude tests, and the resting four for varying amplitude tests. The findings out of the study show a great parallel to Kunnath et al. (1997) study; the dissipated energy is absolutely dependent to the loading history, confinement provided in the RC members drastically influence the energy dissipation of the member along with the increase in ductility.

The laboratory tests those aimed to explore the relation between the reinforced concrete damage and fatigue phenomenon under cyclic loading are limited eventhough the test setup is not complicated. Any laboratory with quasi-static test set-up can easily perform the fatigue tests with the intention of using fatigue formulation in the force-displacement relation. The fatigue tests may be altered by the computer programs those are capable of simulating the laboratory test conditions with certain accuracy. Of course, the success of the numerical analysis is correlated with the capacity of the software employed in. Theoretically, a computer program that is able to use the rational constitutive behavior models (stiffness degrading, strength deterioration, slip-pinching) in the quasi-static analysis should be successful enough. However, the uncertainty of the building conditions of the test samples (concrete receipt, pouring method, reinforcement configuration, and any human-made imperfections) will be ignored in the numerical calculations.

1.4. The Objective and Scope of the Study

After an extensive literature review on the energy-based analysis and seismic design of the structures, the implementation of the energy concept into the structural analysis and earthquake resistant design has not been completed, yet. The next generation earthquake resistant design codes will be based on the combination of strength and deformation-displacement characteristics of the structural members. Hence, concentration of the upcoming studies on energy balance equation will be considerably meaningful effort. Most the studies aiming to develop the energy-based design procedures and methodologies have been focused mainly on the steel structures whereas the similar effort has not been paid to the reinforced concrete structures. A procedure that combines the seismic demand and the structural capacity in terms of energy for the reinforced concrete structures have been missing in the recent literature. Therefore, the research rational of this study is to employ the energy formulations in the analysis and design of reinforced concrete buildings which covers the majority of the structures.

The short-comings of the conventional response spectrum and its use in the current guidelines must be altered by more realistic methods. Because of the simplistic assumptions those are required for the assessment of the inelastic behavior of the structures (i.e. force reduction factor (R) and overlaying the capacity on demand curve) whereas the alternative methods which is energy-based method must be more robust and direct in their results. This study is intended to derive mass normalized input and plastic energy spectra those are related to the displacement ductility, seismic scale and site conditions. Even if the similar spectra are available in the literature, the formation of the energy spectra with respect to the difference seismic scales has not been mentioned in any study. It is meaningful that the direct derivation of the seismic energy demand energy spectra including elastic and inelastic behavior plus with the parameters of the varying seismic scales and soil conditions will be more rational than the use of the conventional spectral methods.

While evaluating the earthquake resistant design of the structures, the resistance of the structures should be also referred in energy principles. However, it is not easy to define

a response history of the structural members that reflects the exact seismic action in the analysis. Therefore, the numerical simulation of the fatigue tests of reinforced concrete members will be a good study for the establishment of the energy dissipation capacity formulations. The fatigue-similar analysis includes the uniform deformation pattern of the structural members. The basis of the low-cycle fatigue approach in the seismic action relies on the findings of the experiments comparing the constant- and random-amplitude deformation histories.

Therefore, the primary objectives of this study are as follows;

- Develop the energy spectra for elastic and inelastic SDOF systems with different seismic scale and site conditions.
- Conduct numerical simulations of constant-amplitude push and pull tests on reinforced concrete members with different shear span, axial force, and longitudinal reinforcement ratio.
- Define the energy dissipation capacity tables for the simulated numerical models regarding the code-based system and section performance levels.
- Recommend a design methodology to find the amount of the longitudinal reinforcement of reinforced concrete members by using energy balance equations.
- Compare the proposed design methodology to the current design methods.

The study is ultimately aimed to develop a design methodology for the reinforced concrete columns those are the main structural elements of the precast type building. Because of the main characteristics of the selected building type and to be able to develop the analysis and design procedures merely based on energy, the following issues are kept out of the scope,

- The shear failure mode of the members is not taken as a parameter in energy formulations due to the fact that modern seismic code provisions require that the shear failure should be prevented in the design of the new buildings.
- Out-of-plane actions and responses of the members (torsion, out-of-bending, etc.) are not cared.

- Since the first mode of the multi-storey buildings resembles the behavior of the Single Degree of Freedom, the Multi Degree of Freedom systems are not being used in this study.

This study is composed of five chapters. The first chapter gives a general overview of the study and the literature of energy-based analysis and design approach.

Chapter 2 introduces the Energy Balance Equation and the components of this equation. By using the convenient constitutive hysteretic models, the response and energy spectra of the several systems having 5 percent Rayleigh damping are computed for different constant ductility levels. In order to establish a basis for the seismic demand, smoothed input and plastic energy spectra as a function of different ductility levels, seismic intensity and site conditions are provided in this chapter.

Chapter 3 deals with the simulation of the fatigue based energy dissipation capacity formulations of the several reinforced concrete structures. The developed algorithm that takes the system and section performance levels into the consideration is presented. The developed algorithm is a generic algorithm which should be extended to different reinforced concrete columns. The energy dissipation capacity tables for the selected cross-sections are also provided in this chapter.

Chapter 4 presents the recommended design methodology for three different reinforced concrete structures, a single column, one-bay frame and one-to-two bay precast building. The sensitivity and comparative analysis to the current design codes are given in this chapter.

Chapter 5 contains the summary, conclusions and future extension of the study.

2. EARTHQUAKE DEMAND IN TERMS OF ENERGY

2.1. Earthquake Excitation: Energy Balance Equation

The main concern of the structural engineers dealing with the analysis of the earthquake induced forces is to formulate the effects of the strong ground motion on the structures, Figure 2.1.

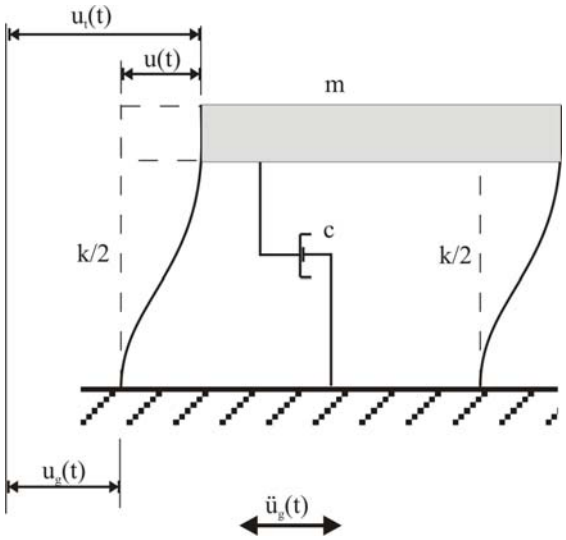

Figure 2.1. SDOF subjected to ground motion

The forces acting on a Single Degree of Freedom (SDOF) system as a function of time can be expressed in two reference systems; displacement of the system with respect to either originating point on the ground (absolute motion terms), or the point of initial position at silence (relative motion terms). The difference of the acting forces between two approaches occurs only at the terms related to the mass of the system. The formulation of the motion of the SDOF system (Chopra, 1995) is as follows;

$$m\ddot{u}_t(t) + c\dot{u}(t) + f_s\left(u(t),\dot{u}(t)\right) = 0 \tag{2.1}$$

where m, c and f_s are the mass and damping factor of the system and the spring (or restoring) force, respectively. The terms of $\ddot{u}_t(t)$, $\dot{u}_t(t)$ and $u(t)$ are the time-histories of

the total displacement, relative velocity and relative displacement of the SDOF system, respectively. However, the Equation 2.1 can be rewritten if one separates the components of the total displacement of the system as;

$$u(t) + u_g(t) = u_t(t) \tag{2.2}$$

Thus, the equation of the motion of the system becomes

$$m\ddot{u}(t) + c\dot{u}(t) + f_s\big(u(t), \dot{u}(t)\big) = -m\ddot{u}_g(t) \tag{2.3}$$

Here, $\ddot{u}_g(t)$ the multiplier of the mass of the system on right side of the equation is the acceleration of the ground motion.

The equation of the motion with relative response values may give a better understanding to the physical meaning of its terms. The first term represents the inertial force of the mass, the second is the damping force due to the friction between structural members, and the third is the spring force trying to restore the system to its initial position. The term on the right side of the equation is simply external force acting on the structure. If the response of the system stays in the elastic range of the members, the third term in the equation 2.3 can be simplified as $ku(t)$ where k is the initial stiffness of the system.

The equation of motion of SDOF system represents the excitation of the ground and the response of the structures as the forces in time-history series, due to the dynamic characterization of the earthquake. The damage potential of the earthquakes and the response of the structures during the earthquakes are conventionally defined with the extreme values of these time-histories.

The most common parameter that defines the severity of an earthquake is the peak values of ground acceleration (PGA) or velocity (PGV) of the record (Kramer, 1990). Nevertheless, there is a strong relation between the damage potential of the ground motion and its PGA values, many researchers indicated that the Peak Values of Ground Acceleration or Velocity may not reflect the severity of the ground motion by itself

(Zahrah, 1981; Akiyama, 1985; Malhotra, 2002). The different parameters those describe the damage potential of the earthquakes were developed by many researchers (Arias Intensity, Housner Intensity, Effective Peak Ground Acceleration etc.).

Since the external and internal forces excited by the earthquake are in equilibrium at any time instance of the ground motion duration, the work created by these internal and external forces should also remain in balance throughout the entire duration. The approach of assuming the energy balance can be formulated by using the equation of motion of a SDOF system (Akiyama, 1985).

The formulation of the energy balance may be written again by caring the absolute and relative motion of the system (Bertero and Uang, 1990). The formulations of these two approaches give out similar equations those differ only with the terms with the mass of the system.

2.1.1. Derivation of Absolute Energy Formulation

Integration of the Equation 2.1 with respect to the displacement of the system, $u(t)$, yields the following equation;

$$\int m\ddot{u}_t(t)du + \int c\dot{u}(t)du + \int f_s du = 0 \tag{2.4}$$

If the Equation 2.4 is rearranged by taking $u_t(t) = u_g(t) + u(t)$ as follows,

$$\int m\ddot{u}_t du_t + \int c\dot{u}(t)du + \int f_s du = \int m\ddot{u}_t du_g \tag{2.5}$$

where the terms are named as Absolute Kinetic Energy, Damping Energy, Absorbed Energy and Absolute Input Energy, respectively. The Equation 2.5 can be re-expressed as in form of;

$$E_k + E_d + E_a = E_I \tag{2.6}$$

Here, the care should be given to the third term on the left side of the equation that includes the energy of elastic and plastic strains. Therefore, this term is also re-expressed as follows;

$$E_a = E_s + E_p \tag{2.7}$$

The physical meaning of the Absolute Input Energy is the work done by total base shear at the foundation level (Bertero and Uang, 1992), as seen in Figure 2.1.

2.1.2. Derivation of Relative Energy Formulation

If the integration of Equation 2.3, instead of Equation 2.1, again with respect to the displacement of the system, $u(t)$, yields the following equation;

$$\int m\ddot{u}(t)du + \int c\dot{u}(t)du + \int f_s du = -\int m\ddot{u}_g(t)du \tag{2.8}$$

Similar to the Absolute Energy Terms, the terms are named as Relative Kinetic Energy, Damping Energy, Absorbed Energy and Relative Input Energy, respectively, as follows;

$$E_k' + E_d + E_a = E_I' \tag{2.9}$$

Once again, the third term of the left hand side of the equation is the summation of the elastic and plastic energies, as in Equation 2.7.

The physical meaning of the Relative Input Energy is the work done by the equivalent force of $-m\ddot{u}_g$ on a fixed based system as in Figure 2.2;

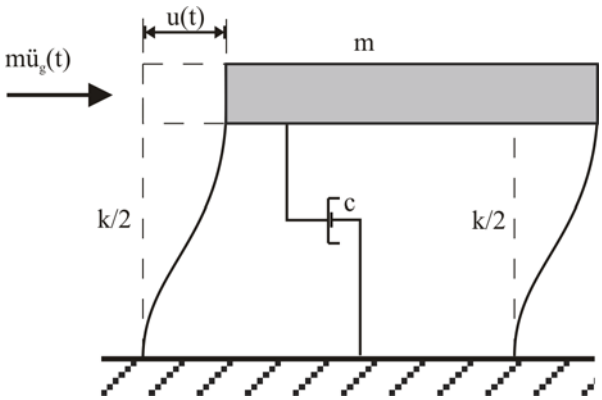

Figure 2.2. Fixed based SDOF system

In this study, the relative energy terms will be employed along the developed Energy Demand and Capacity Methods. Therefore, the Relative and Absolute Energy terms will be shown as E_k, E_I instead of E_k', E_I'. The display of E_k', E_I' in equation 2.9 was to be consistent with the first appearance of the terms in Bertero and Uang (1990). However, the physical meaning of employing relative energy terms in the computations has been favored by the author of this study.

2.1.3. The Energy Mechanisms in the Structures

Each term in equation of motion represents certain forces acting on the structures. The free-body-diagram of a typical SDOF system presents these forces in Figure 2.3. Here the forces of $f_s(t)$, $f_d(t)$, $f_I(t)$ and $p(t)$ are spring, damping, inertia and effective forces, respectively.

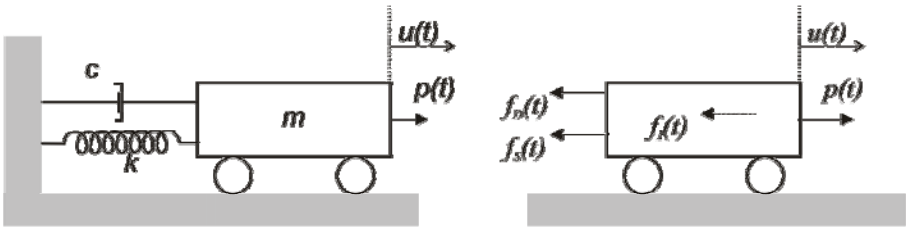

Figure 2.3. Free-Body-Diagram of SDOF system

Alike the equation of motion, the terms in the energy balance equation describe the different physical assets of the structures. If the relations between the derivatives of structural displacement are used in the re-definition of integration terms in Equation 2.8,

each energy term becomes clearer to understand along with the earthquake duration. After some mathematical arrangements in Equation 2.8, the energy terms are expressed in time-histories.

$$\frac{m(\dot{u}(t))^2}{2} + \int c(\dot{u}(t))^2 dt + E_a = -\int m\ddot{u}_g(t)\dot{u}(t)dt \tag{2.10}$$

The third term that is named as "Absorbed Energy" in Equation 2.10 includes the elastic and inelastic (plastic) strain energies, $E_a = E_s + E_p$. The explicit formulation of this term is actually as follows;

$$E_a = \int f_s(t)\dot{u}(t)dt \tag{2.11}$$

However, the elastic strain energy can be formulated with respect to the initial stiffness (k) of the structure, as follows;

$$E_s = \frac{(f_s(t))^2}{2k} \tag{2.12}$$

On the other hand, the formulation of the inelastic (plastic) strain energy is a little bit stringent, since it's computed in the inelastic range of the structural behavior. The common description of the inelastic (plastic) strain energy is the remaining part of the energy balance equation after all other known energy terms are subtracted;

$$E_p = E_I - (E_k + E_d + E_s) \tag{2.13}$$

The conventional approach for the computation of the inelastic (plastic) strain energy is to calculate the total closed area of the spring force vs. displacement hysteresis curves of the system (Mahin and Bertero, 1981). This approach, which was used in this study too, has been the basis for the computation of the plastic energies for the conventional tests conducted in the laboratories (Kunnath, 1996).

It is reckoned that the input energy imparted into the structure is separated into two main groups, (i) recoverable, (ii) irrecoverable energies, as in Figure 2.4.

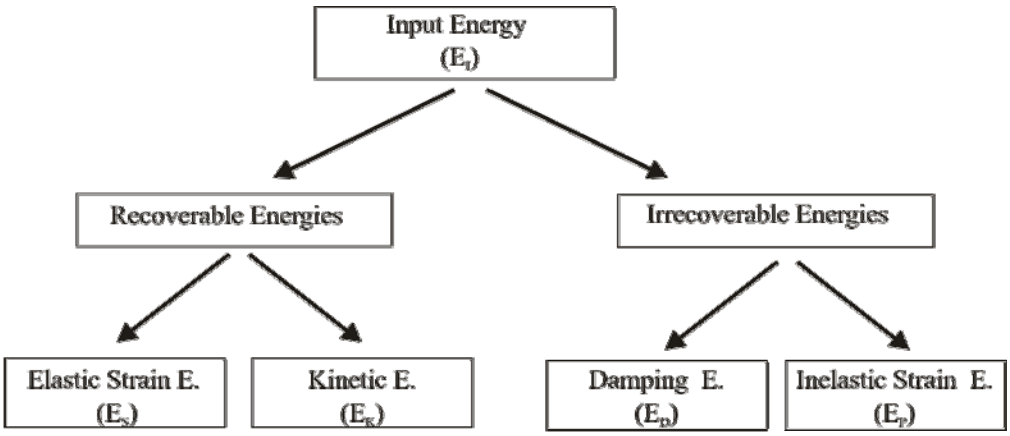

Figure 2.4. Distribution of the energy terms

The fundamental difference between these two groups is the trend of the numerical value along the duration of earthquake. The elastic strain and kinetic energies take values during the main shock of the motion and then diminishes to the end of the shock. However, the damping and inelastic strain energies instantly increase as the vibration of the ground continues. Therefore, at the end of the motion, it's expected that the structure is able to recover the Elastic Strain and Kinetic Energies; on the other hand, it is unable to recover the Damping and Inelastic Strain Energies. This expectation is visualized in the energy time-history graphics in the next sections.

Some portion of the total dissipated energy is directly associated with the damage occurred in the member of the structure. Due to its cumulative nature of the plastic energy, it is possible to quantify the development of the plastic deformations (rotations and displacements) at the member level. This fact has gained considerable attention in recent years for the researchers looking for the relation between the affects of the dynamic forces on the damage of the members (Fajfar, 1994; Dutta and Mander, 2001; Kunnath and Chai, 2003).

2.2. Energy Time-Histories

2.2.1. The Numerical Model of the Structure

This study aims to apply and develop the energy-based analysis and design methodologies for Single Degree of Freedom Systems. Therefore, the energy terms are computed from the evaluation of SDOF system defined in Wong and Yang (2002), Figure 2.5.

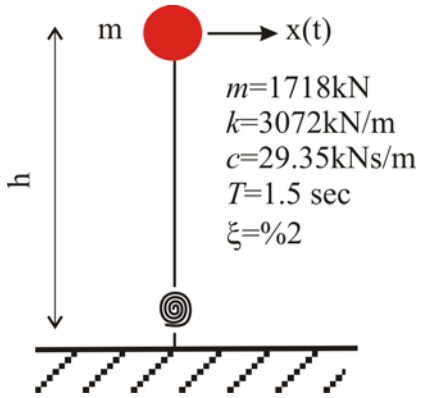

Figure 2.5. The SDOF system used in the computations

Wong and Yang (2002) used linear and Elasto-Perfectly-Plastic Bilinear models in their study. While introducing the energy time-histories computed by using equations 2.10-12, the given model was used in all the calculations of this section. However, the more specific constitutive models representing pure flexural and flexure with slip (pinching) were also used in the derivation of the time-series. These models will be explicitly explained in the later sections.

Prior to the computations of the inelastic analysis, it was assumed that the plasticity and stiffness were distributed along with the height of the member instead of concentrated plastic hinge. However, the mass of the system was taken as lumped on the top of the member to realize the SDOF model.

While evaluating the inelastic response of the SDOF system, the constant displacement ductility of the structure was assumed in the calculations which will be explained in the next sections. This has been achieved by a trial-error method in order to

establish the yield point for the desired (constant) ductility level Kunnath and Hu (2004), Kunnath (2008).

Assuming the viscous damping remained constant along the whole motion is accepted by many researchers. Since this study aims to give a better understanding in the use of energy concept in the analysis and design of the structural members, the alternative viscous damping relations were not taken into the accounts in the present study. The viscous damping ratio of the mathematical model was taken as 5 per cent. However, the effect of the variation of the damping ratio was also analyzed for the sake of briefing the affect on other energy terms.

2.2.2. The Properties of the Earthquake Motions

The analysis of the earthquake records in any study is a very chaotic work for the researcher. The chaotic work starts from the selection of the records and goes on the results of the analysis. Therefore, it is unavoidable to remove some of the records from the initially selected earthquake records during the analysis. In the beginning of this study 428 records were selected from the database of Pacific Earthquake Engineering Research Centre (PEER) in order to avoid the tedious work of correcting the data with respect to similar conditions (noise clearing, filter passing, baseline correction etc.). While developing the energy spectra, some of the records were extracted from the list. The further explanation of the earthquakes used in this study will be given in the next sections.

Based on the chaotic work explained above, only five well-known reference earthquake records employed in the computation of the energy time-histories for different structural and record parameters. These five reference records are summarized in Table 2.1.

Table 2.1. Properties of the reference earthquake records

Ground Motion	PGA (g)	Soil Condition (USGS Classification)	T (sec)	T_d (sec)	Magnitude (Mw)	Focal Distance (km)
Imperial Valley (19.May.1940) 180 component	0.21	C- Deep narrow soil	40	24.11	7.0	8.3
Northridge Sylmar-Hospital (17.Apr.1994) 360 component	0.84	C- Deep narrow soil	20	5.34	6.7	6.4
Chile Llolleo (3.Mar.1985) 10 component	0.71	A- Sandstone and volcanic soil	116	35.85	7.8	4.5
San Salvador (10.Sept.1986) 90 component	0.87	B- Shallow (stiff) soil	10	4.49	5.4	9.0
Kobe-JMA (16.Jan.1995) 180 component	0.80	B- Shallow (stiff) soil	48	5.34	6.9	0.6

The difference of fourth and the fifth columns comes from the definition of the strong ground motion (main shock) duration. Eventough, the baseline corrections and high-band filtering against noise were completed for the raw records; the duration of the motion is re-calculated according to rule expressed by Trifunac and Brady (1975). The effective duration expression of Trifunac and Brady is basically based on accepting that the main shock of a strong ground motion is banded in 5- and 95 per cent of the Arias Intensity (1970) ($t = t_{0.95} - t_{0.05}$). The formulation of the Arias Intensity is given in 2.14.

$$I_a = \frac{\pi}{2g}\int_0^t \left[\ddot{u}_g(t)\right]^2 dt \tag{2.14}$$

The entire and effective durations of the selected earthquakes are plotted in figure 2.6.

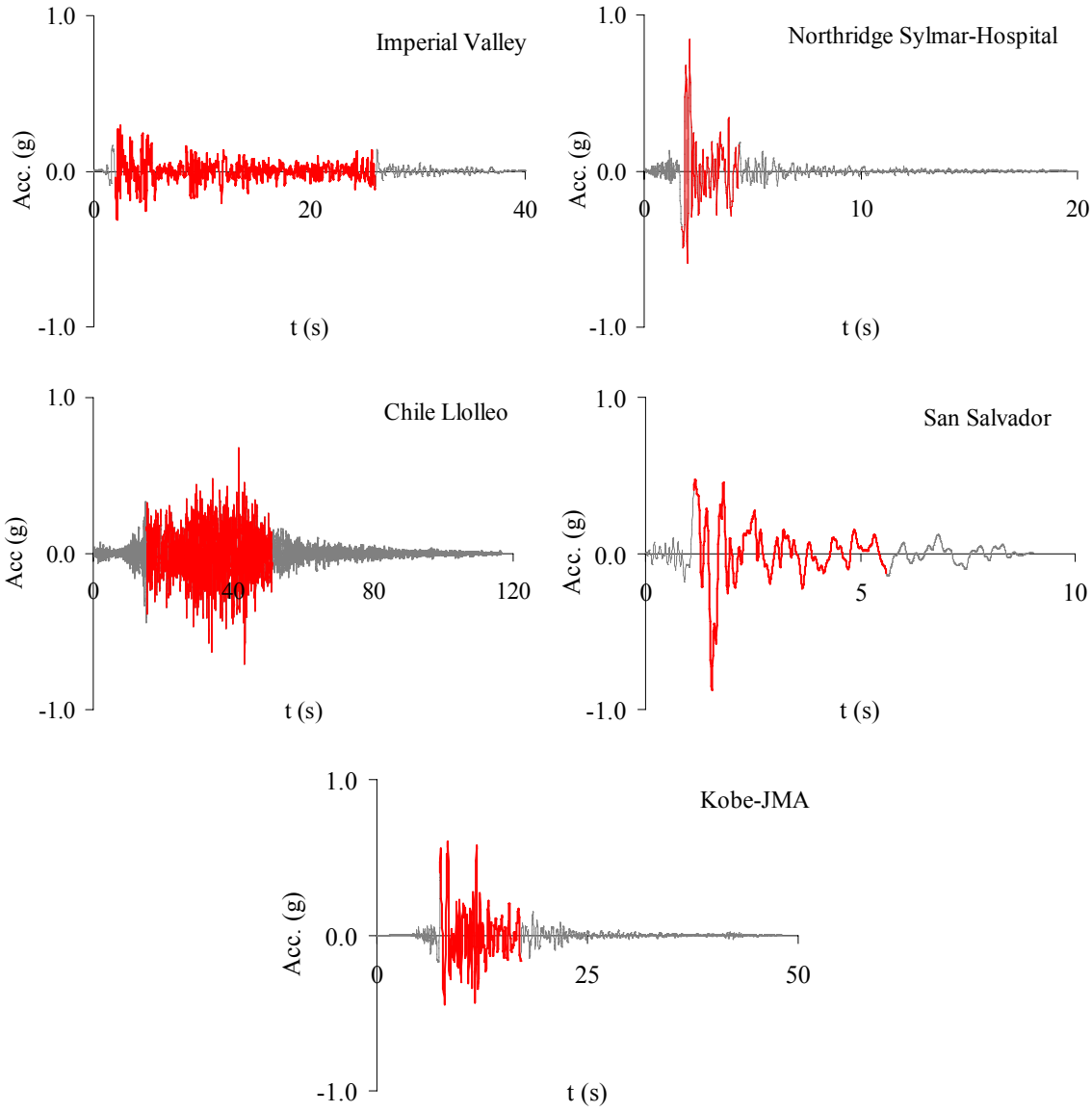

Figure 2.6- Accelerograms of reference earthquake records

Figure 2.7 shows the Fourier Amplitude Spectrum (FAS) of the reference earthquakes. The harmonic nature of the San Salvador and Northridge Sylmar Hospital is clear in Figure 2.7, while Imperial Valley, Chile Llolleo and Kobe-JMA have richer frequency content.

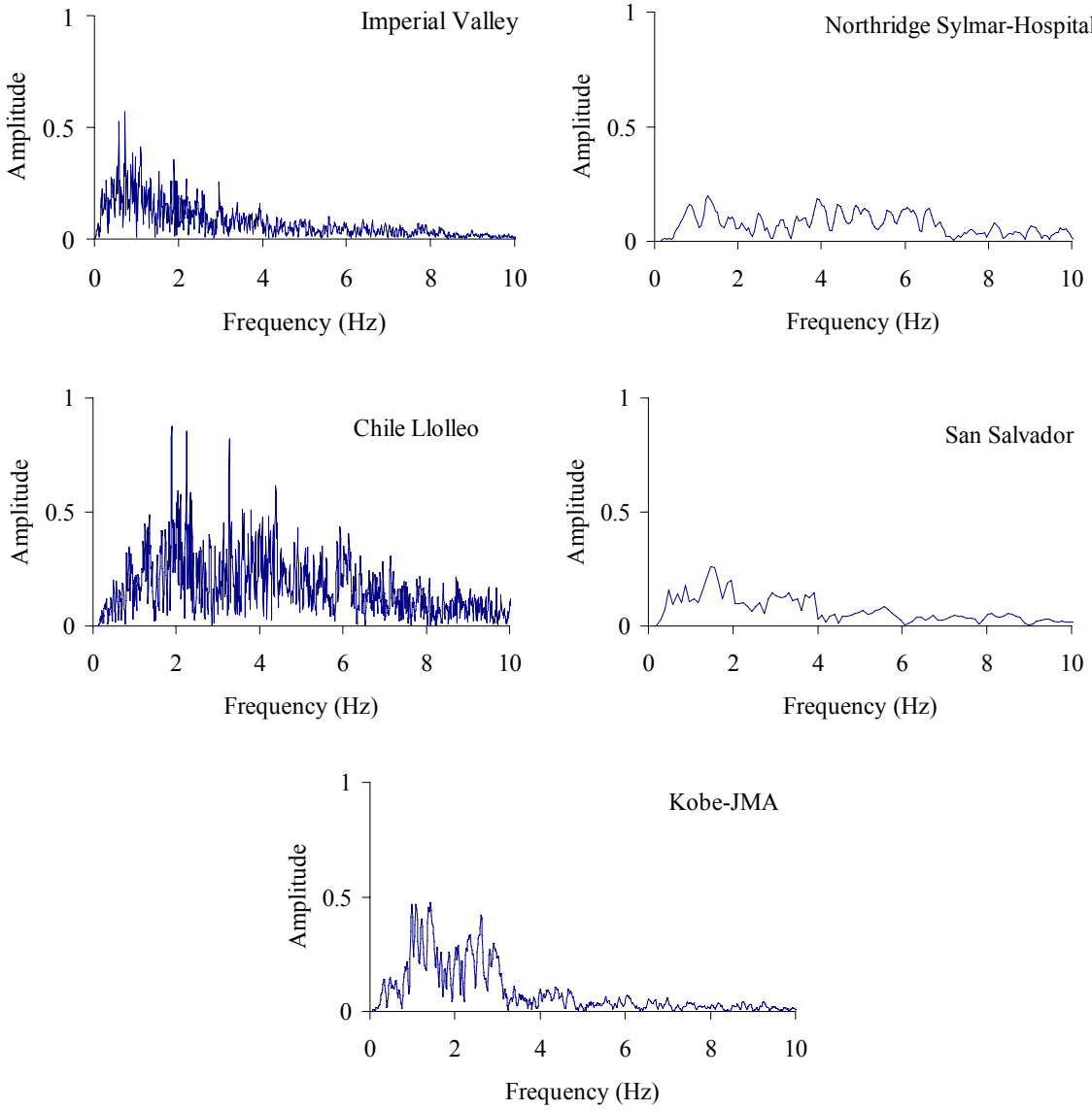

Figure 2.7. FAS of the reference earthquake records

2.2.3. The Energy Terms in Elastic Systems

If the yield strength of a system is higher than the maximum strength demand of the seismic action, it is for sure the structure will not exceed into the inelastic range. The ability of remaining in the elastic range is provided either by adequate deformation or by strength capacity of the members. The relation between the deformation and the strength is basically related through the stiffness, k_i, (or rigidity) which is constant ratio of the shear to the displacement of the member.

Since the restoring force (or spring force) of the system is proportional to the displacement under the seismic force, the term representing the plastic energy in the energy balance equation drops. This yields two specific results; (i) the energy dissipation mechanism duty in the system is assigned to viscous damping, (ii), more important, the damage due to inelastic action does not occur.

Figure 2.8 shows the variation of the energy terms throughout the seismic motion of Imperial Valley (El Centro) in the case linear elastic behavior.

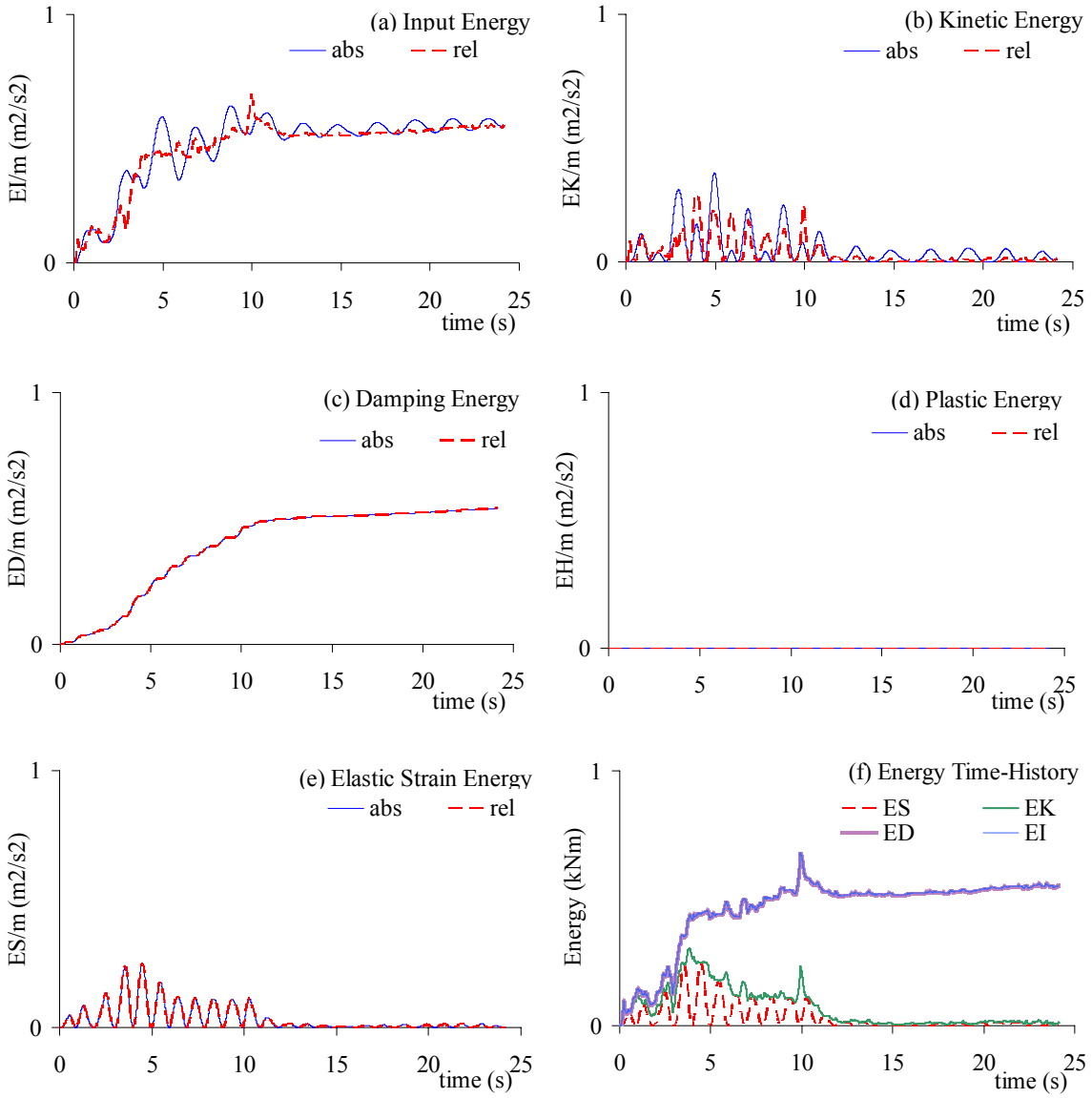

Figure 2.8. Time-history of energy components for elastic SDOF structure with T=1.5s, ξ=5 per cent under Imperial Valley (El Centro) motion

Energy is a scalar term and always positive as in Figure 2.8. The fluctuation of the input energy compared to the damping energy, which looks more stable in accumulation, is due to the fact that this term is the integration of the ground acceleration times structural velocity which have often opposite signs. The integration of the values with opposite signs does not mean that there exists energy leaving the structure. The reduction in the input energy comes from the nature of the drop in the kinetic or elastic strain energies those are independent of the ground motion terms. This is a pitfall that anyone should fall in at first glance on the energy time-histories.

The differences between the relative and absolute energy terms are detectable only in the input and kinetic energies as in Figure 2.8 (a) and (b), while the time-histories of the other energy components are not affected. It is also noticeable that the plastic energy does not exist at any time instance in elastic case. On the other hand, at the end of the motion, the kinetic and elastic strain energies diminish while the damping energy reaches to value equal to the input energy. This fact proves that, if the damping characteristic of the structure is increased (i.e. by providing additional damping devices) the energy imparted into the structure will appreciably change.

Affect of the variation of the damping characteristics of the structure is plotted in Figure 2.9. The Figure 2.9 shows how the energy time-histories of the energy components are affected from the deviation of the damping ratio for 0, 2, 5, 10 and 20 per cent.

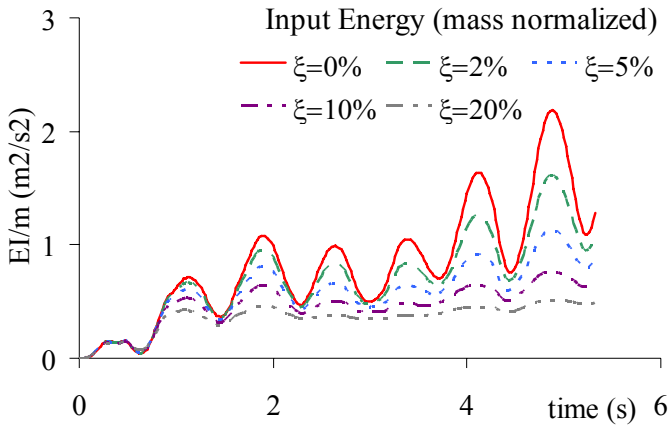

Figure 2.9. The deviation of the Input Energy for the different damping ratios for a SDOF system (T=1.5s) under Northridge Sylmar Hospital motion

The reduction in the Input Energy values with the increase of the damping is actually clear if the response of the structures lightly damped (meaning little resistance against seismic force) and heavily damped (meaning great resistance against seismic force) are compared. Based on the fact that the input energy term is the integration of the structural velocity times ground acceleration, it is obvious that the structure with higher damping will oscillate less then the structure with less damping.

As well as the viscous damping, the stiffness of the system is another structural property that affects the response of the system. While evaluating the response and the energy terms of the SDOF structures, the question of "how does the increasing the stiffness affect the response and energy terms?" arises in the mind right after the observation of the results by increasing damping coefficient. The input energy with normalized the mass is a good manipulation to see how the energy values through the motion duration change with increased stiffness. This is an important finding if the results of these energy time-histories are to be compiled in design spectra (Fajfar et al 1992).

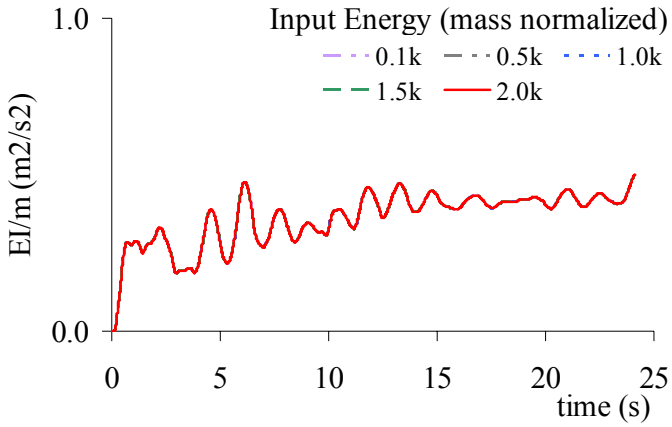

Figure 2.10. The deviation of the Input Energy for the increasing stiffness value for a SDOF system (T=1.5s) under Imperial Valley (El Centro) motion

The severity of the ground motions are generally represented by the peak value of the record. The most common indicator for the damage potential of the ground motion is the peak value of the ground acceleration (PGA). Since the damping and stiffness variations are studied on the input energy time-history of the elastic SDOF system, it would be convenient to scrutinize how increased PGA value challenges the input energy.

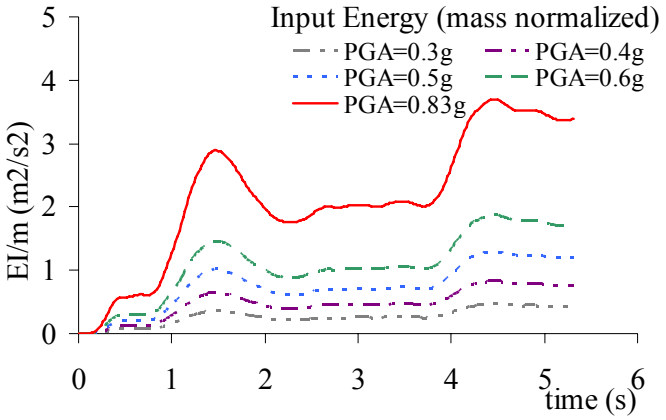

Figure 2.11. The deviation of the Input Energy with the increasing PGA value for a SDOF system (T=1.5s) under Northridge Sylmar Hospital motion

2.2.4. The Energy Terms in Inelastic Systems

The structure with prescribed yielding value (i.e. strength or deformation) may be excited by a strong ground motion that makes the structure exceeds its yield (elastic region boundary) point and goes into inelastic region whilst some permanent deformation occurs. This is a critical case in the earthquake resistant design of the engineered structures. Because, the world-wide accepted philosophy of earthquake resistant design allows the structure to have some permanent deformations (damage) at certain degree. A good expression of this philosophy is found in 1988 edition of the Tentative Commentary to Recommended Lateral Force Requirements (SEAOC Blue Book 1998):

"…Structures designed in conformance with these recommendations should, in general, be able to:

1. *Resist minor levels of earthquake ground motion without damage;*
2. *Resist moderate levels of earthquake ground motion without structural damage, but possibly experience some non-structural damage;*
3. *Resist major levels of earthquake ground motion having an intensity equal to the strangest either experienced or forecast for the building site, without collapse, but possibly with some structural as well as non-structural damage"*

Eventough the strength and deformation capacity of the structures must be provided against seismic actions, it is also known that there must be enough energy dissipation

capacity of the members in cyclic nature of the ground motion (Chopra, 2002; Clough and Penzien, 1995). The current design codes, implicitly, utilizes this requirement by means of the displacement ductility (Teran-Gilmore, 1996). This study aims to develop a good prediction of the seismic demand in terms of energy and, afterward, to recommend a design methodology for the estimation of the reinforcement in the RC columns against earthquake.

In case of the structure goes into the inelastic range due to the excessive seismic force, the relation between the resisting force (spring force) and displacement is not constant any more. Even, this relation becomes more complicated under the reverse-cyclic actions such as the seismic action. For the sake of being simple, the energy time-history computations in this section will be limited for the Elasto-Perfectly-Plastic (*EPP*) behavior model.

Nevertheless the inelastic behavior of the structure is prescribed; it is needed to specify an index that represents the level of the inelastic response. This index can be introduced as the ratio of the elastic spring force to inelastic spring force (yield force)- R force reduction factor, or ratio of the maximum displacement to yield displacement -μ displacement ductility, in order to compare the time-history results. In this study, the displacement ductility level which is assumed as more rational parameter then reduction factor is taken into the evaluation of the energy components.

The earthquake forces exceeding the yield force capacity of the members create permanent deformations (damages). It is known that some portion of the energy imparted into the structure is dissipated by these inelastic deformations. Therefore, inelastic systems have the same energy terms with the addition of the plastic energy, *EH*, (plastic or hysteretic energy). Figure 2.12 shows the time-history series of the energy components, alike to the Figure 2.8 for different ductility levels.

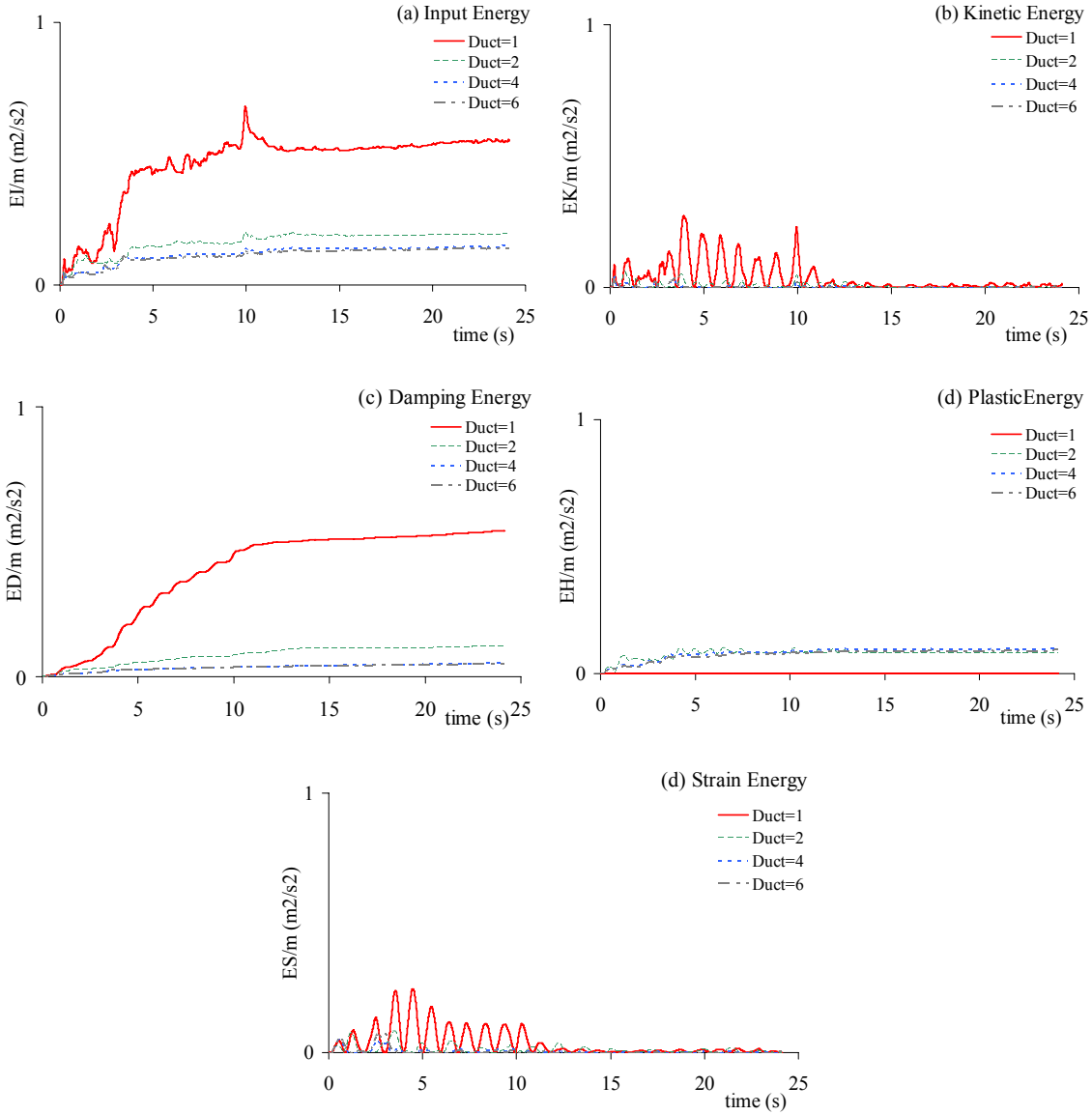

Figure 2.12. Time-history of energy components for inelastic SDOF structure with T=1.5s, ξ=5 per cent and μ=1, 2, 4, 6 under Imperial Valley (El Centro) motion (cont'd)

The distribution of the energy components at any time instance of the motion should be a good indicator to see the variation of these mechanisms. Figure 2.13 show these variations. As seen, the recoverable energy components (*EK* and *ES*) rapidly decay as the structure goes into the inelastic deformations where most of the imparted energy is dissipated by hysteretic and damping mechanisms (energies).

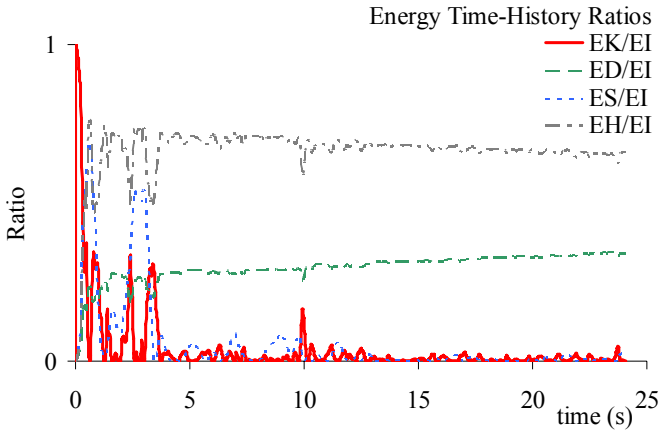

Figure 2.13. Time-history of ratio of the plastic energy to input energy for inelastic SDOF structure with T=1.5s, ξ=5 per cent and μ=1, 2, 4, 6 under Imperial Valley (El Centro) motion

The maximum ratio EH/EI occurs at the during the largest yield excursion at which the 20 per cent of the total hysteretic energy is dissipated, Figure 2.14.

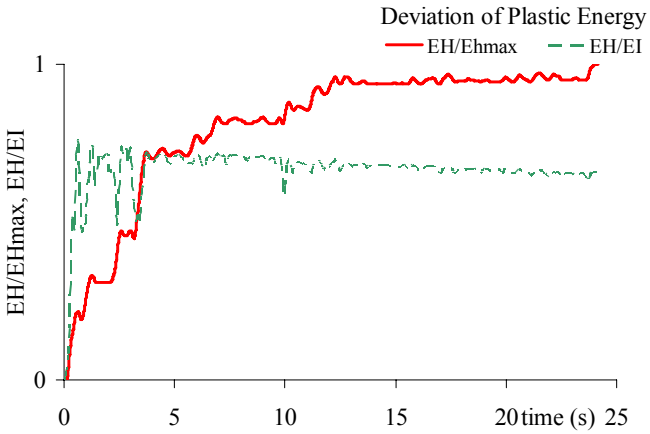

Figure 2.14. Time-history of ratio of the plastic energy to input energy and inelastic energy to total hysteretic energy for inelastic SDOF structure with T=1.5s, ξ=5 per cent and μ= 6 under Imperial Valley (El Centro) motion

The figure 2.14 also indicates that there's a difference between the maximum ratio of hysteretic to input energy ($\max(EH/EI)$) and the ratio of maximum plastic energy to maximum input energy ($EH_{\max}/EI_{\max}$). The ratio of $\max(EH/EI)$ presents the damage

potential of the largest yield excursion, whereas the ratio of $EH_{\max}/EI_{\max}$ reflects the damage potential associated with the total number of yield excursions.

The dissipation of the imparted energy is shared by damping and inelastic strain energies. It is assumed that should the damage of the members are needed to minimize, the damping characteristic of the system must be improve some by means of utilizing additional damping mechanisms in the structure. If the damping characteristic of the structure, which is assumed around 5 per cent for RC buildings and 2 per cent for Steel buildings, rises to 10 to 20 per cent, the share of the inelastic energy significantly reduces which is meaning less damage occurrence, Figure 2.15.

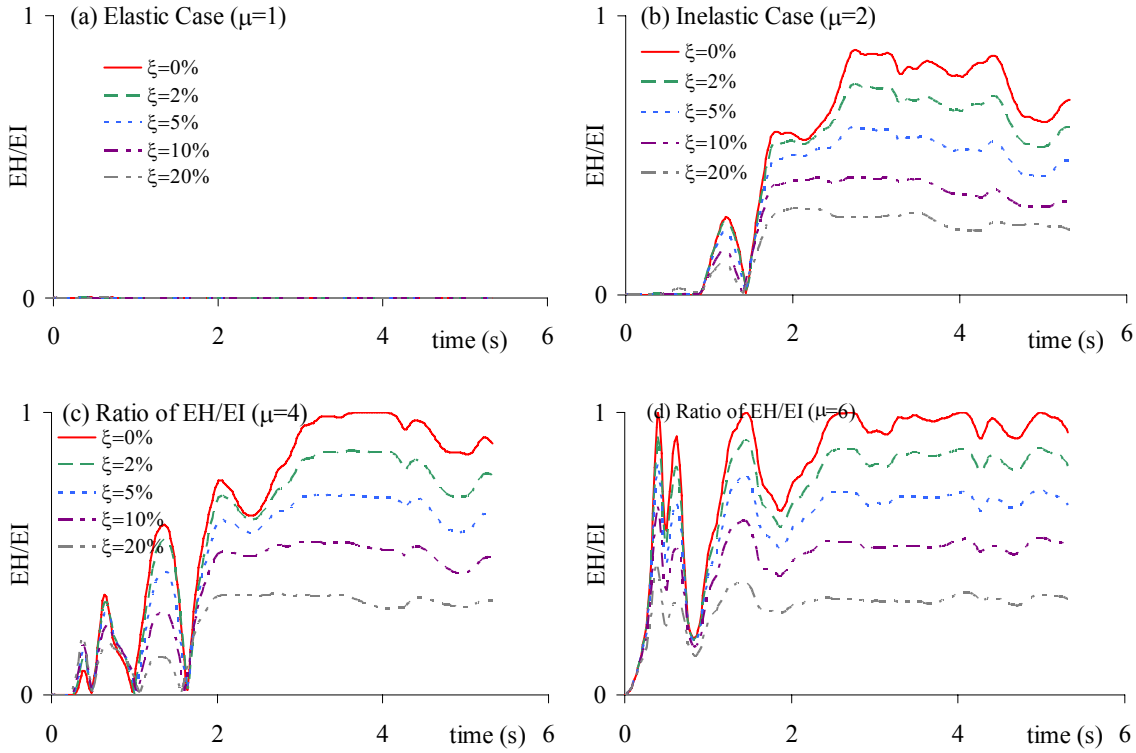

Figure 2.15.The decrease of the plastic energy as the damping ratio and ductility level increases for SDOF system with T=1.5s, ξ=5 per cent under Northridge Sylmar Hospital motion

The stiffness of the structure is inversely proportional to the deformation under seismic loads; the stiffer the structure (greater cross-sections), the less the deformation of the member. This fact confuses the researchers in which stiffness should be selected in the derivation of structural response study, i.e. response spectra. This confusion is solved in

the formulation of the energy components simply by normalizing the mass of the system. This solution brings the stable input and plastic energy time-histories as in figure 2.16.

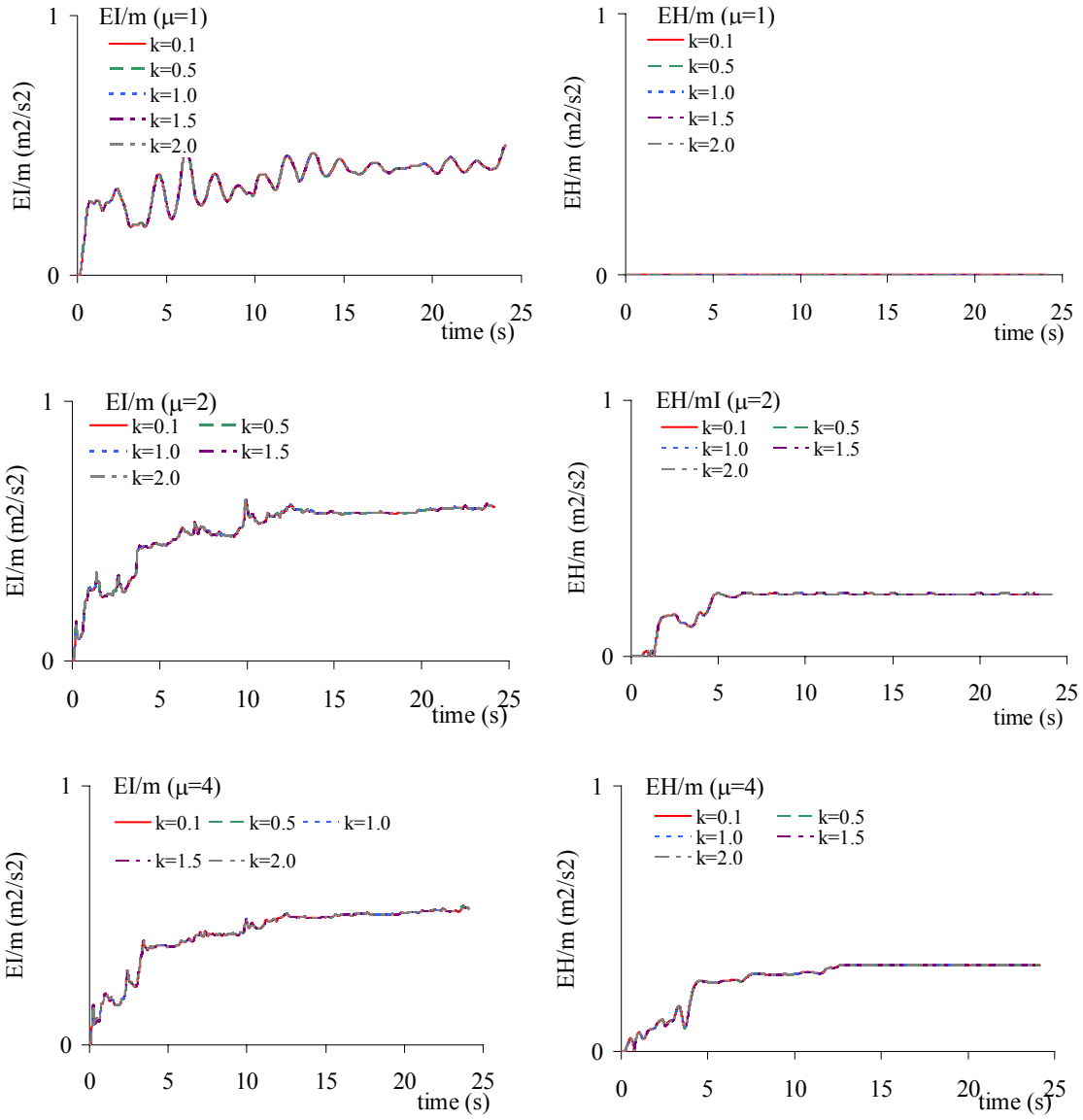

Figure 2.16. The mass normalized input and hysteretic energies of SDOF system with T=1.5s, ξ=5 per cent under Imperial Valley (El Centro)

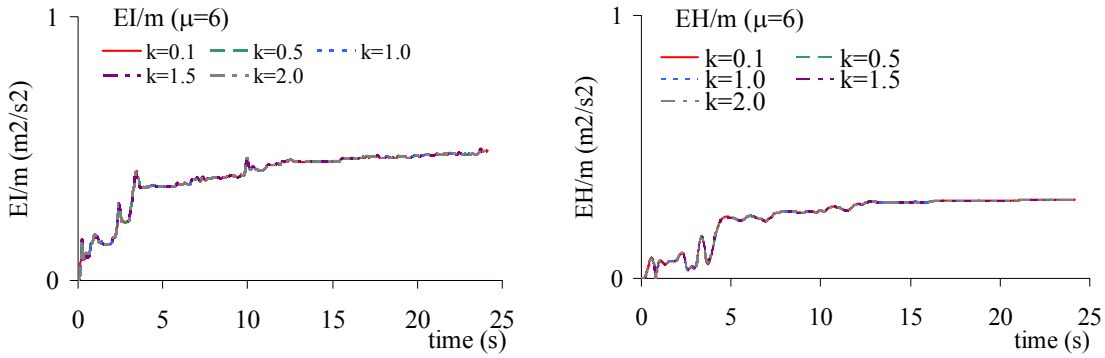

Figure 2.16. The mass normalized input and hysteretic energies of SDOF system with T=1.5s, ξ=5 per cent under Imperial Valley (El Centro) (cont'd)

The severity of the ground motion, hereby it's PGA of the motion; for elastic case was shown that it has proportional contribution to the input energy. If the contribution of the increased PGA value to not only input but plastic energy is studied, the expected results are obtained as in Figure 2.17.

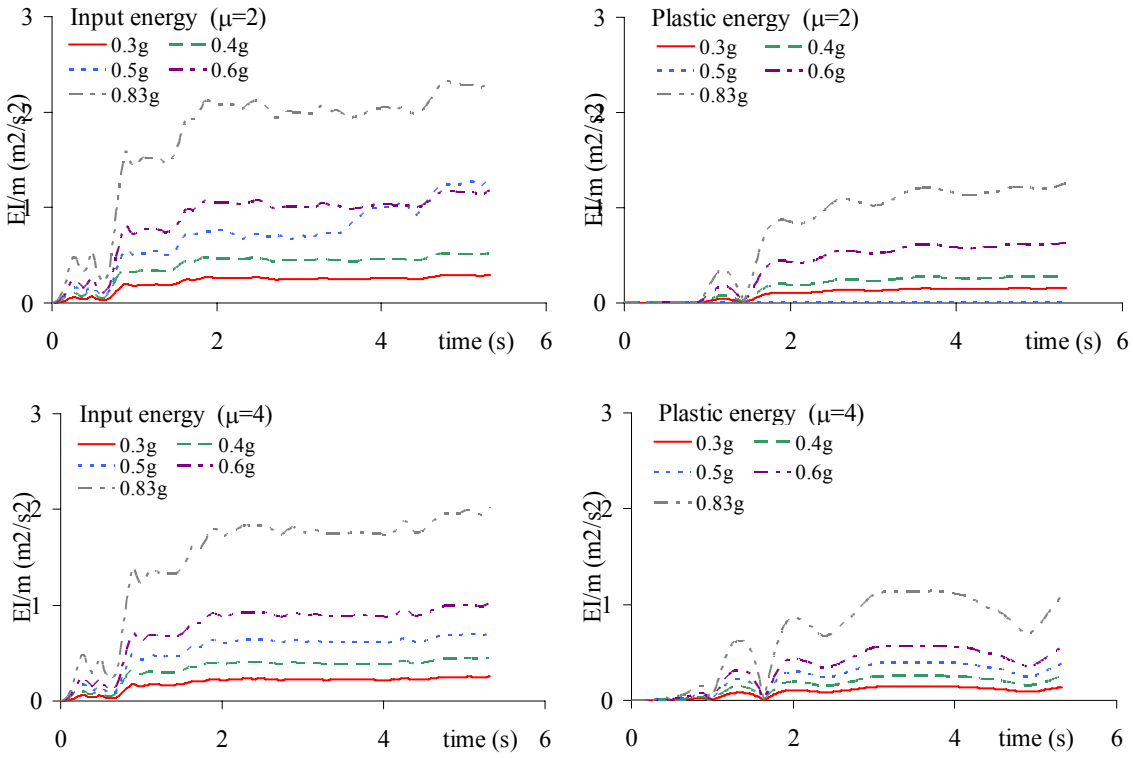

Figure 2.17. The increase of the plastic energy and the ratio of the as the damping ratio and ductility level increases for SDOF with T=1.5s, ξ=5 per cent subjected to Northridge Sylmar Hospital motion

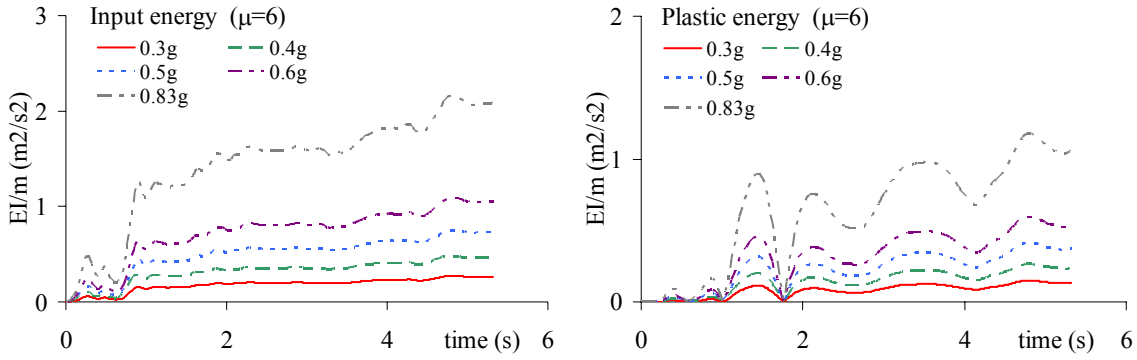

Figure 2.17. The increase of the plastic energy and the ratio of the as the damping ratio and ductility level increases for SDOF with T=1.5s, ξ=5 per cent subjected to Northridge Sylmar Hospital motion (cont'd)

However, it is interesting that the ratio of the hysteretic energy to input energy do not change by the increase of the PGA of the excitation motion, Figure 2.18. Therefore, this ratio should be accepted as good parameter in the prediction of the plastic energy (hysteretic energy) that is related to damage.

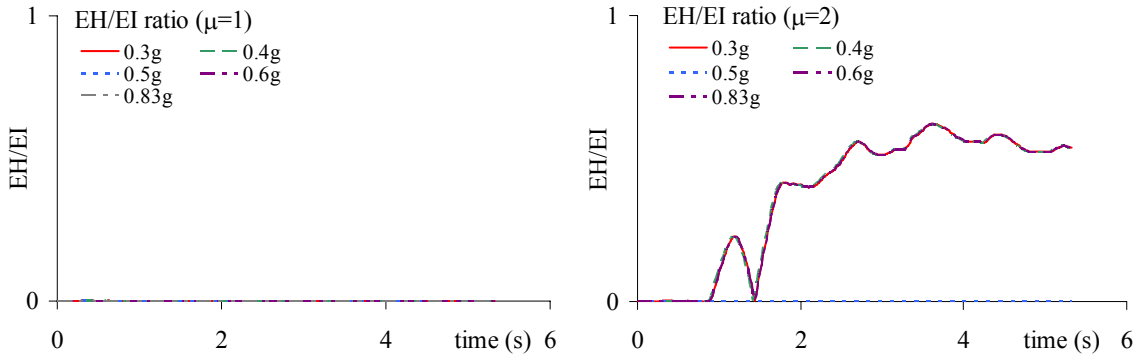

Figure 2.18. Ratio of the inelastic strain to input energy for different PGA values for SDOF with T=1.5s, ξ=5 per cent under Northridge Sylmar Hospital motion

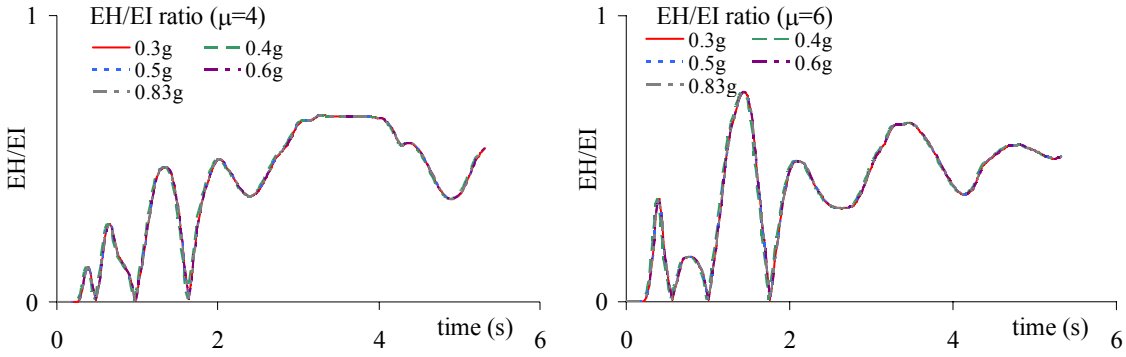

Figure 2.18. Ratio of the inelastic strain to input energy for different PGA values for SDOF with T=1.5s, ξ=5 per cent under Northridge Sylmar Hospital motion (cont'd)

2.3. Energy Spectra

Spectra concept in the analysis of the structures against seismic forces has been widely respected due to its practicability. A spectrum may consist of various parameters (i.e. viscous damping, seismicity, site conditions, ground motion type), hence, it covers a wide range of structures which makes it possible to illustrate many different cases or conditions. The most common used spectra in seismic analysis are the response spectra derived from the response of a SDOF system subjected to ground motion excitation. In point of fact, the response spectra, especially acceleration response spectra, are the basis of the current design codes: force and performance based design approaches.

Even though, the extreme seismic actions or the extreme structural response is in the scope of the earthquake resistant design, it is well known that these approaches ignores the valuable information found in the whole duration of the ground motion (Gupta 1990). This is utilized as the spectral values of energy components are taken at the end of the motion, whereas the values in response spectra are actually the absolute greatest numbers in response time-histories. Taking the extreme values in a response time-history may lead to wrong conclusions. Such a case happens for the two earthquake records whose elastic strength spectra are more or less similar, whereas their input energy spectra are very different from each other in magnitude, Figure 2.19 (Bertero and Uang, 1988).

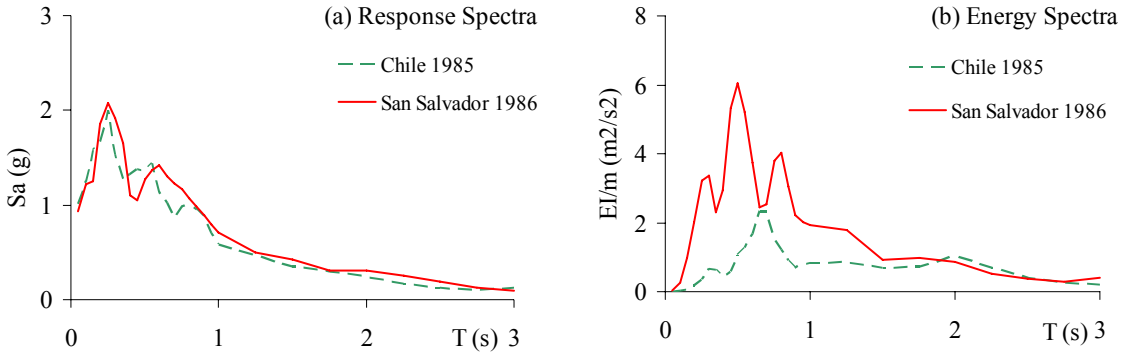

Figure 2.19. The difference between response and energy spectra of two ground motions (Bertero and Uang, 1988)

Figure 2.19 shows the advantage of using energy concepts in the seismic analysis of the structures. Because, the ordinates of a building with T=0.25 s natural period are almost same at the elastic acceleration response spectra which leads to compute the same lateral earthquake forces in the design of the members. on the other hand, the input energy spectra which takes the whole duration and frequency content of these two different earthquakes displays a great difference in their damage potential as the ordinates of T=0.25 s are definitely different. The interesting fact of these earthquakes relies on their duration and frequency content. As seen in Figure 2.6 and 2.7, Chile 1985 looks it lasted longer than San Salvador 1986 and also the Fourier Amplitude Spectrum plots show the frequency content of the Chile is richer than San Salvador. This valuable information is being lost in the compilation of the response spectra.

2.3.1. Introduction to The Energy Spectra

As mentioned in previous section, the whole duration and frequency content of the motion is taken into the account by means of using the energy components (*EI, EK, ED, ES, EH*) at the end of the motion, differing from the conventional computation of response spectra. While deriving the energy spectra, time-history analysis for a SDOF system under earthquake motion is conducted and the results are used in the energy formulations as given in Equations 2.8-2.13. Here, it's pretty straightforward the selection of the ground motions and the assumption of the structural properties, such as mass and stiffness distribution and hysteretic behavior of the system under reverse-cyclic action, do definitely

influence the energy components through the response of the structure. However, this is a fact that it has been respected in the derivation of the conventional response spectra.

In the case of elastic systems, the influence of the properties of the structure (stiffness, damping) and the ground motion record (duration, PGA) on energy components were explained in the previous section. If the ground motion creates lateral forces exceeding the yield level of structure, the inelastic behavior characteristics of the system plays an important role in the response and consequently the energy terms, especially in reverse-cyclic motions. The figure 2.13 displays the deviation of the energy terms in the case of inelastic behavior.

Contrary to the derivation of the elastic spectra (response and energy), inelastic spectra have been the one of the research topic for the researchers for the last 30 years (Fajfar et al., 1992). Two approaches have been developed by the time being; (i) reduction of the elastic spectra through the use of reduction factors, (ii) direct derivation of inelastic spectra through the statistical studies of the spectral obtained by the nonlinear dynamic analysis of structures subjected to the selected ground motions. The second approach that yields more accurate results was considered as the method of the future (Bertero et al 1988). In this study, by the improvement of the computers, the second approach was preferred in the derivation of the energy spectra. Even though the computational effort for obtaining the inelastic spectra is enormous; the developed computer program is able to complete such an analysis in hours. The details of the developed program (flow chart, parameters etc.) will be explained in the following sections.

2.3.2. Constant Ductility

The definition of being inelastic has been occupied the researcher for long time. Such a definition should be utilized with respect to many criteria. Among them, the most popular are based on the strength and deformation of the system.

In order to ease the understanding of the inelastic behavior level; a cantilever column example (SDOF) will be useful. An elastic cantilever column subjected to a seismic motion will response without any change in its spring force-displacement relation (stiffness). If the

same column is required to behave inelastic a border level (yielding) must be determined. Such an assignment of the elastic-inelastic behavior level will produce two ratios of maximum force or displacement to yield force of displacement. Figure 2.20 demonstrates how these ratios are found. The ratios of the forces are called as Force Reduction Factor, *R* and the displacements are as Ductility, μ.

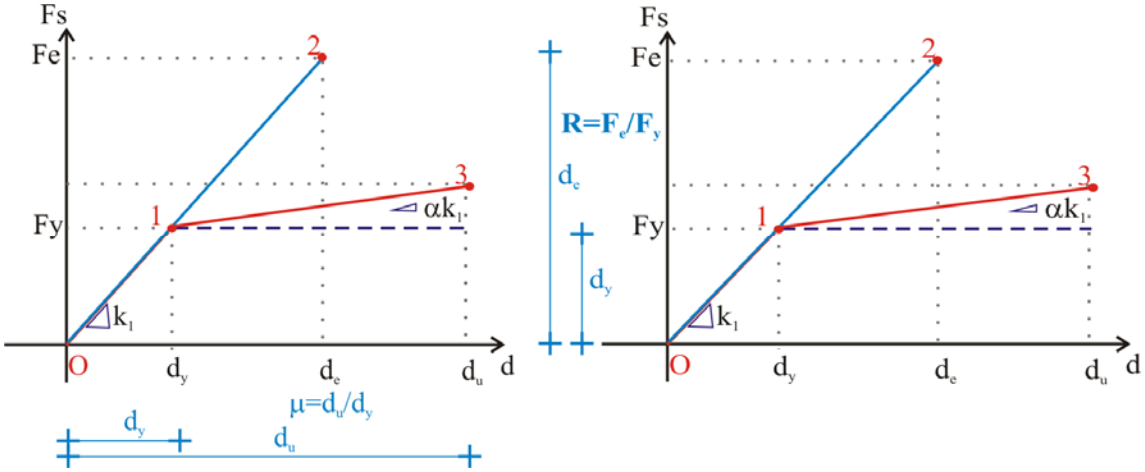

Figure 2.20. Definition of the inelastic behavior level of a SDOF system

In the development of the inelastic energy spectra, it was preferred to employ the constant ductility formulation. Eventough its computation is more time-consuming than the other, the information obtained from the dynamic time-history analysis is more useful. Because, after calculating the elastic demand force level of a particular ground motion from the SDOF system, the different reduced force levels will present the results only for different strength cases. However, the author of this study believes that the scrutinizing the different deformation levels of the systems will produce more accurate and comparable results, rather than force dependent results. Measuring the inelasticity of a member is obvious in sensing the change in the deformation of the system.

2.3.3. Developed Computer Program to Compute the Energy Spectra

Based on the constant ductility concept, a computer program was developed to perform a time-history analysis and then compute the energy terms with respect to the structural properties. The program does an iterative solution technique in order to reach the target ductility (Kunnath and Hu, 2004, Kunnath, 2008). Assuming the initial stiffness of

the system is kept same; the yield level of the system was arranged so that at the end of the motion, the ratio of the maximum displacement to the yield displacement is within a small tolerance range of the target ductility. If the yield level is taken high, resulting the less ductility, the yield level is decreased by the ductility level reaches the target value, Figure 2.21. Once the ductility at that iteration step remains in the tolerance limit of the target ductility (here it was chosen as 5 per cent of the each ductility level), it is assumed that the constant ductility condition is fulfilled for that particular ground motion record.

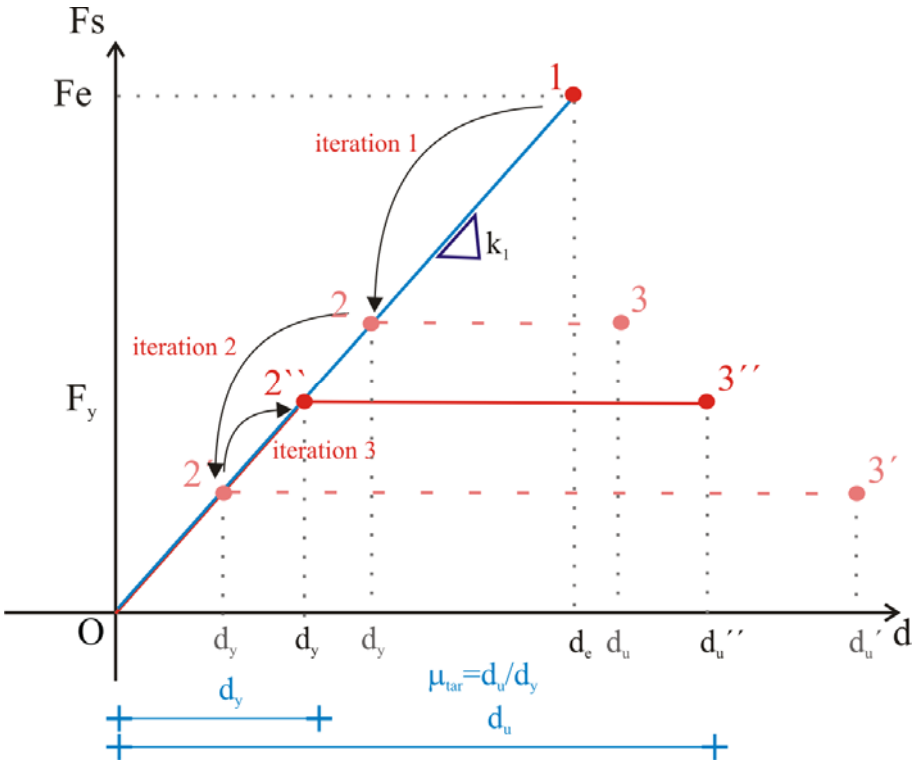

Figure 2.21.Iterative process for target (constant) ductility analysis

The developed computer program based on the constant ductility concept applies the same iteration procedure at every vibration period value ranged between 0.05-3.0 seconds. The selected vibration period covers the majority of the structures occurring in civil engineering. Figure 2.22 displays the flow chart of the developed program.

In order to obtain the time-history response of the SDOF system, reliable analysis software (engine) was used in the mentioned program. The time-history engine of the program was developed in New York State University at Buffalo (Reinhorn et al., 1994), IDARC2D. This program uses tri-linear moment curvature relation for the section properties which allow the user to implement not only strength and stiffness degradation

but also the affects of pinching. The constitutive models those employed in the development of different inelastic energy spectra will be explained in the following sections.

Embedding such a reliable engine into the developed program eased to conduct several parametric studies within the scope of this study. Having such practical analysis tool (combination of parametric input algorithm and solution engine) should lead to improve the findings of this study for the following researchers intending deal with the similar problems.

While considering the range of the ductility level, the constant ductility levels for the elastic and inelastic cases were taken as 1, 2, 4 and 6. Because it is believed that these ductility values represent the majority of the behavior of the inelastic systems. Taking greater values may not be reasonable as in the case of low strength values should not be provided with the practical engineering reasons.

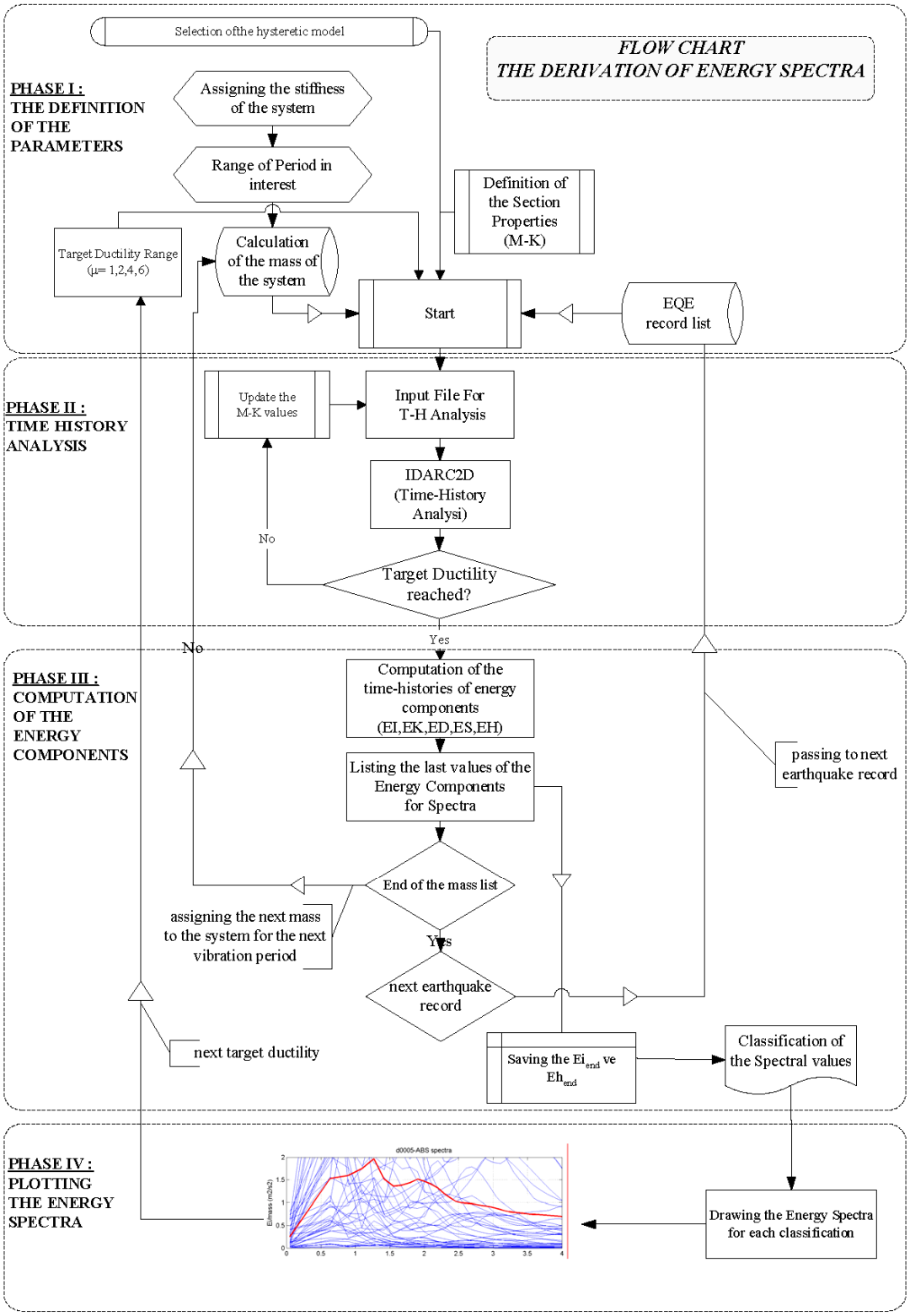

Figure 2.22. Flow chart of the Energy Spectra Program

2.3.4. Constitutive Models

The numerical constitutive models which have been utilized from the statistical studies of the tests results of various structural systems conducted in the laboratories have always been one of the major study topics for the researchers. The behavior of the identical systems under same load conditions may differ from each other just because of the settings of the test system or the quality of the material. The second one is particularly true for the identical Reinforced Concrete systems if the concrete used is poured different times.

Nevertheless, there have been three main parameters in the representation of the behavior of the RC and Steel structures. These parameters, α, β, γ, are used to define the degradation of the stiffness, strength and pinching of the system, respectively, Figure 2.23. The time-history computation program, IDARC2D, is able to use these three parameters in its constitutive models. Therefore, it is possible to describe various constitutive models (Clough, Takeda, Pinching etc.) in the determination of the energy spectra in this study (Reinhorn and Sivaselvan, 1999).

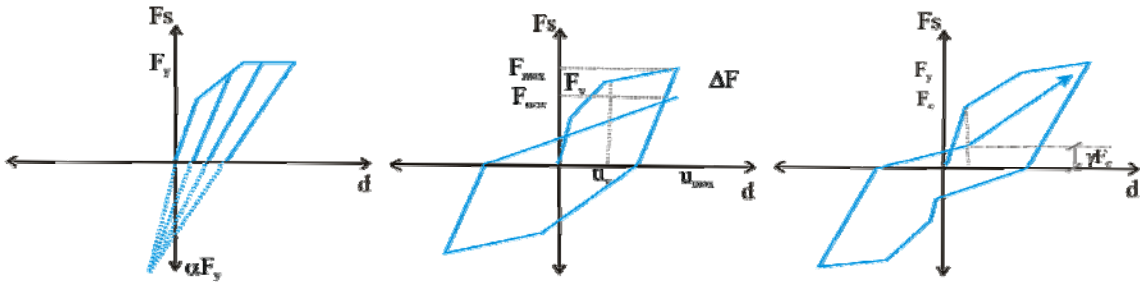

Figure 2.23. Control parameters for the three parameter constitutive models

In order to evaluate the influence of the constitutive model on the energy components of a structure subjected to seismic loading which is in reverse-cyclic and random magnitude nature, 6 different numerical models were considered in the analysis. Eventough the Elasto-Perfectly-Plastic (*EPP*) model is chosen as the reference model in most of the studies, it is convenient to employ the other models for the sake of predicting the energy components for the models representing RC and Steel structures.

The 6 constitutive models are actually classified into two groups; (i) flexural behavior, (ii) flexure with slip models. The first group, flexural behavior includes elasto-perfectly-plastic, bilinear with strength hardening, Takeda, Clough, while the latter group

includes Takeda with slip and Clough with slip. The descriptive schemas of these models are given in Figure 2.24.

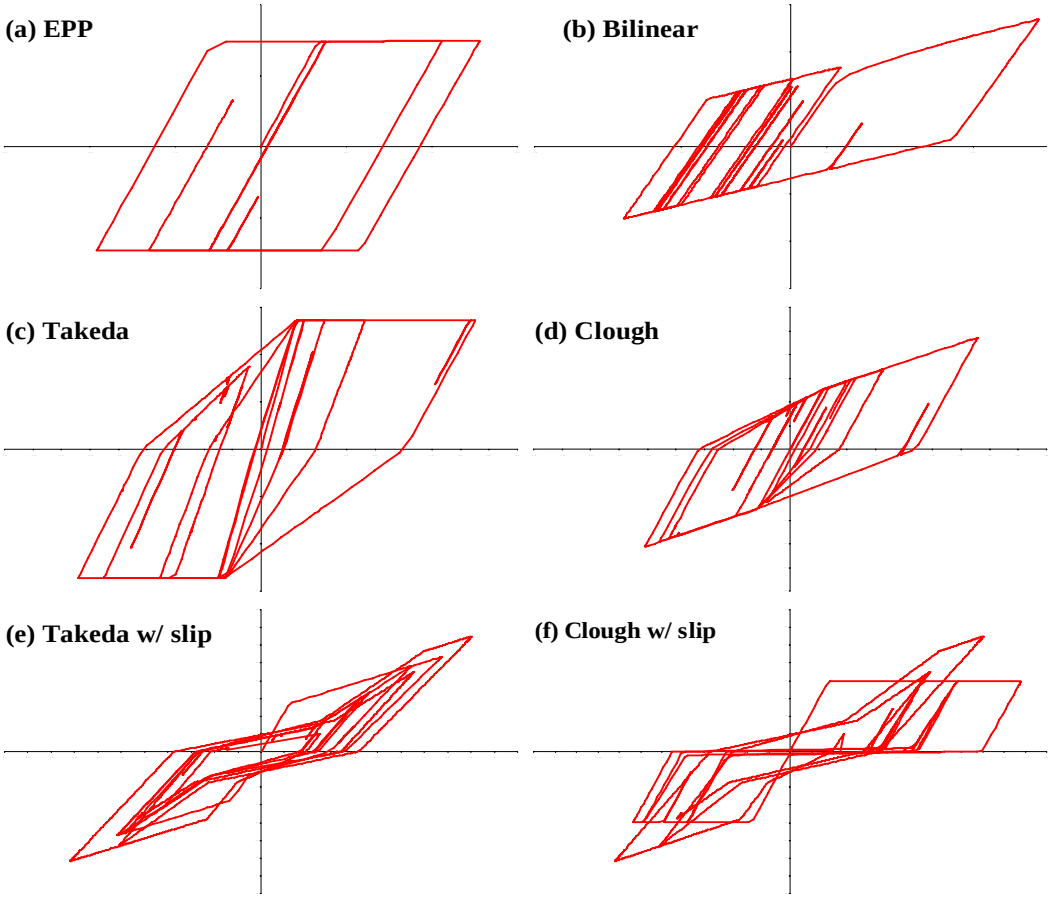

Figure 2.24. Constitutive models used in this study

2.3.4 . Energy Spectra of Different Constitutive Models

The advantage of using energy spectra instead of response spectra may be presented with the evaluation of the other reference earthquakes. Figure 2.25 shows the response and energy spectra of an elastic SDOF system.

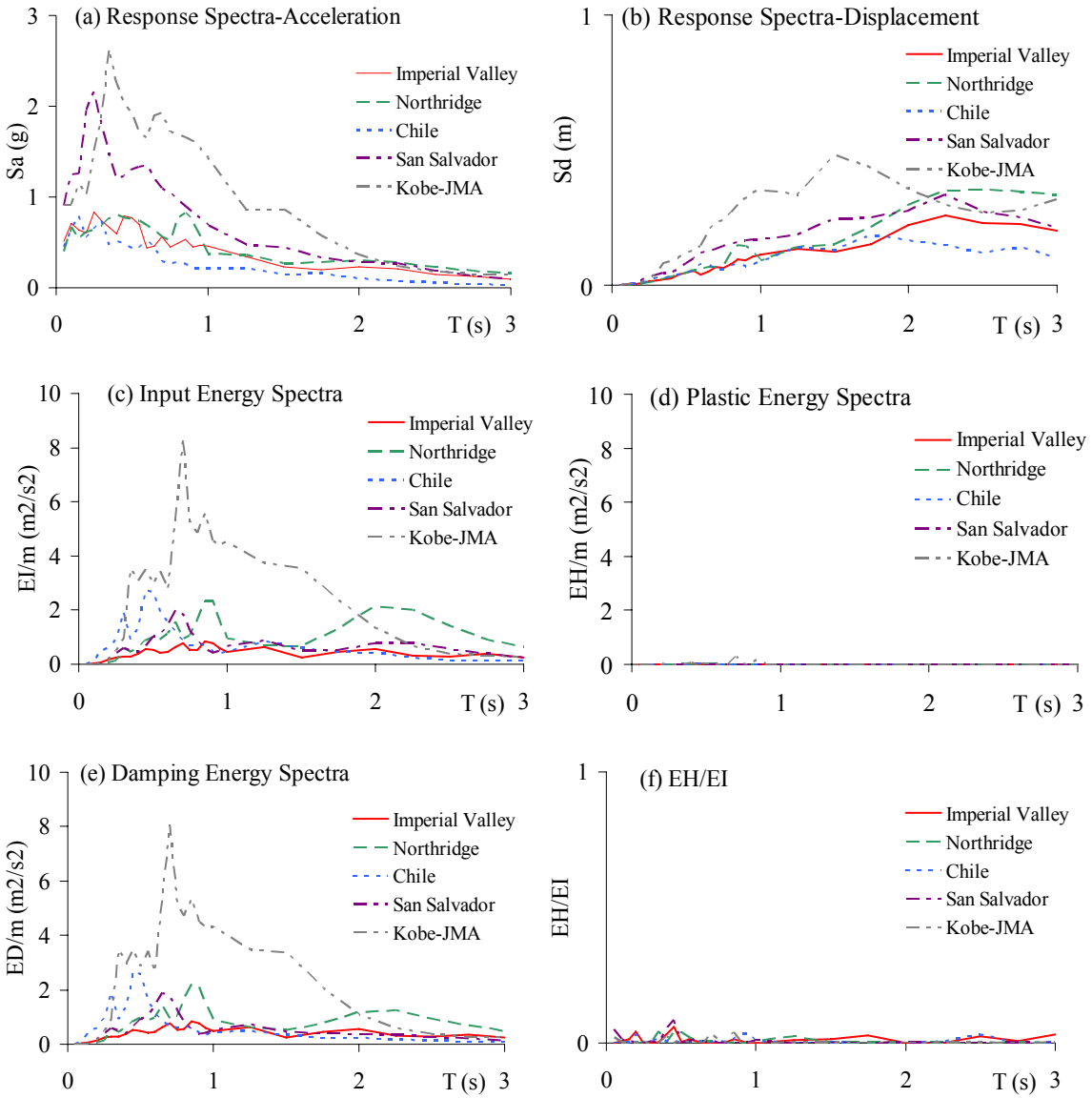

Figure 2.25. Elastic response and energy spectra of SDOF system (ξ=5 per cent)

Chile, San Salvador and Kobe have the highest strength demand for T less then 0.5s, while Kobe has the highest between 0.35 and 2.0 s. Eventough Chile, San Salvador and Kobe have the largest strength demands, it is seen that as come to the higher periods, the displacement demand and input energy imparted tremendously increases, while all other decreases. In the elastic case, all the input energy is dissipated by viscous damping. Therefore the plastic energy does not exist, while the damping energy spectrum is indeed equal to the input energy spectra.

As come to the inelastic behavior, the input energy is dissipated simultaneously by damping and inelastic strain energies. The Figure 2.26 shows how the response and energy spectra differ for different ductility levels.

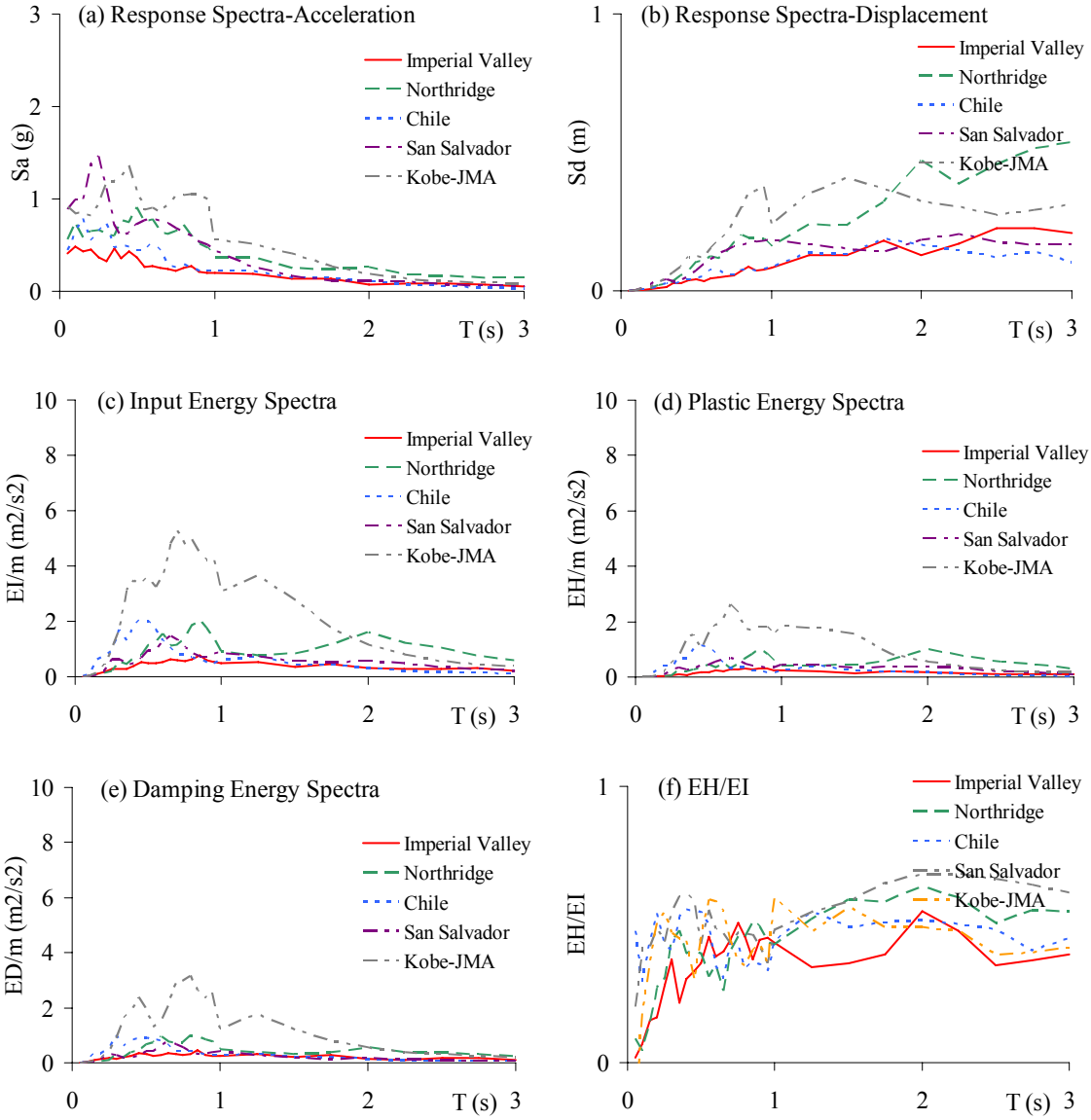

Figure 2.26. Inelastic response and energy spectra of SDOF system (ξ=5 per cent and μ=2)

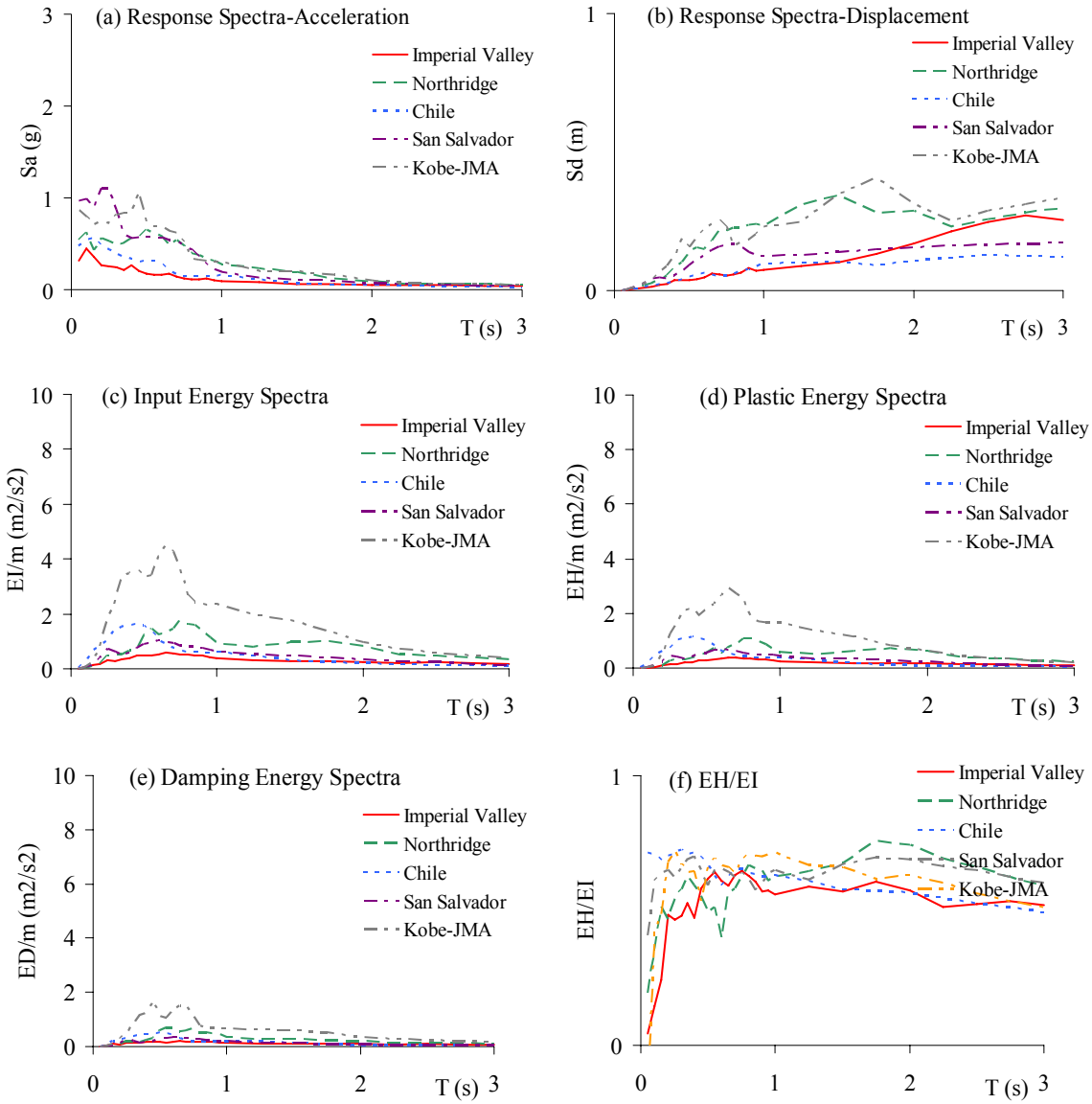

Figure 2.27. Inelastic response and energy spectra of SDOF system (ξ=5 per cent and μ=4)

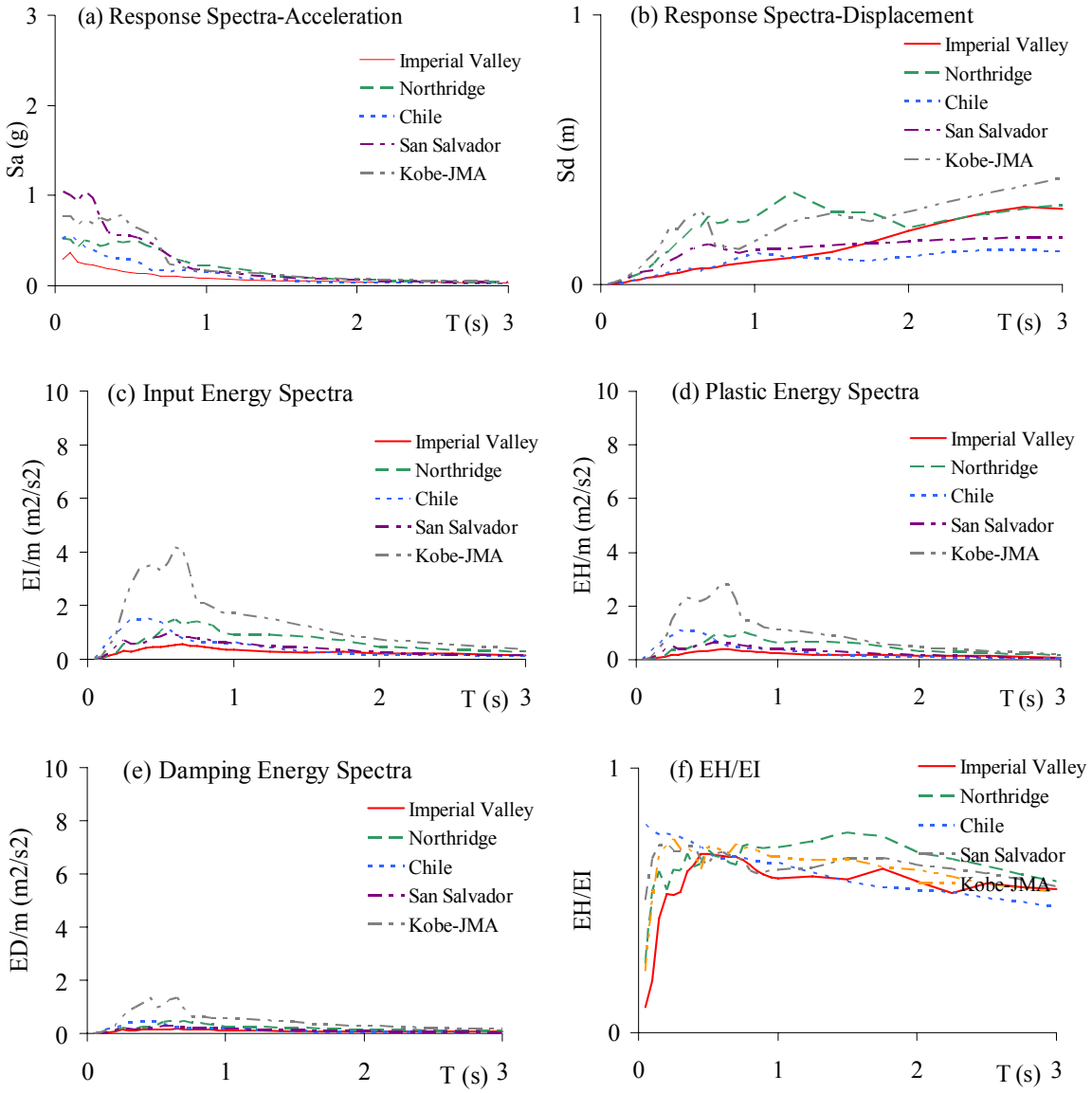

Figure 2.28. Inelastic response and energy spectra of SDOF system (ξ=5 per cent and μ=6)

The interesting fact of the Figures 2.26-2.28 is that as the ductility level of the system increases the almost all the spectral values of acceleration, displacement, input energy, plastic energy and damping energy decreases. However, the ratio of inelastic strain to input energy increases at the same time. This provides that as the ductility level of a system increases, the structure is expected to experience more damage even for the same motion. The damage of the system with higher ductility is likely more severe than the system with lower ductility because the strength of the system (yield point) was decreased in order to reach the target ductility level.

2.3.5. Influence of the Ground Motion Characteristics on Energy Spectra

For design purpose the ground motions can be classified by their severity, duration and frequency content. Eventough there are numerous methods to classify the earthquake motions, the following sections use the most common definitions.

2.3.5.1. Severity. The peak ground acceleration of the motion is the most common term used in the definition of the severity of motion. In the previous sections, the affect of the monotonic increased PGA of a particular motion was studied. Here, the affect of the same study will be carried for the different natural periods, eventually to see the change in the energy spectra, Figures 2.29-2.32.

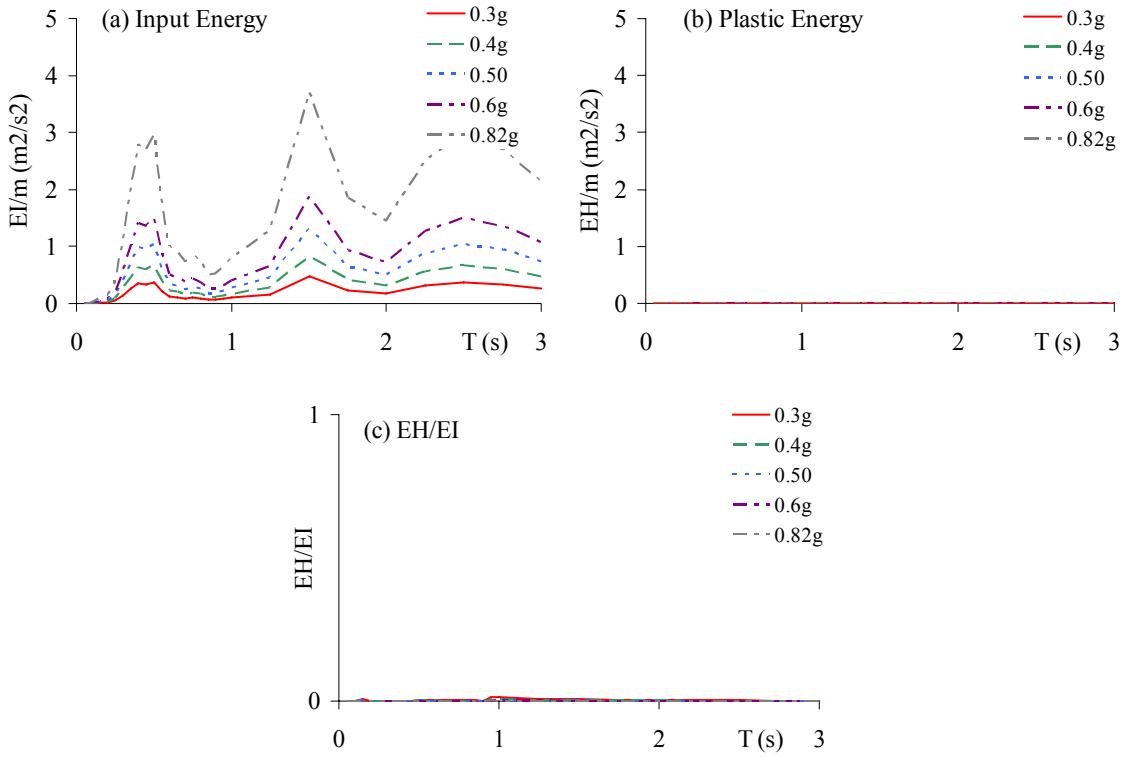

Figure 2.29. Response and energy spectra Northridge Sylmar Hospital motion (μ=1)

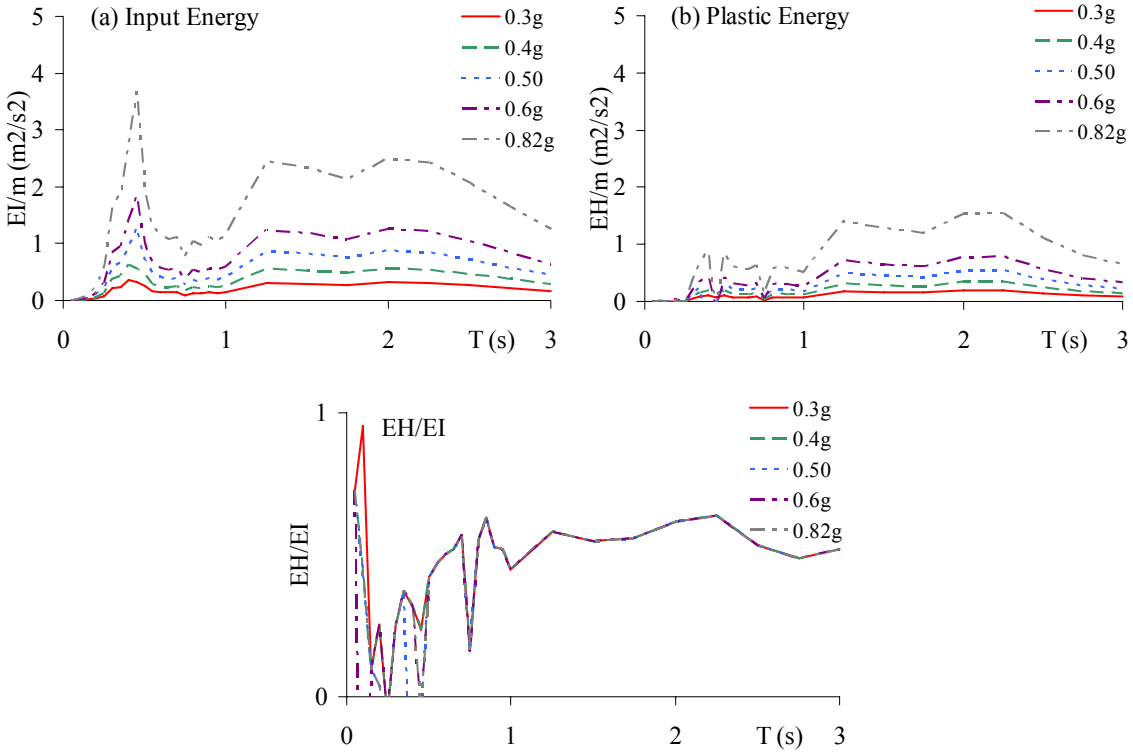

Figure 2.30. Response and energy spectra Northridge Sylmar Hospital motion (μ=2)

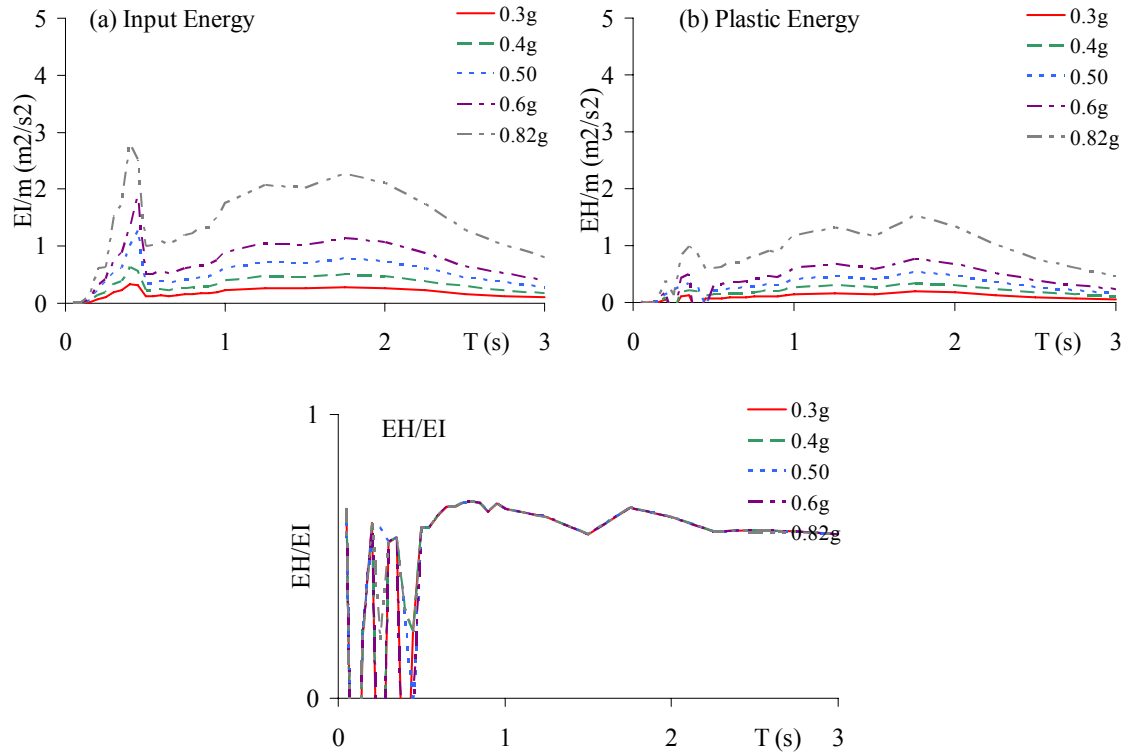

Figure 2.31. Response and energy spectra Northridge Sylmar Hospital motion (μ=4)

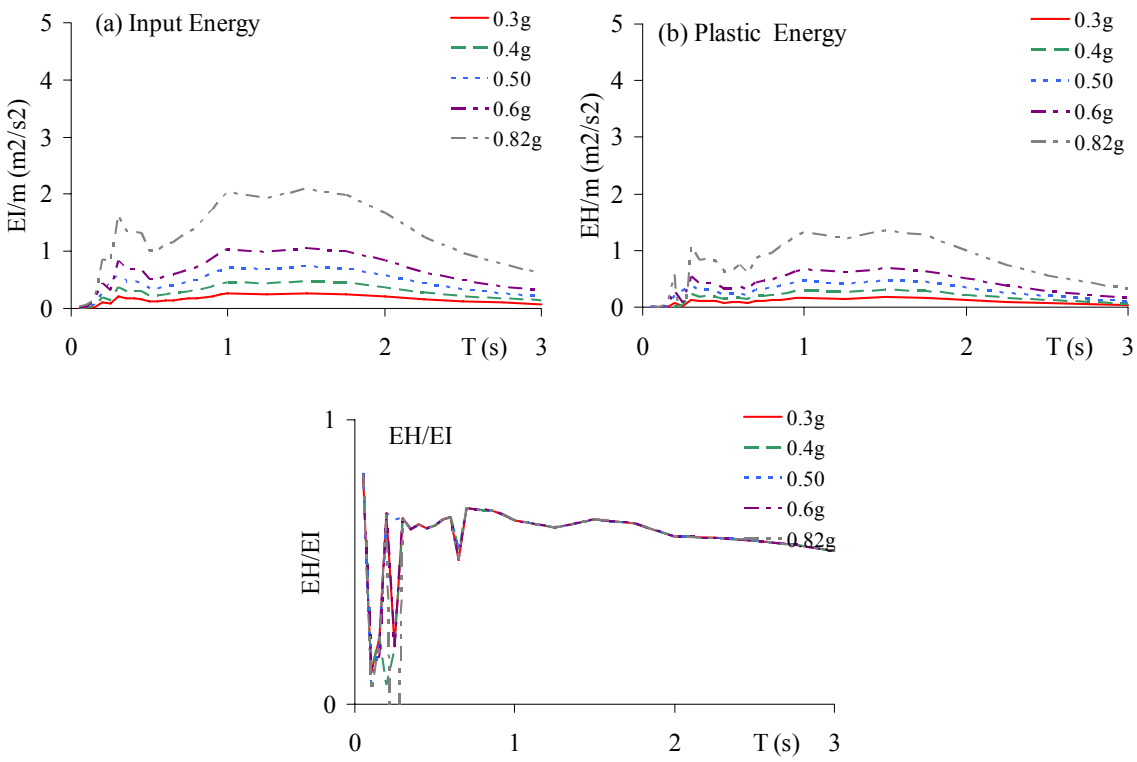

Figure 2.32. Response and energy spectra Northridge Sylmar Hospital motion (μ=6)

2.3.5.2. Duration and Frequency Content. One of the fundamental advantage of using energy concept in the seismic analysis relies on the fact that this approach takes the whole duration and frequency content of the motion in calculations, whereas, the basis of the current seismic codes do not This difference is likely observable in the comparison of Chile 1985 and San Salvador 1986 earthquakes. Having more or less same elastic response spectra and dominant period (Tp=0.25 s) Figure 2.19, the duration of these earthquakes are very different, durations of Chile 1985 and San Salvador are 116 s and 10 s, respectively, Figure 2.6. The similar difference exists in the comparison of the frequency content of the motion, Figure 2.7. However, the input energy and inelastic response spectra for ductility levels of 1 and 6 present the difference of these two earthquakes, Figure 2.33.

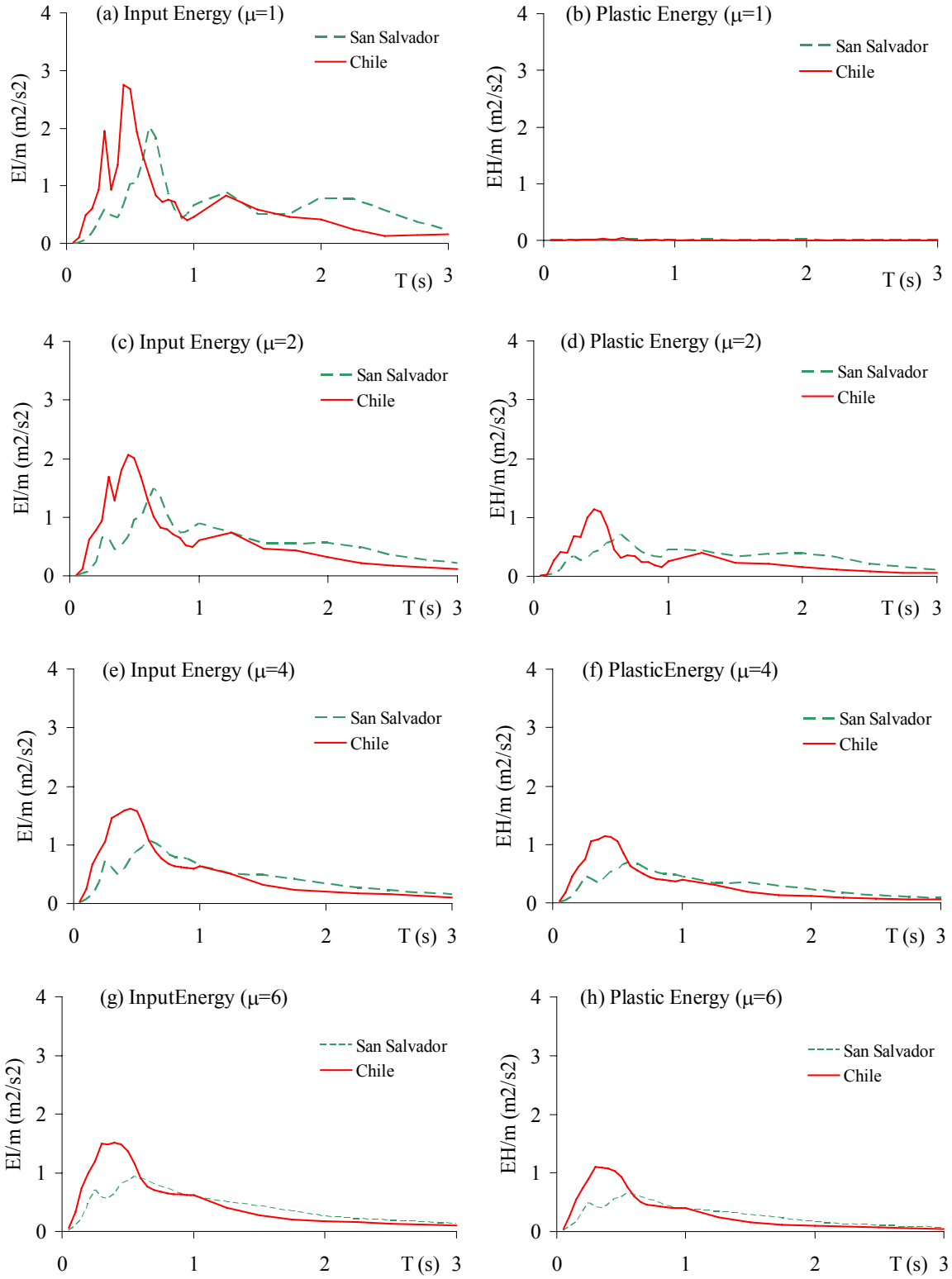

Figure 2.33. Influence of duration of the motion on energies (μ=1, 2, 4, 6)

2.3.5.3. Near-Field Effect. While developing the energy spectra for the analysis of the ground motion excited structures, the approach of direct derivation of the inelastic spectra through the non-linear time-history analysis of the selected earthquake records was considered rather than use of elastic spectra and reducing factors.

In order to conduct the non-linear time-history analysis, horizontal components of 114 station records (total 228 ground acceleration series- detailed in Appendix A) out preliminarily selected 416 records were filtered with respect to their peak ground acceleration (PGA) values. The PGA values of 188 records were either less than 0.15 times g or greater than 0.8 times g, due to the low and exaggerated damage potential, respectively. The common property of the all records is that they were recorded by the accelograms at free-field stations (on surface, single story light building).

The preliminary analysis on the energy spectra derivation shows that the selected earthquake records are needed to be normalizes according to a specific characteristic of the ground motion in order to have a basis for compassion of the time-history results. Therefore, all the selected records were normalized so as their PGA values are all assigned as 0.4g, which is the value with the greatest damage potential as given in Turkish Seismic Code (ABYYHY-2007).

The 228 motion records used in the derivation of the energy spectra are classified with respect to the soil class according to USGS which is also compatible with the classification in Turkish Seismic Code. Table 2.2 shows the shear wave velocity to a depth of 30m;

Table 2.2. USGS soil classification

Class	Limits of the shear wave velocity
A	> 750 m/s
B	360-750 m/s
C	180-360 m/s
D	< 180 m/s

The total number of the records selected for the soil classes of A, B, C and are 6, 82, 106 and 34, respectively. The reason of having comparatively less records in Soil Class A

is due to the fact that the ground motions records preferred from the free-field sites are limited for Soil A and increasing the number of records from other databases would have distracted the main aim of this study. On the other hand, unfortunately, using less motion record for Soil A may have led to the irregular results in spectral study. Thus, the number of the records for Soil A was kept as six.

The numbers of the earthquake motions according to moment magnitude and focal distance values are summarized in table 2.3 and 2.4.

Table 2.3. Distribution of records with respect to moment magnitude

Moment Magnitude	Number of earthquake
$4.0< M_w< 5.0$	32
$5.0< M_w< 6.0$	128
$6.0< M_w<7.4$	68

Table 2.4. Distribution of records with respect to focal distance

Focal Distance	Number of earthquake
$0.0 < D_f <5.0$	36
$5.0 < D_f <12.0$	70
$12.0 < D_f <30.0$	92
$30.0< D_f$	30

As seen in Table 2.3 and 2.4, there has been a better distribution of the records for other properties of the motion.

The damage potential of the selected earthquakes is also viable by their moment magnitude values (ranging from 4.0 to 7.4) which are considered as more reliable mechanical measure rather than Richter Magnitude (M_L), Surface Waver Magnitude (M_s), and Body Wave Magnitude (m_b).

The effects of the near- and far-fault type ground motions have been under the interest of the researchers because of variation of the motion records and consequently the

response of the structures. Near fault ground motions often contain significant waves (Bolt 2004). Especially the directivity effects of the near-fault motions dominate the horizontal motion and appear as pulses with single- or double-sided amplitudes (similar to sinus waves). This is visible in the record of the Northridge Sylmar-Hospital which has a distinct pulse in double-sided Figure 2.34.

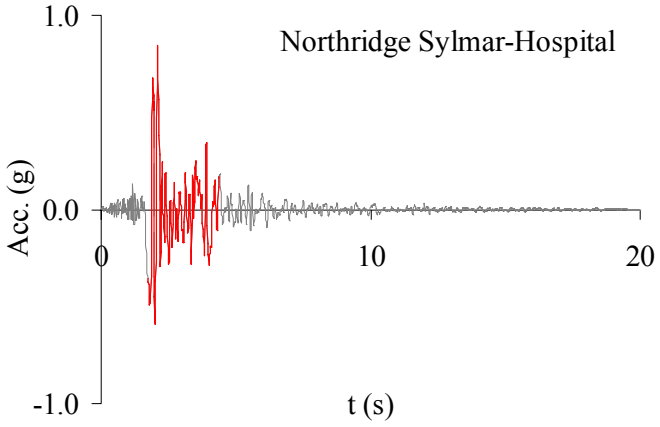

Figure 2.34. Near-fault effect example (double-sided pulse)

Bertero et al (1978) and Anderson and Naeim (1984) showed that near-field ground motions with pulses can induce dramatically high response in fixed-base buildings which is used in this study. Anderson and Bertero (1987) pointed out that the wide acceleration pulses are especially damaging if the width of the pulse is large compared with the natural period of the structure. This is observed in the energy spectra of the Northridge Sylmar-Hospital record, Figure 2.35. As the period of the SDOF system increases, the energy, which is the product of the ground acceleration and relative displacement of the system, imparted into the structure increases.

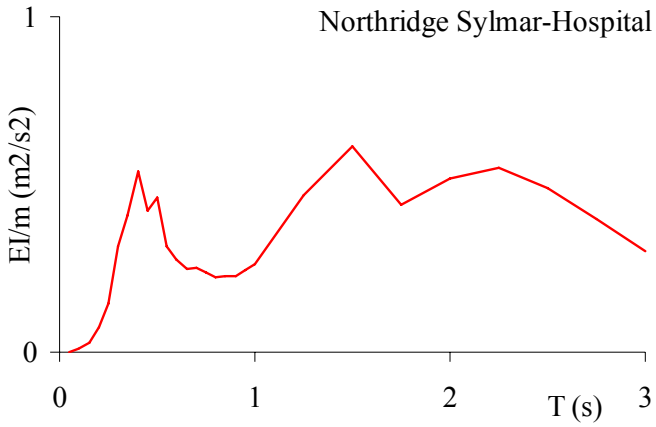

Figure 2.35. Near-fault effect on Input Energy Spectra (μ=1, ξ=5%)

Therefore it was needed to re-evaluate the selected earthquake records in order to avoid the near-fault effects on the energy spectra. It is known that the near-field ground motions with directivity effects tend to have high PGV/PGA ratio, which dramatically influences the response characteristics of the structures (Malhotra 1999). Based on this fact, the selected 228 earthquake records were re-analyzed and some records were excluded from the analysis results.

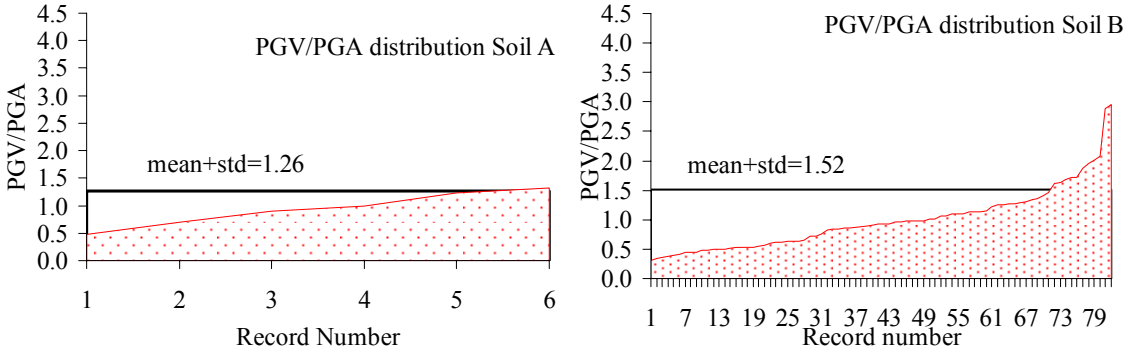

Figure 2.36. PGV/PGA distributions of the records with mean+std

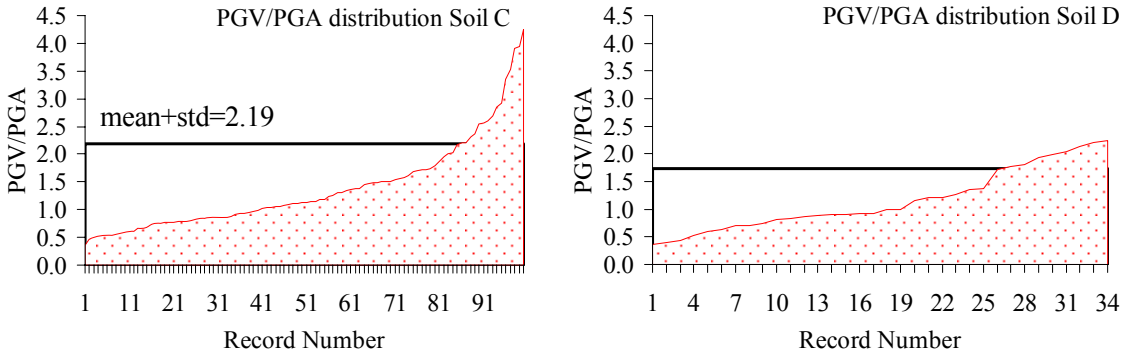

Figure 2.36. PGV/PGA distributions of the records with mean+std (cont'd)

While studying on the 228 records classified for four soil classes, many approaches and methods was attempted in excluding the inappropriate records, from simple eyeballing to very complicated motion and response indexes (RMS motion values, Housner and Arias Intensity etc.). Finally, a two-step approach was performed; (1) statistical evaluation (mean+std. level of PGV/PGA values) and (2) electing according to other ground motion parameter (Housner Intensity). Here, PGV/PGA value is directly correlated to the near-fault effects of the motions (Changhai et al., 2007). Housner Intensity which is the area under the pseudo-velocity spectrum between 0.1 and 2.5 seconds for any viscous damping value, gives an insight in the amplitude and frequency content of the response velocity that is the implicitly influences the input energy (Kramer, 1996). The formulation of the Housner Intensity (1947) is as follows

$$SI(\xi) = \int_{0.1}^{2.5} PSV(\xi, T)dT \tag{2.15}$$

After the exclusion of the records from the group of interest, there was a significant improvement in the form of the Input Energy Spectra, as seen Figure 2.37. As seen in Figure 2.37 (a), the Input Energy ordinates tremendously increase as the natural period of the structure increases as an effect of Near-Fault records. However, after the Near-Fault records excluded from the group of the motions, the trend of the spectral shapes becomes similar to the conventional response spectra. This similarity will be used in the formation of the smoothed design Input Energy Spectra recommended in this study.

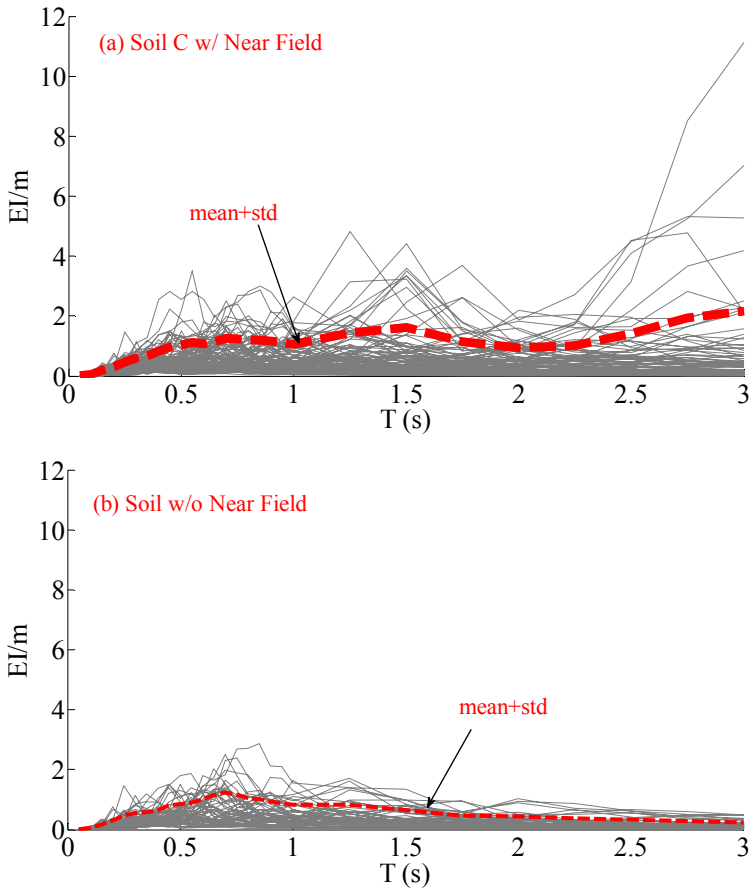

Figure 2.37. Input Energy Spectra for Soil C with and without Near-Field Records

The number of the earthquake records drops from 228 to 145 after the Near-Field and Pulse type records excluded from the second set of motions, as in Table 2.5.

Table 2.5. Number of the Earthquake Records used in the derivation of design spectra

Soil Class	Number of earthquake
A	5
B	66
C	53
D	21

2.3.6 Influence of the Structural Characteristics on Energy Spectra

The energy terms are calculated by using structural properties therefore any change in the structural property would immediately influence the energy response of the structure. However, by normalizing the energy terms with respect to the mass of the system give a chance to compare the influence independent more logically. There are two main structural property, stiffness, ductility and damping, are examined for a given earthquake records, Imperial Valley and Northridge, respectively.

2.3.6.1 Stiffness. The change in the stiffness on energy terms was studied in 2.3.3. Here the change of the stiffness will be studied how it affects structure having variety of initial periods, T=0.05-3.00 s. Figure 2.28 displays the deviation of the input and inelastic strain energies for the SDOF systems having different stiffness values.

For the same ductility level, the energy terms normalized with respect to the mass of the system do not deviate, Figure 2.38.

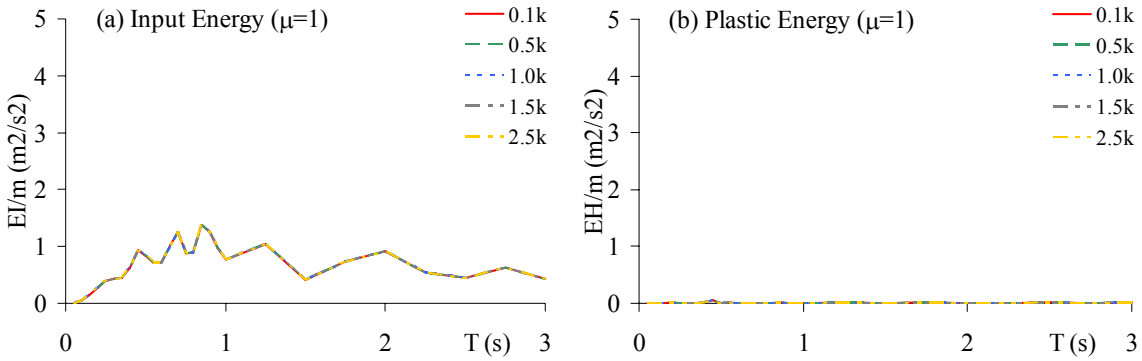

Figure 2.38. Influence of duration of the motion on energies (μ=1, 2, 4, 6) of the system under Imperial Valley (El Centro) motion

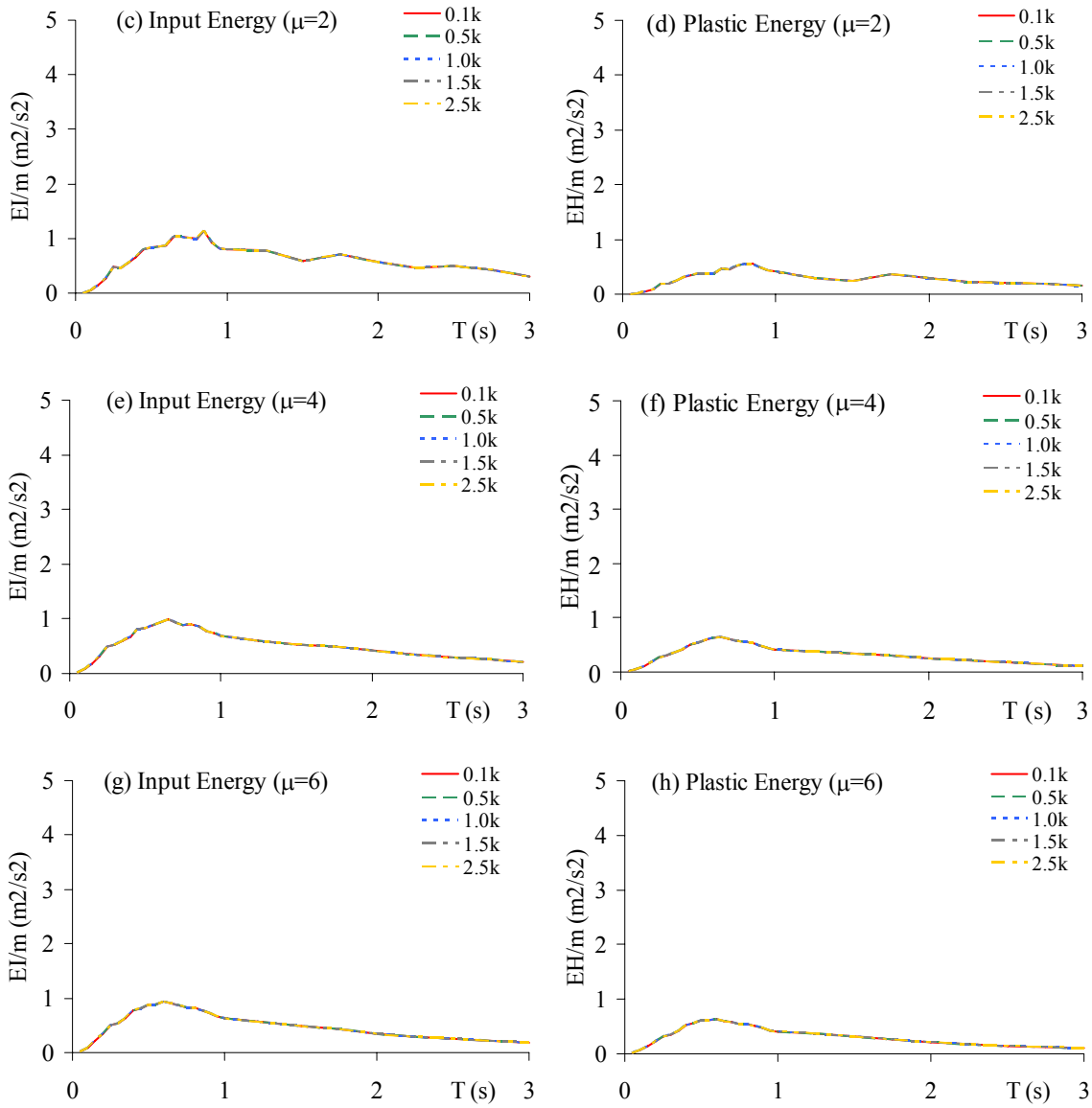

Figure 2.38. Influence of duration of the motion on energies (μ=1, 2, 4, 6) of the system under Imperial Valley (El Centro) motion (cont'd)

2.3.6.2. Ductility. All the spectra showed above displays the importance of the ductility level on the energy terms. The highest value of the energy terms are calculated for the elastic case (μ=1). However, it would be worthwhile to see the ratio of the energy spectra for higher ductility levels to energy spectra of elastic system in order to see at which period range the ductility change has strong influence.

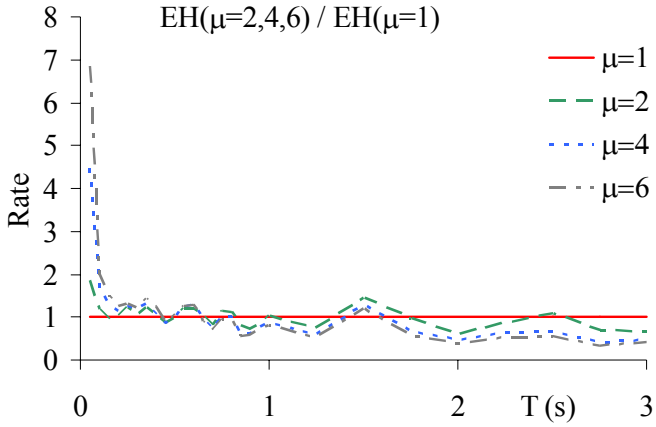

Figure 2.39. Ratio of the inelastic input energies to the elastic input energy of the system under Imperial Valley (El Centro) motion

Figure 2.39 shows the stability of the change of the ductility in terms of input energy. The ratio of the inelastic to elastic input energy changes in the vicinity of 1.5 and 2.5 second.

2.3.6.3. Damping. Damping and inelastic strain are assumed as the energy dissipation mechanisms in the structures. It was shown that that they are not recovered by the structure at the end of the ground motion. Therefore, the imparted energy is shared by these two dissipation mechanisms. Eventough it is assumed that the inherent structural damping is 2- and 5 per cent for steel and RC building, respectively, (Bruneau et al., 1997), this value can be increased by utilizing additional damping mechanisms. This section deals with the change of the portion of the input energy as the damping increases for a SDOF system subjected to Northridge Sylmar Hospital record. Figure 2.40 shows the influence of the damping on the structures at the same ductility level.

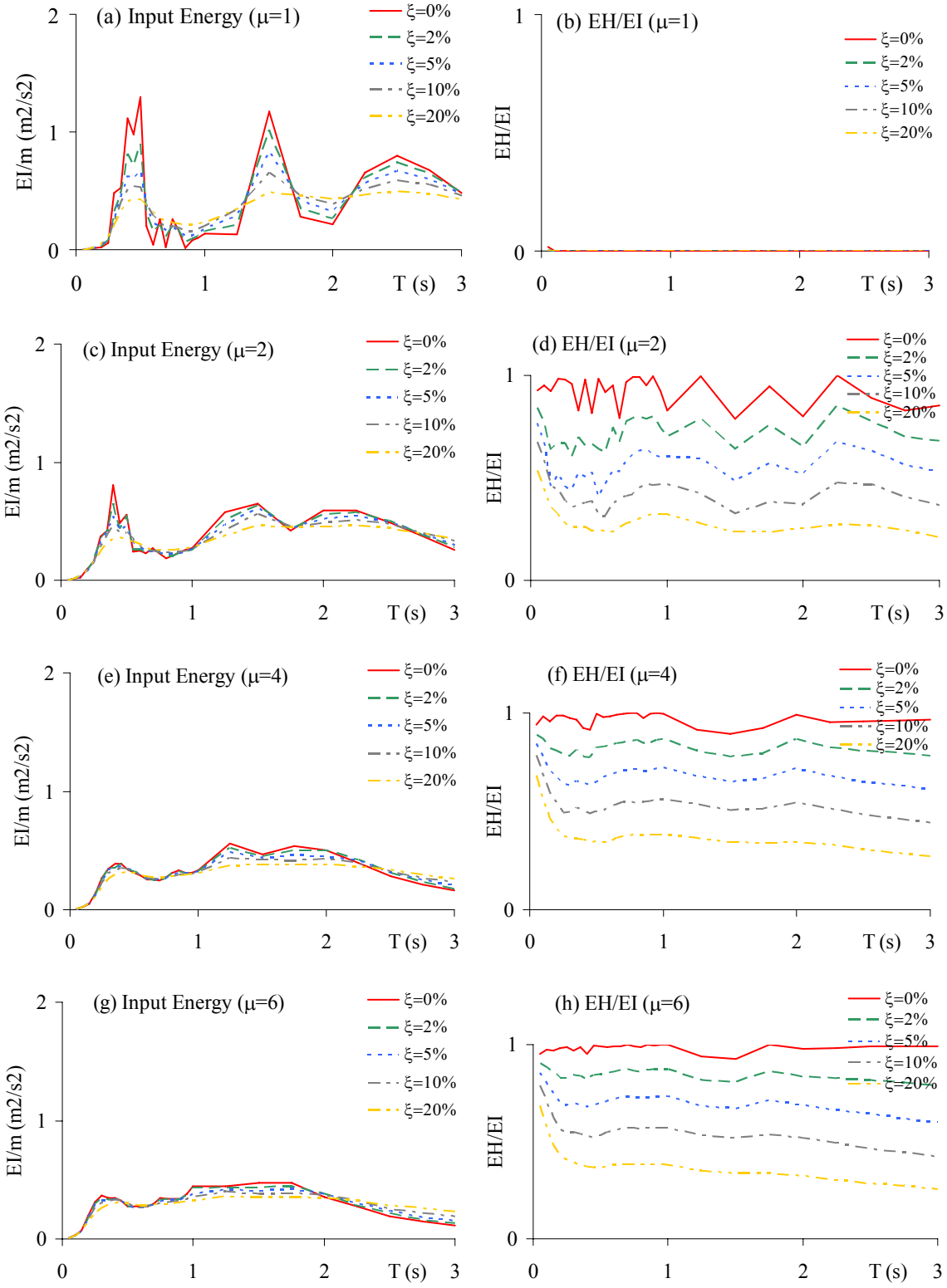

Figure 2.40. Influence of the damping on input energy and plastic energy of the system under Northridge Sylmar Hospital motion

2.3.6.4. Constitutive Models. Researchers have needed to develop mathematical models those represent the behavior of the structural elements (RC, steel or masonry) during the numerical studies. There have been several parameters to define the loading-unloading branches of the force-displacement curves. Among them, the three parameter mathematical models developed by Kunnath et al. (1997) reflect the influence of stiffness, strength and slip change (usually deterioration) have been preferred in this study and briefed in section 2.3.4.

During this study the influence of different constitutive models on the energy demand (input energy) and energy dissipation by plastic actions (plastic energy) was studied and the answer to the question of "which constitutive model should be used in the derivation of earthquake demand in terms of energy?" was sought.

In the case of elastic systems, there's not direct relation between the constitutive models and energy demand value of the structure. However, as come to inelastic behavior there is a strong relation between the input energy and hysteretic model. In section 2.3.6.2, the decrease in the ordinates of the spectra was shown as the ductility level increases for simple Elasto Perfectly Plastic models. However the in the case of different behavior models, the spectral shape of the input and plastic energy do not change only Eventough there are some significant deviation in the ordinates of the spectra. As an example, the input energy spectrum for soil A is shown in Figure 2.41.

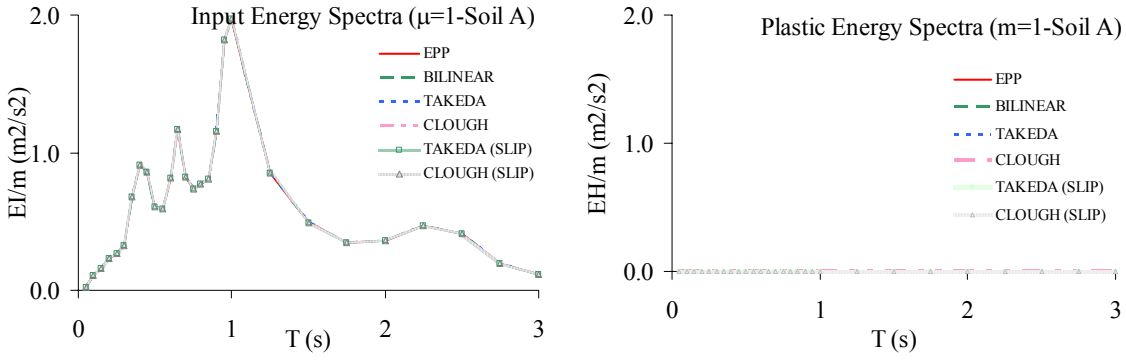

Figure 2.41. Input and plastic energy spectra for various constitutive models

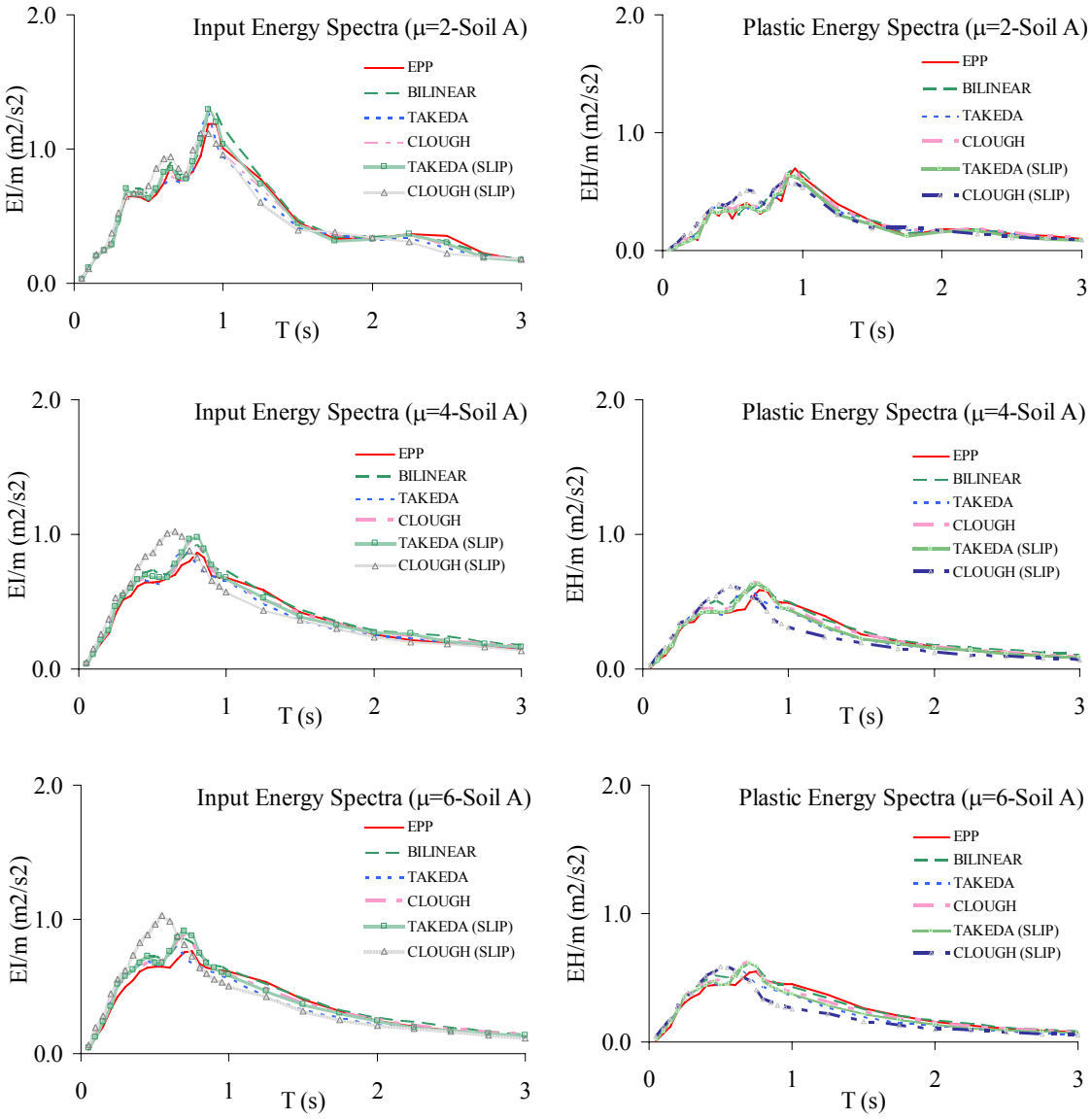

Figure 2.41. Input and plastic energy spectra for various constitutive models (cont'd)

As seen in the figures, there's not significant change in the shape of the spectra however the ordinates of spectral values between 0.5s and 1.5 s deviates. EPP model seems to stay lower than the other models, while the Clough with slip model shows obvious increase between 0.4s and 0.8s.

Similar deviations were observed in the input and plastic energy spectra for other soil classes which are given in Annex B.

Eventough the decrease in the ordinates of both input and plastic energy spectra, the more important indication of the influence of the constitutive model is found in the ratio of the inelastic strain to input energy values. Due to the constant ductility methodology, the strength of the system were arranged so that the SDOF system reaches the target value of the ductility on interest (μ=1, 2, 4 and 6). However the ratio of these two energy values gives a clear value in the evaluation of the energy dissipation due to the plastic deformations (damage), shown in Figure 2.42

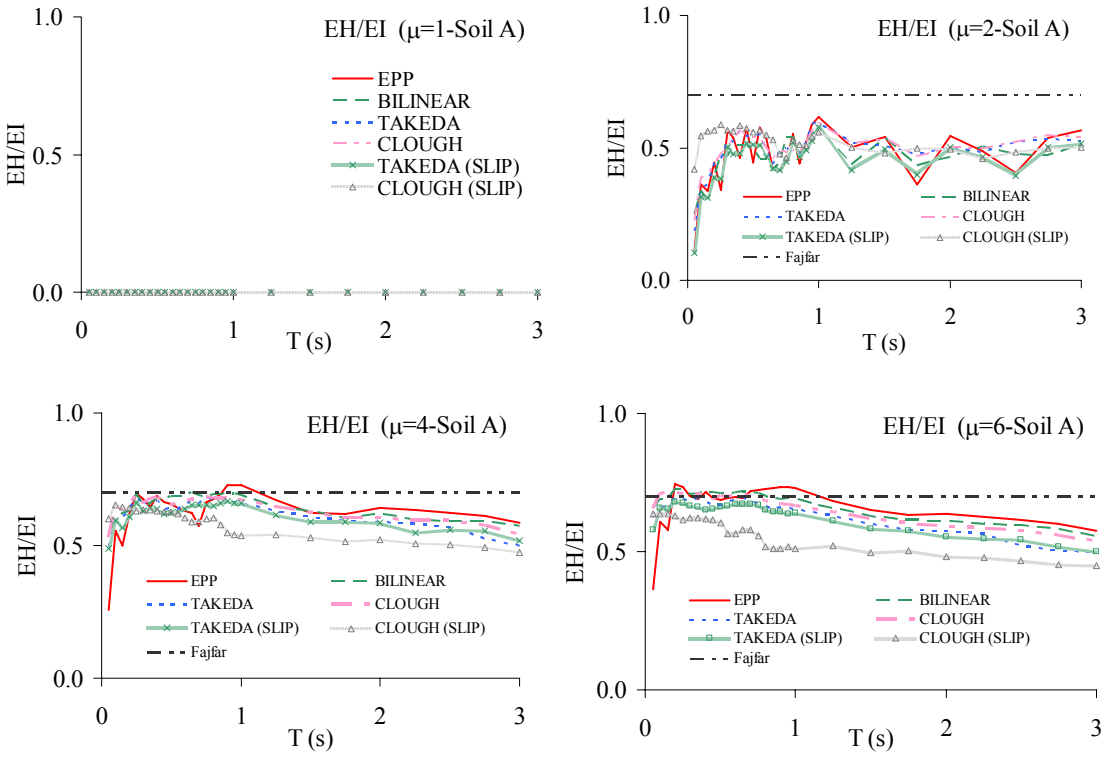

Figure 2.42. Rate of the inelastic strain to input energy for Soil A

The difference in the energy dissipation ratio is obvious for the shear dominated (slip) models compared to the flexural models, especially for μ=6 case. The Clough model with slip is separated from the others right after the 0.2s and kept as the lowest for the rest of the period range. The similar but slight separation is also observed for Takeda with slip model. On the other hand, the Elasto Perfectly Plastic model is almost the highest values as the ductility level increases.

Another interesting fact about the trend of the EH/EI ratio is seen in higher periods at the higher ductility; where it follows and declination trend. This fact should be explained by the response of the structure with high natural periods are more flexural compared to the structures with lower periods. Therefore, the portion of the plastic energy fairly drops. The similar trend was also observed in the other EH/EI spectra for the Soil B, C and D which are given in Annex C. The change in the EH/EI values for EPP model which is widely used in inelastic studies are depicted in figure 2.43 in order to sense declination due to less stiff response.

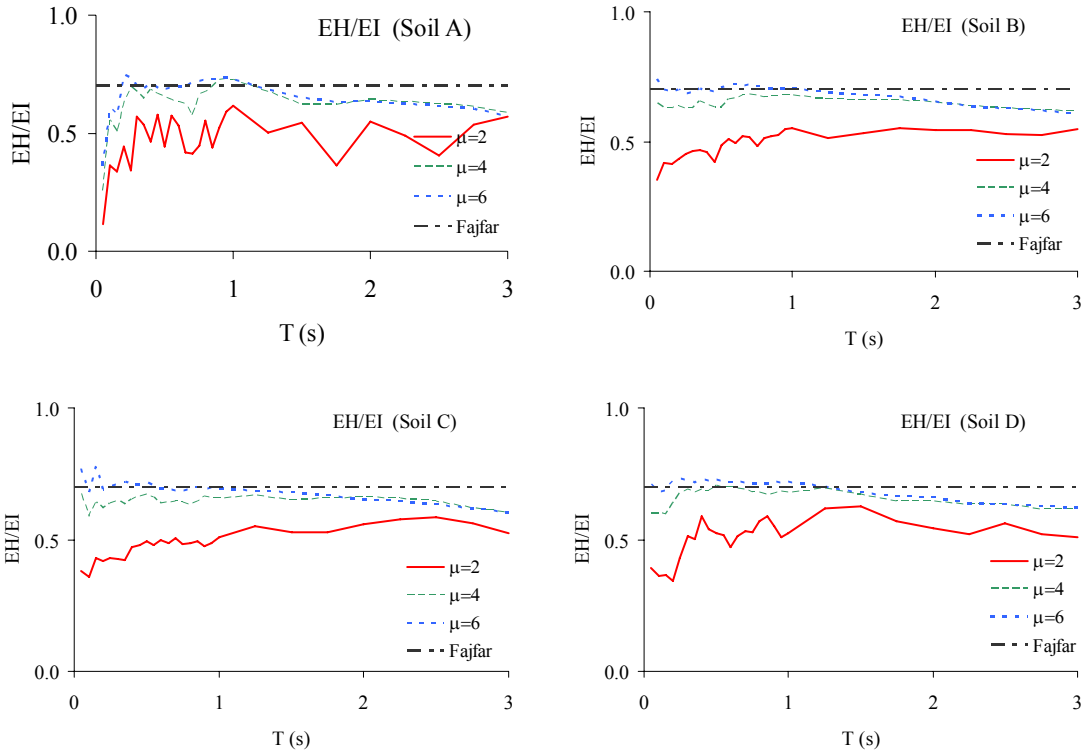

Figure 2.43. Declination of the EH/EI values for EPP model as the increase of ductility level for each soil

It is assumed that the Elasto Perfectly Plastic model is the most appropriate model in obtaining the design energy spectrum since it also covers the vulnerability weakness of the other models those may underestimate the damage potential.

2.4. Design Energy Spectra

Due to the random and erratic nature of ground motions, researchers have looked for the analysis methods those are the simple and accurate. The concept of spectra which describes the most of the terms (response, energy etc) is considered as the most convenient method. The force and performance based analysis-design methods take the spectra concept as the basis. Actually, not only the seismic forces but also all the random and erratic natural motions (wave, wind etc.) are described by means of certain spectra plots. The most common spectral relations in seismic analysis are function of viscous damping and natural period of the structure.

However, development of spectra that is to be used in the analysis and eventually in the design of the structure is still in the concern of the researchers, even though the design spectra have already been in the national seismic design codes. The reason of the discussion relies on the uncertainties of the characteristic of the tectonic plate movement and the probability of the returning of the severe earthquakes. It seems that the evolution of the design spectra in the seismic analysis for every seismic prone region is an endless work.

One of the aims of this study is to use the energy concept in the analysis and design of the structures. This aim brings the fundamental principle of the earthquake resistant design procedure. Bertero and Uang (1992) expressed this principle in a broad view, Table 2.6;

Table 2.6. Principle of earthquake resistant design

Demand	≤	Supply
on Stiffness Strength Stability Energy absorption and dissipation		of Stiffness Strength Stability Energy absorption and dissipation

The relation between the demand of the earthquake and the supply of the structure is not straightforward as seen in Table 2.2. The main difficulty behind this relation is the fact that prior to the calculation of the seismic demand of a structure, a preliminary design (detailing) of the structure should have been done, which means the supply is already

prescribed. The stiffness, strength and stability supply of the structure is evaluated against the demand of the ground motion which is somehow a function of the structural properties. Thus, it comes to an iterative procedure to accomplish a sound design of a structure. While conducting this iterative solution procedure for the inelastic cases, two parameters are considered at every step; ductility (μ) or strength reduction factor (R). However, the most of the inelastic design response spectra are derived from the elastic ones through the use these two dependent parameters. As mentioned above, the more realistic but also the most tedious method of deriving the inelastic design spectra, response of energy, is to compute the mean and mean plus one standard deviation of the Inelastic Spectra, again Response of Energy, corresponding to all time histories likely to occur for a region.

2.4.1. The Design Energy Spectra Proposed By Other Researchers

There is not any national seismic design code that accounts energy-based formulations, except in Japan. The Japanese seismic code employs an energy-equivalent velocity spectrum in the seismic design which was proposed by Akiyama (1985);

$$V_E = \sqrt{\frac{2E_I}{m}} \tag{2.16}$$

Here, E_I represents Input Energy and m is the mass of the system. Akiyama (1985) developed an equivalent velocity spectrum for SDOF and MDOF shear type frames and this spectrum have been the basis of the design codes, Figure 2.44;

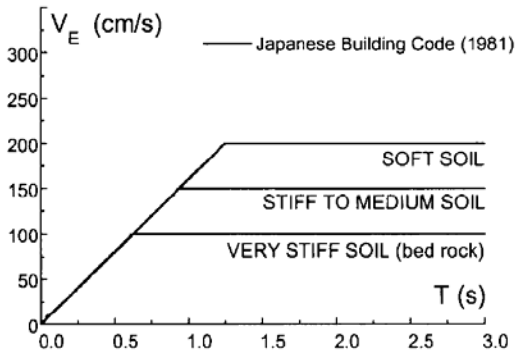

Figure 2.44. Design Energy input spectra in Japanese Building Code (1985)

The energy-based design spectra have been in development for the last 2 decades, because it's provisioned that the next generation seismic codes will include the terms of energy balance equation or its implicit results (cumulative damage vs. plastic energy), Krawinkler (1997). Eventough the energy spectra available in the literature have been kept as concept, the methods of using energy-balance equation in the performance analysis of the buildings (existing or new-designed) motivates the researchers on focusing the relation of energy terms with the strength, stiffness and the deformation of the systems.

Decanini and Mollaioli (1998) proposed an elastic earthquake input energy spectra after the analysis of 298 records for different soil properties. Decanini and Mollaioli showed that the proposed input energy spectra as function of period, soil type, magnitude, focal distance and viscous damping), Figure 2.45. The interesting term in the definition of the spectra is the value of *AEI(0-4)* which is the area of the input energy spectra. While calculating the ordinates of the spectra, this values of a, b, T_1 and T_2 and AEI(0-4) those were derived beforehand are used as in Table 2.7.

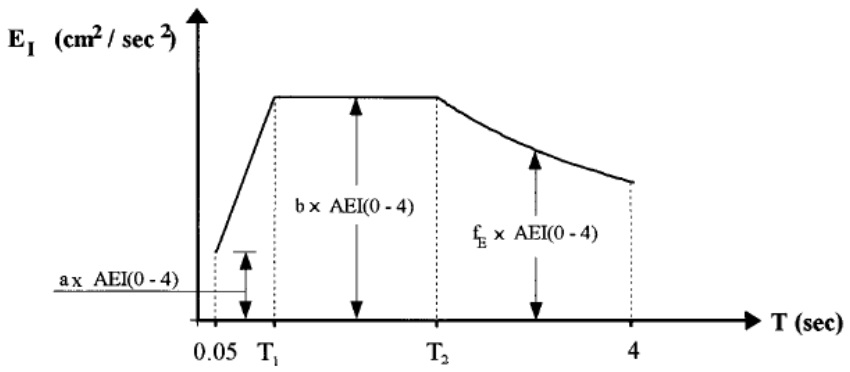

Figure 2.45. Input Energy Spectra proposed by Decanini and Mollaioli (1998)

Here the terms defining the spectral shape of input energy comes from the extensive statistical analysis of the ground motions (excluding Near-Field records), Table 2.7.

Table 2.7. Values of the spectral parameters for elastic systems

Soil Class	a	b	T1	T2	k	SSA(0-4)design
S1	0.30	1.00	0.10	0.50	0.80	1.720
S2	0.20	0.80	0.40	0.90	0.80	1.830
S3	0.10	0.60	0.70	2.20	0.80	1.966

Decanini and Mollaioli (2001) improved their study and proposed an additional method in the estimation of the input energy spectra for inelastic systems. They employed certain hysteretic behavior rules in nonlinear time-history analysis of energy terms and considered that the Elasto Perfectly Plastic behavior model is the more reliable model in accounts of input and plastic energy spectra. Figure 2.46 shows the spectra of the ratio of inelastic strain to input energy as a function of natural period of the system.

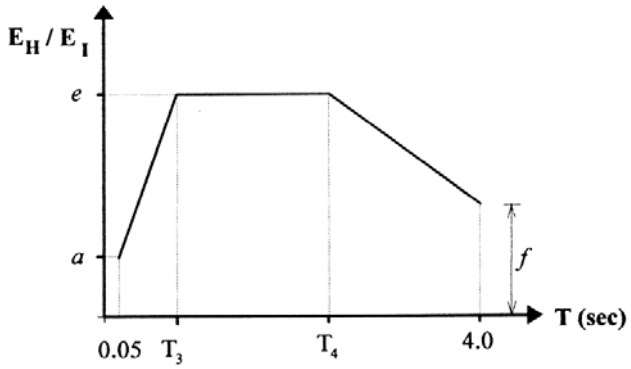

Figure 2.46. Design spectra of EH/EI proposed by Decanini and Mollaioli (2001)

Once again the terms in Figure 2.43 come from the statistical evaluation of the response of SDOF systems subjected to ground motion. Decanini and Mollaioli defined these terms for different soil classes and ductility levels of 2, 4 and 6 which cover the range of most of the frame buildings, as in Table 2.8.

Table 2.8. Parameters characterizing the design EH/EI spectra, EPP model, five per cent viscous damping

Soil Class	μ	a	e	f	T_3 (s)	T_4 (s)
S1	2	0.13	0.45	0.38	0.15	1.6
	4	0.25	0.62	0.47	0.15	1.0
	6	0.30	0.65	0.48	0.15	1.0
S2	2	0.10	0.48	0.40	0.30	2.0
	4	0.12	0.62	0.50	0.25	1.4
	6	0.15	0.66	0.52	0.20	1.2
S3	2	0.01	0.50	0.47	0.60	2.4
	4	0.03	0.65	0.60	0.50	2.2
	6	0.05	0.70	0.62	0.45	1.8

An interesting spectra proposed by Kunnath and Chai (2004) was based on the low-cycle fatigue analysis and correlated damage on the RC structures. They formulated an energy-equivalent velocity (eq 2.17) which is product of the PGV and an amplification factor. The amplification factor was compared to the proposal of Chai et al (1998) and formed as the combination of one straight line up to critical period and then decreasing branch, Figure 2.47.

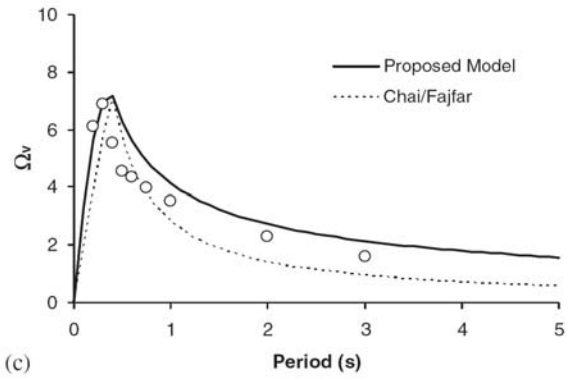

Figure 2.47. Design amplification factor for the energy-equivalent velocity Chai et al. (1998)

$$v_e = \Omega_v(\dot{x}_{g,\max}) \tag{2.17}$$

where the Ω_v is the amplification factor, $\dot{x}_{g,\max}$ is the peak ground velocity of the record. The amplification factor (Ω_v) is defined with respect to the critical period of the ground motion as follow;

$$\Omega_v = \begin{cases} \Omega_v^* \left(\dfrac{2T}{T_c} - \left[\dfrac{T}{T_c} \right]^2 \right) & ; \quad \mathrm{T} < \mathrm{T_c} \\ \Omega_v^* \left[\dfrac{T}{T_c} \right]^{-\lambda} & ; \quad \mathrm{T} > \mathrm{T_c} \end{cases} \tag{2.18}$$

here Ω_v^*, λ and T_c are the peak amplification factor, parameter of the spectral shape and characteristic period of the ground motion. The formulation of the T_c is to be used in the derivation of the design input and plastic energy spectra proposed in this study.

2.4.2. Comparison of the spectra

In earthquake engineering, the response (in this study it's energy) spectrum method is the most commonly used concept because it provides the designer with a rational and simple basis for specifying earthquake demand (Gupta, 1990). If a comparison is made between a time-history analysis of specific motion and response spectrum analysis of the same motion, it may not be clear whether the response spectrum analysis would do much better. However, designing a structure for a potential future earthquake, a spectrum method is much more relevant.

Therefore, while developing the earthquake demand in terms of energy, this study aimed to develop a design energy spectrum in the analysis of the structure apart from conventional strength or deformation view. However, it is worth to note that available database of strong ground motions is far from adequate and itself the major source of uncertainty in the earthquake-resistant design. Therefore, even the proposed design energy

spectra should be accounted as an approximate procedure in earthquake resistant design but with an exception of benefiting from the temporal information that is lost in conventional response spectrum procedures. This fact provides a strong meaning to the proposed design energy spectrum.

Prior to the evaluation of the energy spectra obtained from the aforementioned calculation methods in 2.1, it is necessary to check the reliability of the time history analysis results so far. This is best applicable by comparing the obtained elastic response spectrum of this study to the code based spectrum given in Turkish Seismic Design Code (ABYYHY-2007). The equivalency of the both spectra was validated for the seismic zone 1 (A_0=0.4g), Figure 2.48, whereas it is true for the other seismic zones. The response spectra of the ground motions were represented by the mean plus standard deviation of the max response accelerations obtained during the time history analysis in figure 2.47.

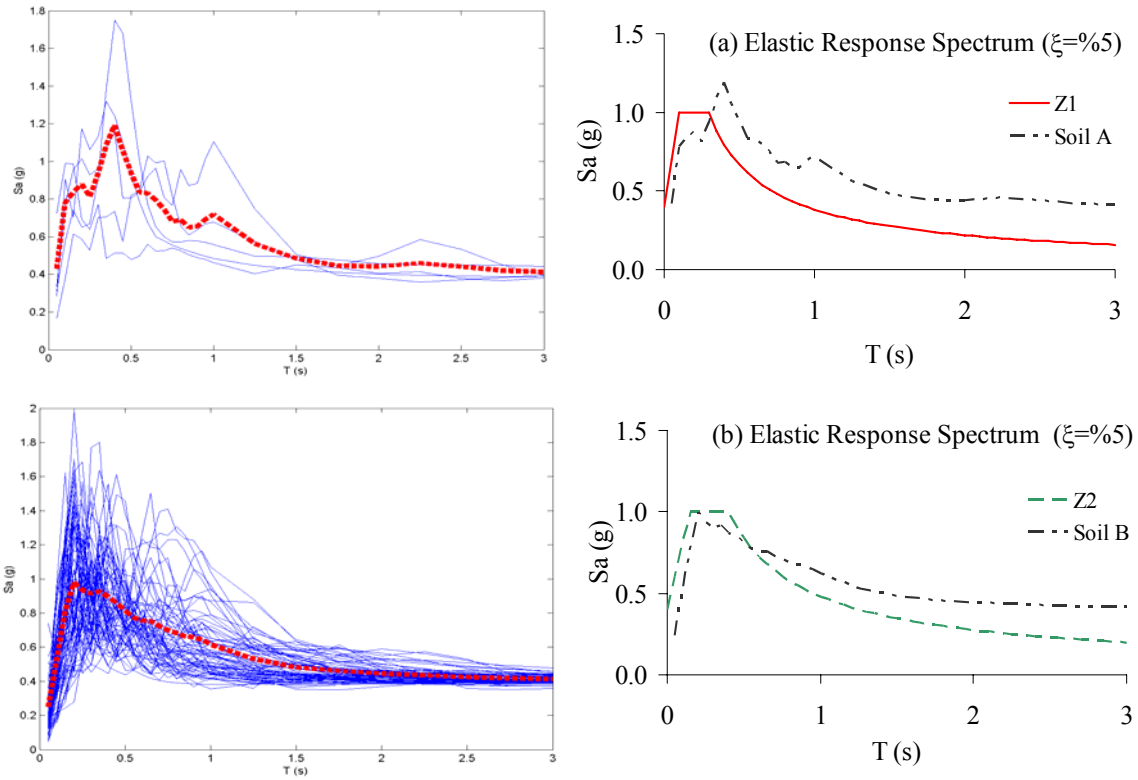

Figure 2.48. Comparison of the acceleration response spectra of the ground motions with the Turkish Seismic Design Code response spectra (A_0=0.4g)

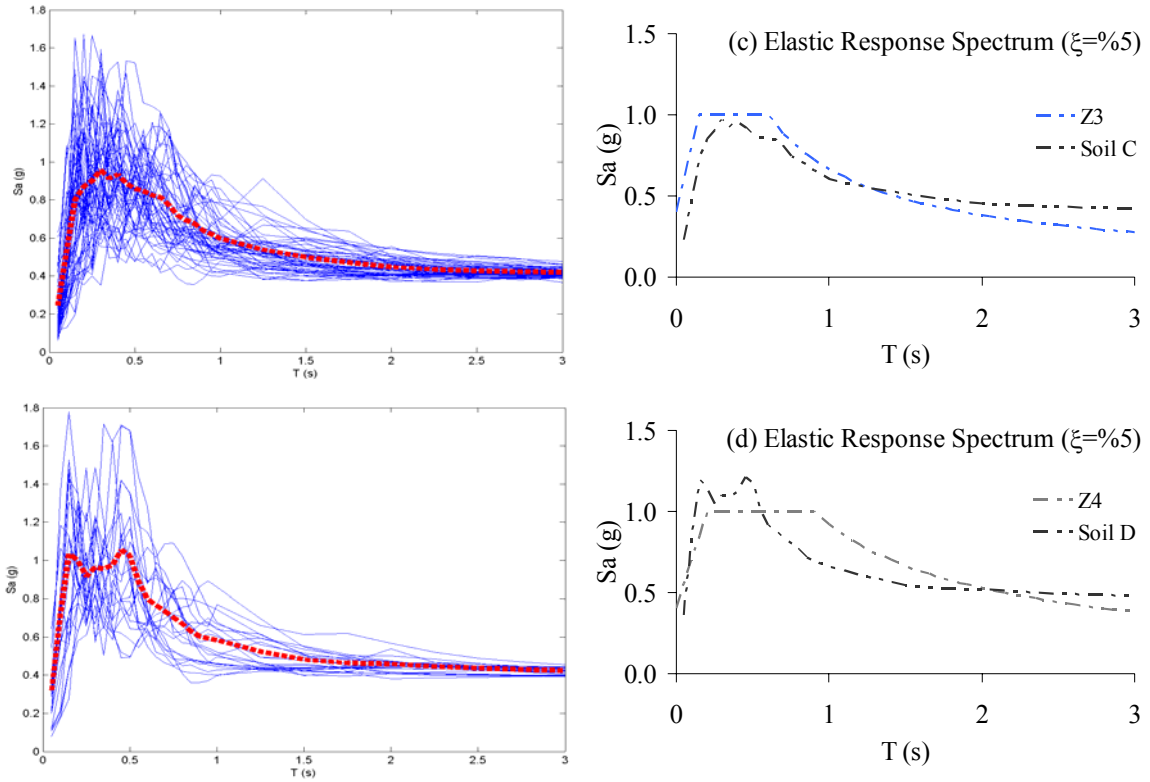

Figure 2.48. Comparison of the acceleration response spectra of the ground motions with the Turkish Seismic Design Code response spectra (A_0=0.4g) (cont'd)

Figure 2.48 shows that the obtained response spectra with the Turkish Seismic Code based spectra are consistent, except for Soil A case in which the comparatively low number of earthquake motion records has been available in PEER database. On the other hand, the spectra of Soil classes B, C and D are very consistent with the Code spectra.

2.4.3. Design Spectra

One of the main aims of this study is to utilize the seismic demand spectra in terms of energy. Since the conventional design spectra are taken the viscous damping, soil type and seismic zone into the consideration, this study should also include the seismic activity occurrence to its scope. Even though, all the spectra examples shown in the earlier sections are the ones from the results of the seismic zone 1 which has 0.4g as its effective ground acceleration, the other seismic zones were also used in the development of the energy design spectra.

There have been considerable discussions on the use of the ground motions in the seismic demand analysis in which way the records should be classified. Due to their erratic nature, duration, intensity and magnitude of the each ground motion record is very different from other. Therefore, it is unavoidable to normalize the records with respect the most applicable parameter that defies the severity of the motion. Several methods are proposed in the literature; however the most common practice of the normalization of the ground motions is to set their peak acceleration to a specific value (Bozorgnia and Campbell, 2004). In this study, in order to be consistent with the ABYYHY (2008), the PGA values of the each record were scaled to the effective ground acceleration values, Table 2.9.

Table 2.9 Effective ground motion acceleration values, ABYYHY (2008)

Seismic Zone	A_0 (g)
1	0.4
2	0.3
3	0.2
4	0.1

In the recent version of the ABYYHY (2008), the earthquake levels are also described in a probabilistic manner and a new parameter called earthquake influence factor was introduced, as in Table 2.10;

Table 2.10 Earthquake Levels and earthquake influence factor, ABYYHY (2008)

Earthquake	EQE influence factor	Probability of exceedence in 50 years	Return Period
Service	~0.5	% 50	72 years
Design	1.0	% 10	474 years
Maximum	~1.5	% 2	2475 years

Based on the given factors and acceleration values, the design spectra in terms of the energy were resulted for the each seismic zone and the earthquake type. Therefore, the proposed input and plastic energy spectra are scaled for the ground motions having 0.1, 0.2, 0.3, 0.4 and 0.6g PGA values.

2.4.3.1. Formulation of the Energy Demand Spectra. In the previous sections it was mentioned that some of the earthquake records from the preliminarily selected were excluded according to PGA, PGV/PGA and Housner Intensity values. In order to derive the most appropriate input energy spectrum that adequately reflects the remaining earthquake records, a probabilistic approach was employed. Such probabilistic approaches have been used since the first attempt of constructing spectra in earthquake resistant analysis. In fact, this probabilistic analysis are nothing else than the smoothing the "average" response (here energy) spectra. The smoothing of the average response spectra were utilized by estimation of the amplification factors those obtained for mean plus one standard deviation spectrum (84.1 per cent probability level) assuming a lognormal distribution (Clough and Penzien, 1995). Figure 2.49 show the distribution of the all earthquake records (PGA=0.4g) and mean plus standard deviation for each soil class.

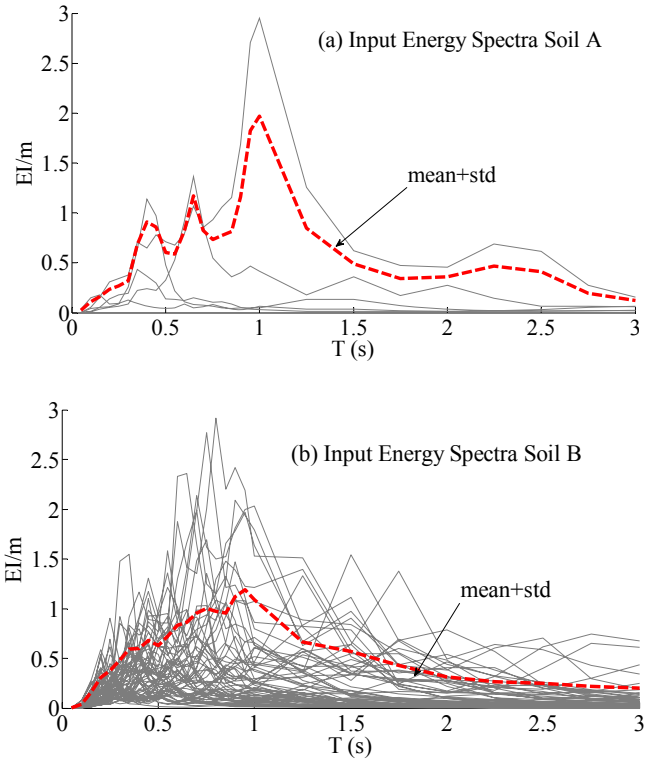

Figure 2.49. Input Energy spectra for different soil (μ=5 per cent and EPP model)

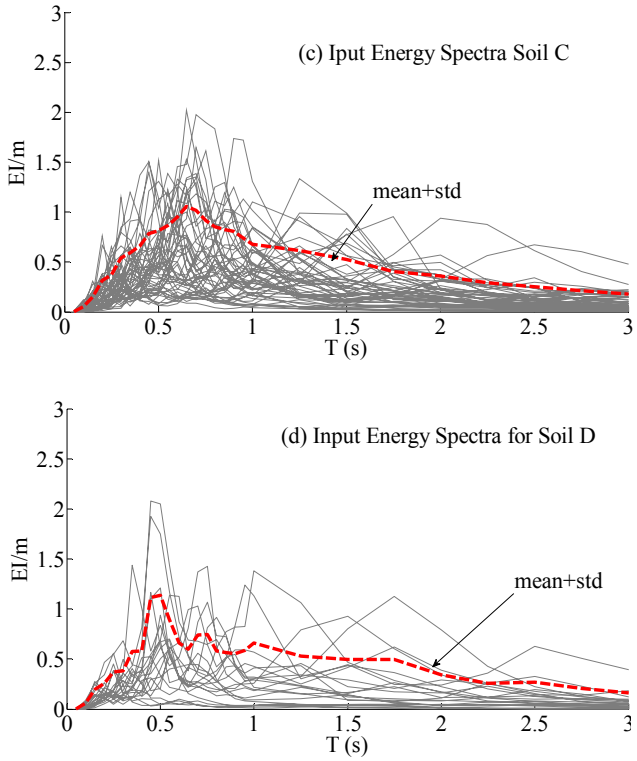

Figure 2.49. Input Energy spectra for different soil (μ=5 per cent and EPP model) (cont'd)

As seen in figure 2.49, the mean plus standard deviation of the energy spectra of the ground motions displays two major trends, a rapid increasing and slightly decreasing branch. Even though this formation resembles the formation of the Kunnath and .Chai (2004), the results of the nonlinear regression analysis show that the ordinates close to the peak period value is subjected to critics due to its sudden increase as in Figure 2.50 and 2.51;

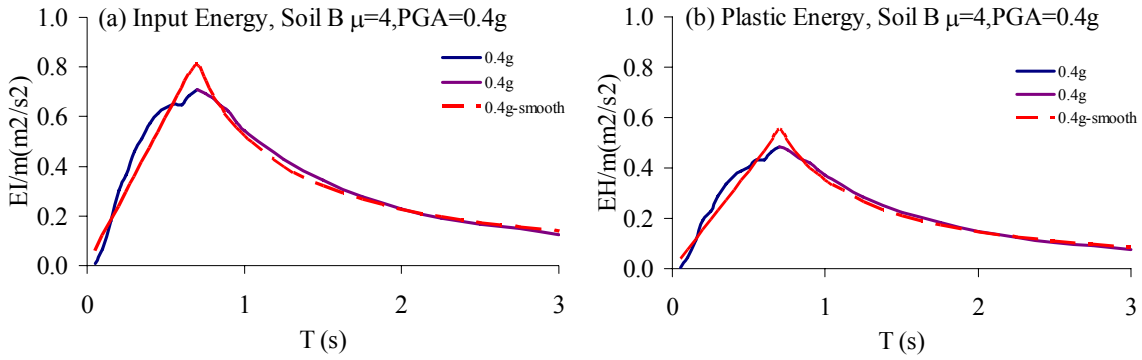

Figure 2.50.The mean+SD and smoothed (regressed) values of the calculated spectra

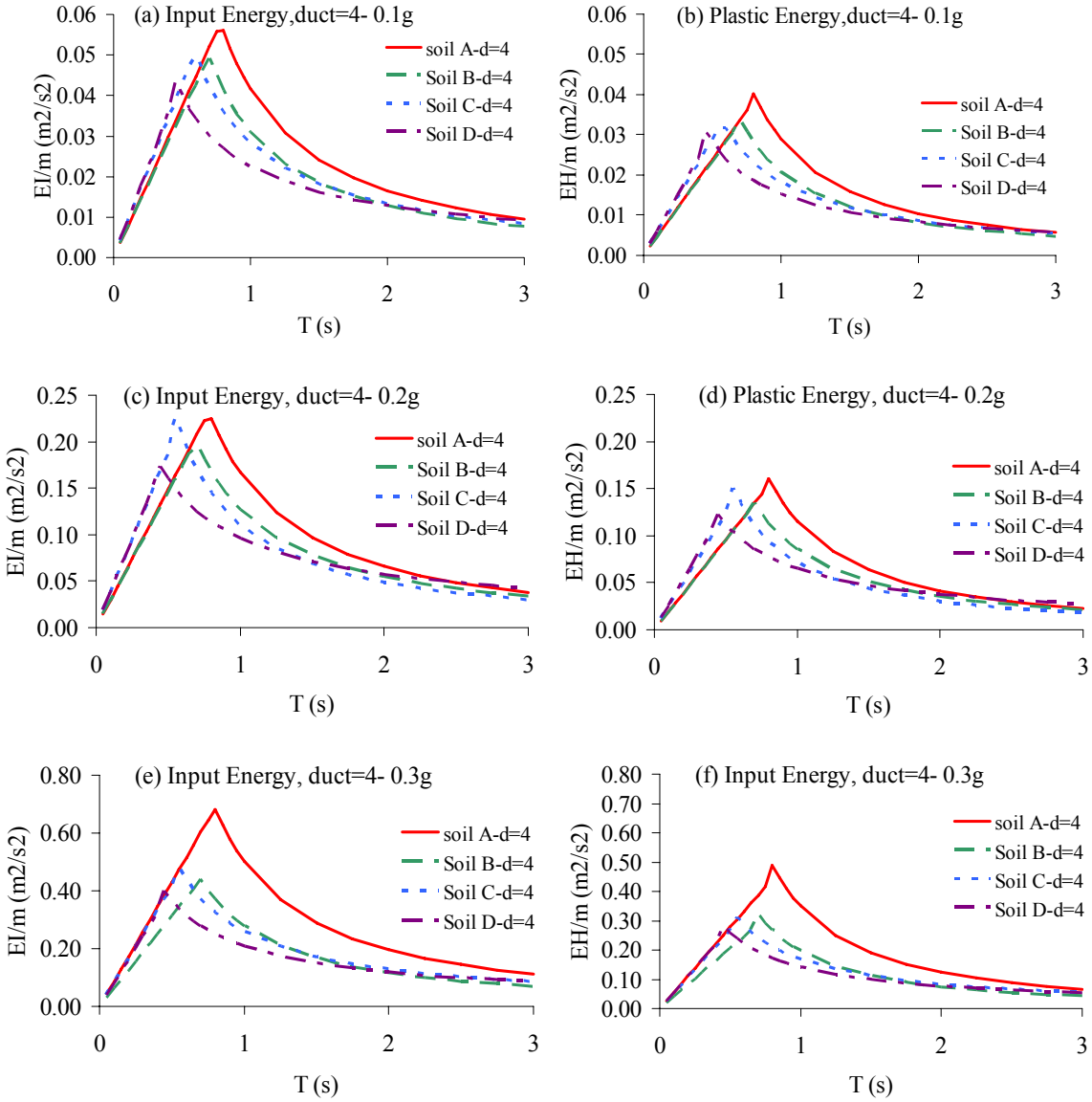

Figure 2.51.Regression Analysis of the mean+SD values of the calculated spectra

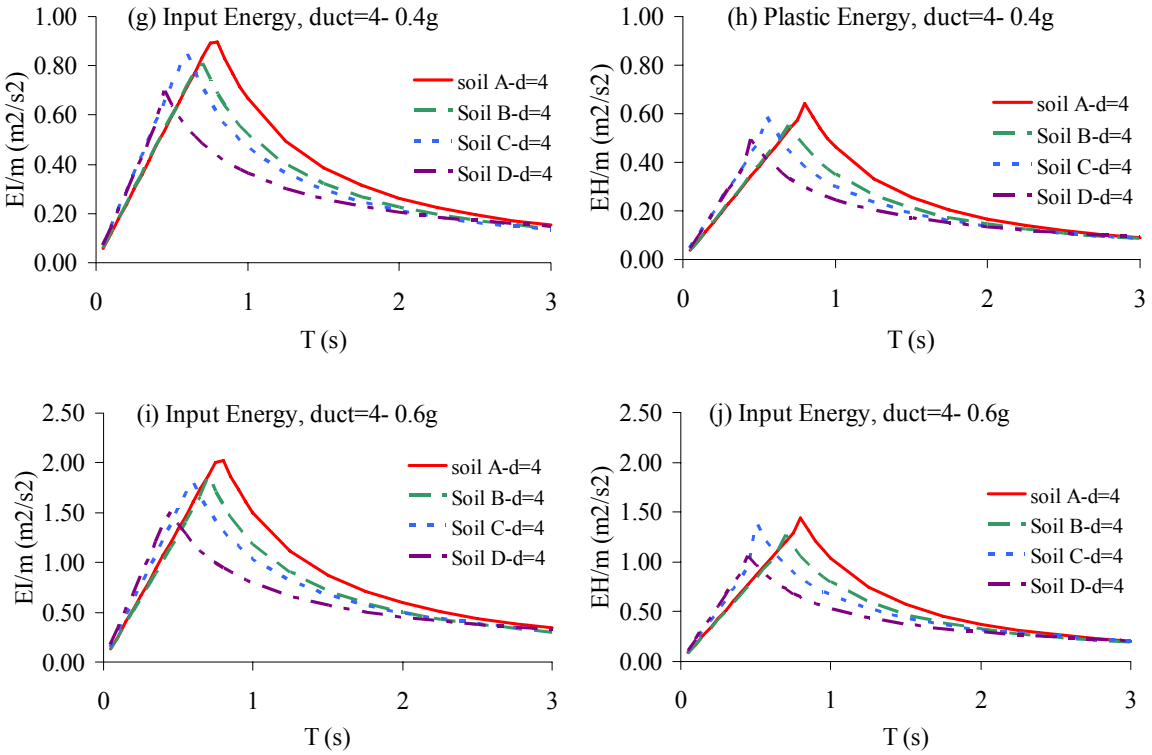

Figure 2.51.Regression Analysis of the mean+SD values of the calculated spectra (cont'd)

The shape of the input and plastic energy spectra may be converted from two major parts to three major parts by simply adding a plateau at a certain ordinate, as in the conventional response spectra described in the codes. Even though it looks very simple to add a constant value to a combined function, it is not as easy as it looks. The starting and ending periods of the plateau are generally related to the soil characteristics. However, the decision of these two certain periods also relate to non-technical issues (especially economy). The most convenient explanation for these important periods are given in Vidic et (1994) where the response of the SDOF systems subjected to several ground motions were used in the comparison of the strength and stiffness of the structures. They proposed a amplification factor based on the results of the time-history analysis.

$$\Omega_a = \begin{cases} 1.0 + 2.5(c_a - 1)T/T_c & ; \quad T \le 0.4T_c \\ c_a & ; \quad 0.4T_c \le T \le T_c \\ 2\pi c_v \left(\dot{x}_{g,\max} \Big/ \ddot{x}_{g,\max} T \right) & ; \quad T_c \le T \end{cases} \tag{2.19}$$

where c_a and c_v are coefficients recommended as 2.5 and 2.0, respectively, and T_c is the characteristic period of the ground motion.

$$T_c = 2\pi \frac{c_a}{c_v} \frac{\dot{x}_{g,\max}}{\ddot{x}_{g,\max}} \tag{2.20}$$

The predominant period T_c is assumed to coincide with period at which peak value of the input energy occurs, Kunnath and Chai 2004. The similar assumption is also employed in this study and the starting and ending periods are taken with respect to periods of the peak energy values for both input and plastic energy dissipation spectra. The only difference of this study is that, the ordinate values given in 2.10 are replaced with the actual ordinates coming from the regression analysis.

The resulting design input and plastic energy spectra are given in the following section.

2.5. Proposed Design Energy Spectra

After an extensive nonlinear time-history analysis conducted on a SDOF system having different behavior models, it was decided that the elasto-perfectly-plastic model displays a upper bound in the determination of the input and plastic demand energies. In order to stay in the safe side of seismic demand values, the EPP model was taken into further consideration for the different structural and ground parameters which are ductility, seismic zone and site conditions. The following sections present the proposed design energy spectra those are applicable for any type of building (i.e. steel, RC or masonry).

2.5.1. Design Input Energy Spectra

The energy imparted into the structure is a reliable parameter in the context of the earthquake resistant design. The input energy is directly related to the soil conditions, severity of the motion and interestingly to the ductility of the structure.

The amount of the input energy is proportional to the severity of the ground motion (seismic activity) since the it is the integration of the velocity response times ground acceleration. The increase in the velocity response of the structure will lead directly increase in the input energy. However, the imparted energy is and inversely proportional to the ductility of the structure. The study has shown that as the ductility of the structure increases, the amount of the input energy decreases. This dilemma should be explained as the ductile structures present larger deformation even though the rate of the deformation is smaller than the less ductile structure. Hence, the decrement in the velocity leads to the impartation of the less input energy.

There are two important features in the proposed response spectra, (i) the first part where the linear increment occurs, last longer than the conventional acceleration response spectrum and (ii) the ordinates of the plateau are different for each soil type at each ductility and seismic zone case. Even though, the range of the first linear part varies from 1/1 to 1.875/1 of the acceleration response spectra, the length of the constant value plateau last longer than acceleration spectra (2/1~10/1 of acceleration spectra). This due to the fact that the response of structure has significant portion in the amount of input energy.

The schematic display of the proposed input energy spectra is given in Figure 2. 52.

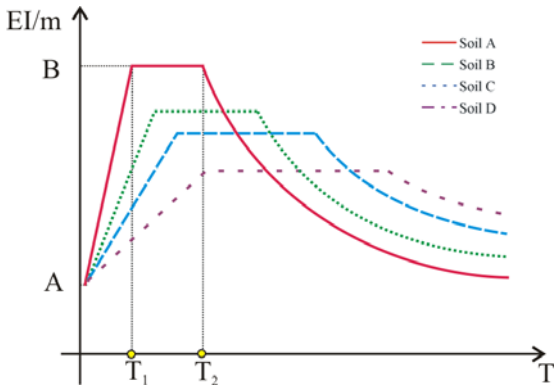

Figure 2.52.Proposed input energy spectra

The formulation of the energy spectra are defined similar to the Equation 2.19 where the constant value is estimated separately for the each parameter.

$$EI/m = \begin{cases} A + (B-A)(T-0.05)/(T_c-0.05) & ; \quad T < T_1 \\ B & ; \quad T_1 < T < T_2 \\ B\left(T_2/T\right)^k & ; \quad T_2 < T \end{cases} \tag{2.21}$$

The procedure recommended by Kunnath and Chai (2004) is applied in the estimation of the corner periods in spectra.

On the other hand, all the spectra values displayed very complex behavior towards the higher periods. In order to smooth the spectra and make consistent with each other, the decreasing branches of the all spectra are formulated in a same way. The power of the formulation is the mean+std value of the estimated power values that is between 0.4-1.6. here the *k* value is taken as 0.9.

2.5.2. Design Plastic Energy Spectra

Direct estimation of the spectral values for given structural (viscous damping, ductility) and site conditions (PGA, soil type) enabled to obtain the plastic energy spectra along with the derivation of the input energy spectra. This is the biggest advantage of benefiting from the constant ductility principle used in the computer program.

As come to the comparison of the plastic energy spectra to the input energy spectra, the most obvious difference comes from the ordinates of the 2nd part of the spectra. Even though the other parts of the spectra have the same trends, the plateau of the spectra is kept higher as the soil softens and resulting the increase of the plastic energy values contrary to the input energy. This may raise a question in mind; “How come plastic energy increases, while input energy decreases?”. The answer to the question relies on the physical meaning of the plastic energy. The plastic energy is directly related to the inelastic behavior (the damage ability) of the structure. As the soil laying beneath the softens it is expected that the ground motion amplifies and the proportion of the plastic energy increases, Figure 2.52. The amplified ground motion is one of the main reasons of the failure of the identical building in near sites that is relatively having hard soil. This fact was experienced in the area of Avcilar during 1999 Kocaeli earthquake. The sites close to Avcilar but having

harder soils encountered little damage on the buildings even if the distance to the epicenter of the earthquake is almost same as in Avcilar.

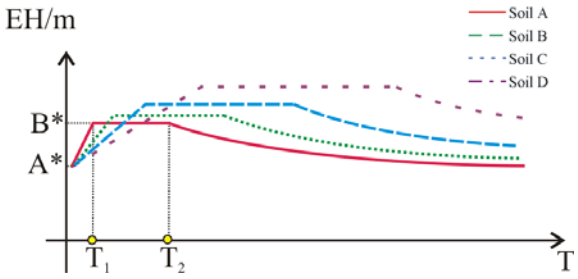

Figure 2.53.Proposed plastic energy spectra

Another important observation was made on the increment of the plastic energy values as the ductility level increases. The damage level on the member is related to the plastic deformation capacity of the system where the ductility is defined as the same way. Therefore, the portion of the plastic energy in the input energy increases as the deformations rises. This is exactly opposite of the trend of the input energy change in front of varying ductility.

The formulation of the plastic energy design spectra is very much similar to the proposed input energy spectra except for the ordinate values of the plateau part.

$$EH/m = \begin{cases} A^* + (B^* - A^*)(T - 0.05)/(T_c - 0.05) & ; \quad T < T_1 \\ B^* & ; \quad T_1 < T < T_2 \\ B^* \left(T_2 / T \right)^k & ; \quad T_2 < T \end{cases} \tag{2.22}$$

An example for the proposed input and plastic energy design spectra for the 1st seismic zone and is given in Figure 2.54, as follows;

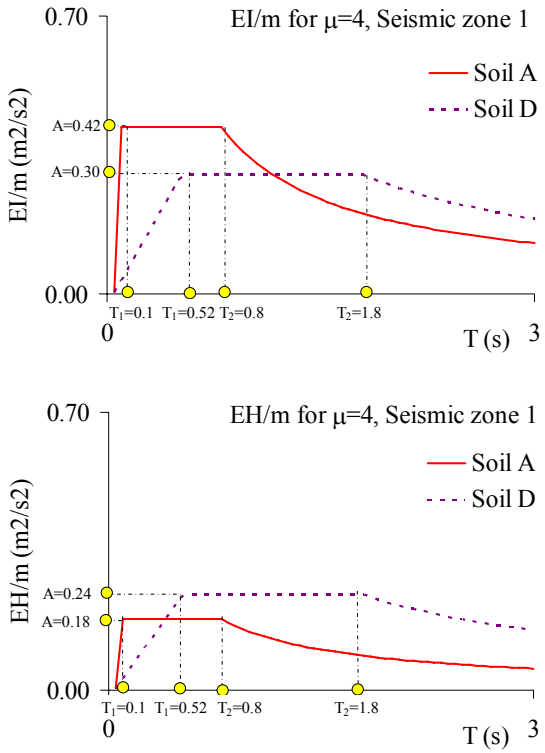

Figure 2.54.A numerical example for proposed design energy spectra

The general view of the input and the plastic for the seismic zone 1 is given in figure 2.55. The values *of A, B, A*, B*, T_1, T_2* and *k* are also summarized in Table 2.11.

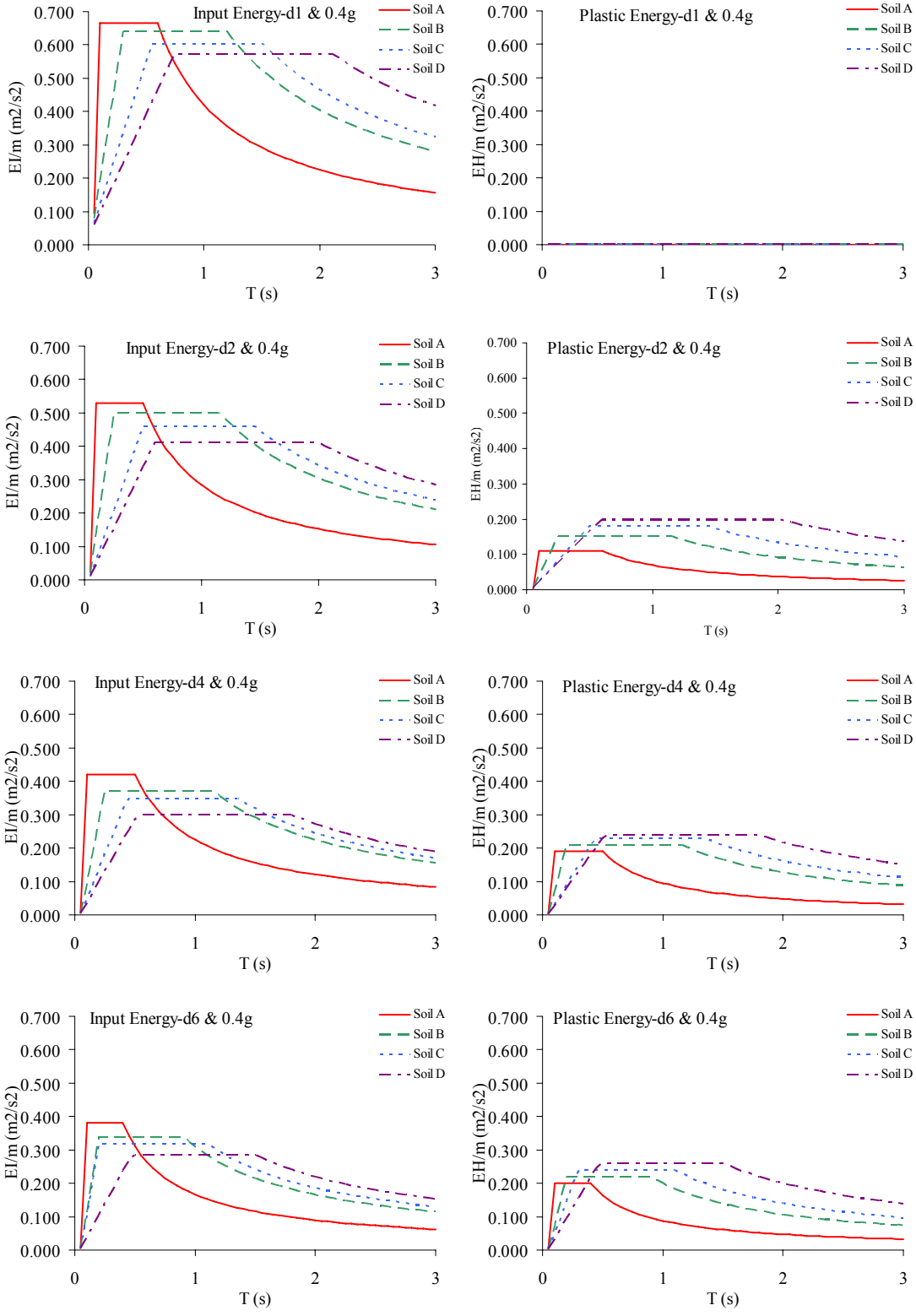

Figure 2.55. The change of the input and plastic energy spectra

Table 2.11. The values of the curves in the proposed input energy spectrum

	Soil A		Soil B		Soil C		Soil D	
	EI/m	EH/m	EI/m	EH/m	EI/m	EH/m	EI/m	EH/m
μ=1								
T1	0.1	0	0.3	0	0.55	0	0.75	0
T2	1	0	1.2	0	1.5	0	2.1	0
A- 0.1g	0.006	0	0.005	0	0.004	0	0.004	0
B- 0.1g	0.042	0	0.04	0	0.036	0	0.032	0
A- 0.2g	0.023	0	0.02	0	0.016	0	0.014	0
B- 0.2g	0.161	0	0.156	0	0.147	0	0.14	0
A- 0.3g	0.054	0	0.042	0	0.036	0	0.03	0
B- 0.3g	0.378	0	0.348	0	0.32	0	0.3	0
A- 0.4g	0.095	0	0.08	0	0.067	0	0.059	0
B- 0.4g	0.665	0	0.64	0	0.603	0	0.575	0
A- 0.6g	0.22	0	0.185	0	0.145	0	0.125	0
B- 0.6g	1.54	0	1.48	0	1.305	0	1.25	0
μ=2								
T1	0.1	0.1	0.25	0.25	0.5	0.5	0.6	0.6
T2	0.9	0.9	1.15	1.15	1.45	1.45	2	2
A- 0.1g	0.005	0.003	0.005	0.002	0.004	0.002	0.004	0.002
B- 0.1g	0.037	0.008	0.035	0.011	0.033	0.013	0.03	0.014
A- 0.2g	0.005	0.003	0.005	0.002	0.004	0.002	0.004	0.002
B- 0.2g	0.153	0.02	0.145	0.027	0.136	0.03	0.12	0.035
A- 0.3g	0.005	0.003	0.005	0.002	0.004	0.002	0.004	0.002
B- 0.3g	0.35	0.035	0.33	0.06	0.31	0.088	0.27	0.126
A- 0.4g	0.005	0.003	0.005	0.002	0.004	0.002	0.004	0.002
B- 0.4g	0.53	0.047	0.5	0.08	0.46	0.116	0.41	0.2
A- 0.6g	0.005	0.003	0.005	0.002	0.004	0.002	0.004	0.002
B- 0.6g	1.32	0.084	1.25	0.143	1.17	0.209	1.05	0.3

Table 2.11. The values of the curves in the proposed input energy spectrum (cont'd)

	Soil A		Soil B		Soil C		Soil D	
	EI/m	EH/m	EI/m	EH/m	EI/m	EH/m	EI/m	EH/m
μ=4								
T1	0.1	0.1	0.25	0.25	0.44	0.44	0.52	0.52
T2	0.8	0.8	1.15	1.15	1.35	1.35	1.8	1.8
A- 0.1g	0.005	0.004	0.004	0.003	0.003	0.003	0.003	0.003
B- 0.1g	0.032	0.01	0.03	0	0.028	0	0.026	0.016
A- 0.2g	0.005	0.004	0.004	0.003	0.003	0.003	0.003	0.003
B- 0.2g	0.128	0.021	0.12	0.026	0.11	0.04	0.1	0.05
A- 0.3g	0.005	0.004	0.004	0.003	0.003	0.003	0.003	0.003
B- 0.3g	0.315	0.11	0.3	0.13	0.285	0.14	0.25	0.15
A- 0.4g	0.005	0.004	0.004	0.003	0.003	0.003	0.003	0.003
B- 0.4g	0.42	0.18	0.37	0.21	0.35	0.23	0.3	0.24
A- 0.6g	0.005	0.004	0.004	0.003	0.003	0.003	0.003	0.003
B- 0.6g	1.1	0.3	1.05	0.4	0.98	0.45	0.85	0.5
μ=6								
T1	0.1	0.1	0.2	0.2	0.3	0.3	0.47	0.47
T2	0.6	0.6	0.9	0.9	1.1	1.1	1.5	1.5
A- 0.1g	0.006	0.003	0.005	0.002	0.004	0.002	0.004	0.002
B- 0.1g	0.03	0.011	0.026	0.013	0.024	0.016	0.022	0.018
A- 0.2g	0.006	0.003	0.005	0.002	0.004	0.002	0.004	0.002
B- 0.2g	0.11	0.025	0.09	0.03	0.085	0.05	0.07	0.06
A- 0.3g	0.006	0.003	0.005	0.002	0.004	0.002	0.004	0.002
B- 0.3g	0.29	0.12	0.25	0.13	0.23	0.15	0.19	0.16
A- 0.4g	0.006	0.003	0.005	0.002	0.004	0.002	0.004	0.002
B- 0.4g	0.38	0.21	0.34	0.22	0.32	0.24	0.28	0.26
A- 0.6g	0.006	0.003	0.005	0.002	0.004	0.002	0.004	0.002
B- 0.6g	1	0.4	0.9	0.5	0.8	0.55	0.75	0.6

3. SEISMIC CAPACITY IN TERMS OF ENERGY

3.1. Definition of Seismic Capacity

The definition of "capacity" of the structures in general and of the member in particular is very changeable from the view of the load or deformation pattern (also said as load/deformation history or memory) those may be either statically or dynamically applied (Surahman, 2008).

The load (axial or shear force, bending or torsion moment) bearing capacities of the structural members have been calculated according to the design philosophies such as "Allowable Stress" and "Limit State" design philosophy. "Limit State Approach" have superseded "Allowable Stress Approach" in the design of reinforced concrete structures since 1960's (Berktay, 2003; Ersoy and Özcebe, 2004).

The relation between the terms of capacity and design is totally correlated in seismic design; this correlation requires an "iterative" manner due to randomness of the excitation. Therefore the capacity definition of the current design codes is summarized in the following sections.

3.1.1. Force-Based Design and Capacity

This design method is relied on the static analysis of the structures those are simple, regular and limited in height. However, most structural design codes are actually based on this simple design practice (UBC-97, ABYYHY-2007 etc.). This method requires a preliminary design in order to calculate the natural period which lead to the seismic force.

The seismic force in Force Based Design (here ABYYHY-2007 is formulated) is defined as base shear, V as follow;

$$V = \frac{A(T) \times W}{R_a(T)} \tag{3.1}$$

where *A(T)* is Spectral Acceleration coefficient depending on the soil condition at site and seismicity on regions, *W* is the building weight, $R_a(T)$ is the load reduction factor that allows the shift from elastic to inelastic demand and *T* is the fundamental period of the structure. This force is recognized as the shear force acting at the base of the structures and it must be distributed along with the height of the building which is assumed having rigid floor diaphragm action as follow;

$$F_i = (V - \Delta F_N) \frac{w_i H_i}{\sum_{j=1}^{N} w_j H_j} \tag{3.2}$$

Where F_i is the lateral seismic force acting on the *i*th storey, w_i is the weight of the i^{th} floor, H_j is the elevation of i^{th} floor, ΔF_N is the additional force applied at the top of the building and *N* is the number of the stories.

The design of the members (here say the longitudinal reinforcement ratio for beams and columns) are obtained according to the member forces from the results of the static analysis of the structure subjected to these equivalent seismic forces acting at floor level. If the preliminary design of the member fails to resist the acting member force, the strength of the structural member is increased either through their section dimensions or increasing the longitudinal reinforcement ratio. However, this modification will change the stiffness of the system, resulting in different structural response and natural period. This improvement requires the use of iterative solution procedures which is unavoidable in seismic design.

As general, the modern design codes do not allow the members vulnerable to shear failure by mandating the use of appropriate confinement around the longitudinal reinforcing bars. Therefore the shear capacity of the RC beams or columns is provided by the code-based ratios that ensures the avoidance of the shear-dominant behavior.

The similar provision against torsion is also applied as the pre-defined ratios. However, this design code has been refined by more rational approach of performance-based introduced in Paulay and Priestly (1992).

3.1.2. Performance-Based Design and Capacity

Starting from 1960's, researchers became interested in the quantification of the inelastic deformation capacity of the structural components which is expressed in terms of displacement ductility capacity, $\mu_{\delta,}$ due to its apparent relationship to the force-reduction factor, *R*, that is commonly used in the reduction of the base shear acceptable inelastic design levels. However, there have been yield deformation has been variously defined by different research groups. Beside this shortcoming, the force-reduction approach considers that particularly structures can be allocated characteristic ductility capacities and accordingly force reduction factors. This complicates the main principles of the force-based design.

Park and Paulay (1976) proposed that the distribution of the strength through the building was more important than the value of the base shear by assuring the plastic hinges occurred in beams rather that the columns (weak beam/strong column). The response of the structure as the hinges occur is imposed by setting then to fulfill several levels of design criteria. These design criteria are serviceable, operational, life safety and near collapse level with expected levels of seismic ground motion (SEAC 2000). Actually performance-based design is an approach considering building performance in future earthquake and based on controlling the dynamic response of the structure within the response thresholds which are established upon the acceptable level of damage that might be measured as risk of casualty, occupancy and economic losses.

The performance-based design is explicitly linked with the strength and deformation capacity of the both structural and non-structural members in a building. This is provided via expressing the status of the deformation state of the members (particularly flexural curvature or strain values) or of the interstory drift of the stories.

In the context of the earthquake resistant design, the failure of the capacity of the members can be defined as the inability of the structure to accommodate the maximum deformability during the ground motion, as follow;

$$\mu_{demand} \leq \mu_{acceptable} \leq \mu_{ultimate} \tag{3.3}$$

here, μ_{demand}, μ_{accep}, $\mu_{ultimate}$ resemble the deformation values of demand of earthquake imposed to the structure, acceptable (or supply) for the structure and ultimate capacity under monotonically increasing deformation, respectively. The acceptance of the member deformation brings out the definition of the various state (or performance level) which the structure should reach or not exceed. The performance levels those are also used in this study are to be explained in detail in the following sections.

An example to the maximum drift angle of the member should be the lesser of (Priestley 2000);

$$\begin{aligned} \theta_{concrete} &= \theta_y + \left(\varepsilon_{concrete}/c - \varphi_y\right)l_p \quad \text{(concrete compression)} \\ \theta_{steel} &= \theta_y + \left(\varepsilon_{steel}/(d-c) - \varphi_y\right)l_p \quad \text{(reinforcement tension)} \end{aligned} \tag{3.4}$$

Here, θ_y is the yield drift angle, φ_y is the yield curvature and l_p is the plastic hinge length.

The material drift limits in equations 3.4 are displayed with the aim of exhibiting how the performance limits at cross-section level could be expressed as the deformation of the system and the curvature of the section are incorporated into the same formula.

Displacement-based design, in particular, and performanced-based design, in general, have been finding larger ground in the countries' design codes due to its more reliable results even though it requires more calculations than the force-based design calculations. how ever, a change of preference from the simple to bit more complex calculations should be accounted as an improvement that would let the alternative method

to be used in seismic analysis and design. The energy-based method is one of the alternative methods but require more complex assumptions and calculations.

3.1.3. Energy-Based Design and Capacity

The performance-based design was developed to overcome the lack of the important issues in force-based design, such as predicting the overall capacity of the building and realistic states of building reaches after the seismic forces were applied. Even though, the performance-based design is able to predict the damage of the member due to inelastic recursions; the general approach to identify the damage at the member is addressed the damage indexes recommended by various researchers, Banon et al (1981), Toussi and Yao (1983), Stephens and Yao (1987), Wang and Shah (1987), Chung et al. (1977 and 1989), Park and Ang (1985), Cosenza and Manfredi (1999), Kappos (1997). These damage indexes are aimed to address the damage of the member subjected to monotonic or seismic forces.

However, the shortcoming of both force- and performance-base design methods is the gap between the ground motion excitation and the inelastic response of the structure which is prone to have damages. The biggest handicap of these methods is the inability of defining the damage occurrence on the member which is in cumulative manner due to the reverse cyclic nature of ground motion with random amplitude (Kunnath and Chai, 2004). Therefore, as well as the strength and deformation capacities of the building and members, the building should have enough energy dissipation reserve during the strong ground motion. Even, Kawashima (1997) noted that the drew attention to consider the residual deformation and strength reserve in defining the damage control performance level after drawing on lessons from the 1995 Kobe earthquake.

All the above mentioned ideas make an alternative design procedure, Energy-Based Design, valuable from the view of incorporating the ground motion, regarding frequency content and duration, which is called Seismic Demand studied in Chapter 2, and response of the structure, regarding the capacity against strength, deformation and energy supply, which is to be studied in current chapter.

3.2. The Concepts Incorporated with the Energy Dissipation Capacity

The scheme of energy in the description of a physical entity (earthquake resistant design parameters like strength or deformation) may not be easily sensed because it is a cross product of force and displacement vectors, those are more perceivable than energy. Therefore, while introducing the seismic capacity in terms of energy, some concepts have been referred in the developed capacity procedure. These concepts have essentially described in the development of the current codes.

3.2.1. Energy Dissipation Due to Inelastic Behavior

The conventional method of approximating plastic energy in structures is obtained as the area enclosed by the force versus displacement response (Mahin and Bertero, 1981). The similar approach has been applied also for the plastic rotation versus moment couple, which is available in the joints of the multi degree systems, where the resisting force and corresponding displacement is unknown (Wong and Yang, 2002).

Since the energy dissipation due to the plastic deformations is related to the area of the hysteresis graphs, the general characteristic of the load-deformation curves defy the amount of the energy dissipation value. For example a RC member with poor confinement subjected to either monotonic or cyclic loads will eventually expose to the excessive shear cracks those reduce the bonding of the longitudinal reinforcement. Therefore, the sudden changes (slip) happen in the stiffness which is the slop of the force-displacement curve, Figure 3.1, Ang et al (1981).

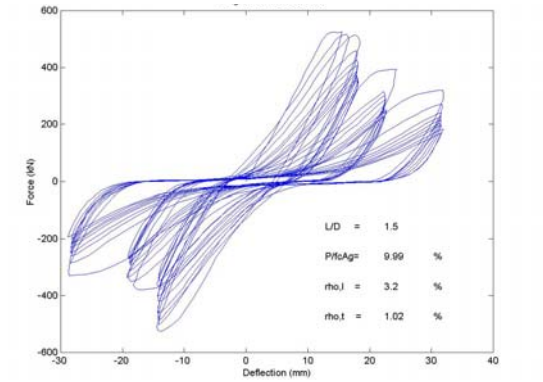

Figure 3.1. Typical shear failure of RC bridge pier Ang et al (1981)

The members which has adequate confinement do have a better resistance than the poor confined members due to the high-ductile behavior that also lets dissipate more energy and damage, Figure 3.2 Paulay and Priestley (1992).

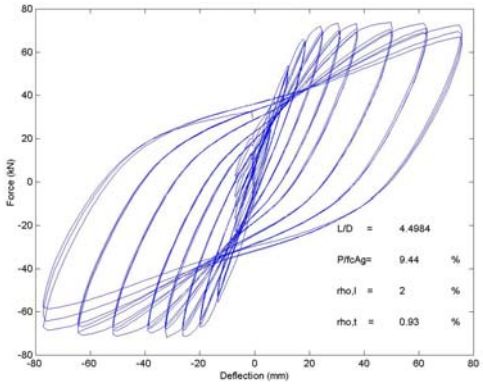

Figure 3.2. Typical flexural behavior of RC bridge pier Kunnath et al (1997)

The energy dissipation values of the members having shear- and flexural-behavior differ in the case of ground motion which was studied in the previous chapter and formulated as;

$$EI = E_{recoverable} + E_{irrecoverable} = (ES + EK) + (ED + EH) \tag{3.5}$$

Several researchers (Akiyama, 1985; Uang and Bertero, 1988; Fajfar et al., 1992; Akbaş, 1996; Decanini and Mollaioli, 1999; Wong and Yang, 2002; Leelataviwat et al., 2002) have agreed on that measuring the damage potential of a ground motion is possible with the promising parameters of EI and $E_{irrecoverable}$. Since the devices those are capable of

dissipate large amount of energy have been the latest research topic, it seems that the damage potential of a ground motion should be particularly focused on plastic energy (*EH*) values.

The fact given above have been the main motivation of this study; development of a methodology that defies the demand of the ground motion and supply of the structure in terms of energy.

3.2.2. Performance of the Structure Subjected To Seismic Forces

3.2.2.1. System Performance Levels. The goal of the earthquake resistant design procedures is that if a structure designed accordingly to its regulations satisfy the criteria defined by the same procedure. In force-based design, these criteria are mainly involved in the level of the forces acting on the member, and interstory drift ratios. As come to performance-based design, these criteria are mainly dependent on the displacement of the members (again via interstory drift ratios) and deformation of the members (strain at the compression concrete and tension steel).

The criteria in performance-based design have been displayed in matrix that is qualitatively explaining the relationship between the ground motion and the performance of the building, Figure 3.23.

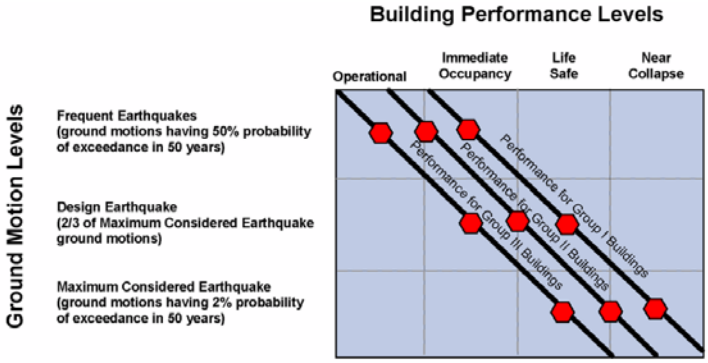

Figure 3.3. Expected building performance (NEHRP Recommended Provisions for Seismic Regulations for New and Other Structures)

The principles of these performance levels are qualitatively expresessed in the recent guidelines, as an example Table 3.1 gives the description of the building performance level in FEMA273;

Table 3.1. Performance levels, qualitative (FEMA 273)

Performance-Level	Explanation
Immediate Occupancy	Structures performing to this level are expected to experience limited stiffness degradation and no significant strength degradation
Life Safety	LS is a state in which significant damage has occurred to the lateral force resisting system, however this damage is repairable, though perhaps not economically.
Collapse Prevention	CP level is intended to be a state of incipient collapse in which the lateral force resisting system has experienced substantial stiffness and strength degradation

The relationship between the lateral force resistance and the damage of the structures is generally described as the monotonically increasing static force vs. top displacement of the structure, Figure 3.4.

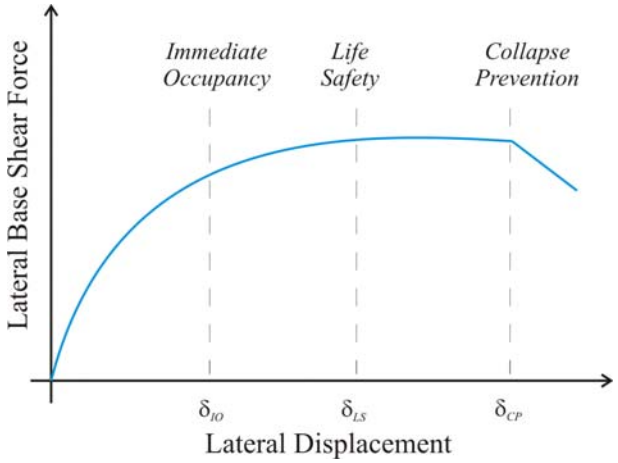

Figure 3.4. Structural performance Levels (FEMA 273)

Even though the descriptions for the system performance levels are well-stated in the design codes (FEMA 273, FEMA 356, ATC 40, 1996), the quantitative description of these levels are not concluded in the design codes. The quantities found in the design guidelines do necessarily take an action of being just “indicative” rather than acceptable criteria for evaluation. The same action holds true in almost all design guidelines of different countries, even in Turkish Seismic Design Code.(ABYYHY-2007)

On the other hand, the quantities those are named as indicative were assumed as an origin of start in this study since the systems evaluated are singled degree freedom systems (cantilever beam/columns). The system performance values available in design codes are given in Table 3.2;

Table 3.2. Performance levels, quantitative

Performance Levels	FEMA 356	ABYYHY-2007
Immediate Occupancy	% 1	% 1
Life Safety	% 2	% 3
Collapse Prevention	% 4	% 4

As seen in Table 3.1, the values of ABYYHY-2007 are almost same, except LS, with FEMA 356. Therefore, the limit values in the derivation of the energy dissipation capacity study were taken according to ABYYHY-2007.

3.2.2.2. Section Performance Levels. It was mentioned that there are certain acceptance criteria for the performance levels in which the structures should satisfy during the ground motion. The similar approach of applying the performance level at the member (especially RC members due to its deteriorating nature) has been correlated with the damage occurred during the reverse cyclic action.

The current design guidelines have included the values of the critical section rotation (or accordingly curvature or axial strain) values at the sections based on the extensive laboratory tests and numerical analysis conducted by different researchers, Gülkan and

Sözen (1974), Rothe and Sözen (1983),Bracci et al. (1995), Browning et al. (2000), Gupta and Krawinkler (2000), Lehman et al. (2000).

The section performance levels have been segmented according to the axial strains in the compression in cover and core concrete and tension in steel as follow;

Table 3.3. Section performance levels- axial strain rates (DBYYH-2007)

Performance Levels	Concrete (compression)	Steel (tension)
Minimum	*0.035*	*0.010*
Safety	$0.035+0.01\times(\rho_s/\rho_{sm})\le 0.0135$	*0.040*
Collapse	$0.004+0.0114\times(\rho_s/\rho_{sm})\le 0.018$	*0.060*

In this study the maximum values of the materials were taken into the account while evaluating the limit state of the member for the proposed capacity procedure since it demonstrates the extreme condition of the member can experience, Figure 3.7.

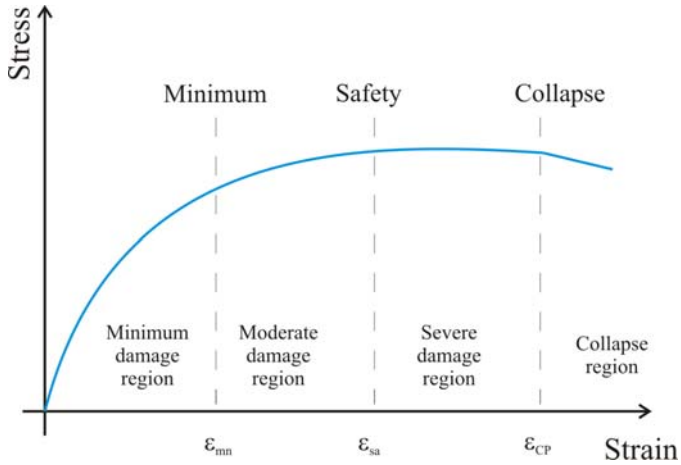

Figure 3.5. Section performance Levels (ABYYHY-2007)

3.2.3. Damage of the Member

While addressing the damage at the member level (local damage), many researchers proposed that a dimensionless index (generally between 0 and 1, from minor to severe, respectively) should be used in the definition how much the member suffered from the

applied force, either monotonic or dynamic. These damage indexes may be classified into five classes, as follow

3.2.3.1. Non-Cumulative Indices. The simplest form of the damage indices are ductility and interstory drift.

The ductility (μ) ratio is defined as rotation (θ), curvature (ϕ) or displacement (δ). As an example of the rotation ductility;

$$\mu_\theta = \theta_m / \theta_y \tag{3.6}$$

where θ_m and θ_y are the maximum and yield rotations, respectively. Here the calculation of the maximum rotation is easy to obtain contrary to the fact that the greatest challenge comes from the definition of the yielding of the system. Mostly it is related to the steel in tension which reaches to the yield strain, in spite of that the concrete in the core of the section may not lose its strength (Park, 1986).

The interstory drift is the most referred indicator in damage assessment. There have been attempts to interrelate the maximum and permanent drift values (Toussi and Yao 1983; Krawinkler et al., 2003). Even though its simplicity, this value do fail to take account of the effects of the reverse cycling actions of the seismic events.

3.2.3.2. Deformation-Based Cumulative Indices. These indices were inspired from the extending ductility concept to cover the cyclic loads. Stephens and Yao (1987) developed a damage index based on the displacement ductility while caring the positive and negative displacement, as follow;

$$D = \sum \left(\frac{\Delta\delta^+}{\Delta\delta_f} \right)^{1-br} \tag{3.7}$$

where $r = \Delta\delta^+ / \Delta\delta^-$, $\Delta\delta_f$ is the value of $\Delta\delta^+$ in a single-cycle test to failure and *b* is a constant. Stephens and Yao recommended the values of $\Delta\delta_f$ and b as 10 per cent and 0.77, respectively.

Since seismic loading of RC elements results high ductility over several cycles, the classical idea of low-cycle fatigue formulation has been also found attractive in the development of the deformation-based indices. Jeong and Iwan (1988) use an extension of Miner's rule by combining it with another well-known law Coffin-Manson, as follow;

$$D = \sum_i {n_i \mu_i} / {C} \tag{3.6}$$

where $c = n_f \mu$ and n_f is the number of cycles to failure at a selected ductility, μ.

The idea of employing the low-cycle fatigue concept have been the topic of two extensive test studies conducted in Building and Fire Research Laboratory, USA and METU, Turkey. The similar test setups for bridge columns at BFRL (Kunnath et al., 1997) and for beams at METU (Erberik, 2002) were used to find the energy dissipation characteristics under constant amplitude displacement controlled tests which is actually nothing else than the low-cycle fatigue application. The both tests resulted in their own damage formulations and indexes.

Kunnath et al. (1997) developed the a formulation that uses the Coffin-Manson relationship in the prediction of the damage in the circular bridge piers, as follow;

$$2N_f = \left(\frac{8.25}{\mu_c} \right)^4 \tag{3.7}$$

where μ_c is the cyclic displacement ductility factor. Kunnath and Chai (2003) have developed this formulation lately to derive the cumulative damage based inelastic cyclic demand spectrum.

Erberik and Sucuoğlu (2003) developed a total damage index from the test results of the beam under constant (representing fatigue) and variable amplitude (representing seismic action) tests, as follows;

$$Dn = \frac{\mu_{e,m} - 1}{\mu_u - 1} + \frac{\mu_{e,m}}{\mu_u - 1}\left(\frac{4}{5E_{h,n_{eq,n}}} - 1\right) \tag{3.8}$$

Here, the first term on the right-hand side represents damage due to maximum effective ductility, and the second term represents damage due to low-cycle fatigue at $n_{eq,n}$ cycles.

3.2.3.3. Energy-Based Cumulative Indices. The first damage index based on energy dissipation was proposed by Gosain et al (1977), as follow;

$$D_e = \sum_i \frac{F_i \delta_i}{F_y \delta_y} \tag{3.9}$$

By assuming that the remaining capacity of the member which has 75 per cent of the yield strength due to cyclic loading is negligible, the cycles beyond 75 per cent of the yield strength is ignored.

Another energy formulation was developed by Kratzig et al. (1989) based on the primary and following half-cycles of the repeated action. For the positive half-cycles the cumulative damage function is defined as;

$$D^+ = \frac{\sum E^+_{p,i} + \sum E^+_p}{E^+_f + \sum E^+_i} \tag{3.10}$$

in which E_{pi} is the energy in primary half cycle, E_i is the energy in a following half-cycles and E_f is the energy absorbed in a monotonic test to failure. The computed positive and negative indices, they are put into a formula of the overall damage index as follow;

$$D = D^{+} + D^{-} - D^{+}D^{-} \tag{3.11}$$

The inclusion of the follower half-cycle energy terms in both numerator and denominator of Equation 3.11 means that they contribute considerably less to the damage index than the primary terms.

3.2.3.4. Combined Indices. The most widely used cumulative damage indices is the one developed by Park and Ang (1985), as follows;

$$D_{PA} = \frac{\delta}{\delta_u} + \beta \frac{\int dEH}{F_y \delta_u} \tag{3.12}$$

where δ represents the maximum displacement demand and β is a constant determined experimentally and ranging between -0.3 to 1.2, δ_u is the ultimate displacement of monotonic increasing load (push-over), δ_y and F_y are the yield displacement and strength, respectively. The term in the second of the right-hand side of the equation includes the energy dissipation of the system ($\int dEH$). The advantages of this index are its simplicity and the fact that it has been calibrated by enormous amount of test data including shear and bond instances. Cosenza et al (1990) showed the similar results if the β value is taken as 0.15 which was proposed by Park and Ang since it was median of values obtained experimentally.

The researchers attempted to develop the Park and Ang damage index for the different test cases and proposed different ranges describing the damage occurred on the members, Park et al. (1985), Kunnath et al. (1987), Stone and Taylor (1993), Ghobarah et al. (1997), Augusti and Ciampoli (2008). However, it was generally considered that the D_{PA} should take a value between 0 (at rest condition) and 1 (total collapse). The proposed limits of the D_{PA} index are summarized in Tables 3.4-3.5;

Table 3.4. Damage levels and corresponding D_{PA} values- Park et al (1987)

Damage Conditions	D_{PA} values
No damage (minor cracking)	<0.1
Minor damage (light cracking)	0.1≤ D_{PA}<0.25
Moderate damage (severe cracking, localized spalling)	0.25≤ DPA<0.40
Severe damage (crushing of concrete, reinforcement exposed)	0.40≤ DPA<1.0
Collapse	1.0≤ DPA

Table 3.5. Damage levels and corresponding D_{PA} values- Stone and Taylor (1993)

Damage Conditions	D_{PA} values
No damage (Minor cracking)	<0.11
Repairable (Extensive spalling but inherent stiffness remains)	0.11≤ D_{PA}<0.40
Irreparable- (Still standing but failure imminent)	0.40≤ D_{PA}<0.77
Collapsed	0.77≤ D_{PA}

Table 3.6. Damage levels and corresponding D_{PA} values- Ghobarah et al (1997)

Damage Conditions	D_{PA} values
Elastic limit	0.05
Minor damage limit	0.14
Repair limit	0.40
Collapse prevention	0.60
Collapse	1.00

This index was implemented in the original release of IDARC nonlinear time-history program that was used in the development of the energy demand spectra in Chapter 2. The recent release of IDARC (IDARC2D- 6.0) uses a modified version of Park and Ang Index,

in which the moment and curvature terms are used instead of force and displacement, as follows;

$$D_{PA} = \frac{\phi_m - \phi_y}{\phi_u - \phi_y} + \beta \frac{\int dEH}{M_y \phi_u} \tag{3.13}$$

In this study, the formulation of 3.13 and the damage conditions given in Table 3.6 were used in the determination of the energy dissipation capacity of the RC members which was the basis of the proposed design procedure, as explained in following sections.

3.3. Proposed Energy Dissipation Capacity Procedure

Proposing a procedure in the derivation of the capacity is a very challenging attempt in earthquake resistant design, due to the complex terms of references. The uncertainties are exceptionally high in the prediction of the seismic forces those are reverse-cyclic, absolutely random and random in frequency and in duration. Therefore, finding the exact solution to the equation of motion of a SDOF system subjected to a future earthquake motion is impossible even after many years of research (Nakashima, 1997). This fact makes the any procedure, aiming to define the capacity of the engineering structures safe and sound against earthquakes, nothing else than an approximate approach. More than 200 steel buildings those were constructed according to the latest design codes in Los Angeles experienced severe damage during the Northridge earthquake, Whittaker et al. (1998).

Researchers have been addressing the most compatible design procedures based on the latest data of both earthquake ground motion records in demand prediction and the extensive laboratory test results those reflect the nature of the seismic action as much as they can. However, in spite of the all efforts, there must be a margin of safety in the assumption of the procedures describing the seismic force, deformation and lately energy dissipation capacity of the structures and their structural members.

This study proposes an energy dissipation capacity procedure for the reinforced concrete members (cantilever beam and columns) while taking into the account of the "structural performance" concept and low cycle-fatigue theory. Even if the studied systems

are very simple structures, they represent the precast structures and bridges those are widely used in civil engineering. Therefore, the procedure described here must be improved if the energy dissipation capacities of more complex structures are needed.

3.3.1. Hysteretic Behavior In The Energy-Dissipation Capacity Procedure

Current design codes limit the interval of the lateral reinforcement in RC members in order to prevent the shear-dominant behavior, ACI 318, ABYYHY-2008. Because, the damage of the ductile the members can be controlled up to certain load or deformation level unlike the sudden failure of the brittle systems (shear). Based on this provision, the constitutive rules representing the flexure behavior of the members have been utilized in the development of the proposed design procedure and shear failure is kept out-of-scope.

The numerical model parameters used in this study have been obtained from the full-scale RC column tests conducted in Structural and Earthquake Engineering Laboratory of ITU using earthquake simulated loads. Analytical calculations were performed to derive the hysteretic behavior rules by using IDARC2D a non-linear time-history analysis program which can evaluate the numerical models under static, quasi-static and dynamic loading. In Sürmeli (2008), quasi-static analysis was performed for each specimen by applying piecewise linear cyclic displacement history as in the experimental study in order to simulate the hysteretic behavior of the full-scale RC test specimen. The success of the obtained hysteretic behavior was satisfactory enough as seen in Figure 3.6;

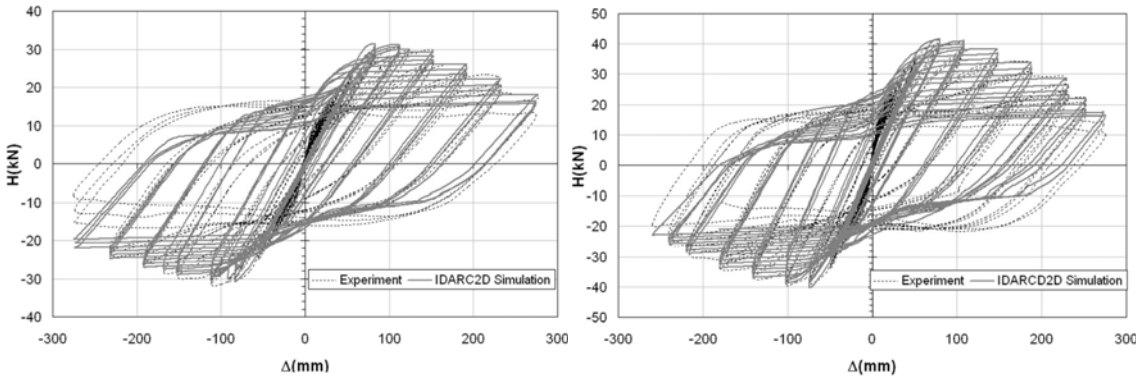

Figure 3.6. Comparison of the base shear vs. top displacement relations between experimental and numerical works

It is possible to define the hysteretic rules as tri-linear or smooth curves with respect to the parameters representing the change in stiffness, strength and shear of the system in IDARC2D program (Reinhorn and Sivaselvan, 1999; Sivaselvan and Reinhorn 2001). While developing the energy demand spectra in chapter 2, the generic tri-linear behavior rules were employed since they represent the widely used flexural and shear-slip mathematical models, such Clough, Takeda with and without slip. However, it is required to utilize more realistic behavior rules in the development of the energy-dissipation capacity of the RC members due to the need of being more rational regarding the natural behavior of such an element. Sürmeli (2008) obtained the most appropriate hysteretic rule parameters used in IDARC2D program, Table 3.7;

Table 3.7. Parameters of the smooth hysteretic model Sürmeli (2008)

Specimen no	α	β_1	β_2	R_s	σ	λ	N	η
S30_18	4	0.10	0.10	0.08	0.02	0.60	2	0.49
S35_18	3	0.10	0.12	0.07	0.02	0.60	2	0.49
S40_20	4	0.10	0.12	0.13	0.06	0.60	2	0.49

The given parameters developed for the test results of the specified specimens; however, in developing the energy-dissipation capacity of the members, the mean values were used in the hysteretic behavior rule.

Table 3.8. Parameters of the smooth hysteretic model used in this study

α	β_1	β_2	R_s	σ	λ	N	η
3	0.10	0.10	0.09	0.03	0.60	2	0.49

3.3.2. The Properties of The Structural Members Evaluated In The Capacity Procedure

The flexural behavior of the structural members is desired in the current design guidelines. The best way to describe the flexural properties of a member is through the moment-curvature relation that is related to the geometric and strength properties of the

cross section and the material that was made of. A moment-curvature relation give a clear idea of the cracking, yielding and ultimate capacity of the members since the curvature is directly related to the chord rotation at the cross-section. The damage due to the flexural forces (axial force and bending moment) can be explicitly observed in the moment-curvature plots.

Therefore, a set of moment-curvature relationship for square sections (30x30 cm, 40x40 cm and 50x50 cm) were calculated by using a section analysis program, XTRACT which calculates the moment-curvature values and strains in concrete compression and steel tension. These results are used in the prediction of which state the cross-section reaches under the given loading condition. The section analysis program, XTRACT is also capable of calculating the P-M interaction relations that is very important in the response of the RC members in case of axial loading exists (RC columns).

The greatest advantage of IDARC2D is the fact that the skeleton of the program was based on the laboratory researches. Therefore, it is possible to establish a numerical model by using almost all available data that is employed in the laboratory tests. This fact enables the researchers to simulate the experimental work as much good as in the numerical studies. The current study is really based on the success of the IDARC2D program that is capable of performing static, dynamic, quasi-static and adaptive push-over analysis.

The analysis program of IDARC accepts the tri-linear moment-curvature relationship. Therefore, it was needed to idealize the results of XTRACT program by converting to consistent line series. Even though, the XTRACT program is capable of idealizing the curves except for cracking point; a small program based on the idea presented in Reinhorn (1997) was written in MATLAB that converts the cross-section analysis results to tri-linear relationship, Figure 3.7.

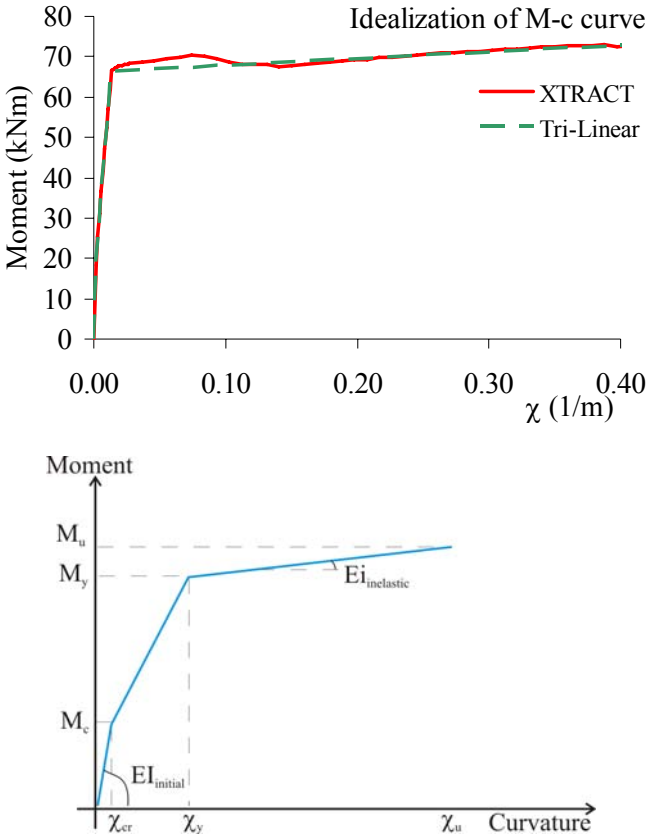

Figure 3.7. Idealization of moment-curvature relationship

Should there present the axial load on the RC members, the response of the member changes due to its composite content. This is calculated as in the axial force-moment interaction diagram which has certain points those describe the crucial physical changes in the member. The analysis program of IDARC2D takes also this information into the numerical model, which improves the accuracy of the analysis. The characteristic point of the P-M interaction curve that must be included in the analysis is shown in Figure 3.8.

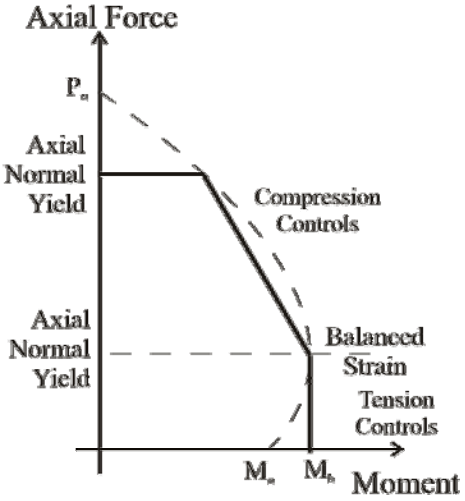

Figure 3.8. Interaction diagram and the modeling parameters

While developing the energy-design capacity procedure, commonly used structural members having cross section dimensions of 30x30, 40x40 and 50x50 were chosen as the case elements. In fact, the developed procedure is easily adopted for the different cross-sections since the behavior of the section is defined as in moment-curvature relationship instead of detailed geometric descriptions. The three set of members were assumed that they have symmetric longitudinal reinforcement and well confinement, confinement interval is 10 cm as given in the design codes (ABYYHY-2007, ACI318). The longitudinal reinforcement ratio of the all cases ranges from one to four percent of the gross area of the section, Figure 3.9. Minimum and maximum values of this range are stipulated by the current design codes.

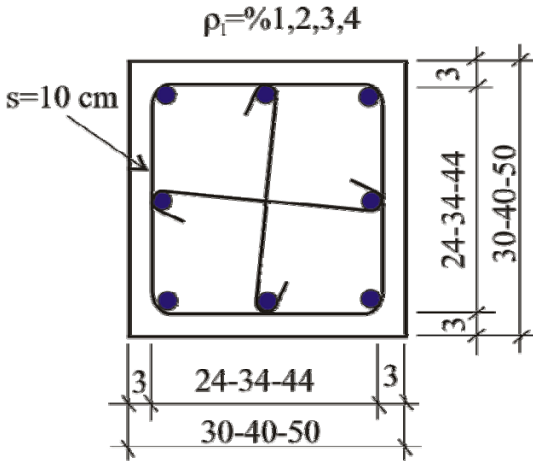

Figure 3.9. Reinforcement detail of the cases

The strength of the materials used in the numerical models have been differed in the concrete as 20 MPa and 25 MPa, while the yield and ultimate strength of the longitudinal and lateral reinforcement are 420MPa and 550 MPa, respectively, as in Figure 3.10.

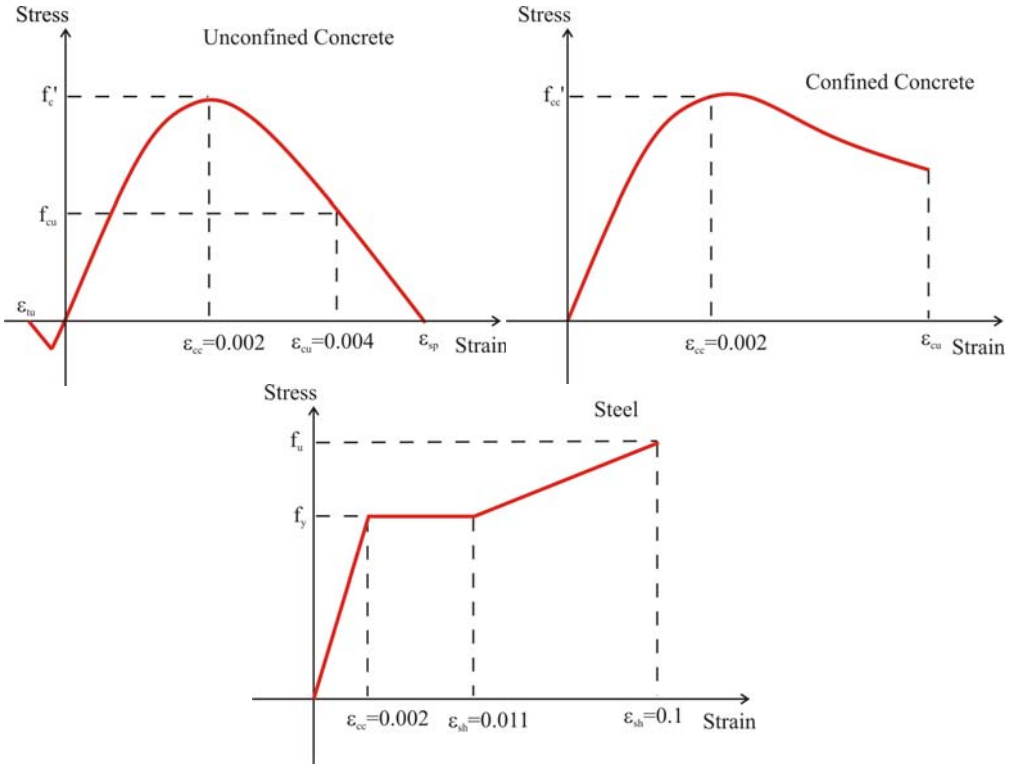

Figure 3.10. Material models used in this study

(Mander unconfined/confined concrete model, reinforcing steel with hardening)

As come to the member geometry, in order to confirm the flexural member ratio of the height-to-section dimension which is greater than 10, the height of the member were taken 3m, 4m and 5m. It is worth to say that, the axial load level of the case members are less then twenty per cent of their capacity. Thus, the buckling of the column members were not investigated.

3.3.3. Low-Cycle Fatigue Theory

Even though the fatigue philosophy was developed for the metals in 1940's, Miner (1945), Manson (1953) and Coffin (1954), this philosophy has been found a large basis in

the earthquake response of the structures studies. Contrary to the metals, the earthquakes result low in cycle but incredibly high in amplitude of structural response. Many researchers developed the analysis and design procedures by modifying the formulations developed in the classical fatigue theory.

Among these research studies, two laboratory tests those, conducted in Building and Fire Research Laboratory (BFRL), Maryland and Middle East Technical University (METU), Ankara, resulted very interesting findings in the application of fatigue in earthquake resistant design. They were aimed to compare the results of the constant amplitude and variable amplitude quasi-static pull-and-push test on the Reinforced Concrete column and beams.

The first test in BFRL investigated the cumulative damage in RC circular bridge piers. 12 identical quarter-scale bridge columns were tested in two phases (i) constant amplitude (low-cycle fatigue characteristic) and (ii) variable amplitude (seismic characteristic) tests. The results of both phases used in the determination of the effects of the load path on cumulative damage, Figure 3.11.

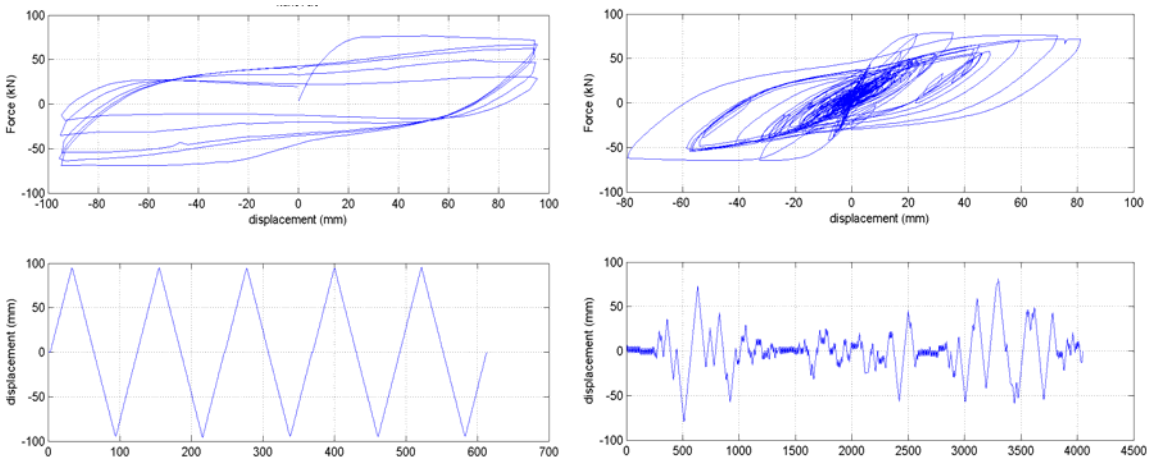

Figure 3.11. Test protocols conducted in BFRL 1997 (PEER database)

Test observations indicate two potential failure modes: low cycle fatigue of the longitudinal reinforcing bars and confinement failure due to rupture of the spirals. The former mode is mainly due to the large displacement amplitudes in excess of 4 per cent

lateral drift, while the latter is due to larger number of smaller amplitude cycles. The study concludes two important findings:

- *"Energy-dissipation capacity of members is path-dependent; hence, models of seismic damage that rely on measures of energy dissipation cannot predict failure in it is not related to ductility.*
-
- *Standard cyclic testing may provide information on the behavior of members and the potential effects of certain material and geometric parameters on seismic response, but must not and can not be used as a measure of energy-dissipation capacity of members."*
-

The first conclusion given above convince the author to avoid the differencing path in the capacity procedure, while the latter supports this idea in a way that the constant amplitude test should be preferred rather than monotonically increasing or varying amplitude analysis.

The second test on the low-cycle fatigue study was conducted in METU used the cantilever RC beams. Total 17 RC beams in three groups were used in the constant and variable amplitude tests. The groups of the specimen were classified according to the test protocol; (i) one in monotonic type of loading, (ii) twelve specimens with constant amplitude, (iii) four specimens with variable amplitude. This second reference test aimed to investigate the low-cycle fatigue principles in conjunction with the damage prediction and hysteretic rule definition by assessing the energy dissipation characteristics of the RC members. However, two of the conclusions which the study reaches have a gained substantial feature on the development of the proposed energy-dissipation capacity procedure;

- *"The most stable response parameter obtained from the experimental results is the dissipated energy per cycle. A normalized form of cyclic energy dissipation may characterize the global dynamic performance of structural systems satisfactorily.*
-
- *For short period systems with five per cent viscous damping, hysteretic to input energy ratio, EH/EI, seems to be constant and independent of the type of the motion. As the period*

increases, the ratio decreases indicating that more of the energy imparted to the structure is dissipated by viscous damping rather than hysteretic damping."

The first conclusion encourage to utilize the fatigue principle in the proposed energy-dissipation capacity procedure while the second conclusion substitutes the capacity design procedure into the design methodology complemented with the energy demand spectra study given in the previous chapter.

3.3.4. Application of Low-Cycle Fatigue Philosophy Combined With the Performance Theory

The crucial point in the displacement-based design is the state limits defined as the structures should satisfy during the ground motions. This theory have been introduced the engineers to select which performance level that the structure is expected to satisfy. This selection is -in reality- left to the owner of the building who should consider the cost of the retrofitting of his/her building if it experiences earthquake motion. The flexibility of selecting the performance level according to the building owner however gives huge responsibility to the designer who should not forget the main principles of the engineering; (i) most economic design, (ii) no compromising from the safety of the residents living or working in the building.

The proposed energy-dissipation procedure combines the low-cycle fatigue theory and performance level approach for RC members (cantilever beams/columns) by displacing the tip of the member with constant amplitude that is defined with respect to the system performance level drift ratios, whilst the deformation at the critical section is kept below the pre-defined performance level. The back and forth displacing the system is repeated (i) the damage index of Park and Ang reaches its performance value, given in table 3.6, or (ii) the strength of the system drops 20 per cent of the maximum strength. The first stop criteria was explained in details, however, the latter is a generally accepted rule in the laboratory tests (Razvi and Saatcioglu,1994). This quasi-static constant amplitude simulation is utilized for three cross section with their four different longitudinal reinforcement ratio and the axial load ratios of zero-, five-, ten- and twenty per cent of its axial load capacity. These axial load ratios represent the commonly designed load levels on

beams and columns. In excess of 20 per cent load carrying ratio, displacement ductility of the member tremendously drops which avoids the flexural behavior under adequate ductility.

In order to utilize the briefly explained procedure, a computer program was developed in MATLAB, and the algorithm of the program is given in Figure 3.12;

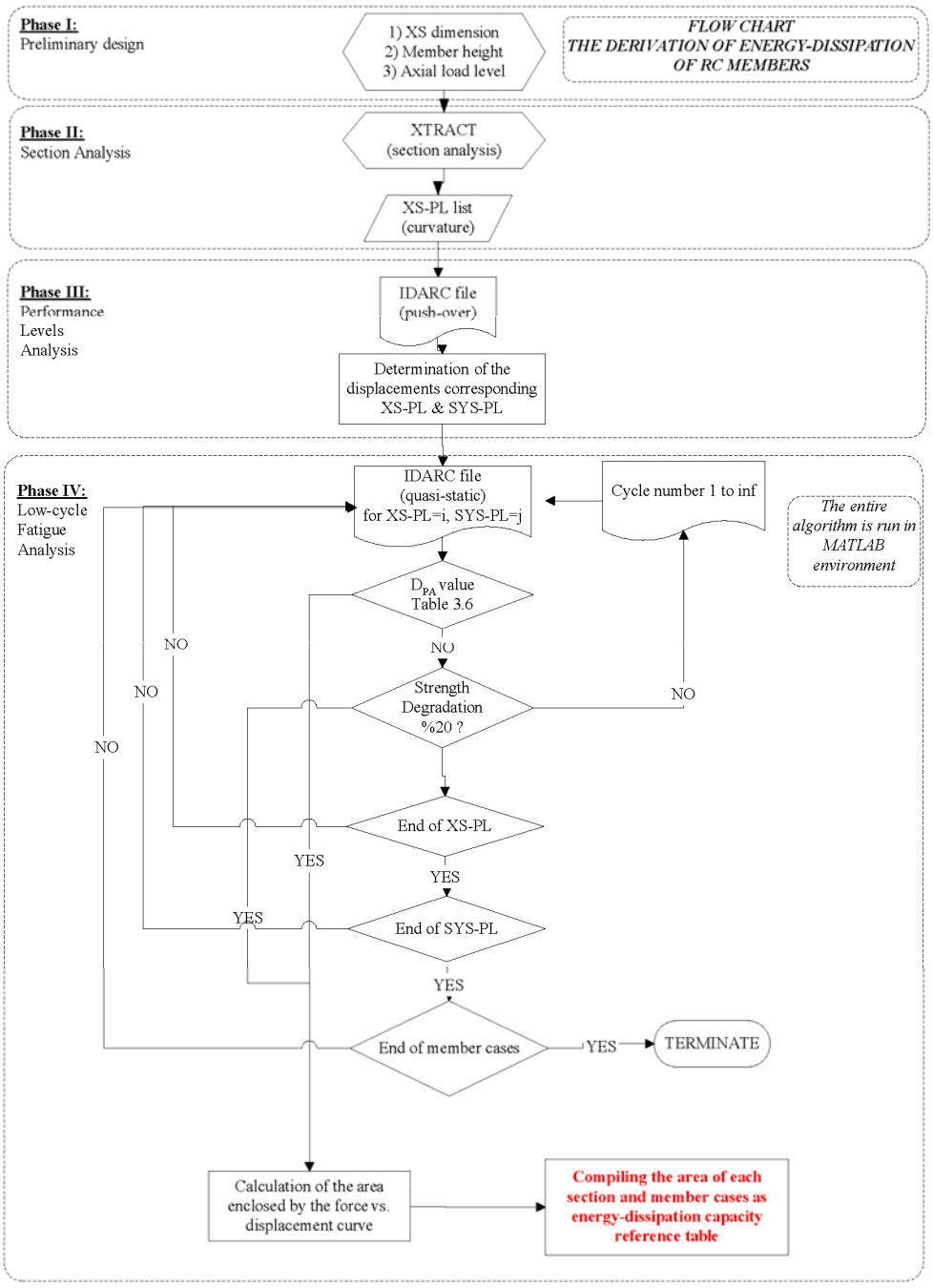

Figure 3.12. the algorithm of energy-dissipation capacity procedure

The challenging of the introduction of the performance level comes from the comparison of the system and section performance levels, which have commonly met in displacement values. This is provided by investigating the results of the monotonic increasing static analysis (push-over) which gives the deformation and the lateral load carrying capacity of a member. Probably, the most confusing point in the section is to combine the section and performance levels on the same graphic. In spite of the fact it may not be true for Multi Degree of Freedom Systems due to the complex section damage distribution (or performance states), it is possible in the case of SDOF system, a fixed base and free end system which is actually nothing else than a single column or beam. A push-over analysis results not only resisting force vs. top displacement, it is also calculated the elastic and plastic rotations and consequently the curvature at the critical section where likely the damage occurs as in Figure 3.13.

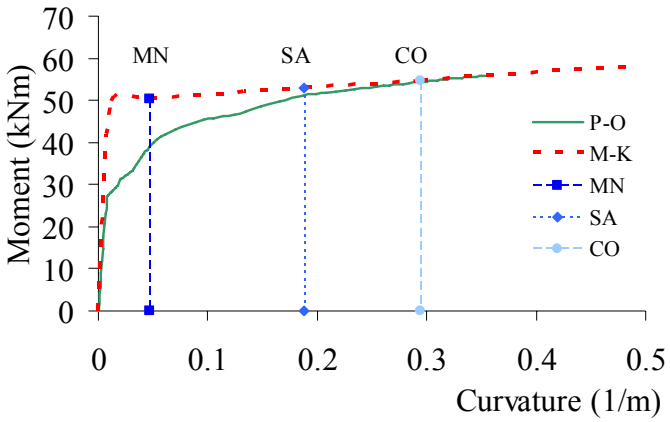

Figure 3.13. Combination of MK from P-O and XTRACT

After determined the curvatures where the performance damages occur, the corresponding displacement values and, beside, the system performance level displacement (as of drift ratios Table 3.2) are depicted on the same plot, Figure 3.14. For the each Section-System Performance Level pairs, the most appropriate displacement value is taken as the amplitude of the quasi-static test simulation which was described in Figure 3.12.

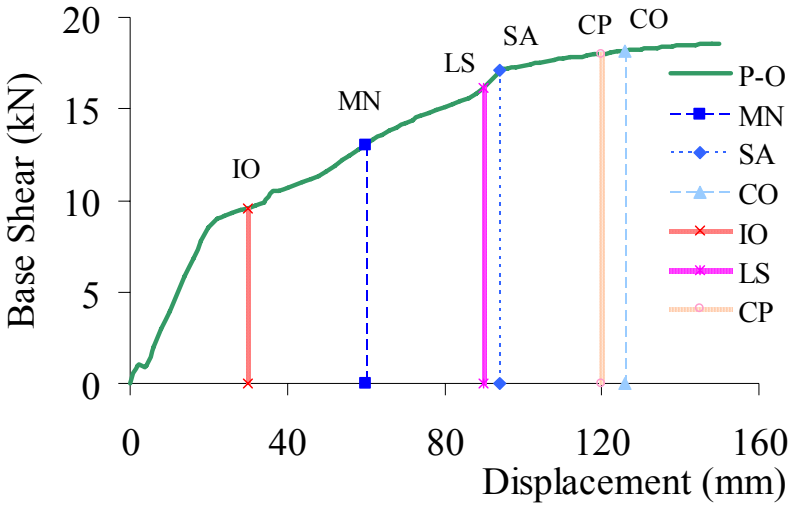

Figure 3.14. Combination of force-displacement from P-O and XTRACT

As an example, if the member is supposed to remain in the limits of Immediate Occupancy (IO) and Minimum damage (MN) level, the constant amplitude of the tip displacement is taken as the 30 cm drawn as the first line on the far left under push-over come which resembles the displacement of the Immediate Occupancy level.

An example of the low-cycle fatigue test result is given in figure 3.15 where the constant amplitude and the deterioration is obvious.

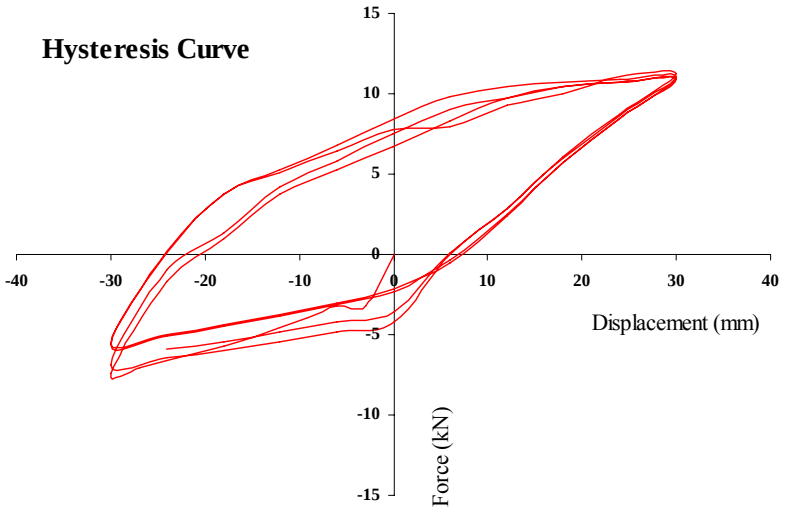

Figure 3.15. A typical example for low-cycle fatigue hysteresis

3.4. Energy Dissipation Capacity

The proposed energy dissipation capacity procedure is introduced for a range of RC members that represent the commonly used in civil engineering. This representation enables this study on the development of the algorithm rather than the optimization according to the current design methods. This limitation may be welcomed since the procedure requires only the moment-curvature relation of the interested section and the rest is the same for all members.

On the other hand, the work done by the external forces and the resistance of the corresponding internal forces establish the energy capacity equation. The basic definition of the work requires the external force acting on the member and the deformation of the member. Therefore, the origin of the energy dissipation capacity procedures start from the establishment of the cross section and the member that the section is assigned. It might be paradigmatic to take the system height into the capacity formulations; however, there is not any other way to describe the energy dissipation of the system that is not geometrically defined. This challenging assumption is utilized with respect to the shear span ratios of the flexural members. the definition of the shear span is the rate of the length of the memner to the perpendicular depth of the section and this parameter has been widely used in the laboratory tests those research the affects of some terms (i.e. reinforcement ratio, confinement, axial load ratio), Berry et al. (2004). The range of the shear span affects the behavior of the RC member as explained in Ersoy and Özcebe (2004). The ratio lower than 3 is prone to the sudden drop of the shear resistance that leads to brittle failures, the ratio between 3 to 7 may suffer from the shear cracks unless the adequate confinement is provided, and finally, the ratio greater than 7 performs a flexural behavior. The upper limit of the shear span is limited to 10 in EC8 which is also respected in this study. Based on the adequate confinement along the height of the member is provided, the shear span ratio range is taken from 3 to 10.

The width of the columns is not taken into the consideration because the moment curvature relations of the columns 3~4 times larger than the effective depth are not significantly different from the rectangular columns. However, the reduction of the width

of the section reduces the curvatures tremendously. Thus, the studied column members are taken as rectangular and commonly used in the precast column design.

As come to the longitudinal reinforcement ratio, all the design guidelines mandate the use of minimum reinforcement in the RC members while also limit the upper ratio. The interval of the longitudinal reinforcement was taken as %1 percent between minimum and maximum values of one to four per cent, respectively.

A similar approach is also seen in the classification of the axially loaded members. The axial load level changes the flexural behaviors, as seen in preceding sections. Therefore, for the sake of having a flexural behavior, the axial load level is kept between 0 to 20 per cent of the axial load capacity. Due to the sudden drop of the moment capacity of the high axial load levels, it was not intended to enlarge this study to this special type of the columns.

Table 3.9. The geometric and mechanical properties of the studied members

Definition	Range
Cross Section Dimension (a-b)	Square sections of 30cm, 40cm and 50cm
Shear Span (S)	3-10
Concrete strength (fc)	20MPa and 25 MPa
Reinforcement yield and ultimate strength (fy & fsu)	420MPa and 550MPa
Longitudinal reinforcement ratio (ρ_l)	% 1, 2, 3, 4
Axial Load level (P/P0)	% 0, 5,10, 20

The aim of these different properties of the models is to investigate the influence of each property on the energy-dissipation values of the members in low-cycle fatigue loading. The following chapters present the variation of the energy-dissipation values of the each case that was called as “energy-dissipation capacity” for the given performance levels.

3.4.1. Influence of the Geometric Properties

Since the energy-dissipation capacity is dependent on the section and the member properties, therefore, the following sections discuss how they affect the energy dissipation.

3.4.1.1. Cross-Section Dimension. The deformation capacity of a member is directly related to its moment of inertia which is the function of section dimensions. It is expected that the larger the section, stiffer the member. Therefore, the ability of the tip deflection of the inversed cantilever systems will dramatically reduced. This act will increase the flexural rigidity of the system if one would like to deform it up to certain level. As seen in Figure 3.16, the displacement controlled test simulation of low-cycle fatigue yielded the energy dissipation results that confirm the expectation expressed above. Figure 3.16 show that the area enclosed by the dictated tip deflection versus resisting force increases as the gross section dimensions increase for all span shear ratios of a system at different performance levels.

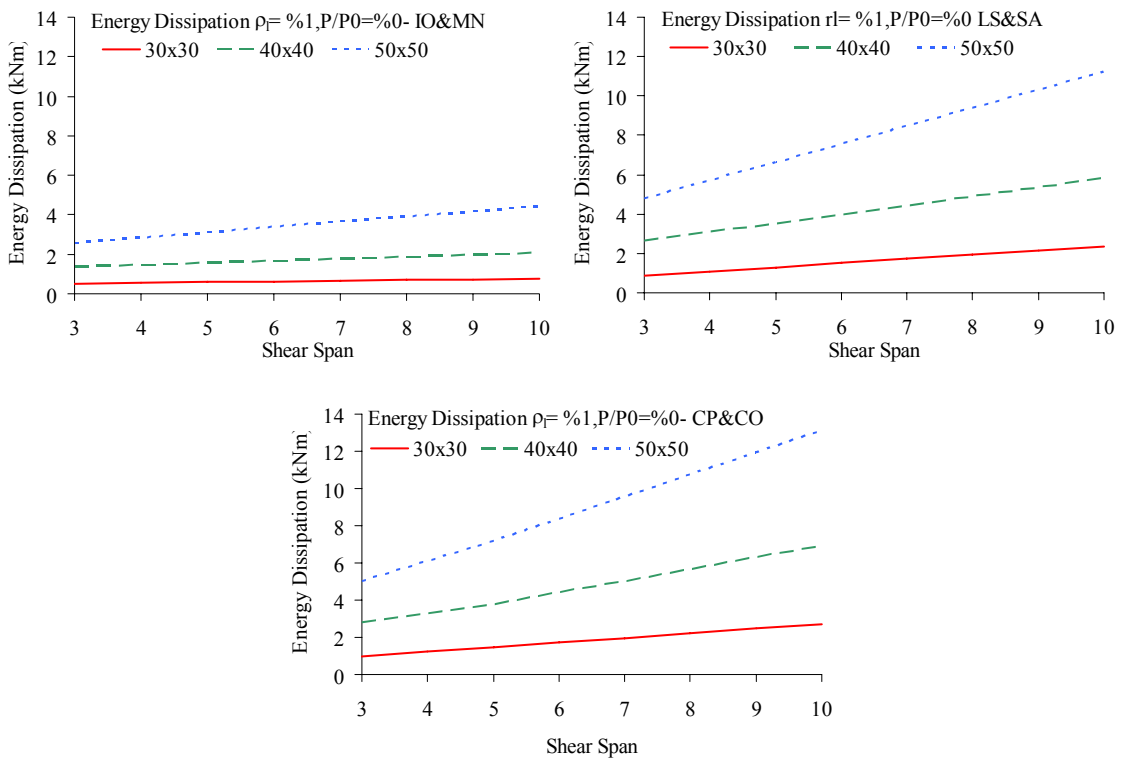

Figure 3.16. Influence of cross-section dimensions on energy dissipation capacity for the performance different performance levels

3.4.1.2. The Shear Span. It is known that the shear span of flexural member confronts a characteristic similarity for the member's resisting force. Nevertheless what the shear span rates are, the resisting forces, and corresponding bending moments at the bottom, are almost same. However this is not true for the tip deflection of the member. This is easily observed in the energy dissipation graphics given in Figure 3.17. The energy dissipation of a member with different cross section is plotted.

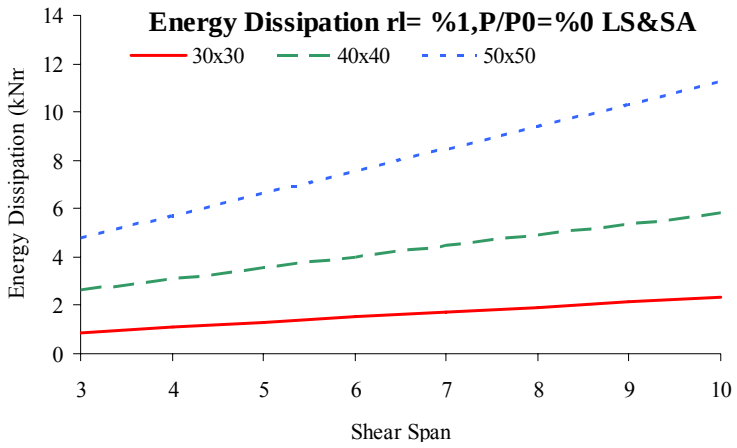

Figure 3.17. Influence of shear span (30x30cm, %1 reinforcement)

3.4.2. Influence of The Mechanical Properties

The mechanical properties of the members should be classified as to

(i) The reinforcement configuration (ρ_l)

(ii) Axial load level (N)

3.4.2.1. The Reinforcement Configuration. The increase in the amount of the longitudinal reinforcement in the RC sections does not significantly affect the flexural stiffness and ductility as compared to its affect on the strength which tremendously increases, Figure 3.18.

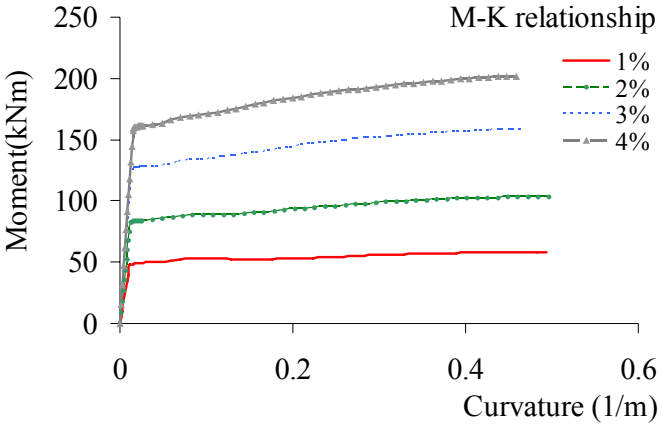

Figure 3.18. The influence of reinforcement ratio on M-K relationship

Then a question rises in mind that "how does the increase in reinforcement ratio change the energy-dissipation, Even though the flexural stiffness of the section does not change significantly?"

Since the energy dissipation is proportional to the deformation amount and the force resistance of the member, there must be a relation between the flexural behavior of the member and its energy-dissipation. Actually this is obvious when the lateral force-capacity curves are compared as in Figure 3.19

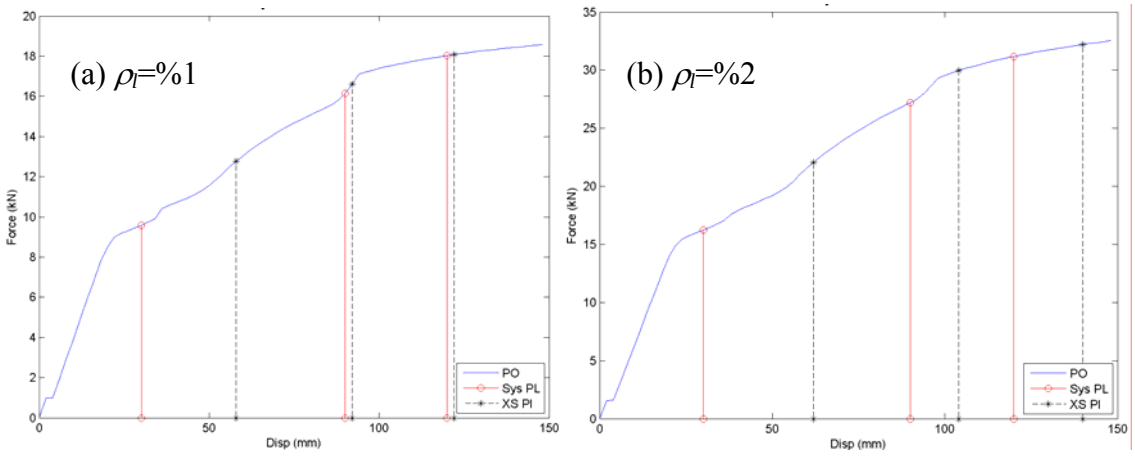

Figure 3.19. The influence of reinforcement ratio on lateral load carrying capacity (3m in height and 30x30cm in section dimensions)

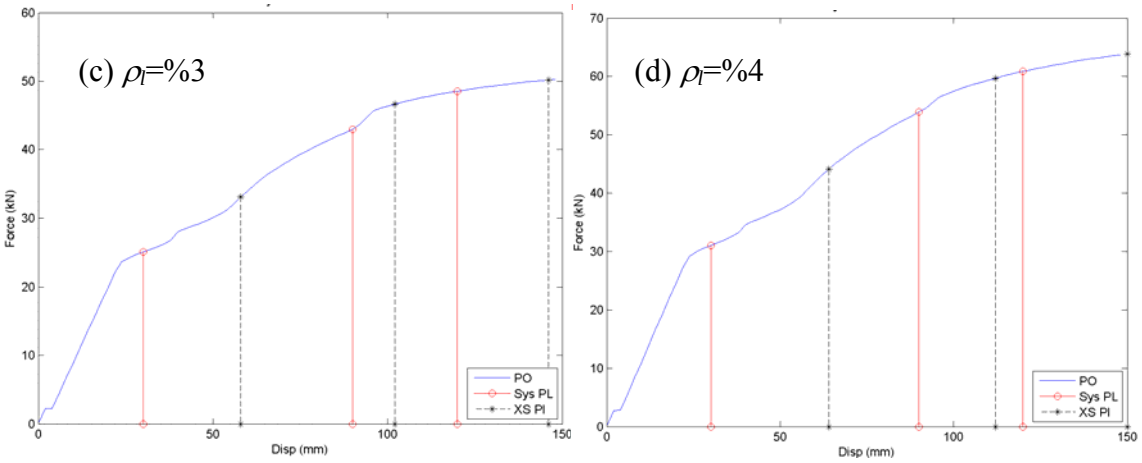

Figure 3.19. The influence of reinforcement ratio on lateral load carrying capacity (3m in height and 30x30cm in section dimensions) (cont'd)

As seen in Figure 3.20, the deformation capacity of the member is almost same for all different ρ_l values; however, the load carrying level significantly increases as the ρ_l values increases. Another significant change is observed in the section performance levels, which resembles the damage in the section. The section performance levels shift to the right likely as the strength of the section increases.

As come to the question asking the relationship between the increase in the longitudinal reinforcement and the energy-dissipation capacity, the Figure 3.20 shows increase trend for different ρ_l values, as expected.

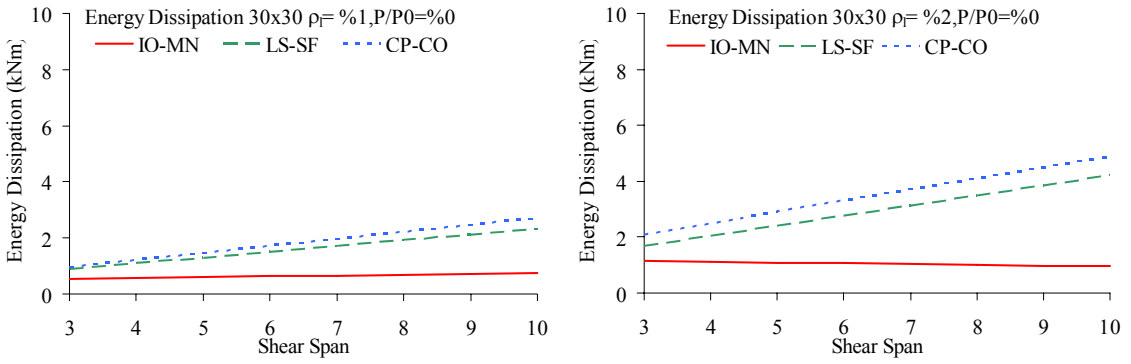

Figure 3.20. The influence of reinforcement ratio

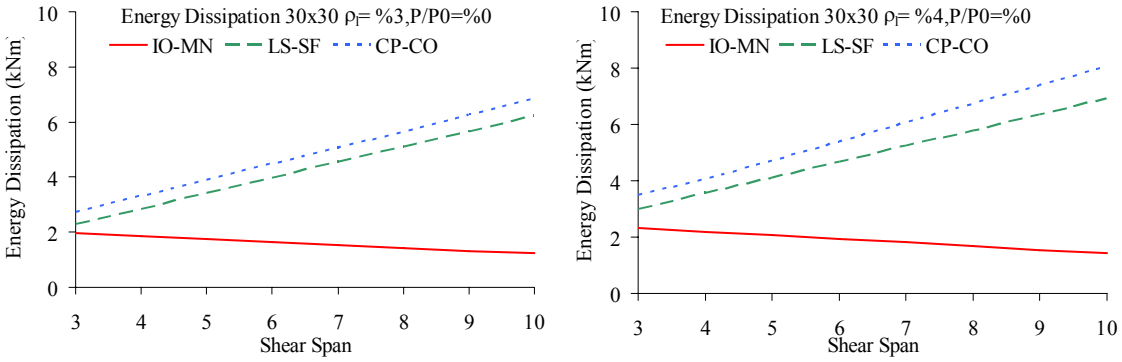

Figure 3.20. The influence of reinforcement ratio (cont'd)

As seen in Figure 3.20, the increase in the reinforcement ratio lets the increase in the energy dissipation due to the fact that the strength of the member increases even if the initial stiffness is not changed. But increased strength means the increased resistance and the higher ordinates of the hysteretic loops. Eventually, this results the increment in the area of the loops.

However, Figure 3.20 also shows that there is declination for the performance level or IO & MN that is close to the elastic region. It seems paradigmatic to see such a trend opposite of the others at first glance. But this act comes from the higher resistance of the system having greater reinforcement ratio. As will be seen in next section, the increase of the axial load will change this strange reduction.

3.4.2.2. Axial Load Level. One of the crucial issues for the RC members is the axial load level, because axial loads acting on the flexural members significantly change the lateral load and moment carrying capacity, and displacement ductility (Ersoy, 2002). The best practice is given by the moment curvature relationship of the same member with and without axial loads, as in Figure 3.21; similar to the increment of the longitudinal reinforcement ratio, the strength of the section increases, while the ductility enormously drops.

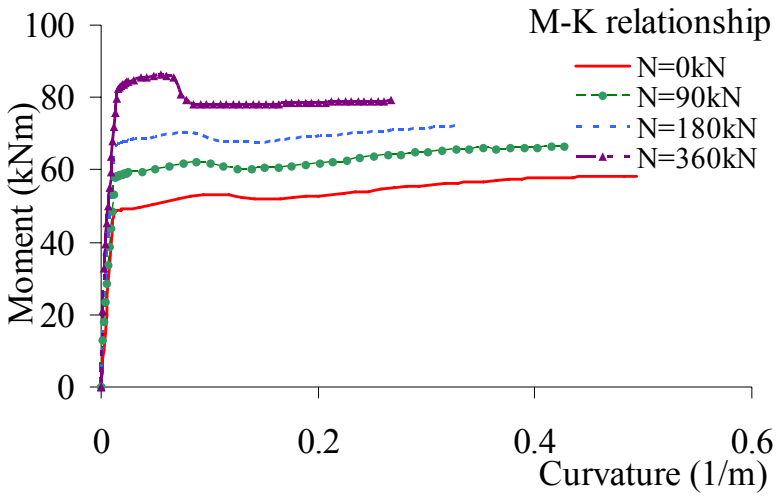

Figure 3.21. The influence of axial load on M-K relationship

The increase in the axial load acting on the member also changes the energy-dissipation of the member since the deformation of the member is associated with the flexural stiffness of the member.

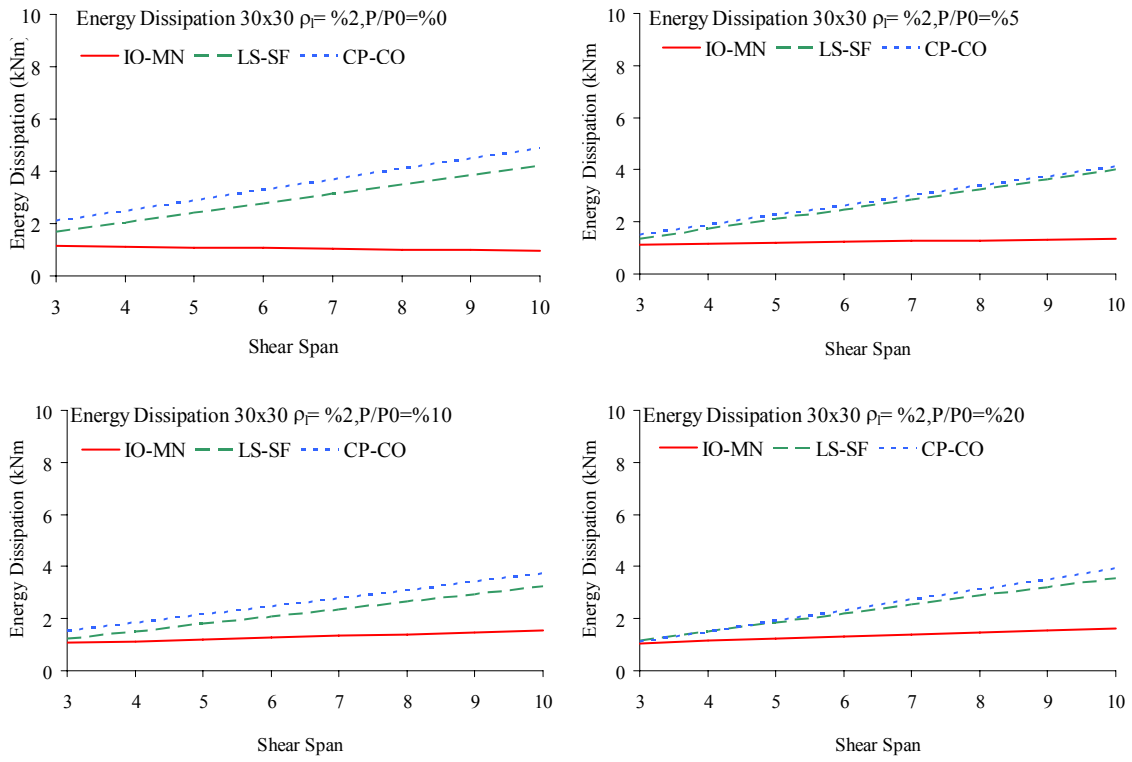

Figure 3.22. The influence of axial load on energy dissipation

3.4.3. Energy-Dissipation Capacity Charts and Tables

The results of the low-cycle fatigue analysis for the varying gross sections and the shear span of the system and also different reinforcement ratio and axial load levels are plotted into the design charts below and the table of the energies is given in Appendix D;

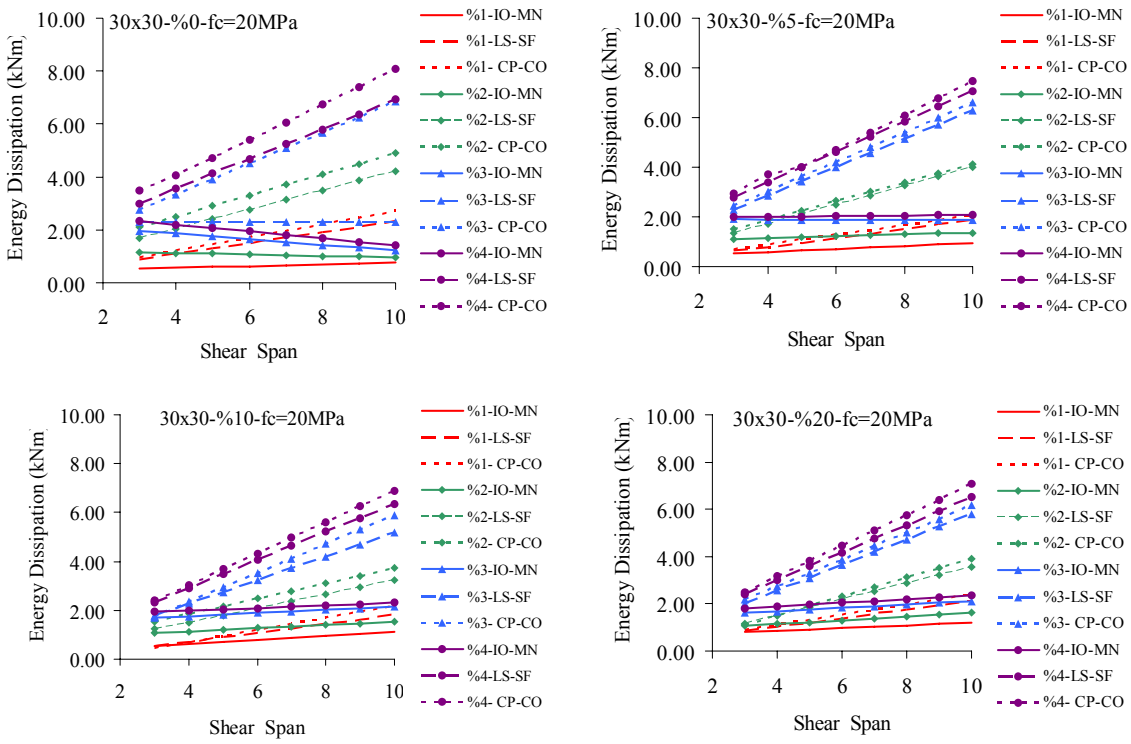

Figure 3.23. The energy dissipation chart of 30cmx30cm section (20MPa)

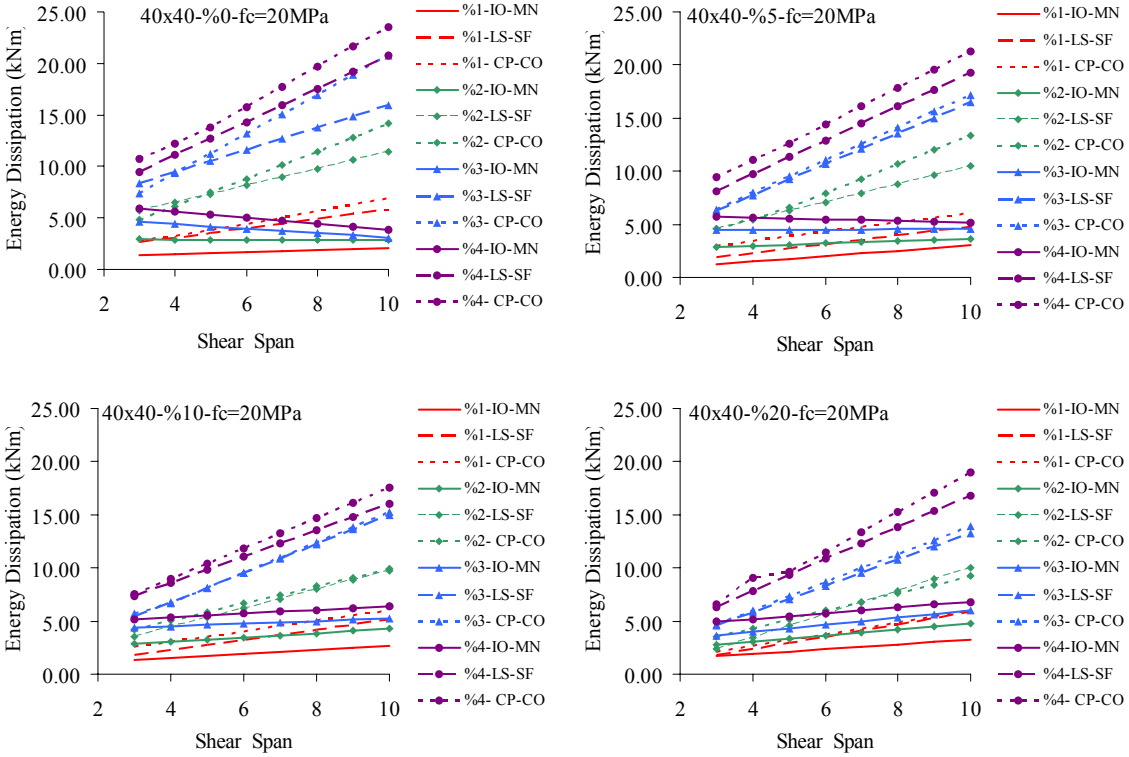

Figure 3.24. The energy dissipation chart of 40cmx40cm section (20MPa)

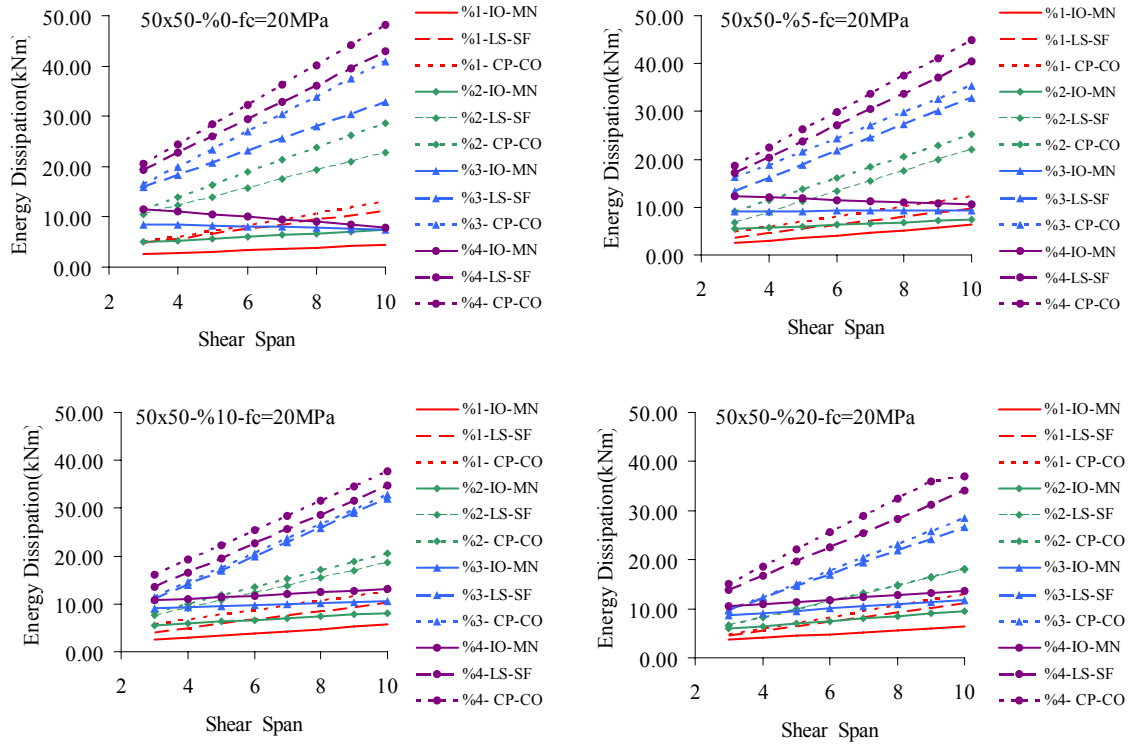

Figure 3.25. The energy dissipation chart of 50cmx50cm section (20MPa)

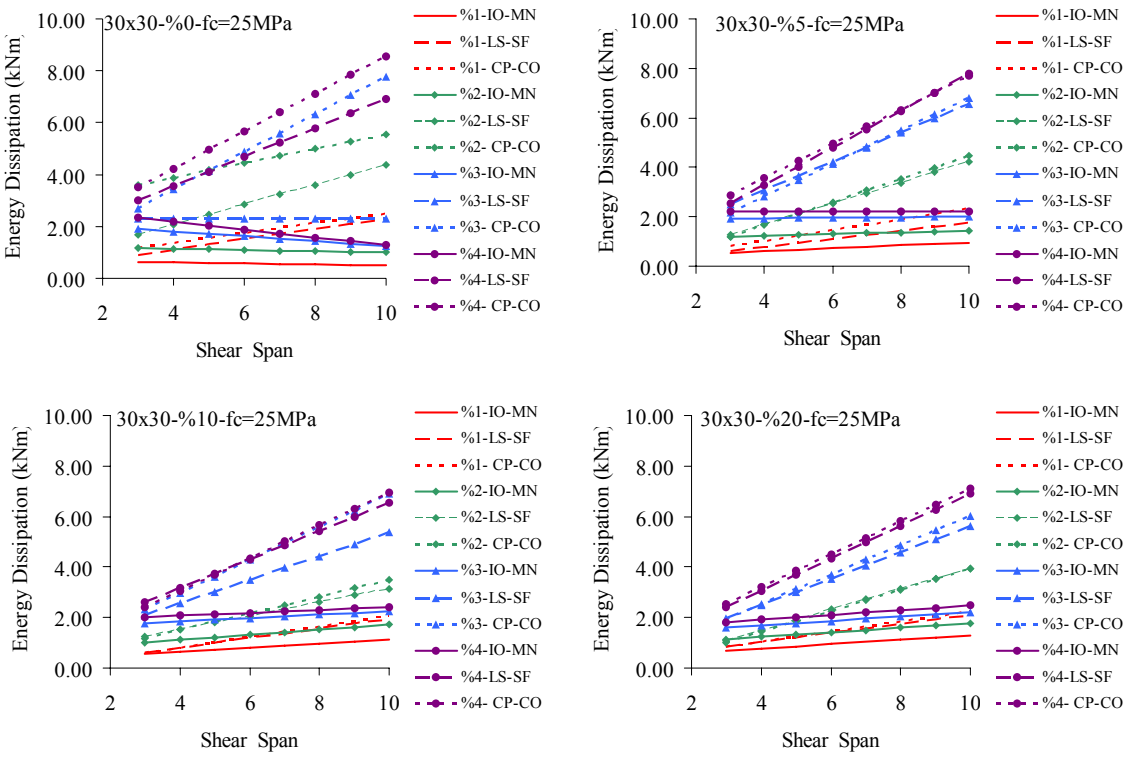

Figure 3.26. The energy dissipation chart of 30cmx30cm section (25MPa)

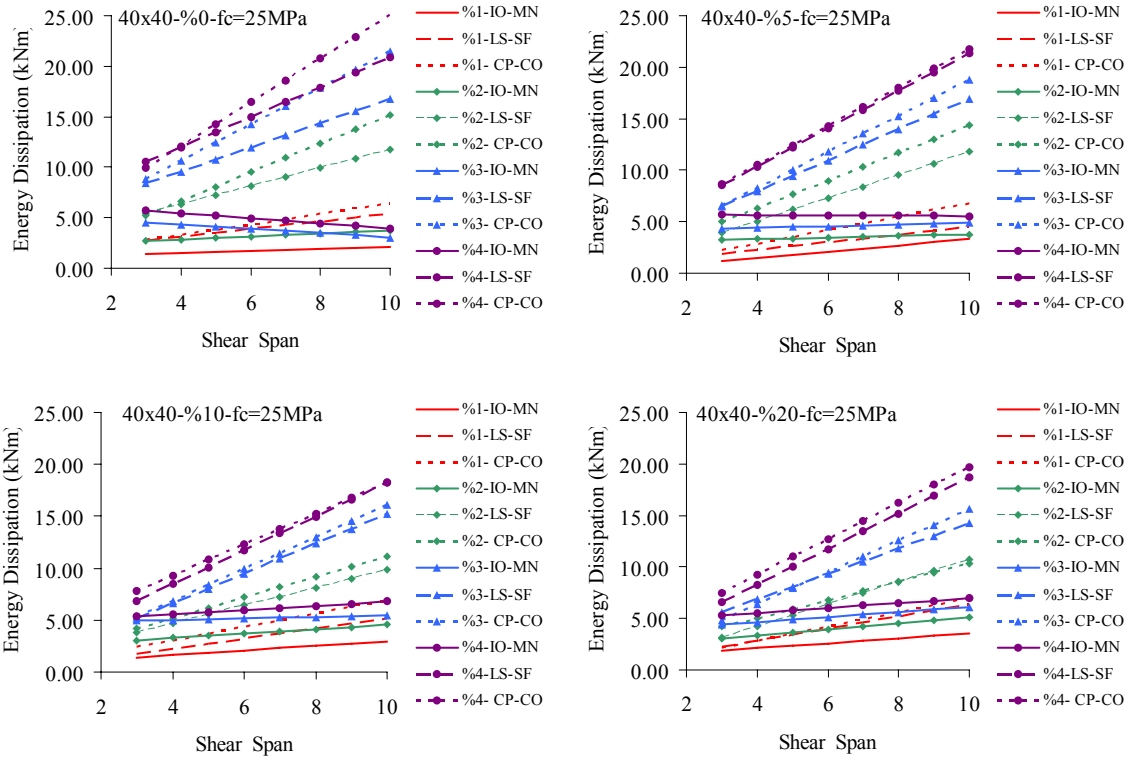

Figure 3.27. The energy dissipation chart of 40cmx40cm section (25MPa)

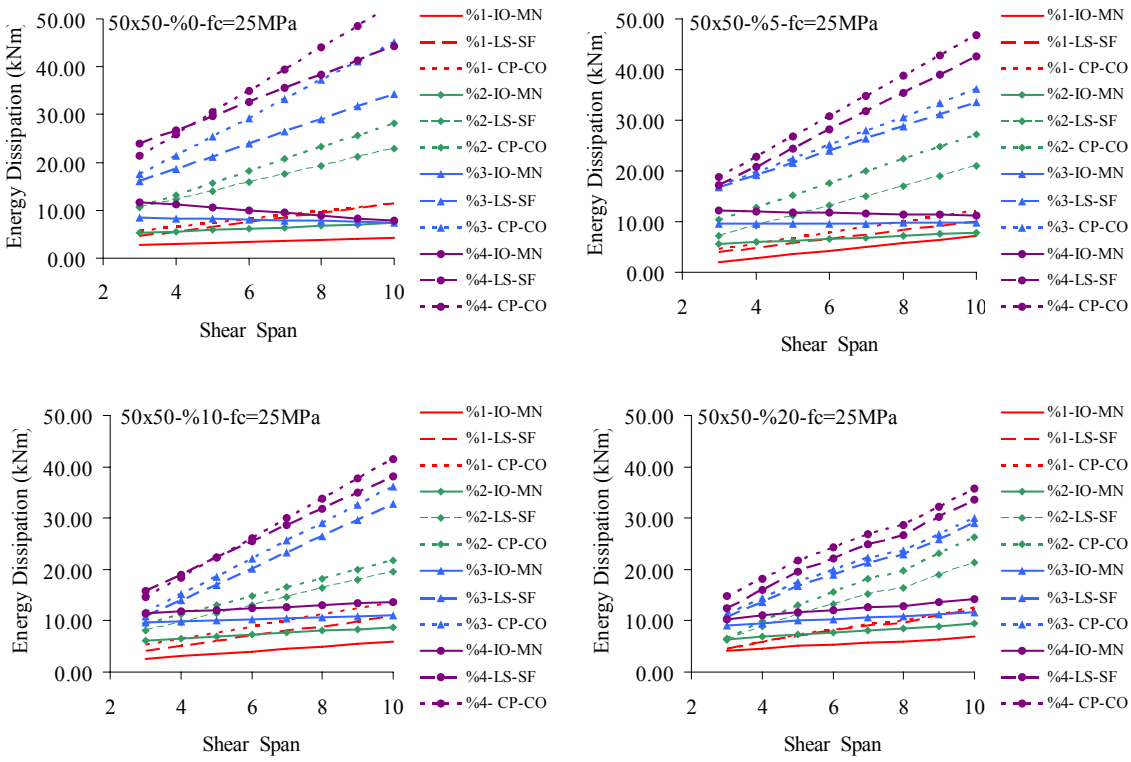

Figure 3.28 . The energy dissipation chart of 50cmx50cm section (25MPa)

4. DESIGN METHODOLOGY

4.1. Earthquake Resistant Design of the Structures

4.1.1. Description of Earthquake Resistant Design

Since the beginning of 1900's, structural engineers have been taking major load sources into their design considerations. One of these major load sources is the earthquakes caused by the strong ground motions. It is well known that the earthquake resistant design is a set of proposed procedures those are developed according to the latest knowledge in the seismology and in the structural behavior (material and configuration of the vertical and horizontal load carrying components).

As the database of the ground motion records increase, the possibility of understanding this phenomenal natural disasters increases. This has been recently in the classification of near- and far-field earthquakes. The probabilistic approach in understanding the types of earthquakes at a specific site needs to have more record sample. The method to succeed this goal is (i) to place ground motion record instrumentations at certain locations and monitor their findings or (ii) to use satellite images calibrated with GPS measurements that real time monitor the ground movements. The latest technological improvements in the data acquisition techniques assist the researchers on their way to obtain more data in shorter period then it was used to be.

On the other hand, the development of the material science and its applications in the buildings as well as the introduction of the additional mechanical systems (active/passive control systems) give the chance to revise the right hand side of the basic formulation in the earthquake resistant design; "demand < capacity". Even if the development of the material and mechanical systems penetrate the civil engineering major so slow than the others, it is the likely happens that the next generation building codes will be based on alternative principles and concepts, as defended in this study.

Energy-based structural analysis and design of the conventional buildings is yet early on the way of implementation into the guidelines. There are too many things to do in the understanding of the response of the structures excited by the ground motions. However, this study gives a perspective in the analysis and design of Single Degree of Freedom (SDOF) systems totally from the view of energy components.

4.1.2. The Basis of the Proposed Design

The fundamental principles in the design of a structure are to keep it sustainable under the severe conditions those are expressed technically, sociologically and economically. Every major disaster brings up new questions on researchers' mind about the mistakes and the missing parts in the analysis and design of the systems.

Structural engineers try to satisfy the basic rule in the design "*demand* < *supply*". The most critical decision in the implementation of this rule is whether to take it as it is, or take a certain portion of both sides. In elastic design, beside the material safety factors, the equation is tried to be fulfilled as it is. However, in inelastic design, the both sides of equation are factored with proper values while optimizing the supply of the building which will not risk the human life.

The design principle for the proposed design methodology is the same as given above. Different from the conventional analysis and design methods, the proposed methodology does not take any safety factor even though the inelastic actions are in the consideration. The values used in the demand and capacity procedures are the nominal values. This assumption may sound like there is a dilemma, however, as mentioned before, the aim of this study is to give an understanding in the response of the structures (steel, RC and masonry) subjected to earthquakes and to recommend a design method for the RC systems. Therefore, all the attention was paid to the development of a sound design. The factored/reduced energy based design is out of scope in this study.

This dogmatic assumption is actually correct since the all components in the analysis and capacity formulations are derived directly. Any kind of conversion from one case to

another was not benefitted. The inelastic demand spectra (input and plastic energy) are derived directly from the inelastic behaviors defined with the displacement ductility and the capacity of the RC systems is directly obtained from the inelastic deformations prescribed by the performance limits. This makes the proposed design methodology different from the conventional design methods.

This study recommends a design methodology for reinforced concrete structures those behaviors is similar to Single Degree of Freedom Systems. The most convenient structure resembling the SDOF systems are the precast buildings and the bridges. The behavior of these structures is named as SDOF systems because their description is nothing else than the cantilever columns (Fischinger,2008).

4.2. Energy Based Design

4.2.1. Identification of the Target Buildings for the Proposed Design Method

Even though the engineered structures range from the underground structures to the tall buildings, the basic structure that the civil engineers deal with is the Single Degree of Freedom Systems. The first modes of the multi-story buildings resemble the SDOF behavior (Clough and Penzien, 1995). However, there are some structures those are commonly used in the daily life are behave almost same as the SDOF systems. The single storey-multi bay frame type buildings may be exemplified as factories, depots, garages, bridges, electric poles, water tanks etc.

This study targets to impellent the energy-based design methodology for the precast frame buildings. This type of the buildings is very simple to construct and used very much especially in industrial buildings. One of the major facts observed in 1999 Kocaeli earthquake is that the most of the damaged precast buildings were suffered from the poor construction techniques and underestimation of the seismic forces. Due to its importance of precast structures in the social life, many research projects were started in order to assess the design parameters of the precast systems. Two of these project was completed in European Laboratory of Structural Assessment (ELSA) laboratories at Ispra/ Italy (Ferrera

and Negro,2004;Toniolo,2007); “Seismic Behavior of Reinforced Concrete Structures: Test on the Precast Prototype” and “Seismic Behavior of precast concrete structures with respect to Eurocode 8”, respectively. The three dimensional one-to-two bay 6 precast columns connected with rigid beams and slab were tested by using pseudo-dynamic test techniques. Both studies looked for the different aspects of the precast buildings. The first one compared the behavior of the cast-in-situ and precast buildings, while the latter one checked the safety of the shear span aspect ratio of the precast buildings. The findings of the both tests were presented in many places and implanted into the Eurocode 8 code.

Figure 3.1.and 3.2 show the detail and the picture of the precast system before the PSD tests, respectively;

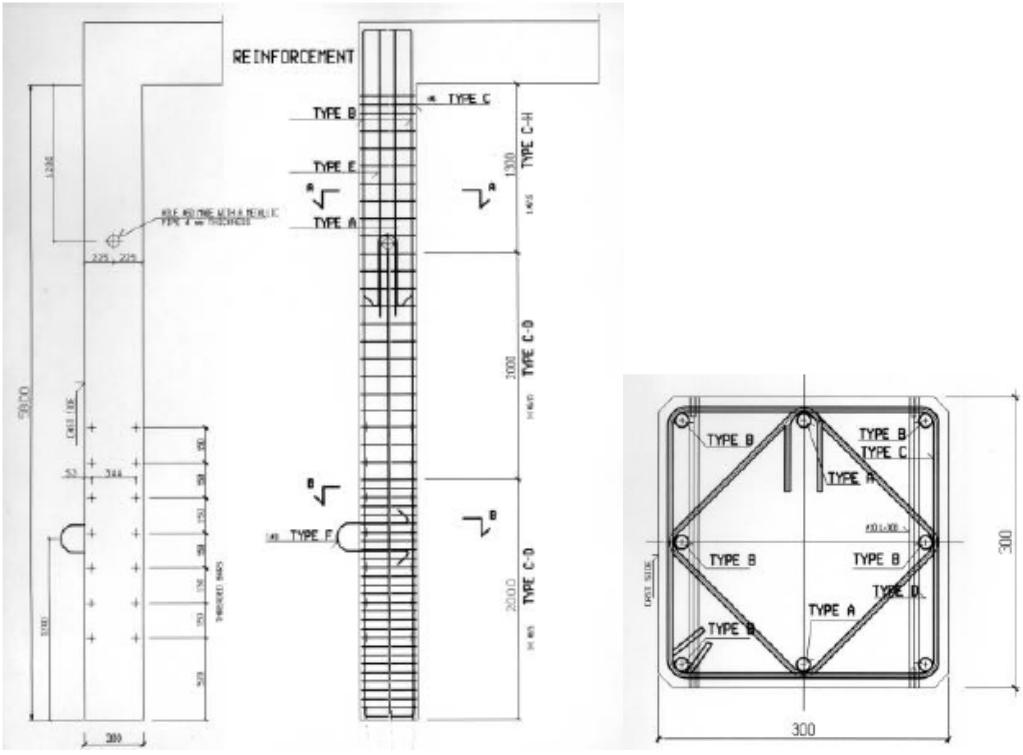

Figure 4.1. The details of the precast building, Ferrera and Negro (2004)

Figure 4.2. The picture of the precast building, Ferrera and Negro (2004)

After the pseudo-dynamic test series the over all structure is given in Figure 3.3 and the beam-column joint in Figure 3.4.

Figure 4.3. The picture of the deformed precast building, Ferrera and Negro (2004)

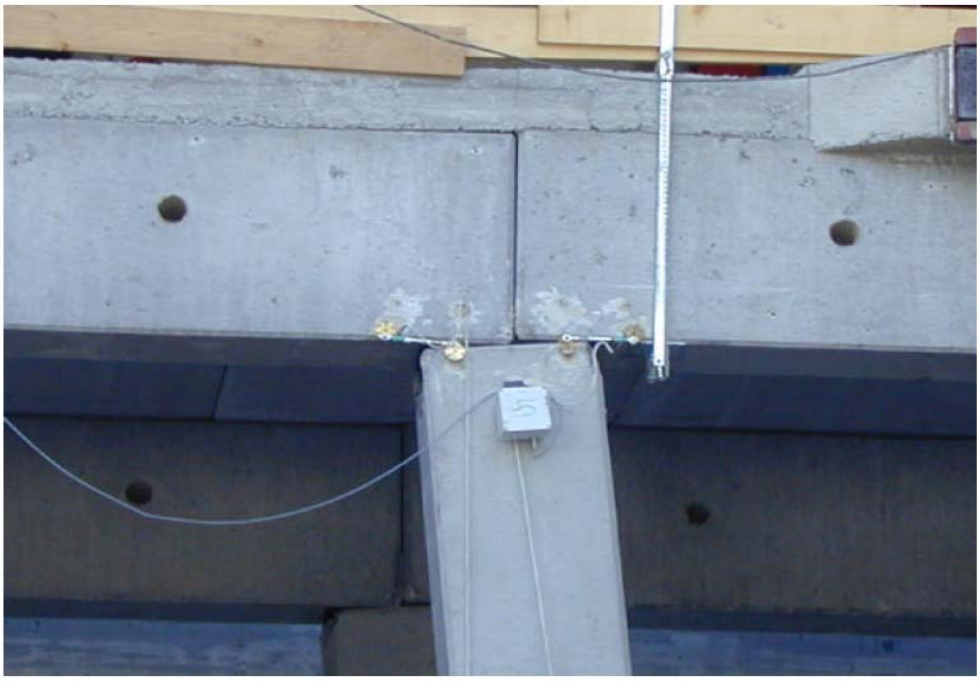

Figure 4.4. The beam-column joint of the precast building, Ferrera and Negro (2004)

As stated in their final reports, the overall structures behaved alike the shear frames, transiting to one direction. Even though the plastic deformations were observed at the bottom of the columns, the end of the beams were not affected from the lateral loading. This observation of both tests proves the precast buildings behave in their 1st mode that is nothing else than the behavior of the SDOF systems.

Beside the observations of the tests, the numerical models of the precast building yielded the similar results (Ferrera et al., 2004; Fischinger, 2008) used the results of the second tests and calibrated the numerical model and displayed that the each identical column can be successfully modeled in numerical analysis to represent the entire system.

According to the findings of the stated tests and the numerical studies, the proposed energy-based design method can be extended to the analysis and design of the 2 and 3 dimensional precast buildings, as will be explained in the following sections.

4.2.2. Proposed Design Procedure

The proposed design procedure for the RC columns is the combination of the ideas of the analysis procedures (explained in Chapter 2) and the capacity procedure (explained in Chapter 3) those are in energy terms .

The steps of the proposed design are explained as follow;

1. The preliminary design:
    a. The engineer assigns the gross section dimensions to each column.
    b. The cracked section flexural stiffness for each column is estimated.
    c. The vibration period of the system according to the cracked sections is calculated.
    d. The axial load levels of the each column are calculated.
2. Plastic Energy Demand:
    a. Prior the calculation of the seismic energy demand, the seismic zone and the site conditions are defined.
    b. For the defined seismic zone and the site condition, the engineer selects the appropriate plastic energy spectra for the ductility levels of 2, 4 and 6.
    c. The cracked section period is marked on the spectra and the corresponding plastic energy values are calculated.
    d. The list of the mass normalized plastic energy values of each ductility levels are multiplied by the mass of the system.
    e. The total plastic energy demand value is distributed among the columns according to their flexural rigidities.
    f. The last step concludes the seismic demand analysis of the structure in terms of energy.
3. Energy Dissipation Capacity:
    a. At the end of the previous step, the plastic energy demand due to the ground motion on each column is calculated.

b. The calculated plastic energy value is placed on the appropriate energy dissipation capacity table or charts those are classified according to the axial load level, concrete strength.
c. The engineer finds the preliminarily assigned section and the corresponding shear span and controls the longitudinal reinforcement ratio and its performance limits. It is the engineer who will decide the demand ductility level and the supply of the member with respect to the performance.
d. Since the system performances are defined as the drift ratio of the system, the only difference between the different cross sections is the member performance that is related to the strains of the concrete and reinforcement.
e. If the engineer can not find the adequate energy dissipation for the assigned cross section within the reinforcement range of 1-to-4-per-cent, it is needed to change the cross section dimensions.
f. Similar to the current design codes, changing the member dimensions change the lateral stiffness of the entire system and requires restarting of the analysis again.
g. This iterative approach is carried out until the seismic plastic energy demand is kept under the energy dissipation supply of the structure for the desired performance region.

The flow chart of the proposed design methodology explained above is given in Figure 4.5.

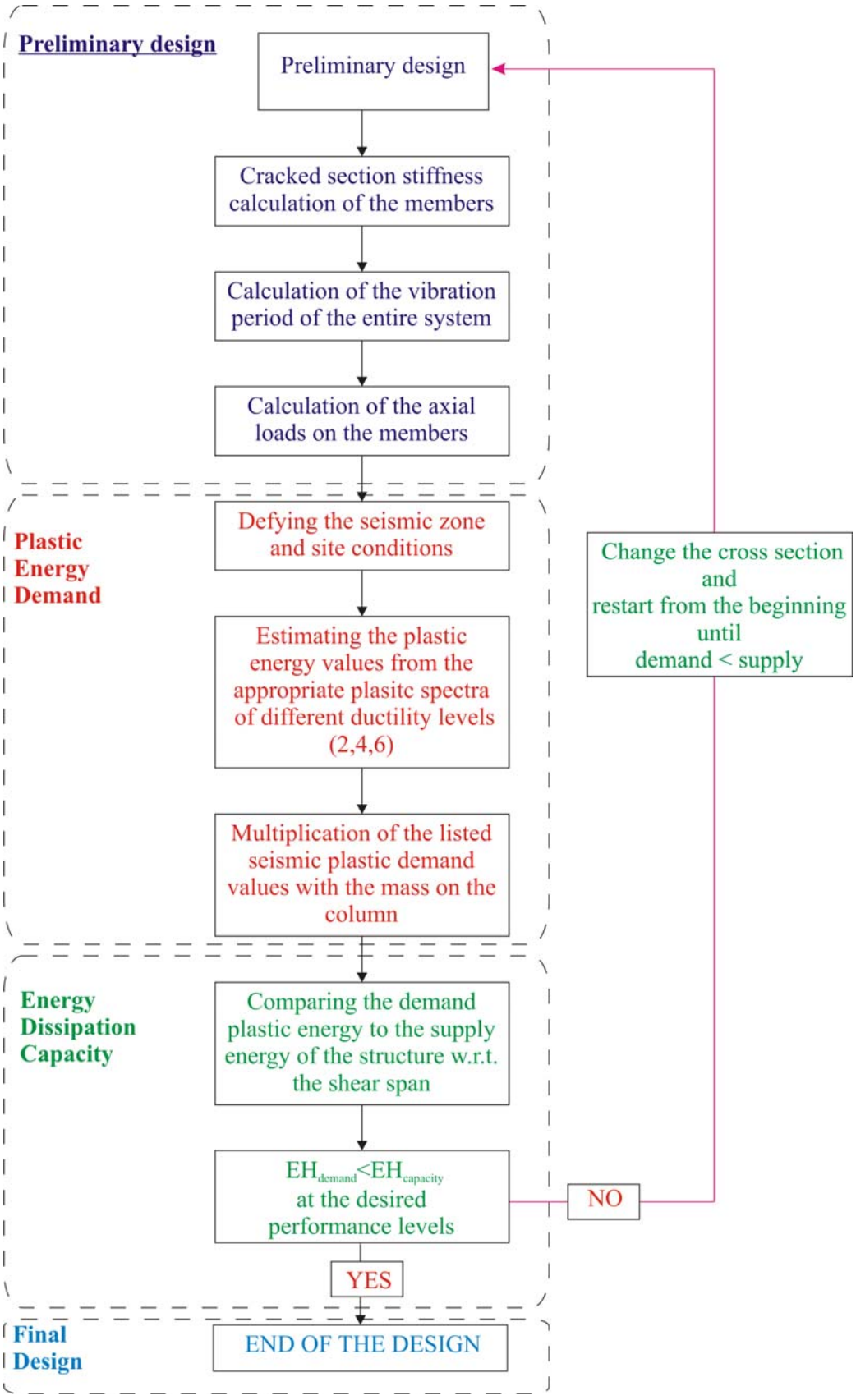

Figure 4.5 Flow chart of the proposed design

4.3. Design Examples

The following sections give the examples of the different structures and the comparison of the proposed design with the force-and displacement-based design methods those are described as in ABYYHY (2008).

In order to compare the results of the three methods, the damage level of the members kept as “Safe (SA)” and the system performance is kept as “Life Safety (LS)”.

4.3.1. Single Column Example

In order to establish a base for the comparison of the proposed design methodology with the current methods, a cantilever column with a mass on top of it (Figure 4.6) was studied with various different axial load level, seismic zone and site condition as briefed in Table 4.1.

Table 4.1. The parameters of the single column example

Definition	Range
Axial load levels	% 5, 10, 20
Seismic zone	1^{st} , 4^{th}
Site conditions	Z1, Z4

The illustration of the single-column example is given in Figure 4.6.

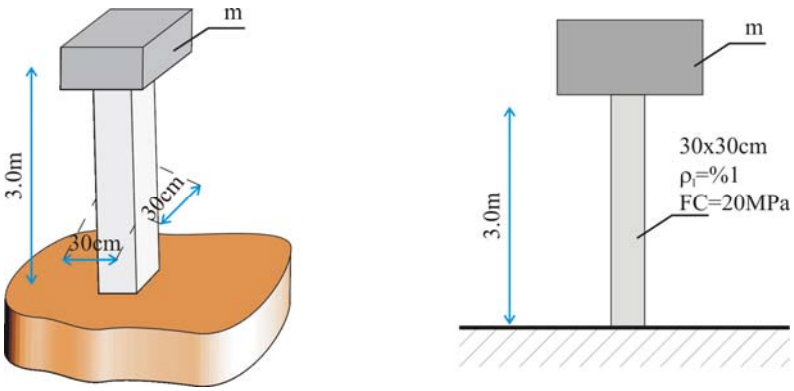

Figure 4.6 Single column example

The geometrical (section dimensions, height) and mechanical properties (concrete strength, longitudinal reinforcement ratio, transversal reinforcement ratio, axial load level) were selected according to TSE500-2000 and ABYYHY (2008). The concrete strength is assigned as 20MPa and the yield and ultimate strength of reinforcement is as 420MPa and 550MPa, respectively. In order to avoid the shear failure, the interval of the transversal reinforcement is taken as 15cm, as the half of the depth of the section.

The section of the system is taken as 30x30cm with one-per-cent longitudinal reinforcement ratio as preliminary design. The height of the column was selected as 3.00 m so that this covers the all the shear span ratios of the cross sections those were used in the previous chapter. There are 16 cases those were analyzed and designed according to force-, displacement- and energy-based methods, (FB, DB, EB), respectively. The cases are separated into three main groups according to the axial load level. Each set is also classified in two sets as uncracked and cracked sections. Each subgroup is evaluated on the most and least severe seismic cases. The results are given in Tables 4.2 to 4.4.

The cases of 1, 2, 3.1, 3, 4, 6, 8, 10 and 12, all three methods consider the preliminary design of the member is adequate. The only difference is that FB takes case 2 as “MINIMUM (MN)” where the other two take it as “SAFE (SA)”. The common sides of these cases are they are located in 4^{th} seismic zone and on Z4 soil.

The cases of 4.1, 6.1, 8.1, 10.1 and 12.1 are the ones that the revisions were made for all three cases. The methods generally increased the stiffness (larger section) from 30x30cm to 40x40 cm with one-per-cent or 50x50cm with one-per-cent.

However, the EB method has changed cases 5 and 7 of being inadequate in ductility of in stiffness. Therefore, it may be expressed that the energy based formulations give a little bit safe results.

The advantage of using DB method to the FB is that the system performance is also expressed, while EB adds the inelastic response of the member through the ductility level during the seismic loading.

Table 4.2. The results of the Force-Based Design of the single column

Case	P/P0	mass (kNs2/m)	T (s)	Seismic Zone	Site Condition	Force Based Design				
						Preliminary Design		Final Design		
						Member Performance	System Performance	Member Performance	System Performance	REVISION
1	5%	9.17	0.41	Z1	1	MN (30x30 & %1)	-	MN (30x30 & %1)	-	NONE
2	5%	9.17	0.41	Z4	4	MN (30x30 & %1)	-	MN (30x30 & %1)	-	NONE
2.1	5%	9.17	0.41	Z4	1	SA (30x30 & %1)	-	SA (30x30 & %1)	-	NONE
3	5%	9.17	0.65	Z1	1	MN (30x30 & %1)	-	MN (30x30 & %1)	-	NONE
4	5%	9.17	0.65	Z4	4	MN (30x30 & %1)	-	MN (30x30 & %1)	-	NONE
4.1	5%	9.17	0.65	Z4	1	SA (30x30 & %1)	-	SA (30x30 & %1)	-	NONE
5	10%	18.35	0.58	Z1	1	SA (30x30 & %1)	-	SA (30x30 & %1)	-	NONE
6	10%	18.35	0.58	Z4	4	MN (30x30 & %1)	-	MN (30x30 & %1)	-	NONE
6.1	10%	18.35	0.58	Z4	1	CO (30x30 & %1)	-	SA (40x40 & %1)	-	LARGER SECTION
7	10%	18.35	0.92	Z1	1	SA (30x30 & %1)	-	SA (30x30 & %1)	-	NONE
8	10%	18.35	0.92	Z4	4	SA (30x30 & %1)	-	SA (30x30 & %1)	-	NONE
8.1	10%	18.35	0.92	Z4	1	FA (30x30 & %1)	-	SA (40x40 & %1)	-	LARGER SECTION
9	20%	36.70	0.82	Z1	1	SA (30x30 & %1)	-	SA (30x30 & %1)	-	NONE
10	20%	36.70	0.82	Z4	4	SA (30x30 & %1)	-	SA (30x30 & %1)	-	NONE
10.1	20%	36.70	0.82	Z4	1	FA (30x30 & %1)	-	SA (50x50 & %1)	-	LARGER SECTION
11	20%	36.70	1.06	Z1	1	CO (30x30 & %1)	-	SA (50x50 & %1)	-	LARGER SECTION
12	20%	36.70	1.06	Z4	4	SA (30x30 & %1)	-	SA (30x30 & %1)	-	NONE
12.1	20%	36.70	1.06	Z4	1	FA (30x30 & %1)	-	SA (50x50 & %1)	-	LARGER SECTION

Table 4.3. The results of the Displacement-Based Design of the single column

Case	P/P0	mass (kNs2/m)	T (s)	Seismic Zone	Site Condition	Displacement Based Design				
						Preliminary Design		Final Design		
						Member Performance	System Performance	Member Performance	System Performance	REVISION
1	5%	9.17	0.41	Z1	1	MN (30x30 & %1)	LS	MN (30x30 & %1)	LS	NONE
2	5%	9.17	0.41	Z4	4	MN (30x30 & %1)	IO	MN (30x30 & %1)	IO	NONE
2.1	5%	9.17	0.41	Z4	1	SA (30x30 & %1)	LS	SA (30x30 & %1)	LS	NONE
3	5%	9.17	0.65	Z1	1	SA (30x30 & %1)	LS	SA (30x30 & %1)	LS	NONE
4	5%	9.17	0.65	Z4	4	MN (30x30 & %1)	LS	SA (30x30 & %1)	LS	NONE
4.1	5%	9.17	0.65	Z4	1	CO (30x30 & %1)	FA	SA (40x40 & %1)	LS	LARGER SECTION
5	10%	18.35	0.58	Z1	1	SA (30x30 & %1)	LS	SA (30x30 & %1)	LS	NONE
6	10%	18.35	0.58	Z4	4	SA (30x30 & %1)	LS	SA (30x30 & %1)	LS	NONE
6.1	10%	18.35	0.58	Z4	1	CO (30x30 & %1)	FA	SA (40x40 & %1)	LS	LARGER SECTION
7	10%	18.35	0.92	Z1	1	SA (30x30 & %1)	LS	SA (30x30 & %1)	LS	NONE
8	10%	18.35	0.92	Z4	4	SA (30x30 & %1)	LS	SA (30x30 & %1)	LS	NONE
8.1	10%	18.35	0.92	Z4	1	FA (30x30 & %1)	FA	SA (40x40 & %1)	LS	LARGER SECTION
9	20%	36.70	0.82	Z1	1	CO (30x30 & %1)	LS	SA (40x40 & %1)	LS	LARGER SECTION
10	20%	36.70	0.82	Z4	4	SA (30x30 & %1)	LS	SA (30x30 & %1)	LS	NONE
10.1	20%	36.70	0.82	Z4	1	FA (30x30 & %1)	FA	SA (50x50 & %1)	LS	LARGER SECTION
11	20%	36.70	1.06	Z1	1	FA (30x30 & %1)	FA	SA (40x40 & %1)	LS	LARGER SECTION
12	20%	36.70	1.06	Z4	4	SA (30x30 & %1)	LS	SA (30x30 & %1)	LS	NONE
12.1	20%	36.70	1.06	Z4	1	FA (30x30 & %1)	FA	SA (50x50 & %1)	LS	LARGER SECTION

Table 4.4. The results of the Energy-Based Design of the single column

Case	P/P0	mass (kNs2/m)	T (s)	Seismic Zone	Site Cond.	Energy Based Design						REVISION
						Preliminary Design			Final Design			
						Member Perf.	System Perf.	Ductility	Member Perf.	System Perf.	Ductility	
1	5%	9.17	0.41	Z1	1	MN (30x30 & %1)	LS	4	MN (30x30 & %1)	LS	4	NONE
2	5%	9.17	0.41	Z4	4	MN (30x30 & %1)	IO	6	MN (30x30 & %1)	IO	6	NONE
2.1	5%	9.17	0.41	Z4	1	SA (30x30 & %1)	LS	4	MN (30x30 & %1)	LS	4	NONE
3	5%	9.17	0.65	Z1	1	SA (30x30 & %1)	LS	6	MN (30x30 & %1)	LS	6	NONE
4	5%	9.17	0.65	Z4	4	MN (30x30 & %1)	IO	6	MN (30x30 & %1)	IO	6	NONE
4.1	5%	9.17	0.65	Z4	1	MN (30x30 & %1)	LS	2	SA (40x40 & %1)	LS	6	Larg. Sect.
5	10%	18.35	0.58	Z1	1	FA (30x30 & %1)	FA	-	SA (40x40 & %1)	LS	6	Larg. Sect.
6	10%	18.35	0.58	Z4	4	MN (30x30 & %1)	IO	6	MN (30x30 & %1)	IO	6	NONE
6.1	10%	18.35	0.58	Z4	1	FA (30x30 & %1)	FA	-	SA (40x40 & %1)	LS	6	Larg. Sect.
7	10%	18.35	0.92	Z1	1	FA (30x30 & %1)	FA	-	SA (30x30 & %2)	LS	6	More. Reinf
8	10%	18.35	0.92	Z4	4	MN (30x30 & %1)	IO	6	MN (30x30 & %1)	IO	6	NONE
8.1	10%	18.35	0.92	Z4	1	FA (30x30 & %1)	FA	-	SA (40x40 & %1)	LS	6	Larg. Sect.
9	20%	36.7	0.82	Z1	1	FA (30x30 & %1)	FA	-	SA (40x40 & %2)	LS	6	Larg. Sect. More. Reinf.
10	20%	36.7	0.82	Z4	4	MN (30x30 & %1)	IO	6	MN (30x30 & %1)	IO	6	NONE
10.1	20%	36.7	0.82	Z4	1	FA (30x30 & %1)	FA	-	SA (50x50 & %1)	LS	6	Larg.Sect.
11	20%	36.7	1.06	Z1	1	FA (30x30 & %1)	FA	-	SA (40x40 & %2)	LS	6	Larg. Sect. More. Reinf.
12	20%	36.7	1.06	Z4	4	FA (30x30 & %1)	FA	-	MN (30x30 & %1)	IO	6	NONE
12.1	20%	36.7	1.06	Z4	1	FA (30x30 & %1)	FA	-	SA (50x50 & %1)	LS	6	Larg.Sect.

Table 4.5. Energy demand and supply values for single column example

Case	Ductility	Preliminary Design		Final Design	
		EH_Demand	EH_Supply	EH_Demand	EH_Supply
1	1	0.00	0	0.00	0
	2	1.01	1.89	1.01	1.89
	4	1.65	1.89	1.65	1.89
	6	1.93	1.89	1.93	1.89
2	1	0.00	0	0.00	0
	2	0.09	1.89	0.09	1.89
	4	0.12	1.89	0.12	1.89
	6	0.14	1.89	0.14	1.89
2.1	1	0.00	0	0.00	0
	2	1.21	1.89	1.21	1.89
	4	1.69	1.89	1.69	1.89
	6	2.05	-	2.05	1.89
3	1	0.00	0	0.00	0
	2	1.01	1.89	1.01	1.89
	4	1.65	1.89	1.65	1.89
	6	1.79	1.89	1.79	1.89
4	1	0.00	0	0.00	0
	2	0.13	1.89	0.13	1.89
	4	0.15	1.89	0.15	1.89
	6	0.17	1.89	0.17	1.89
4.1	1	0.00	0	0.00	0
	2	1.83	1.89	1.07	3.35
	4	2.20	-	1.51	3.35
	6	2.38	-	1.82	3.35
5	1	0.00	0	0.00	
	2	1.83	1.89	1.07	3.35
	4	2.20	-	1.51	3.35
	6	2.38	-	1.82	3.35
6	1	0.00	0	0.00	0
	2	0.25	1.89	0.25	1.89
	4	0.29	1.89	0.29	1.89
	6	0.33	1.89	0.33	1.89
6.1	1	0.00	0	0.00	0
	2	1.83	1.89	1.07	3.35
	4	2.20	-	1.51	3.35
	6	2.38	-	1.82	3.35
7	1	0.00	0	0.00	0
	2	1.99	-	1.99	3.23
	4	2.87	-	2.87	3.23
	6	2.62	-	2.62	3.23
8	1	0.00	0	0.00	0
	2	0.25	1.89	0.25	1.89
	4	0.29	1.89	0.29	1.89
	6	0.33	1.89	0.33	1.89

Table 4.5. Energy demand and supply values for single column example (cont^d)

Case	Ductility	Preliminary Design		Final Design	
8.1	1	0.00	0	0.00	0
	2	3.67	-	1.99	3.23
	4	4.40	-	2.87	3.23
	6	4.77	-	2.62	3.23
9	1	0.00	0	0.00	0
	2	4.05	-	4.05	7.29
	4	6.44	-	6.61	7.29
	6	5.82	-	7.71	7.29
10	1	0.00	0	0.00	0
	2	0.25	1.89	0.25	1.89
	4	0.29	1.89	0.29	1.89
	6	0.33	1.89	0.33	1.89
10.1	1	0.00	0	0.00	0
	2	7.34	1.89	3.38	6.44
	4	8.81	1.89	4.74	6.44
	6	9.54	1.89	5.71	6.44
11	1	0.00	0	0.00	0
	2	3.50	1.89	4.05	7.29
	4	4.99	1.89	6.61	7.29
	6	4.62	1.89	6.54	7.29
12	1	0.00	0	0.00	0
	2	0.25	1.89	0.25	1.89
	4	0.29	1.89	0.29	1.89
	6	0.33	1.89	0.33	1.89
12.1	1	0.00	0	0.00	0
	2	7.34	1.89	5.62	9.86
	4	8.81	1.89	7.88	9.86
	6	9.54	1.89	9.54	9.86

4.3.2. One-Bay Frame System

A more realistic example of one bay-one story system, Figure 4.7, is examined in order to see how the total plastic demand energy can be distributed among the columns that support that mass of the precast systems. The mass of the system is calculated for the slab with 4m in width and carrying 25kN/m2 uniform load that is actually more for the ordinary precast systems.

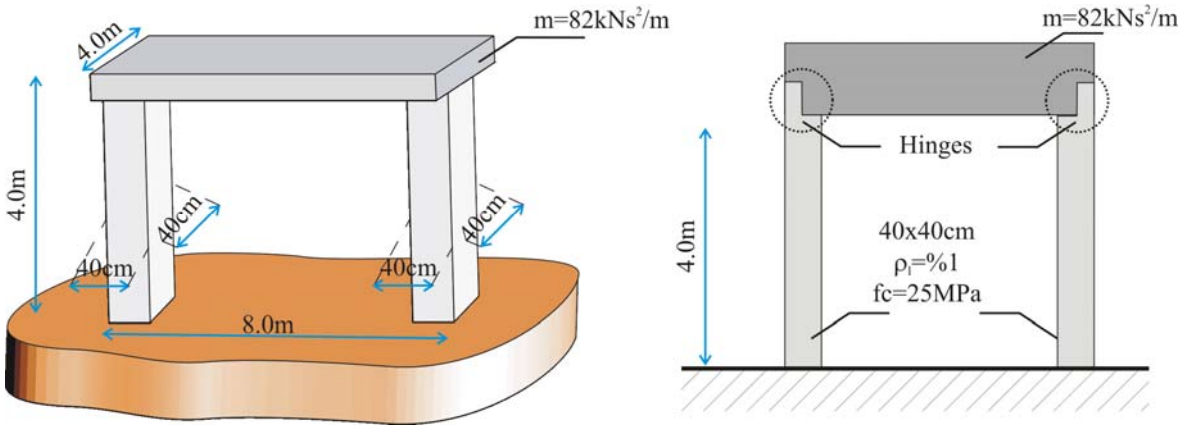

Figure 4.7. One-bay & one-story frame example

Since the previous single column example provides the sensitivity analysis of the seismic parameters, this example is intended to demonstrate the energy-based design for coupling columns. Therefore, only 4 cases will be examined, which are separated as uncracked and cracked sections in seismic zone 1 and resting on hard and soft soils.

Table 4.6. The parameters of the frame example

Definition	Range
Axial load levels	% 10
Seismic zone	1st
Site conditions	Z1, Z4

The dimensions and the mechanical properties of the frame are taken according to TSE500-2000 and ABYYHY (2008). Different from the previous example, the concrete strength is taken as 25MPa while the reinforcement remains same as 420MPa, and

550MPA yield and ultimate strengths, respectively. The distance between the transversal reinforcement was taken as 20cm, half of the cross section depth.

The four cases were analyzed and designed according to the Force Based (FB), Displacement Based (DB) and Energy Based (EB). The results of the all three methods are given in Table 4.6 -4.8.

The cases of 13 and 15 where the uncracked sections are used have been adequately designed in the beginning. Therefore, any revision was not applied.

However, there are some interesting results in the cases of 14 and 16. Each of the design methods revised the sections and the reinforcement. The Force-based design required larger cross section for 14, but required more reinforcement for 16. Meanwhile, the Displacement-based design not only increased the section of cases 14 and 16, but also increased the reinforcement ratio in order to bring the system from FA & FA to SA & LS section and system performance levels, respectively. On the other hand, according to energy-based design, the sections were adequately reinforced for SA & LS performance levels. But at that option, the ductility demand and the supply of the frame is just 2 instead 4. Because the 4 ductility is preferred the reinforcement ratios were increased from two to three while the sections remained in their dimensions.

Table 4.10 displays the seismic plastic energy demand and the energy dissipation supply of the system for preliminary and final designs.

Table 4.7. The results of the Force-Based Design of the frame system

Case	P/P0	mass (kNs2/m)	T (s)	Seismic Zone	Site Condition	Force Based Design				
						Preliminary Design		Final Design		
						Member Performance	System Performance	Member Performance	System Performance	REVISION
13	10%	42.56	0.74	Z1	1	MN (40x40 & %2)	-	MN (40x40 & %2)	-	NONE
14	10%	42.56	0.74	Z4	1	FA (40x40 & %2)	-	SA (50x50 & %1)	-	Larger Section
15	10%	42.56	1.16	Z1	1	MN (40x40 & %2)	-	MN (40x40 & %2)	-	NONE
16	10%	42.56	1.16	Z4	1	FA (40x40 & %2)		SA (40x40 & %3)	-	More. Reinf

Table 4.8. The results of the Displacement-Based Design of the frame system

Case	P/P0	mass (kNs2/m)	T (s)	Seismic Zone	Site Condition	Displacement Based Design				
						Preliminary Design		Final Design		
						Member Performance	System Performance	Member Performance	System Performance	REVISION
13	10%	42.56	0.74	Z1	1	MN (40x40 & %2)	LS	MN (40x40 & %2)	LS	NONE
14	10%	42.56	0.74	Z4	1	FA (40x40 & %2)	FA	SA (50x50 & %2)	LS	Larg. Sect More Reinf.
15	10%	42.56	1.16	Z1	1	MN (40x40 & %2)	LS	MN (40x40 & %2)	LS	NONE
16	10%	42.56	1.16	Z4	1	FA (40x40 & %2)	FA	SA (50x50 & %2)	LS	Larg. Sect More Reinf.

Table 4.9. The results of the Energy-Based Design of the frame system

Case	P/P0	mass (kNs2/m)	T (s)	Seismic Zone	Site Cond.	Energy Based Design						REVISION
						Preliminary Design			Final Design			
						Member Perf.	System Perf.	Ductility	Member Perf.	System Perf.	Ductility	
13	10%	42.56	0.74	Z1	1	SA(40X40 & %2)	LS	6	SA(40X40 & %2)	LS	6	NONE
14	10%	42.56	0.74	Z4	1	SA(40X40 & %2)	LS	2	SA(40X40 & %3	LS	6	More Reinf.
15	10%	42.56	1.16	Z4	1	SA(40X40 & %2)	LS	6	SA(40X40 & %2)	LS	6	NONE
16	10%	42.56	1.16	Z1	1	SA(40X40 & %2)	LS	2	SA(40X40 & %3	LS	6	NONE

Table 4.10. Energy demand and supply values for frame system

Case	Ductility	Preliminary Design		Final Design	
		EH_Demand	EH_Supply	EH_Demand	EH_Supply
13	1	0.00	0	0.00	0
	2	4.49	8.11	4.49	8.11
	4	7.33	8.11	7.33	8.11
	6	7.08	8.11	7.08	8.11
14	1	0.00	0	0.00	0
	2	8.14	8.11	8.14	12.37
	4	9.77	-	9.77	12.37
	6	10.58	-	10.58	12.37
15	1	0.00	0	0.00	0
	2	3.58	8.11	3.58	8.11
	4	5.05	8.11	5.05	8.11
	6	4.72	8.11	4.72	8.11
16	1	0.00	0	0.00	0
	2	8.14	8.11	8.14	12.37
	4	9.77	-	9.77	12.37
	6	10.58	-	10.58	12.37

4.3.3. Three Dimensional Frame Example

A three dimensional frame system similar to the prototype of Ferrera and Negro (2004) study was selected in order to demonstrate that the energy-based design is also applicable for ordinary three dimensional precast structures, Figure 4.8.

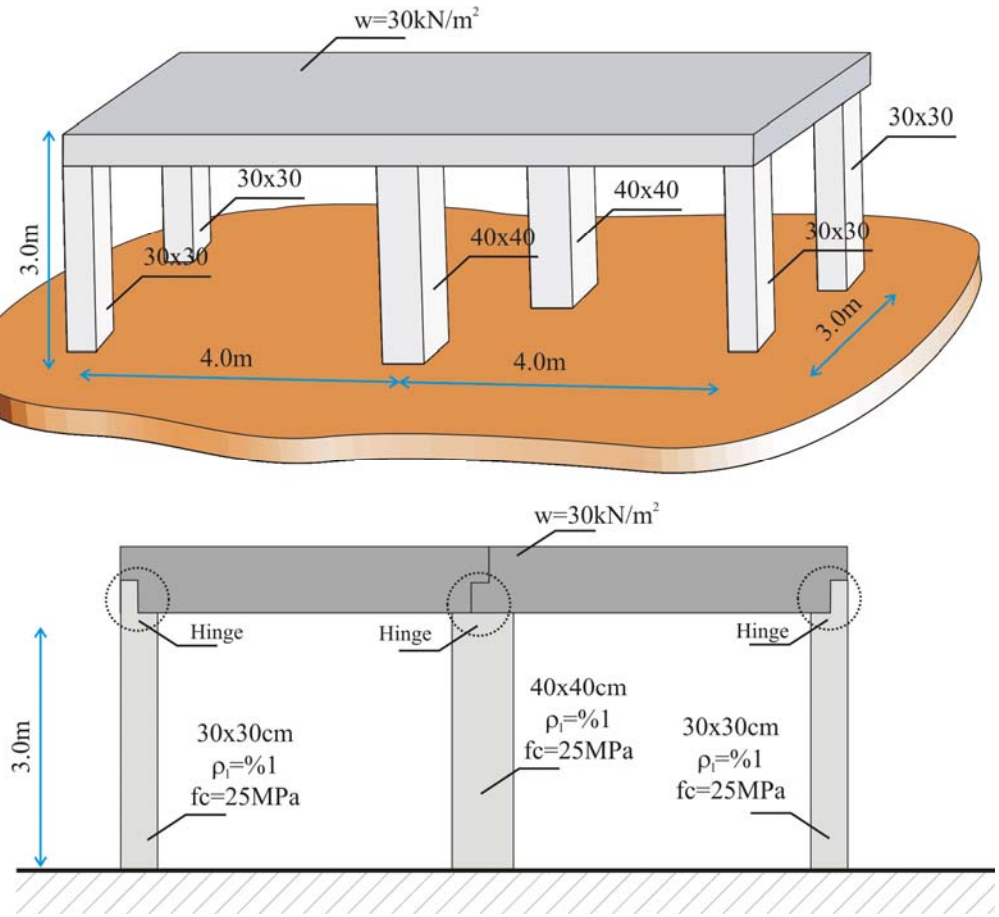

Figure 4.8. Three dimensional frame system

The geometric and mechanical properties of the model are assigned according to TS500-2000 and ABYYHY (2008). The height of the structure is 3.0m, and the plan dimensions are 8m by 3.0 m. The rigid slab that is pinned connected to the columns are carrying 30kN/m^2 uniform load.

The column configuration was selected different from the Ferrera and Negro (2004) in order to show how the seismic plastic energy is distributed among the columns of the system. The seismic zone was taken as 1st zone and the soil type is Z3.

The results of the all three design are given in Tables 4.11 to 4.13. As seen in the force- and displacement-based designs the preliminary design of the columns sections with one-per-cent longitudinal reinforcement was found adequate however, the energy based design considers the 40x40cm columns are not ductile enough. Therefore, the longitudinal reinforcement ratio was increased from one-per-cent to two-per-cent in order to rise the ductility level of the system.

Table 4.11. The results of the Force-Based Design of the three dimension building

Case	P/P0	mass (kNs2/m)	T (s)	Seismic Zone	Site Condition	Force Based Design				
						Preliminary Design		Final Design		
						Member Performance	System Performance	Member Performance	System Performance	REVISION
17	5%	74	0.35	Z3	1	MN (40x40 & %1) MN (30x30 & %1)	-	MN (40x40 & %1) MN (30x30 & %1)	-	NONE
18	5%	74	0.56	Z3	1	MN (40x40 & %1) MN (30x30 & %1)	-	MN (40x40 & %1) MN (30x30 & %1)	-	NONE

Table 4.12. The results of the Displacement-Based Design of the three dimension building

Case	P/P0	mass (kNs2/m)	T (s)	Seismic Zone	Site Condition	Displacement Based Design				
						Preliminary Design		Final Design		
						Member Performance	System Performance	Member Performance	System Performance	REVISION
17	5%	74	0.35	Z1	1	MN (40x40 & %1) MN (30x30 & %1)	LS	MN (40x40 & %1) MN (30x30 & %1)	LS	NONE
18	5%	74	0.56	Z3	1	MN (40x40 & %1) MN (30x30 & %1)	LS	MN (40x40 & %1) MN (30x30 & %1)	LS	NONE

Table 4.13. The results of the Energy-Based Design of the three dimension building

Case	P/P0	mass (kNs2/m)	T (s)	Seismic Zone	Site Cond.	Energy Based Design						REVISION
						Preliminary Design			Final Design			
						Member Perf.	System Perf.	Ductility	Member Perf.	System Perf.	Ductility	
17	5%	74	0.35	Z1	1	MN (40x40 & %1) MN (30x30 & %1)	LS	2 6	MN (40x40 & %2) MN (30x30 & %1)	LS	6 6	More Reinf. 40x40 NONE
18	5%	74	0.56	Z3	1	MN (40x40 & %1) MN (30x30 & %1)	LS	2 6	MN (40x40 & %2) MN (30x30 & %1)	LS	6 6	More Reinf. 40x40 NONE

Table 4.14. Energy demand and supply values for three dimension building

Case	Ductility	Preliminary Design				Final Design			
		EH_Demand		EH_Supply		EH_Demand		EH_Supply	
		30x30	40x40	30x30	40x40	30x30	40x40	30x30	40x40
17	1	0.00	0.00	0.00	0	0.00	0.00	0.00	7.84
	2	0.86	2.76	1.77	3.58	0.86	2.76	1.77	7.84
	4	1.30	4.10	1.77	-	1.30	4.10	1.77	7.84
	6	1.72	5.50	1.77	-	1.72	5.50	1.77	7.84
18	1	0.00	0.00	0.00	0	0.00	0.00	0.00	7.84
	2	1.30	4.10	1.77	-	1.30	4.10	1.77	7.84
	4	1.65	5.27	1.77	-	1.65	5.27	1.77	7.84
	6	1.72	5.50	1.77	-	1.72	5.50	1.77	7.84

5. SUMMARY AND CONCLUSIONS

5.1. Summary

The earthquake resistant design philosophy was relied on the strength of the structures. Beginning from the 1990's a new philosophy appeared and the deformation was introduced as a design tool. It is still challenging to use deformation of the systems in the design. Even though the latter method requires more computational effort, it provides more information than the classical force based methods. The displacement of the system brings up the valuable information on member deformation those are directly related to the damage occurrences. The most important contribution of the displacement based design is to introduce the limit states of the systems and their members. This contribution lead the engineers to evaluate their design calculations in a better way than the strength based formulations where there is not a chance to see how much the structures affected from the variation of the member configurations.

However the displacement based method also has some deficiencies in the definition of the demand of the earthquake and capacity of the building. It still uses the elastic response spectrum in the definition of the demand forces. It is well-known that the derivation of the elastic response spectra comes from the use of the extreme values of response histories of the buildings. However, this approach is prone to lose much information provided by the ground motion record and more important by the response of the structure. On the other hand the capacity of the building is also relied on a method that is subjected to serious critics regarding the damage occurrences. Nonlinear static analysis may be good in understanding the capacity of structure in extreme loadings, but most probably it falls short in the determination of the reversed cycling loadings.

Based on the facts given above, an alternative analysis and design tool was necessary in the earthquake resistant design. The implied tool must clear the uncertainties in the derivation of the demand actions and also determination of the seismic capacity of the buildings.

This study used the energy balance equation and energy concept the analysis and design of the structures. Even if the energy may not be relevant in the structural calculations, it might be helpful in the understanding the complex relation between the excitation force and its deformation on the buildings.

In order to set up a analysis basis in the earthquake resistant design, the well know dynamic equation of motion was re-stated in terms of energy and the terms in this equation was assessed as the energy mechanisms in the structure. It was shown that the imparted seismic energy is either stored or dissipated during the motion duration. The mechanisms that store the imparted energy are the kinetic and strain energy sources which are nothing else then the well known kinetic-potential energy couples in physic. One exists if the other one does not, vice versa. However, the energy dissipated in the structure is of the engineers' interest since they are directly related to the damage of the members.

This study aimed to highlight which features of the ground motions' and the structures affect the energy imparting and dissipation through the members by examining the energy response time-histories of a Single Degree of Freedom system. Several parameters (from the severity of the motion, to the damping of the structure) were used in the study to see which one is effective in the understanding of the damage occurrence. Among these studies, it was seen that the best parameter that is able to clarify the affect of the ground motion was the plastic energy mechanism. Therefore, the motivation on the development of an analysis procedure was concentrated on the inelastic action of the systems. To cover the constitutive models describing the majority of the buildings (steel, RC, masonry) were used in the analysis and found out that the elasto-perfectly-plastic model represent the other models within a safe margin. Than, it was the author's decision to use the elasto-perfectly-plastic model in the development of the analysis procedure.

In order to define the variation of the energy components for different buildings, the spectra concept was used in the formulations. Apart from the classical spectra formulation, the developed computer program was able to derive the input and plastic energy spectra for a given inelastic action defined as its ductility.

This study succeeded to define the energy input and plastic spectra as the demand parameters for the different seismic zones and soil conditions and also for the different ductility level of the buildings directly obtained from the energy balance equation of the inelastic systems. The obtained input and plastic energy spectra were smoothed in order to establish the design spectra for the practicing engineers.

On the other hand, the energy dissipation philosophy was employed in the definition of the capacity of the structural components of deteriorating systems (mostly referred as reinforced concrete systems). While developing the energy dissipation capacities of the RC members, it was needed to have the information about the boundary conditions of the members interested in the design. Even if it may seem irrelevant to use the system information along with the section information, there is not any other option to relate the energy dissipation capacity of a member with its geometrical and mechanical properties.

In order to establish the energy dissipation capacity of a RC member, a set of cross sections with different dimensions and varying reinforcement configuration was used as a reference table. The geometry of the structural component was related to the depth of the section which is actually the shear span of the member. These basic assessments enabled the author to compute an algorithm that determines the energy dissipation capacities for the RC sections. While developing the algorithm, for the sake of being realistic the behavior of the real RC column were used instead of the widely accepted mathematical models.

The algorithm of energy dissipation capacity is relied on two important issues those are valid for structures (i) low-cycle fatigue and (ii) cumulative damage occurrences.

The biggest advantage of using the energy concepts in the earthquake resistant design is the ability of examining the reversed cyclic actions and examining the cumulative damage occurrences those are not included in the current design philosophies.

The developed energy dissipation capacity algorithm also uses the performance limit statements of the displacement based design method. The use of such a limit statements makes the energy dissipation and the damage occurrence monitored throughout the seismic demand spectral values those are obtained from the use of the entire motion record.

The success of expressing the energy demand of the ground motion and the energy supply of the structure enables to set up a design methodology for the RC structures with single story-multi bay frames. The most typical example for this type of buildings is the precast industrial buildings and the bridges.

The proposed design methodology was used in the analysis and the design of the three structures from one-to-three dimensional systems having very different structural properties.

5.2. Conclusions

The following conclusions can be stated based on the conducted numerical analyses which were calibrated with the findings of the experimental tests. The comments stated below are limited to the assumptions made in the selection of the numerical models and the systems. Therefore, any critical assumption or the simplifications have been expressed where appropriate. The findings of this study may not be generalized in real life cases; however it is the author's believe that the findings of this study gained an alternative view in earthquake resistant analysis and design in terms of energy.

The following items are related with the demand of the ground motion, hence used in the analysis of the structures against earthquakes;

- The energy balance of the both side of the equation is valid throughout duration of the motion. Therefore, it is easy to monitor the developments in the structure.
- Use of relative response histories in the energy components formulation is a better choice than the use of absolute response even if the last values of the responses are same. This is practically obvious for input energy component which fluctuates more in the case of absolute response formulations that might be deceptive.
- The energy imparted into the structure is very sensitive to the structural properties and ground motion parameters simultaneously because the input energy is the product of the motion record and the response of the structure.

- The input energy is also sensitive to the viscous damping of the system. Increase in the damping ratio makes drastic decrease in the input energy.
- The increase in the viscous damping of the system also reduces plastic energy of the system which prevents the damage occurrences. The idea of increasing the damping characteristic of the systems by additional mechanisms relies on this simple fact.
- The important energy component in the structures for the damage occurrence is the plastic energy demand of the earthquake. Therefore it is important to supply the adequate energy dissipation capacity to the systems is important in the earthquake resistant design.
- The demand of the earthquakes on the structures is used to derive from the response of the structures. However, this might be deceptive due to the fact that such an action takes extreme value of the response history. But the duration and the frequency content of the record may not be taken into the consideration. This may lead to great mistakes in the estimation of the earthquake demand.
- The reason of benefiting from the energy concept is to include the entire record into the estimation of the earthquake demand. By this way, the more realistic earthquake analysis should be available.
- The spectral values of the input and plastic energy components also display the behavior of the stiff (low natural period) and flexible (high natural period) structures. The energy demand and the damage occurrence likeliness is more for the low period structures (around 0.1~0.7s) than the long period structures.
- Even though the similar spectral shape is seen in the energy spectra, the fundamental periods (or the characteristic periods) of the ground motions are different from the periods found in response spectra. Therefore, the length of the plateau starts later and lasts longer than the acceleration response spectrum.
- The spectral values of the near field records show difference from the far field records. The trend of the input energy spectra towards the long periods start increasing whereas its just opposite for the far field records.

- The input and plastic energy spectra are very sensitive to the change of the ductility. Even though the difference may not be visible between the ductility level of 4 and 6, the reduction of the input energy is greater while the ductility shifts from 2 to 4 and 6.
- It is seen that as the ductility increase the input energy values decreases while the plastic energy values increase. This is one of the major conclusions of this study. Because this proves that contrary to the general view of assuming EH/EI is a stable parameter, it is shown that there is a reverse relation between the input and plastic energies.
- The unstable relation of EH/EI leaded this study to determine the plastic energy spectra apart from the input energy spectra. By this way, the damage due to the ground motion is better described than the conventional response spectra methods.
- The constitutive rules of the structures are very dominant in the ratio of the plastic to the input energy values. As the pinching character of the system increases the amount of the input energy values do not significantly change, but the ratio of the plastic to input energy changes drastically. The lowest ratios of the plastic to input energy were observed in the slip models, whereas the Elasto-perfectly-plastic behavior draws the envelope of the all values.
- The change of the site conditions also affect the EH/EI ratio. As the site conditions soften, the ratio increases especially in the mid-periods.

The following items are related with the energy dissipation capacity of the reinforced concrete columns;

- Since the definition of the energy and the capacity of the members is difficult, it is needed to use some principles that help to understand the energy concept.
- The developed algorithm relies on the low-cycle fatigue analysis that is true for the earthquake induced vibrations.
- Even though the basic formulation for the low-cycle fatigue requires the life-cycle and damage coefficients, the developed algorithm benefits from the fatigue-like deformation pattern that is constant amplitude cyclic displacement pattern.

- The fatigue-like deformation pattern allows identifying the performance levels of the members and the systems that is used in the assessment of the constant amplitude of the cyclic deformation. Therefore, the amount of the energy dissipated is related to these performance levels.
- While applying constant amplitude protocol, the damage occurrences are monitored with respect to the damage indexes.
- The damage index used in the developed algorithm is Park and Ang index that is calibrated for the cantilever systems as in the studied examples.
- The developed algorithm is used for a set of typical RC sections. However, it is possible to include different RC sections by using their moment-curvature relations.
- The energy dissipation tables of the sections are establishment with respect to the shear span of the member where the section is used. The reason of employing the member geometry is that the boundary conditions are required in the formation of the system performances. Otherwise, use of constant-amplitude test may not be possible.
- The energy dissipation increases as the system passes to the next performance level.
- As the stiffness of the section increases the energy dissipation also increases due to the fact the increased stiffness require more force in order to reach the predefined displacement amplitude.
- The increment in the shear span also increases the energy dissipation values except for the minimum section and immediate occupancy system levels. Even the declining trends happen in the low axial but high reinforcement levels.
- The increase of the reinforcement ratio increases the energy dissipation capacity even though the system performance level is not changed. The system performance level is related to the lateral deformation of the system that is directed by the dimensions of the section not the reinforcement ratio. However, for the cases where the section performance governs the limit state, the energy dissipation increases. This is true for the high shear span ratios with low axial force levels.

- Axial load level drastically reduces the energy dissipation. This is due to the increased strength but decrease strain values, which means the system reaches the serious damage levels at early loadings.
- The chartered and tabulated energy dissipation values for the selected cross sections assist the engineers to decide which performance level is satisfied and the residual energy dissipation capacity of the member that would help to improve the retrofitting style (more confined or more strengthened)
- The concrete compression strength increases the energy dissipation of the systems.

The energy demand and the energy dissipation capacity algorithms are combined in a design methodology. Based on the solved cases the following items are listed;

- The proposed design methodology may need more computational effort to derive the energy dissipation values. But once they are obtained, the design method does not need even computer analysis like push-over.
- The design methodology of the RC members is applicable only for inelastic cases. Because the elastic case do not have any energy dissipation.
- The proposed design method was used for the full and cracked RC section and it was seen that use of the cracked section gives more reliable results as it is expected as a design criterion.
- The proposed method results the section and system performance levels beside the inelastic behavior level measured as displacement ductility.
- The three cases were solved by using force-, displacement- and energy-based methods. The expected service levels from the all three methods were safe in section and life safety of the system. Force-based design empirically states the section performance. Displacement-based design gives out section and system performances. But energy-based design method gives out the both performance levels and also the expected ductility.
- It is the designer’s choice to select which performance and ductility levels should be reached. Energy-based design provides more information to the designer about the behavior of the system just by using plastic energy concept.

- The results of the solved cases show that even if the reinforcement ratios are close for all three methods, the force-based method allows the sections to have more damage than the displacement-based method. However, the energy-based method gives out bit more reinforcement for the same performance level. This should be due to the amplitude of the test system that was kept constant.

5.3. Future Work

By the introduction of the energy dissipation mechanisms into the structures, it is not difficult to predict that the future construction guidelines will be based on “Energy” principles. Therefore, any attempt in the development of the seismic analysis and design of the buildings in terms of energy would be meaningful.

The one would like to carry on the developed algorithms and the proposed design method; he/she may do the followings,

- The energy demand algorithm is developed only for the single degree of freedom systems. Therefore, this algorithm should be extended to the multi degree of freedom systems.
- The displacement ductility of the SDOF systems was taken into the energy demand calculations. However, the strength change should also be taken as another design parameter.
- The developed energy dissipation capacity algorithm is used for cantilever systems. If the both-end-fixed systems are implemented into the algorithm, there might be a chance to examine the beam elements.
- The system performance level was defined according to the drift ratio. Another definition might be employed as a basis for system performances.

APPENDIX A: EARTHQUAKES USED IN THE ANALYSIS

#	PEER NAME	TYPE	SOLI	M_w	ΔT	EFFECT. DURAT.
1	P0006-I-ELC180	strikeslip	C	M7	0.01	24.1
2	P0006-I-ELC270	strikeslip	C	M7	0.01	24.0
3	P0031-C05085	strikeslip	C	M6	0.01	6.5
4	P0031-C05355	strikeslip	C	M6	0.01	7.5
5	P0032-C08050	strikeslip	C	M6	0.01	13.1
6	P0032-C08320	strikeslip	C	M6	0.01	10.6
7	P0034-TMB205	strikeslip	B	M6	0.01	4.4
8	P0034-TMB295	strikeslip	B	M6	0.01	5.5
9	P0052-PEL090	reversenormal	C	M6	0.01	10.5
10	P0052-PEL180	reversenormal	C	M6	0.01	11.2
11	P0056-ORR021	reversenormal	B	M6	0.01	14.5
12	P0056-ORR291	reversenormal	B	M6	0.01	15.4
13	P0140-DAY-LN	reversenormal	B	M7	0.02	12.3
14	P0140-DAY-TR	reversenormal	B	M7	0.02	12.4
15	P0144-TAB-LN	reversenormal	C	M7	0.02	16.5
16	P0144-TAB-TR	reversenormal	C	M7	0.02	16.1
17	P0148-G02050	strikeslip	C	M5	0.005	7.5
18	P0148-G02140	strikeslip	C	M5	0.005	4.2
19	P0149-G03050	strikeslip	C	M5	0.005	8.9
20	P0149-G03140	strikeslip	C	M5	0.005	8.7
21	P0150-G04270	strikeslip	C	M5	0.005	8.5
22	P0150-G04360	strikeslip	C	M5	0.005	11.5
23	P0151-G06230	strikeslip	B	M5	0.005	3.2
24	P0151-G06320	strikeslip	B	M5	0.005	3.6
25	P0159-H-AEP045	strikeslip	C	M6	0.01	7.1
26	P0159-H-AEP315	strikeslip	C	M6	0.01	7.0
27	P0160-H-AGR003	strikeslip	B	M6	0.01	13.2
28	P0160-H-AGR273	strikeslip	B	M6	0.01	12.7
29	P0161-H-BCR140	strikeslip	C	M6	0.005	9.7
30	P0161-H-BCR230	strikeslip	C	M6	0.005	9.7
31	P0162-H-BRA225	strikeslip	C	M6	0.005	14.6
32	P0162-H-BRA315	strikeslip	C	M6	0.005	13.9
33	P0163-H-CXO225	strikeslip	C	M6	0.005	11.0
34	P0163-H-CXO315	strikeslip	C	M6	0.005	14.2
35	P0165-H-CPE147	strikeslip	B	M6	0.01	29.7
36	P0165-H-CPE237	strikeslip	B	M6	0.01	36.2
37	P0166-H-CHI012	strikeslip	C	M6	0.01	20.1
38	P0166-H-CHI282	strikeslip	C	M6	0.01	22.1
39	P0170-H-DLT262	strikeslip	C	M6	0.01	45.8
40	P0170-H-DLT352	strikeslip	C	M6	0.01	39.3
41	P0171-H-ECC002	strikeslip	C	M6	0.005	10.2
42	P0171-H-ECC092	strikeslip	C	M6	0.005	11.4
43	P0172-H-EMO000	strikeslip	C	M6	0.005	8.2
44	P0172-H-EMO270	strikeslip	C	M6	0.005	6.6
45	P0175-H-E03140	strikeslip	D	M7	0.005	11.0
46	P0175-H-E03230	strikeslip	D	M7	0.005	14.1
47	P0176-H-E04140	strikeslip	C	M6	0.005	6.5
48	P0176-H-E04230	strikeslip	C	M6	0.005	9.8

#	eqe_list	type	soil	magn	DTVERI	DURATION_EFF
49	P0177-H-E05140	strikeslip	C	M6	0.005	8.2
50	P0177-H-E05230	strikeslip	C	M6	0.005	9.4
51	P0178-H-E06140	strikeslip	C	M6	0.005	11.4
52	P0178-H-E06230	strikeslip	C	M6	0.005	8.4
53	P0179-H-E07140	strikeslip	C	M6	0.005	6.8
54	P0179-H-E07230	strikeslip	C	M6	0.005	4.8
55	P0180-H-E08140	strikeslip	C	M6	0.005	6.8
56	P0180-H-E08230	strikeslip	C	M6	0.005	5.8
57	P0181-H-E10050	strikeslip	C	M6	0.005	12.8
58	P0181-H-E10320	strikeslip	C	M6	0.005	11.7
59	P0182-H-E11140	strikeslip	C	M6	0.005	8.4
60	P0182-H-E11230	strikeslip	C	M6	0.005	7.8
61	P0185-H-EDA270	strikeslip	C	M6	0.005	6.9
62	P0185-H-EDA360	strikeslip	C	M6	0.005	6.6
63	P0186-H-HVP225	strikeslip	C	M6	0.005	11.8
64	P0186-H-HVP315	strikeslip	C	M6	0.005	12.5
65	P0190-H-SHP000	strikeslip	C	M6	0.01	10.0
66	P0190-H-SHP270	strikeslip	C	M6	0.01	7.5
67	P0203-A-E06140	strikeslip	C	M5	0.005	6.5
68	P0203-A-E06230	strikeslip	C	M5	0.005	2.0
69	P0237-A-CVK090	strikeslip	D	M6	0.005	6.3
70	P0237-A-CVK180	strikeslip	D	M6	0.005	5.1
71	P0241-B-CVK090	strikeslip	D	M5	0.005	3.8
72	P0241-B-CVK180	strikeslip	D	M5	0.005	3.5
73	P0266-CPE045	strikeslip	B	M6	0.01	8.6
74	P0266-CPE315	strikeslip	B	M6	0.01	7.6
75	P0317-PTS225	strikeslip	B	M5	0.005	14.7
76	P0317-PTS315	strikeslip	B	M5	0.005	16.5
77	P0319-WSM090	strikeslip	C	M5	0.005	6.6
78	P0319-WSM180	strikeslip	C	M5	0.005	5.9
79	P0320-WLF225	strikeslip	D	M5	0.005	8.4
80	P0320-WLF315	strikeslip	D	M5	0.005	9.2
81	P0451-G03000	strikeslip	C	M6	0.005	15.3
82	P0451-G03090	strikeslip	C	M6	0.005	19.1
83	P0452-G04270	strikeslip	C	M6	0.005	13.2
84	P0452-G04360	strikeslip	C	M6	0.005	12.5
85	P0453-G06000	strikeslip	B	M6	0.005	7.3
86	P0453-G06090	strikeslip	B	M6	0.005	6.5
87	P0454-HVR150	strikeslip	C	M6	0.005	15.2
88	P0454-HVR240	strikeslip	C	M6	0.005	10.6
89	P0458-AND250	strikeslip	B	M6	0.005	6.8
90	P0458-AND340	strikeslip	B	M6	0.005	5.2
91	P0518-CFR225	reverseobligue	B	M6	0.005	7.6
92	P0518-CFR315	reverseobligue	B	M6	0.005	6.1
93	P0519-DSP000	reverseobligue	B	M6	0.005	6.6
94	P0519-DSP090	reverseobligue	B	M6	0.005	7.4
95	P0528-MVH045	reverseobligue	B	M6	0.005	5.1
96	P0528-MVH135	reverseobligue	B	M6	0.005	6.3
97	P0530-NPS210	reverseobligue	B	M6	0.005	4.6
98	P0530-NPS300	reverseobligue	B	M6	0.005	5.2
99	P0531-PSA000	reverseobligue	C	M6	0.005	13.6

#	eqe_list	type	soil	magn	DTVERI	DURATION_EFF
100	P0531-PSA090	reverseobligue	C	M6	0.005	15.6
101	P0535-H08000	reverseobligue	B	M6	0.005	8.3
102	P0535-H08090	reverseobligue	B	M6	0.005	7.0
103	P0548-B-ZAK270	strikeslip	D	M5	0.005	8.5
104	P0548-B-ZAK360	strikeslip	D	M5	0.005	10.6
105	P0551-A-BEN270	strikeslip	D	M7	0.005	16.3
106	P0551-A-BEN360	strikeslip	D	M7	0.005	12.6
107	P0553-A-LAD180	strikeslip	D	M6	0.005	11.6
108	P0553-A-LAD270	strikeslip	D	M6	0.005	14.7
109	P0555-A-ZAK270	strikeslip	D	M6	0.005	6.1
110	P0555-A-ZAK360	strikeslip	D	M6	0.005	8.1
111	P0595-A-ALH180	reversenormal	B	M6	0.005	5.3
112	P0595-A-ALH270	reversenormal	B	M6	0.005	5.8
113	P0624-A-GRV060	reversenormal	B	M5	0.005	5.6
114	P0624-A-GRV330	reversenormal	B	M5	0.005	3.3
115	P0629-A-ING000	reversenormal	B	M6	0.005	7.5
116	P0629-A-ING090	reversenormal	B	M6	0.005	11.1
117	P0630-A-116270	reversenormal	B	M6	0.005	9.3
118	P0630-A-116360	reversenormal	B	M6	0.005	6.4
119	P0642-A-OBR270	reversenormal	B	M5	0.005	8.0
120	P0642-A-OBR360	reversenormal	B	M5	0.005	7.1
121	P0683-A-LUR090	reversenormal	D	M5	0.005	6.9
122	P0683-A-LUR180	reversenormal	D	M5	0.005	5.4
123	P0701-A-TAR000	reversenormal	B	M5	0.005	6.4
124	P0701-A-TAR090	reversenormal	B	M5	0.005	4.9
125	P0707-A-WHD062	reversenormal	D	M5	0.005	9.1
126	P0707-A-WHD152	reversenormal	D	M5	0.005	7.4
127	P0714-B-OBR270	reverseobligue	B	M5	0.005	5.3
128	P0714-B-OBR360	reverseobligue	B	M5	0.005	6.2
129	P0720-B-PTS225	strikeslip	B	M6	0.005	10.3
130	P0720-B-PTS315	strikeslip	B	M6	0.005	11.1
131	P0724-B-CAL225	strikeslip	C	M6	0.005	11.8
132	P0724-B-CAL315	strikeslip	C	M6	0.005	11.6
133	P0725-B-ICC000	strikeslip	C	M6	0.005	14.2
134	P0725-B-ICC090	strikeslip	C	M6	0.005	17.5
135	P0729-B-SUP045	strikeslip	B	M6	0.005	12.3
136	P0729-B-SUP135	strikeslip	B	M6	0.005	12.3
137	P0730-B-WSM090	strikeslip	C	M6	0.005	18.7
138	P0730-B-WSM180	strikeslip	C	M6	0.005	16.2
139	P0733-G01000	reverseobligue	A	M7	0.005	6.5
140	P0733-G01090	reverseobligue	A	M7	0.005	3.7
141	P0734-CYC195	reverseobligue	A	M7	0.005	15.2
142	P0734-CYC285	reverseobligue	A	M7	0.005	12.1
143	P0735-G02000	reverseobligue	C	M7	0.005	11.0
144	P0735-G02090	reverseobligue	C	M7	0.005	9.2
145	P0736-G03000	reverseobligue	C	M7	0.005	6.2
146	P0736-G03090	reverseobligue	C	M7	0.005	11.2
147	P0737-G04000	reverseobligue	C	M7	0.005	12.9
148	P0737-G04090	reverseobligue	C	M7	0.005	14.5
149	P0742-AGW000	reverseobligue	C	M7	0.005	15.8
150	P0742-AGW090	reverseobligue	C	M7	0.005	17.5

#	eqe_list	type	soil	magn	DTVERI	DURATION_EFF
151	P0743-AND270	reverseobligue	B	M7	0.005	10.3
152	P0743-AND360	reverseobligue	B	M7	0.005	10.7
153	P0744-CAP000	reverseobligue	C	M7	0.005	11.7
154	P0744-CAP090	reverseobligue	C	M7	0.005	13.1
155	P0745-CLS000	reverseobligue	B	M7	0.005	6.8
156	P0745-CLS090	reverseobligue	B	M7	0.005	7.9
157	P0746-GMR000	reverseobligue	C	M7	0.005	11.3
158	P0746-GMR090	reverseobligue	C	M7	0.005	9.0
159	P0748-SFO000	reverseobligue	C	M7	0.005	10.5
160	P0748-SFO090	reverseobligue	C	M7	0.005	11.2
161	P0753-A02043	reverseobligue	D	M7	0.005	8.4
162	P0753-A02133	reverseobligue	D	M7	0.005	11.8
163	P0761-CLD195	reverseobligue	B	M7	0.005	13.2
164	P0761-CLD285	reverseobligue	B	M7	0.005	11.3
165	P0764-GIL067	reverseobligue	B	M7	0.005	5.0
166	P0764-GIL337	reverseobligue	B	M7	0.005	4.8
167	P0767-HWB220	reverseobligue	B	M7	0.005	10.1
168	P0767-HWB310	reverseobligue	B	M7	0.005	12.4
169	P0769-HSP000	reverseobligue	D	M7	0.005	13.3
170	P0769-HSP090	reverseobligue	D	M7	0.005	21.1
171	P0774-SLC270	reverseobligue	C	M7	0.005	12.0
172	P0774-SLC360	reverseobligue	C	M7	0.005	11.0
173	P0779-STG000	reverseobligue	B	M7	0.005	9.3
174	P0779-STG090	reverseobligue	B	M7	0.005	8.1
175	P0780-WVC000	reverseobligue	B	M7	0.005	11.1
176	P0780-WVC270	reverseobligue	B	M7	0.005	10.7
177	P0789-SVL270	reverseobligue	C	M7	0.005	20.2
178	P0789-SVL360	reverseobligue	C	M7	0.005	20.2
179	P0807-EUR000	reversenormal	B	M7	0.005	20.8
180	P0807-EUR090	reversenormal	B	M7	0.005	19.9
181	P0809-PET000	reversenormal	C	M7	0.005	17.8
182	P0809-PET090	reversenormal	C	M7	0.005	16.1
183	P0810-RIO270	reversenormal	B	M7	0.005	15.4
184	P0810-RIO360	reversenormal	B	M7	0.005	10.9
185	P0816-JOS000	strikeslip	B	M7	0.005	27.2
186	P0816-JOS090	strikeslip	B	M7	0.005	26.1
187	P0873-LCN000	strikeslip	A	M7	0.005	13.4
188	P0873-LCN275	strikeslip	A	M7	0.005	13.1
189	P0881-YER270	strikeslip	C	M7	0.005	17.6
190	P0881-YER360	strikeslip	C	M7	0.005	18.9
191	P0883-ORR090	reversenormal	B	M6	0.005	9.1
192	P0883-ORR360	reversenormal	B	M6	0.005	8.6
193	P0884-HOL090	reversenormal	C	M6	0.005	12.0
194	P0884-HOL360	reversenormal	C	M6	0.005	10.7
195	P0887-ARL090	reversenormal	B	M6	0.005	13.0
196	P0887-ARL360	reversenormal	B	M6	0.005	13.5
197	P0897-DWN090	reversenormal	C	M6	0.005	17.3
198	P0897-DWN360	reversenormal	C	M6	0.005	14.4
199	P0903-BLD090	reversenormal	B	M6	0.005	16.6
200	P0903-BLD360	reversenormal	B	M6	0.005	17.4
201	P0905-CCN090	reversenormal	B	M6	0.005	13.2

#	eqe_list	type	soil	magn	DTVERI	DURATION_EFF
202	P0905-CCN360	reversenormal	B	M6	0.005	13.7
203	P0912-OBR090	reversenormal	B	M6	0.005	11.0
204	P0912-OBR360	reversenormal	B	M6	0.005	11.3
205	P0927-NWH090	reversenormal	C	M6	0.005	5.9
206	P0927-NWH360	reversenormal	C	M6	0.005	5.5
207	P0928-PKC090	reversenormal	B	M6	0.005	10.1
208	P0928-PKC360	reversenormal	B	M6	0.005	9.9
209	P0934-SYL090	reversenormal	C	M6	0.005	6.8
210	P0934-SYL360	reversenormal	C	M6	0.005	5.3
211	P1041-KAK000	strikeslip	D	M6	0.005	13.2
212	P1041-KAK090	strikeslip	D	M6	0.005	12.9
213	P1043-KJM000	strikeslip	B	M6	0.005	8.4
214	P1043-KJM090	strikeslip	B	M6	0.005	9.5
215	P1046-NIS000	strikeslip	D	M6	0.005	9.7
216	P1046-NIS090	strikeslip	D	M6	0.005	11.2
217	P1054-SHI000	strikeslip	D	M6	0.005	10.3
218	P1054-SHI090	strikeslip	D	M6	0.005	11.8
219	P1056-TAZ000	strikeslip	D	M6	0.005	4.6
220	P1056-TAZ090	strikeslip	D	M6	0.005	3.7
221	P1057-TAK000	strikeslip	D	M6	0.005	11.4
222	P1057-TAK090	strikeslip	D	M6	0.005	9.9
223	P1096-DZC180	strikeslip	C	M7	0.005	11.8
224	P1096-DZC270	strikeslip	C	M7	0.005	10.6
225	P1540-DZC180	strikeslip	C	M7	0.005	11.0
226	P1540-DZC270	strikeslip	C	M7	0.005	10.8
227	P1547-BOL000	strikeslip	C	M7	0.005	8.5
228	P1547-BOL090	strikeslip	C	M7	0.005	9.4

APPENDIX B: THE COMPUTER PROGRAM FOR THE DERIVATION OF THE ENERGY SPECTRA

```
% INELASTIC SPECTRA ANALYZING PROGRAMME
% WRITTEN BY AHMET ANIL DINDAR- adindar@iku.edu.tr
% on 17 NOVEMBER 2008, Tuesday
% the program runs based on target ductility ratio value
%% CLEANING
clc,clear,close all,fclose all;
% format short
tic
%% PROGRAM BAŞLAR
%% TRY-CATCH OLAYI
 try
%% DEPREM DATASININ OKUNMASI İLE PROGRAM BAŞLAR :)
EQE_READER_index=menu('Select the EQE file option','Read from list','Select from folder');
   switch EQE_READER_index
      case 1
        [file path]=uigetfile({'*.txt';'*.dat';'*.*'},'Select the EQE file');
        EQE_LIST_FILE=[path,file]; % file in which the EQE files are listed
        File_List=(textread([EQE_LIST_FILE],'%s'))';
      case 2
         % Tek bir dosya DEPREM DOSYASININ OKUTULMASI
        [File_Lis,path,Filter_index] = uigetfile({'*.*'});
        File_List{1,1}=File_Lis;
   end
%% LOGGING
  % Filing
   mkdir('LOG');
   log=fopen(([pwd,'\LOG\LOG- ',datestr(now,'ddmmyyyy-HHMM'),'.dat']),'w+'); % Bu log file ne
güzel!
   screen_log=fopen(([pwd,'\LOG\SCREEN LOG- ',datestr(now,'ddmmyyyy-HHMM'),'.dat']),'w+');
% Bu log file ne güzel!
%% KAÇINCI ANALİZ OLDUĞUGUNUN BELİRLENMESİ
analiz_sayisi_degeri=menu('Analiz Sayisi','1. analiz','2. analiz','3. analiz','4. analiz','5. analiz');
   switch analiz_sayisi_degeri
      case 1
         analiz_sayisi=1 ;
      case 2
         analiz_sayisi=2;
      case 3
          analiz_sayisi=3 ;
      case 4
         analiz_sayisi=4 ;
      case 5
         analiz_sayisi=5;
   end
% mail gönderilmesi
  mail_report2('PR023-START: ',[num2str(analiz_sayisi),' on ',datestr(now,'ddmmyyyy-HHMM')])
%% LET'S CHANGE THE EQE UNIT TO G
unit_factor=menu('select the units of the EQE file','g','m/sec','cm/sec2');
  switch unit_factor
     case 1
        unit_converter=1;
     case 2
        unit_converter=9.81 ;
     case 3
        unit_converter=981   ;
  end
```

```
%% TYPE_EQE_DURATION
TYPE_EQE_DURATION=menu('select the duration type','normal','effective');
%% PGA index
PGA_index=menu('select the PGA value','Original','0.1','0.2','0.3','0.6','other');
   switch PGA_index
%              case 1
%                 PGA=max(abs(agg3));  % PGA degeri
       case 2
          PGA=0.1 ;          % PGA degeri
       case 3
          PGA=0.2 ;          % PGA degeri
       case 4
          PGA=0.3 ;          % PGA degeri
       case 5
          PGA=0.6 ;          % PGA degeri
       case 6
          PGA=input('Değerli kardeşim, hadi verini sen gir (g)  : ') ;
   end
%% SYSTEM HEIGHT
height=3000 ; % in milimeter
%% Damping of the system
dampingratioindex=menu('select critical damping ratio','% 0','% 2','% 5 ','% 10','other');
   switch dampingratioindex
      case 1
         dampingratio=0 ;
      case 2
         dampingratio=2 ;
      case 3
         dampingratio=5 ;
      case 4
         dampingratio=10 ;
      case 5
        dampingratio=input('Değerli kardeşim, hadi verini sen gir (%)  : ') ;
   end
%% PROGRAM TERMINITION TIME
terminate_time=menu('SELF-DESTRUCTION','YES','NO');
  switch terminate_time
     case 1
        self_destrution_time=input('Enter the time of self-destruction (0700) : ');
         fprintf(screen_log,' %s : SELF-DESTRUCTION SET as %f \n',datestr(now,'ddmmyyyy-
HHMM'),self_destrution_time) ;
         fprintf(' %s : SELF-DESTRUCTION SET as %f \n',datestr(now,'ddmmyyyy-
HHMM'),self_destrution_time) ;
      case 2
         fprintf(screen_log,' %s : NO SELF-DESTRUCTION \n',datestr(now,'ddmmyyyy-HHMM')) ;
         fprintf(' %s  : NO SELF-DESTRUCTION \n',datestr(now,'ddmmyyyy-HHMM')) ;
  end
%% PERIOD DEFINITION
% The period range is defined in this section
   period_range=[(0.05:.05:1.0),(1.25:.25:3.0)]' ; % GEnerally 0.05-3.0 sec
%% STIFFNESS DEFINITION
bending_stiffness=1*10^10 ; % [1*10^10;2*10^10;4*10^10] -> Stiffness Range (kN.mm2)
stiffness=3*bending_stiffness/(height^3) ; % "k" value (kN/mm)
%% NON-LINEARITY TOLERANCE AND DUCTILITY
   tolerance=0.05 ;
   tar_duc=[1;2;4;6]; % This is the range of the ductility
   convergence_limit=20 ;
%% PROGRAMIN BAŞLAMASI
for i=1:size(File_List,2) ; % The loop for EQE's
```

```
file=File_List{1,i}   ; % Temp. assignment of EQE to a pivot variable
% Hazırlık
  % duration coeff
    duration_coeff=1 ; % bu rakam deneme ile belirlendi
  % düktilite tablosunun index counterı
    index_counter=1;
  % Recalling the EQE file from its nest
    path=['D:\aad\EQES\'];
    EQE_FILE_NAME=[path,file]; %
  % sonucların konacağı dosya yaratılırsa
    mkdir([pwd,'\RESULTS\',file(1:end-4)]); %
%       mkdir([pwd,'\RESULTS\',file(1:end-4),'\TH']); %
%% DEPREM HEADER OKUTULURSA
   fid_EQE=fopen(EQE_FILE_NAME) ; % EQE file opening
   counter=1;
    while counter<5 ; % SADECE ILK 4 SATIR OKUNACAK- "HEADER LINES" !
      tline=fgets(fid_EQE) ;
      % 2. satır- Olay adı
        if counter==2
          EQE_EVENT_NAME=tline(1:min(findstr(tline,'/'))-3) ;
        end
      % 4. satır- data sayısı ve kısıtlanması
        if counter==4
          wp1=strfind(tline,',') ;
          NOOFDATA=str2num(tline(6:wp1-1));
        % checking the NOOFDATA for the limitation :)
          if NOOFDATA>6500
             NOOFDATA=6500;
          end
          wp2=strfind(tline,'DT=') ;
          wp3=strfind(tline,'SEC') ;
          DTVERI=str2num(tline(wp2+3:wp3-1));
        end
       % bir sonraki satıra geçiş counterı
       counter=counter+1  ;
    end
   % header'dan çıkan bilgi ile deprem süresinin hesabı
    DURATION=NOOFDATA*DTVERI ; % DEPREM SURESININ HESABI
   %  dosyanın kapanması
    fclose(fid_EQE) ;
% End of reading Header
%% ŞİMDİ DE DEPREM DATASI OKUTULURSA
 % eğer varsa eqe datasını silelim
   delete([pwd,'\eqe_temp.dat'])
 % şimdi deprem datası okunur ve sonra da düzeltilerek yeniden yazılır!
   EQE_file=fopen(EQE_FILE_NAME); % Mevcut EQE data
   EQE_file_new=fopen([pwd,'\eqe_temp.dat'],'a+'); % EQE'nin yeni dosyası
   counter2=1 ; % EQE içinde headerlines'ı atlamak için counter değeri
    % şimdi EQE file okunuyor !
    while ~feof(EQE_file)
      tline = fgets(EQE_file); % EQE file her bir satır
      if counter2<5 % Headerline'ı atlamak için
      else
        fprintf(EQE_file_new,'%s',tline);
      end
      counter2=counter2+1 ;
    end
  fclose (EQE_file) ;
  fclose (EQE_file_new) ;
```

```
        % NOTE "neden bilemedim ama şu anda dosyaya yazdığım veriyi tekrar MATLAB içine alıyorum"
            agg1=dlmread([pwd,'\eqe_temp.dat'])/unit_converter; % unit_converter: converts the input file to "g" units
                delete([pwd,'\eqe_temp.dat'])  % ilginç eqe_temp.dat siliniyor
        %   TODO "burasini biraz toparlamalı sanırım ileride"
            agg2=reshape(agg1',[size(agg1,1)*size(agg1,2),1]); % Burada tek kolona indirgeme var.
             agg3=agg2(1:NOOFDATA,1); % Tamamdır, burada limitlenmiş data var, aslında bir fark yok
               % ŞİMDİ PGA HESABI OLSUN
          %% EQE kaydının PGA'ye göre normalize edilmesi
               switch PGA_index
                  case 1
                     PGA=max(abs(agg3));  % PGA degeri
               end
               % işte burada eqe scale ediliyor :)
                 agg3=PGA*(agg3/(max(abs(agg3))));  % agg3 normalize ediliyor :)
          %% EFFECTIVE DURATION CALCULATION (TRIFUNAC-BRADY)
           % Arias Intensity
                 Ia=(pi/(2*9.81))*cumtrapz(agg3.^2)*DTVERI ; % Arias Intensity
                  Ia_05=.05*Ia(end) ; % 0.05 of Arias Intensity- LOWER
                  Ia_95=.95*Ia(end) ; % 0.95 of Arias Intensity- UPPER
           % EQE duration selection- Pre-defined
              switch TYPE_EQE_DURATION
                 case 1
                  % All record
                     agg4=agg3 ;
                     NOOFDATA_EFF=size(agg4,1) ;
                     DURATION_EFF=DTVERI*NOOFDATA_EFF ;
                     t1=size(agg3,1);
                     t2=size(agg3,1);
                 case 2
                   % Indexed time instants
                     t1=find(Ia<Ia_05) ; % time less than 0.05 of Ia
                      t1=t1(end) ;
                     t2=find(Ia>Ia_95) ; % time greater than 0.95 of Ia value;
                      t2=t2(1)-1   ; % son değeri aralığa almak için
                   % effective ground acceleration seri is
                     agg4=agg3(t1:t2) ;
                     NOOFDATA_EFF=size(agg4,1) ; % T-F kuralı gereği "EFF" ifadeleri geldi
                     DURATION_EFF=DTVERI*NOOFDATA_EFF ;
              end
           % plotting the values
              figure(i),
               plot((DTVERI:DTVERI:DURATION),agg3,'r'),hold on, % EQE ilk hal
               plot((DTVERI:DTVERI:DTVERI*t2),agg3(1:t2),'b'), % EQE son hal-I
               plot((DTVERI:DTVERI:DTVERI*t1),agg3(1:t1),'r') % EQE Son hal-II
                 title(['Effective Ground Acc-',file(1:end-4)]),grid on
                 xlabel('t (sec)'),ylabel('acc (g)'),YLim([-1,1])
                 saveas(gcf,[pwd,'\RESULTS\',file(1:end-4),'\',file(1:end-4),'-Effective Ag.png']) ;
              close
          %% DEPREM VERISININ DEĞERLENDIRILMESININ IDARC IÇIN YAZILMASI
              delete('eqe.dat'); % folderdaki mevcutun silinmesi
               dlmwrite('eqe.dat',agg4);  % IDARC için verinin yazılması
              % Results klasöründe yerine kopyalama
               dlmwrite([pwd,'\results\',file(1:end-4),'\',file(1:end-4),'- Eff eqe.dat'],agg4);    % effective verinin dosyaya yazılması
          %% ABSOLUTE VALUE ANALİZ İÇİN HIZIN HESAPLANMASI
               agg5=agg4*9.81 ; % şimdi burada enerji hesabı için m/s2 birimine çevirdim
                 vgg=cumtrapz(agg5)*DTVERI ;
```

```
                dgg=cumtrapz(vgg)*DTVERI ;
        %% VERİLEN EQE KAYDI İÇİN HEDEF DÜKTİLİTE İÇİN SPECTRA'NIN BELİRLENMESİ
        initial=1;
        for j=1:size(period_range,1) ; % Her bir period değeri için spectral loop
            for k=1:size(tar_duc,1);  % Düktilite listesinin gözden geçirilmesi
                mkdir([pwd,'\RESULTS\',file(1:end-4),'\',num2str(tar_duc(k,1)),'\TH\']); %
            %% ŞİMDİ DE IDARC INPUT DOSYASINI HAZIRLAYALIM
                % BURADA PERIOD DEGERI DEĞİŞİMİ YAPILIYOR VE DONGUYE GIRIYOR
                % Başlangıç değerlerinin belirlenmesi
                % Period range'nden ilgili değer
                    period=period_range(j) ;
                % calculation of the weight
                    weight=(period/(2*pi))^2*stiffness*9810 ; % This is the weight in kN
                % iterative degerlendirme için başlangıç degerleri
                stopper=1 ; % bu aslında bir counter değeri değil mi
        % NOTE "ŞU ANDA BURASI DENEMEDE 121108-2259"
            if initial==1;
                pyp_carpan=1 ; % PYP'nin ilk değerini ayarlamak için gerekiyor
                EI=2.00E+10 ;
                PYP=(weight*height*PGA)*pyp_carpan ;
                PYP_matrix=[PYP;0;0]      ;
            elseif initial==2
                PYP=PYP_matrix(1,1);
            elseif initial==3
                PYP=PYP_matrix(2,1);
                stopper=2 ;
            elseif initial==4
                PYP=PYP_matrix(2,1);
                stopper=2 ;
            end
        % NOTE "ŞU ANDA BURASI DENEMEDE 121108-2259"
        %               pyp_carpan=2 ; % PYP'nin ilk değerini ayarlamak için gerekiyor
        %               PYP=(weight*height*PGA)*pyp_carpan ;
        %               PYP_matrix=[PYP;0;0]   ;
                % IDARC dosyalarının hazırlanması
                while 1  % Hocam, şimdi burası resmin koptuğu yerdir.

                    %% işte çok kritik bir yer daha, eğer saat belli bir değerde ise 0800 gibi
                    %% otomatik program durdur ve verileri sakla komutu vereceğim.
                        if terminate_time==1 && str2num(datestr(now,'HHMM'))>self_destrution_time &&
str2num(datestr(now,'HHMM'))<(self_destrution_time+30);
                            mail_report2(['PR023-BREAK:',file(1:end-4),',      d=',num2str(tar_duc(k,1)),'      on
'],datestr(now,'ddmmyyyy-HHMM'))
                            fclose all
                        quit
                        end
                    %% NOTE DENEME
                    % PYP'nin güncellenmesi
                        PCP=0.99*PYP ;
                    % input file'ın yazılması
                        fid_BOS=fopen('PR023-input(BOS).DAT') ;
                        fidd_YENI=fopen('PR023-input.dat','w+') ;
                        while ~feof(fid_BOS) ;
                            tline = fgets(fid_BOS);
                            tline=strrep(tline,'WEIGHT',num2str(weight)) ;
                            tline=strrep(tline,'HEIGHT',num2str(height)) ;
                            tline=strrep(tline,'STIFFNESS',num2str(bending_stiffness)) ;
                            tline=strrep(tline,'PYP_VALUE',num2str(PYP)) ;
                            tline=strrep(tline,'PCP_VALUE',num2str(PCP)) ;
```

```
                    tline=strrep(tline,'UYP_VALUE',num2str(1.02*PCP/bending_stiffness)) ;
                    tline=strrep(tline,'PGA',num2str(PGA)) ;
                    tline=strrep(tline,'DURATION',num2str(DURATION_EFF)) ;
                    tline=strrep(tline,'NOOFDATA',num2str(NOOFDATA_EFF)) ;
                    tline=strrep(tline,'DTVERI',num2str(DTVERI)) ;
                    tline=strrep(tline,'DTHESAP',num2str(DTVERI/20)) ;
                    tline=strrep(tline,'DAMPINGRATIO',num2str(dampingratio)) ;
                    fwrite(fidd_YENI,tline);
                end
                fclose(fid_BOS) ;
                fclose(fidd_YENI);
            % IDARC VERISI HAZIRLANDI %%%%%%%%%%%%%%%%%%%
            %% RUNNING IDARC
        %          ! idarc2d_6.0.exe
                winopen idarc2d_6.0.exe ; % iste IDARC çalışmas satırı
             % pause miktarının belirlenmesi
               pause(duration_coeff*NOOFDATA_EFF/500)      ;
             %% READING THE RESULTS
        %                Reading the response file
[story_time,story_disp,story_drift,story_shear,story_absacc,story_damagebeamslab,story_damagecolwall,sto
ry_relvel,story_relacc]...
            =textread(['PR023-story.out'],'%f %f %f  %f %f %f %f %f %f','headerlines',10); % iste o
muhtesem satir
    %--------------------------TEST ET---------------
          % DIKKAT ÖNEMLİ BİR KONTROL: BURADA IDARC ÇÖZÜMÜNÜN EKSİKLİĞİ
KONTROL EDİLİYOR
            if size(story_relvel,1)-size(vgg,1)<0 ;
               duration_coeff=duration_coeff+2 ;
               fprintf(screen_log,' %s %s : duration düzeltildi %.0f sn\n',datestr(now,'ddmmyyyy-
HHMM'),file(1:end-4),duration_coeff) ;
               fprintf(' %s %s : duration düzeltildi %.0f sn\n',datestr(now,'ddmmyyyy-
HHMM'),file(1:end-4),duration_coeff) ;
               continue
            end
    %--------------------------TEST ET---------------
         % converting files in "mm" to "m"
            story_drift=story_drift(1:end-1,1)/1000; story_shear=story_shear(1:end-1,1); % drift and shear
of the story
            story_disp=story_disp(1:end-1,1)/1000;
            story_relvel=story_relvel(1:end-1,1)/1000 ; story_absvel=story_relvel+vgg ;
            story_relacc=story_relacc(1:end-1,1)/1000; story_absacc=story_absacc(1:end-1,1)/1000; % ---
--->>>> UNIT CONVERSION
            time=story_time(1:end-1,1);
         % Reading the column data file

[column_time,phibot,momentbot,phitop,momenttop,axialforce,column_drift,column_shear,rotbot,plasrotbot,r
ottop,plastrotbot]...
            =textread('COL_001.prn','%f %f %f  %f %f %f %f %f %f %f %f %f','headerlines',4); % iste
o muhtesem satir
         % converting files in "kN.mm" to "kN.m"
            column_momentbot=momentbot(1:end-1,1)/1000;      column_momenttop=momenttop(1:end-
1,1)/1000;  % moment values
            column_phibot=phibot(1:end-1,1)*1000   ;   column_phitop=phitop(1:end-1,1)*1000   ;   %
curvature values
            column_rotbot=rotbot(1:end-1,1); column_rottop=rottop(1:end-1,1) ; % rotation values
            column_shear=column_shear(1:end-1,1);
              %% READING THE DEFORMED FILE and finding the ductility values
             % READING THE DEFORMED FILE
                 [vy,dy]=deformed_file_reader ;
```

```
        %% end of reading results
%%%%%%%%%%%%%%%%%%%%%%%%%%%%%%%%%%%%%
        du=max(abs(story_disp)) ;
        ductility=du/dy   ;
        vy=vy*weight ;
        % tabiki duc. de ayarlanıyor
        if isinf(ductility)==1
            ductility=1 ;
        end
      %% INDEXING THE RESPONSES
       index(index_counter,1:7)=[PYP, tar_duc(k,1), abs(vy), abs(dy), dy,
polyarea(story_drift,story_shear), ductility] ;
       index=sortrows(index,[-1]) ; % this command sorts the index matrix wrt the PYP values
         fprintf(screen_log,'  %s  %s      %.0f  p=%.3f  d=%.0f  PYP=%.0f  d_now=%.2f
\n',datestr(now,'ddmmyyyy-HHMM'),file(1:end-4),stopper,period,tar_duc(k,1),PYP,ductility) ;
         fprintf('  %s  %s      %.0f  p=%.3f  d=%.0f  PYP=%.0f  d_now=%.2f
\n',datestr(now,'ddmmyyyy-HHMM'),file(1:end-4),stopper,period,tar_duc(k,1),PYP,ductility) ;
      %% NEW PYP VALUE DEFINITION
  %% eğer sistem kafadan inelastic başlarsa diye.
         if k==1 && stopper==1 && ductility>1
           pyp_carpan=pyp_carpan+1 ;
           PYP=(weight*height*PGA)*pyp_carpan ;
           PYP_matrix=[PYP;0;0]     ;
           index_counter=index_counter+1 ; % bu index'i arttırır NOTE "indexi arttırmak için"
           continue
         end
  % şimdi burada ilk adımın döngüde kullanılması için bir hareket yapıyorum.
         if tar_duc(k,1)==1 && ductility==1 % linear durumda ilk etapta durmak için
            fprintf(screen_log,'%s %s convergence = %.5f \n "artık analiz bitti !
"\n',datestr(now,'ddmmyyyy-HHMM'),file(1:end-4),abs(tar_duc(k,1)-ductility)/tar_duc(k,1)*100);
            fprintf('%s %s convergence = %.5f \n "artık analiz bitti ! " %s %s
\n',datestr(now,'ddmmyyyy-HHMM'),file(1:end-4),abs(tar_duc(k,1)-ductility)/tar_duc(k,1)*100);
            index_counter=index_counter+1 ; % bu index'i arttırır NOTE "indexi arttırmak için"
           break
         elseif stopper==1 && ductility < (1+tolerance)*tar_duc(k,1)%
                   PYP=mean(PYP_matrix(1:2,1)) ;
                   PYP_matrix=[PYP_matrix(1,1);PYP;PYP_matrix(2,1)] ;
                   PYP_matrix=sort(PYP_matrix,'descend') ;
         else
           if ductility>=(1-tolerance)*tar_duc(k,1) && ductility<=(1+tolerance)*tar_duc(k,1) ;
             fprintf(screen_log,' %s %s convergence = %.5f \n "artık analiz bitti !
"\n',datestr(now,'ddmmyyyy-HHMM'),file(1:end-4),abs(tar_duc(k,1)-ductility)/tar_duc(k,1)*100);
             fprintf(' %s %s convergence = %.5f \n "artık analiz bitti !
"\n',datestr(now,'ddmmyyyy-HHMM'),file(1:end-4),abs(tar_duc(k,1)-ductility)/tar_duc(k,1)*100);
             index_counter=index_counter+1 ; % bu index'i arttırır NOTE "indexi arttırmak için"
             break
           elseif ductility > (1+tolerance)*tar_duc(k,1)%
             PYP=mean(PYP_matrix(1:2,1)) ;
             PYP_matrix=[PYP_matrix(1,1);PYP;PYP_matrix(2,1)] ;
             PYP_matrix=sort(PYP_matrix,'descend') ;
            % şimdi bir önlem alalım sonsuz döngüye karşılık
            if stopper==convergence_limit
              fprintf(screen_log,' %s %s converge olmadı\n',datestr(now,'ddmmyyyy-
HHMM'),file(1:end-4))
              fprintf(' %s %s converge olmadı \n',datestr(now,'ddmmyyyy-HHMM'),file(1:end-
4))
                      mail_report2(['PR023-DIVERGENCE:',file(1:end-
4)],datestr(now,'ddmmyyyy-HHMM'))
              break
```

```
                        end ;
                       elseif ductility<(1-tolerance)*tar_duc(k,1)
                          PYP=mean(PYP_matrix(2:3,1)) ;
                          PYP_matrix=[PYP_matrix(2,1);PYP;PYP_matrix(3,1)] ;
                          PYP_matrix=sort(PYP_matrix,'descend') ;
                        % şimdi bir önlem alalım sonsuz döngüye karşılık
                        if stopper==convergence_limit
                           fprintf(screen_log,' %s %s converge olmadı\n',datestr(now,'ddmmyyyy-
HHMM'),file(1:end-4))
                           fprintf(' %s %s converge olmadı \n',datestr(now,'ddmmyyyy-HHMM'),file(1:end-
4))
                                    mail_report2(['PR023-DIVERGENCE:',file(1:end-
4)],datestr(now,'ddmmyyyy-HHMM'))
                            break
                        end ;
                       end
                    end
            stopper=stopper+1  ;
            index_counter=index_counter+1 ; % bu index'i arttırır
                 end % "iterative durum için loop sonu"
            %% PLOTTING THE RESULTS
        %                       plot(story_drift,story_shear), grid on, title(['PGA=',num2str(PGA),'-
weight=',num2str(weight),',  vy=',num2str(vy),'  ,  dy=',num2str(dy),'  ,du=',num2str(du),'
,duct=',num2str(ductility)]),xlabel('disp (m)'),ylabel('force (kN)')
        %                       saveas(gcf,['Ductility=',num2str(tar_duc(k,1)),',  PGA=',num2str(PGA),',
vy=',num2str(vy),'-weight=',num2str(weight),'-duct=',num2str(ductility),'.png'],'png')
        % %                 pause
        %                 close all

spectra(j,1:5,k)=[max(abs(story_shear)),max(abs(story_drift)),max(abs(story_relvel)),max(abs(story_relacc))
,max(abs(story_absacc))];
        %%      % NOTE "işte buradan sonra energy mevzusu başlayacak"
             %% ENERJI ANALIZI ----------------------------------------------------------------
                 mass=(weight)/9.81; % now mass is kN-m
                 damping=(dampingratio/100)*2*mass*(2*pi/period) ; % 5% ratio
                 %% bakalım kuvvet balance nasıl? % NOTE "buradadurdurk"
                 force_inertia=mass*story_relacc ; force_damping=damping*story_relvel ;
                 force_resisting=story_shear ; force_effective=mass*agg5 ;
                    force_error=force_inertia+force_damping+force_resisting+force_effective ;
                 %% sonuçları kayıt etmek
                     % TH klasörü içinde

response=[time,period*ones(size(time,1),1),mass*ones(size(time,1),1),damping*ones(size(time,1),1),stiffnes
s*1000*ones(size(time,1),1),story_drift,story_relvel,story_absvel,story_relacc,story_absacc,story_shear,agg5
,force_error];
                        dlmwrite([pwd,'\results\',file(1:end-4),'\',num2str(tar_duc(k,1)),'\TH\',file(1:end-4),'-
',num2str(j),'-RTH.dat'],...
                            response,'delimiter','\t');
                      % spectra için
                        response_spectra(j,1:14,k)=[period  ,mass,damping,stiffness*1000,ductility,
max(abs(response(:,6:13))),max(Ia)] ; % spectra için kullanılacak
                 %% enerji analizi
                    % absolute energy
                      abs_Ei=mass*cumtrapz(dgg,story_absacc) ;
                      abs_Ek=mass*(story_absvel.^2)/2 ;
                      abs_Ed=damping*cumtrapz(story_disp,story_relvel) ;
                      abs_Es=0.5*stiffness*1000*(story_disp.^2) ;
                      abs_Eh=cumtrapz(story_disp,story_shear) ;
                    % ENERGY VALUES
```

```
                    abs_energy_error=abs_Ei-(abs_Ek+abs_Ed+abs_Es+abs_Eh) ;
                    abs_ENERGY=[abs_Ei,abs_Ek,abs_Ed,abs_Es,abs_Eh,abs_energy_error] ;
                % relative energy time-history
                    rel_Ei=-1*mass*cumtrapz(story_disp,agg5) ;
                    rel_Ek=mass*(story_relvel.^2)/2 ;
                    rel_Ed=damping*cumtrapz(story_disp,story_relvel) ;
                    rel_Es=0.5*stiffness*1000*(story_disp.^2) ;
                    rel_Eh=cumtrapz(story_disp,story_shear) ;
                  % ENERGY VALUES
                    rel_energy_error=rel_Ei-(rel_Ek+rel_Ed+rel_Es+rel_Eh) ;
                    rel_ENERGY=[rel_Ei,rel_Ek,rel_Ed,rel_Es,rel_Eh,rel_energy_error] ;
                 % recording the energy
                  % TH klasörü içinde
                        dlmwrite([pwd,'\results\',file(1:end-4),'\',num2str(tar_duc(k,1)),'\TH\',file(1:end-
4),'-',num2str(j),'-ETH.dat'],...
                    [abs_ENERGY,rel_ENERGY],'delimiter','\t');
                  % spectra için

energy_spectra_max(j,1:12,k)=[period,mass,max(abs_Ei),max(abs_Ek),max(abs_Ed),max(abs_Es),max(abs_
Eh),...

max(rel_Ei),max(rel_Ek),max(rel_Ed),max(rel_Es),max(rel_Eh)]; % maximum değerlerin alınmsı ile spectra
olması

energy_spectra_end(j,1:12,k)=[period,mass,abs_Ei(end),abs_Ek(end),abs_Ed(end),abs_Es(end),abs_Eh(end),
...

rel_Ei(end),rel_Ek(end),rel_Ed(end),rel_Es(end),rel_Eh(end)]; % maximum değerlerin alınmsı ile spectra
olması
              %% printing the Input Energy
                 % abs values
                 figure
                  subplot(3,1,1:2),plot(time,abs_Ek,'b--'),hold on
                              plot(time,(abs_Ek+abs_Es),'g-.'),
                                 plot(time,(abs_Ek+abs_Es+abs_Ed),'r-.'),
                                    plot(time,(abs_Ek+abs_Es+abs_Ed+abs_Eh),'m.'),
                                       plot(time,abs_Ei,'k')
                     title(['abs       ETH-       ',file(1:end-4),'      -      T=',num2str(period),'      s      -
','d=',num2str(tar_duc(k))]),grid on
                     ylabel('Ei/mass (m2/s2)'),xlim([0,time(end)]);
                  subplot(3,1,3),plot(time,agg5),ylabel('ag (m/s2)'),grid,xlim([0,time(end)])
                     saveas(gcf,[pwd,'\RESULTS\',file(1:end-4),'\',num2str(tar_duc(k,1)),'\TH\',file(1:end-
4),'-',num2str(j),'-abs TH.png']) ;
                     close
                  % rel values
                  figure
                  subplot(3,1,1:2),plot(time,rel_Ek,'b--'),hold on
                              plot(time,(rel_Ek+rel_Es),'g-.'),
                                 plot(time,(rel_Ek+rel_Es+rel_Ed),'r-.'),
                                    plot(time,(rel_Ek+rel_Es+rel_Ed+rel_Eh),'m.'),
                                       plot(time,rel_Ei,'k')
                     title(['rel       ETH-       ',file(1:end-4),'      -      T=',num2str(period),'      s      -
','d=',num2str(tar_duc(k))]),grid on
                     ylabel('Ei/mass (m2/s2)'),xlim([0,time(end)]);
                  subplot(3,1,3),plot(time,agg5),ylabel('ag (m/s2)'),grid,xlim([0,time(end)])
                     saveas(gcf,[pwd,'\RESULTS\',file(1:end-4),'\',num2str(tar_duc(k,1)),'\TH\',file(1:end-
4),'-',num2str(j),'-rel TH.png']) ;
                     close
          %    % saving the variables into
```

```
%                save ([pwd,'\results\',file(1:end-4),'\',num2str(tar_duc(k,1)),'\',file(1:end-4),'.mat']);
    %% BİR SONRAKİ DÜKTİLİTE İÇİN İŞLEM YAPTIRMAK
        if k==size(tar_duc,1)
            continue
        elseif isempty(find(index(:,end)>tar_duc(k+1,1)))==1 ;
%               initial=1 ; % PYP ilk değerini değerlendirmek için
            PYP_matrix=[index(end,1);0;0];
            initial=2; % böylece PYP linearlikten kurtuluyor...
            index_counter=index_counter-1 ; % indexte duplicate olmasın diye
             continue
        elseif (find(index(:,end)>tar_duc(k+1,1)))>2
            new_pyp_matrix=find(index(:,end)>tar_duc(k+1,1)) ;
            PYP_matrix_start=new_pyp_matrix(1) ;
            PYP_matrix(1,1)=index(PYP_matrix_start-1,1);
            PYP_matrix(3,1)=index(PYP_matrix_start,1);
            PYP_matrix(2,1)=0.5*(PYP_matrix(1,1)+PYP_matrix(3,1)) ;
            initial=3; % böylece PYP linearlikten kurtuluyor...
        elseif (find(index(:,end)>tar_duc(k+1,1)))==2
            PYP_matrix(1,1)=index(1,1) ;
            PYP_matrix(3,1)=index(2,1) ;
            PYP_matrix(2,1)=0.5*(PYP_matrix(1,1)+PYP_matrix(3,1));
            initial=4 ;
            continue
        end
%-------------------------------------------------------------------------
     end  % "ductility range için loop sonu" (değişken "k")
       %% log file'a yazma
        fprintf(log,'%s : %s \n',datestr(now,'ddmmyyyy-HHMM'),file(1:end-4));
    % yeniperiyotta başlangıç şartları
       clear index ;
       initial=1;
        index_counter=1 ;
    end % period range için loop sonu (değişken "j")
   %% ARTIK SPECTRALAR OLUŞTURULUYOR
    for k=1:size(tar_duc,1)
        % writing into the files
            % relative energy into file
              dlmwrite([pwd,'\results\',file(1:end-4),'\',num2str(tar_duc(k,1)),'\',file(1:end-4),'-EnSp
max','.dat'],...
                  energy_spectra_max(:,1:12,k),'delimiter','\t','-append') ;
              % ftp-push
%                 comp_name=getenv('COMPUTERNAME');
%                 comp_name2=comp_name(5:end);
%                  ftp_remote=ftp('10.254.10.90',comp_name2,comp_name2) ;
%                    mput(ftp_remote,[pwd,'\results\',file(1:end-4),'\',num2str(tar_duc(k,1)),'\',file(1:end-
4),'-EnSp max','.dat']) ;
              % absolute energy into file
                dlmwrite([pwd,'\results\',file(1:end-4),'\',num2str(tar_duc(k,1)),'\',file(1:end-4),'-EnSp
end','.dat'],...
                 energy_spectra_end(:,1:12,k),'delimiter','\t','-append') ;
              % ftp-push
%                  ftp_remote=ftp('10.254.10.90',comp_name2,comp_name2) ;
%                    mput(ftp_remote,[pwd,'\results\',file(1:end-4),'\',num2str(tar_duc(k,1)),'\',file(1:end-
4),'-EnSp end','.dat']) ;
             % spectral values into file
                dlmwrite([pwd,'\results\',file(1:end-4),'\',num2str(tar_duc(k,1)),'\',file(1:end-4),'-
RS','.dat'],...
                 response_spectra(:,1:10,k),'delimiter','\t','-append') ;
              % ftp-push
```

```
        %                   ftp_remote=ftp('10.254.10.90',comp_name2,comp_name2) ;
        %                     mput(ftp_remote,[pwd,'\results\',file(1:end-4),'\',num2str(tar_duc(k,1)),'\',file(1:end-
4),'-RS','.dat']) ;
                    % plotting the results
                      % Energy Spectra
                        figure
                         subplot(2,1,1),plot(energy_spectra_max(:,1,k),energy_spectra_max(:,3,k),'r'),hold
on,plot(energy_spectra_max(:,1,k),energy_spectra_max(:,8,k)),grid on
                            title(['Ei spectra of ',file(1:end-4)]),xlabel('t (sec)'),ylabel('Ei (max) (m2/s2)')
                            legend('absolute','relative')
                         subplot(2,1,2),plot(energy_spectra_end(:,1,k),energy_spectra_end(:,3,k),'r'),hold
on,plot(energy_spectra_end(:,1,k),energy_spectra_end(:,8,k)),grid on
                             xlabel('t (sec)'),ylabel('Ei (end) (m2/s2)')
                            legend('absolute','relative')
                         saveas(gcf,[pwd,'\results\',file(1:end-4),'\',num2str(tar_duc(k,1)),'\',file(1:end-4),'-EI
spectra'],'png')
                         close gcf
                       % Response Spectra
                        figure
                         subplot(3,1,1),plot(response_spectra(:,1,k),response_spectra(:,6,k),'b'),grid on
                         title(['Response Spectra of ',file(1:end-4)]),ylabel('Sd (m/s)')
                         subplot(3,1,2),plot(response_spectra(:,1),response_spectra(:,7),'b'),grid          on,ylabel('Sv
(m/s)')
                         subplot(3,1,3),plot(response_spectra(:,1),response_spectra(:,10),'b'),grid        on,ylabel('Sa
(m/s2)')
                         saveas(gcf,[pwd,'\results\',file(1:end-4),'\',num2str(tar_duc(k,1)),'\',file(1:end-4),'-
RS'],'png')
                         close gcf
                end
                  %% BU KAYIT BİTTİ
                    mail_report2(['PR023-BITTI:                ',file(1:end-4)],[num2str(analiz_sayisi),'                on
',datestr(now,'ddmmyyyy-HHMM')]);
                   % yenikayıt başlarken
                    clear index ;
                    initial=1;
                     index_counter=1 ;
        end % "EQE kayıtları için loop sonu" (değişken "i")
        end_time=toc ;
           mail_report2('PR023-END:',[num2str(analiz_sayisi),'  on  ',datestr(now,'ddmmyyyy-HHMM'),'
Gecen Süre : ',num2str(end_time/3600),' saat'])
           fprintf(screen_log,' %s %s geçen tam süre %f\n',datestr(now,'ddmmyyyy-HHMM'),file(1:end-
4),end_time) ;
           fprintf(1,' %s %s geçen tam süre %f sn\n',datestr(now,'ddmmyyyy-HHMM'),file(1:end-
4),end_time) ;
        transporter_function
        catch
          %% program biter
           end_time=toc ;
           err = lasterror;
           mail_report2(['PR023-FAIL:',file(1:end-4)],[num2str(analiz_sayisi),' on ',datestr(now,'ddmmyyyy-
HHMM'),' Gecen Süre : ',num2str(end_time/3600),' saat',' ',err.message,'line @ ',num2str(err.stack.line)])
           fprintf(screen_log,' %s %s geçen eksik süre %f\n',datestr(now,'ddmmyyyy-HHMM'),file(1:end-
4),end_time) ;
           fprintf(1,' %s %s geçen eksik süre %f sn\n',datestr(now,'ddmmyyyy-HHMM'),file(1:end-
4),end_time) ;
           rethrow(err) ;
        end
        % %% END  OF THE FILE %%
           fclose all;
```

APPENDIX C: THE COMPUTER PROGRAM FOR THE DERIVATION OF THE ENERGY DISSIPATION CAPACITY

```
%% BA ELEMANLARIN ENERJI YUTMA MIKTARINI HESABI ICIN SABIT GENLIKLI QUASI-STATIC TEST
%% PROGRAMI
% ahmet anıl dindar- adindar@iku.edu.tr- 29.mart.2009 pazar
tic
%% temizlik
   clc,clear,close all,fclose all;
         delete('*.dat');
      delete('*.out');
      delete('*.prn');
%% let's rock
 mail_report2('PR025-START-CAon ',datestr(now,'ddmmyy-HHMM')) ;
try
%% A- DEFINING THE CASES
% % 1 system height
%    height_list_range=[3000;4000;5000] ;
%    height_list_index=menu('yukseklik','3000','4000','5000');
%    height_list=height_list_range(height_list_index);
% 2 cross-section names
   xs_name_list_range={'30x30';'40x40';'50x50'};                    % section types
   xs_name_index=menu('Sec bakalımsectionunu','30','40','50');
   xs_name_list=xs_name_list_range(xs_name_index);
% 1 system height
height_list=str2num(xs_name_list{1}(1:2))*[3;4;5;6;7;8;9;10]*10;
% 3 reinforced concrete class
   fc_list=[20;25] ;
   fc_list_index=menu('fc degeri','20','25');
   fc_list=fc_list(fc_list_index);
% 4 confinement type
   confinement_type_list={'c'} ;
% 5 axial load level
   load_level_list=[0;5;10;20] ;
% 6 long. reinforcement ratio
   rho_l_list=[1;2;3;4] ;
% 7  section performance names
   xs_pl_names={'MN';'GV';'GC'}  ;
% 8 system performance levels as drift ratio
   drift_ratio_list=[0.01;0.03;0.04] ;          % Subject to change of course
   sys_pl_names={'LS';'IO';'CP'} ;
% 9 Park & Ang values for system performance values
   parkang_list=[0.2;0.4;0.6] ;
% analiz adım miktarı
   DTanaliz=cellstr('0.1') ;
% LOG file
mkdir([pwd,'\LOG'])
log_name=datestr(now,'ddmmyy-HHMM');
% a) upto failure log için
   fid_log_failure=fopen([pwd,'\LOG\',log_name,'-LOG-failure.txt'],'a+') ;
   fprintf(fid_log_failure,'%s, %s, %s, %s, %s, %s, %s, %s, %s, %s, %s, %s, %s \n','date','height','xs_name','fc','confinement_type','load_level','rho_l','sys_performance_dr_list','XS_performance_dr_list','ca_disp','no_of_iteration','fid_parkang','dissipated_energy');
% b) Performance'lar için
   fid_log_performance=fopen([pwd,'\LOG\',log_name,'-LOG-performance.txt'],'a+') ;
```

```
   fprintf(fid_log_performance,'%s, %s, %s, %s, %s, %s, %s, %s, %s, %s, %s, %s, %s, %s, %s
\n','date','height','xs_name','fc','confinement_type','load_level','rho_l','sys_performance_dr_list','XS_performa
nce_dr_list','ca_disp','no_of_iteration','P&A level','fid_parkang','dissipated_energy');
%% B- BÜYÜK DÖNGÜLER BAŞLAR
for i=1:size(height_list,1)
height=height_list(i,1) ; % sanırım bu zekice bir hareket
   for j=1:size(xs_name_list,1)
   xs_name=xs_name_list{j,1} ;
      for k=1:size(fc_list,1)
      fc=fc_list(k,1) ;
         for m=1:size(confinement_type_list,1)
         confinement_type=confinement_type_list{m,1} ;
            for n=1:size(load_level_list,1)
            load_level=load_level_list(n,1) ;
               for p=1:size(rho_l_list,1)
                  rho_l=rho_l_list(p,1) ;
% Now I start to create the IDARC file
% analysis name
   analysis_name_1=strcat(xs_name,'-',num2str(height),'-',num2str(rho_l),'-',num2str(fc),'-
',confinement_type,'-',num2str(load_level)) ;
   analysis_name_mk=strcat(xs_name,'-',num2str(rho_l),'-',num2str(fc),'-',confinement_type,'-
',num2str(load_level)) ;
% the mk_module
   fid_mk_module=fopen([pwd,'\mk-modules\',analysis_name_mk,'.dat'],'r') ;
   counter1=1 ;
   while counter1<4
      tline=fgets(fid_mk_module) ;
      % axial force ayrımı
      if counter1==1
         weight=cellstr(tline) ;
      end
%       if counter1==2
%          EI1P=cellstr(tline) ;
%       end
      if counter1==3
         EA=cellstr(tline) ;
      end
     counter1=counter1+1 ;
   end
   fclose(fid_mk_module) ;
   [curvature,moment]=textread([pwd,'\mk-modules\',analysis_name_mk,'.dat'],'%f %f','headerlines',3);
   % şimdi IDARC içindei ayarlamaları yapalım
   PCP=moment(2,1);
   PYP=moment(3,1);
   UCP=curvature(2,1);
   UYP=curvature(3,1);
   UUP=curvature(7,1);
   EI1P=PCP/UCP;
   EI3P=(          ((moment(7,1)-moment(3,1))/(curvature(7,1)-curvature(3,1)))          /          ((moment(3,1)-
moment(1,1))/(curvature(3,1)-curvature(1,1))) )*100 ;
% the sub-modules for IDARC input file
%%%%%------- IDARC DOSYALARI BAŞLAR-------%%%%
% ONCE PUSH-OVER ADIMI
   analysis_name_po=strcat(analysis_name_1,'-po');
   % IDARC systemfile creation
      fid_IDARC_sys=fopen('IDARC.dat','w') ;
      fprintf(fid_IDARC_sys,'%s.dat\n',analysis_name_po) ;
      fprintf(fid_IDARC_sys,'%s-out.dat',analysis_name_po) ;
      fclose(fid_IDARC_sys) ;
```

```
   % NOW THE IDARC FILE IS OPENED
   fid_IDARC=fopen([analysis_name_po,'.dat'],'w'); % the IDARC input file
     % tanımlama module is implemented
         fid_tanimlama=fopen('PR025-tanimlama-po.txt') ;
         while ~feof(fid_tanimlama)
            tline=fgets(fid_tanimlama) ;
            tline=strrep(tline,'ANALYSIS_NAME',analysis_name_1) ;
            tline=strrep(tline,'HEIGHT',num2str(height)) ;
            tline=strrep(tline,'WEIGHT',weight{1}) ;
            tline=strrep(tline,'EI1P',num2str(EI1P)) ;
            tline=strrep(tline,'EA',EA{1}) ;
            tline=strrep(tline,'PCP',num2str(PCP)) ;
            tline=strrep(tline,'PYP',num2str(PYP)) ;
            tline=strrep(tline,'UYP',num2str(UYP)) ;
            tline=strrep(tline,'UUP',num2str(UUP)) ;
            tline=strrep(tline,'EI3P',num2str(EI3P)) ;
            fwrite(fid_IDARC,tline) ;
         end
         fclose(fid_tanimlama) ;
     % push-over modulu is impelemented
        fid_pushover=fopen('PR025-pushover.txt') ;
        while ~feof(fid_pushover)
            tline=fgets(fid_pushover) ;
            tline=strrep(tline,'HEIGHT',num2str(height)) ;
            tline=strrep(tline,'WEIGHT',weight{1}) ;
            fwrite(fid_IDARC,tline) ;
        end
        fclose(fid_pushover) ;
     % 3rd module is implemented
         fid_sonuclar=fopen('PR025-sonuclar.txt') ;
         while ~feof(fid_sonuclar)
            tline=fgets(fid_sonuclar) ;
            tline=strrep(tline,'ANALYSIS_NAME',analysis_name_1) ;
            fwrite(fid_IDARC,tline) ;
         end
         fclose(fid_sonuclar) ;
   fclose(fid_IDARC) ;
   %% yuce IDARC'ın çalışması
     winopen idarc2d_6.0.exe
     pause (3)
 % let's read the push-over analysis results

[time_po,phibot_po,momentbot_po,phitop_po,momenttop_po,axialforce_po,column_drift_po,column_shear_
po,rotbot_po,plasrotbot_po,rottop_po,plastrotbot_po]...
   =textread('COL_001.prn','%f %f %f  %f %f %f %f %f %f %f %f %f','headerlines',4); % iste o muhtesem
satir
% hemen push-over sonuçlarını bir yerlere götürelim
   mkdir([pwd,'\RESULTS\',analysis_name_1]) ;
   copyfile('COL_001.prn',[pwd,'\RESULTS\',analysis_name_1,'\',analysis_name_1,'-po.prn']);
   movefile([xs_name,'*.dat'],[pwd,'\RESULTS\',analysis_name_1]);
   movefile('story.out',[pwd,'\RESULTS\',analysis_name_1,'\',analysis_name_1,'-story.prn']);
%------------------------------- END OF PUSH-OVER ANALYSIS -------------------------------%
% burada hemen system performans noktalarını belirleyelim.
for r=1:size(drift_ratio_list,1)
  drift_ratio=drift_ratio_list(r,1) ;
  % drift ratio'ların listesi
     dummy1=find(column_drift_po<=drift_ratio*height) ;
     sys_performance_dr_list(r,1)=dummy1(end);
% xs_performance'ların disp karşılığı
```

```
      dummy2=find(phibot_po<=curvature(3+r,1)) ;
      xs_performance_curv_list(r,1)=dummy2(end);
end
%% bunu resmedelim hemen
figure (1)
plot(column_drift_po(1:end-1,1),column_shear_po(1:end-1,1)),hold on
for dummy3=1:3

plot([column_drift_po(sys_performance_dr_list(dummy3,1)),column_drift_po(sys_performance_dr_list(dum
my3,1))],[0,column_shear_po(sys_performance_dr_list(dummy3,1))],'r-o')

plot([column_drift_po(xs_performance_curv_list(dummy3,1)),column_drift_po(xs_performance_curv_list(d
ummy3,1))],[0,column_shear_po(xs_performance_curv_list(dummy3,1))],'k--*')
end
title(['Push-Over Analysis of ',analysis_name_1])
xlabel('Disp (mm)'),ylabel('Force (kN)'),legend('PO','Sys PL','XS Pl','Location','SouthEast')
saveas(gcf,[pwd,'\RESULTS\',analysis_name_1,'\',analysis_name_1,'-po & PL.png'])
close(figure(1))
%% ------------------------------- CA ANALYSIS --------------------------------%
% şimdi artık burada system performance ile sabit genlik hesabı için analize başlarız
      delete('*.dat');
      delete('*.out');
      delete('*.prn');
% constant amplitude disp. magnitude
for r=1:size(xs_pl_names,1)  % işte burası section performans döngüsü
   for q=1:size(sys_pl_names,1) % burası da sistem performans döngüsü noktası
         ca_disp=column_drift_po(min(xs_performance_curv_list(r,1),sys_performance_dr_list(q,1)),1);
      % the UUP and EI3P verileri güncellenir- ki ben burayı eksikyapmışım.
      % UUP=curvature(3+q);
      %                 EI3P=(((moment(3+q,1)-moment(3,1))/(curvature(3+q,1)-curvature(3,1)))                /
(moment(3,1)/curvature(3,1)))*100 ;
      % şimdi bu noktadan itibaren yeniden IDARC dosyaları yazılır
      % şimdi QS analiz
         analysis_name_qs=strcat(analysis_name_1,'-qs-',sys_pl_names{r,1},'-',xs_pl_names{q,1});
      % IDARC systemfile creation
         fid_IDARC_sys=fopen('IDARC.dat','w') ;
         fprintf(fid_IDARC_sys,'%s.dat\n',analysis_name_qs) ;
         fprintf(fid_IDARC_sys,'%s-out.dat',analysis_name_qs) ;
         fclose(fid_IDARC_sys) ;
      %%%---- İŞTE BURASI ITERATION OLAN YER ----%%%%
      %% CA DEĞERİ BELLİ SAYISI
      no_of_iteration=2 ;
      parkang=0  ;
      counter1=1 ;
      counter2=2 ;
      counter3=1;
      parkang_range(1,1)=0;
         while no_of_iteration<=600
            clear ca_disp_seri
            % displ. pattern
            for s=1:no_of_iteration
               ca_disp_seri(s,1)=((-1)^s)*ca_disp;
            end
            ca_list=[0;ca_disp_seri;0] ;% işte burası acayip bir şey olacak
            noofamplitudes=size(ca_list,1) ;
            % NOW THE IDARC FILE IS OPENED
            %     analysis_name_qs=strcat(analysis_name_1,'-qs');
            fid_IDARC=fopen([analysis_name_qs,'.dat'],'w'); % the IDARC input file
              % tanımlama module is implemented (PO ile aynı)
```

```
                fid_tanimlama=fopen('PR025-tanimlama-ca.txt') ;
                while ~feof(fid_tanimlama)
                   tline=fgets(fid_tanimlama) ;
                   tline=strrep(tline,'ANALYSIS_NAME',analysis_name_1) ;
                   tline=strrep(tline,'HEIGHT',num2str(height)) ;
                   tline=strrep(tline,'WEIGHT',weight{1}) ;
                   tline=strrep(tline,'EI1P',num2str(EI1P)) ;
                   tline=strrep(tline,'EA',EA{1}) ;
                   tline=strrep(tline,'PCP',num2str(PCP)) ;
                   tline=strrep(tline,'PYP',num2str(PYP)) ;
                   tline=strrep(tline,'UYP',num2str(UYP)) ;
                   tline=strrep(tline,'UUP',num2str(UUP)) ;
                   tline=strrep(tline,'EI3P',num2str(EI3P)) ;
                   fwrite(fid_IDARC,tline) ;
                end
                fclose(fid_tanimlama) ;
             % QS modulu is impelemented
             fid_quasistatic=fopen('PR025-quasistatic.txt') ;
             while ~feof(fid_quasistatic)
                tline=fgets(fid_quasistatic) ;
                tline=strrep(tline,'WEIGHT',weight{1}) ;
                tline=strrep(tline,'DTANALIZ',DTanaliz{1}) ;
                tline=strrep(tline,'NOOFAMPLITUDES',num2str(noofamplitudes)) ;
              if strcmp(cellstr(tline),'CADH')==1
                fprintf(fid_IDARC,'%.2f\n',ca_list) ;
                tline='';
                fwrite(fid_IDARC,tline) ;
              end
              fwrite(fid_IDARC,tline) ;
             end
              fclose(fid_quasistatic) ;
              % 3rd module is implemented
                fid_sonuclar=fopen('PR025-sonuclar.txt') ;
                while ~feof(fid_sonuclar)
                   tline=fgets(fid_sonuclar) ;
                   tline=strrep(tline,'ANALYSIS_NAME','kolon') ;
                   fwrite(fid_IDARC,tline) ;
                end
                fclose(fid_sonuclar) ;
           fclose(fid_IDARC) ;
           %% yuce IDARC'ın çalışması
            winopen idarc2d_6.0.exe
            pause (3)
           % let's read the push-over analysis results

[time_ca,phibot_ca,momentbot_ca,phitop_ca,momenttop_ca,axialforce_ca,column_drift_ca,column_shear_c
a,rotbot_ca,plasrotbot_ca,rottop_ca,plastrotbot_ca]...
           =textread('COL_001.prn','%f %f %f  %f %f %f %f %f %f %f %f','headerlines',4); % iste o
muhtesem satir
           % dlmwrite('barrak.dat',[phibot_ca,momentbot_ca],'delimiter','\t')
            dissipated_energy=polyarea(column_drift_ca,column_shear_ca) ;
           % şimdi dur-devam kriterlerini koyalım7
           % once park-ang okuması
              fid_parkang=fopen([analysis_name_qs,'-out.dat']) ;
              while ~feof(fid_parkang)
                 tline=fgets(fid_parkang) ;
                 if strncmp(cellstr(tline),'    OVERALL STRUCTURAL DAMAGE',29)==1
                    parkang=str2num(tline(35:end))  ;
                 end
```

```
            if strcmp(cellstr(tline),'******** CHOLESKY DECOMPOSITION FAILED ********')==1
               parkang=0 ;
               mail_report2(['PR025-OOOOPPPS-',analysis_name_qs,'  on  '],datestr(now,'ddmmyy-
HHMM')) ;
            end
         end
         fclose(fid_parkang);
         parkang_range(counter2,1)=parkang ;
      % şimdi PARK-ANG değerlendirmesi
         if  parkang>=parkang_list(counter3,1)  &&  parkang_range(counter2-
1,1)<parkang_list(counter3,1);
            fprintf(fid_log_performance,'%s, %s, %s, %s, %s, %s, %s, %s, %s, %s, %s, %s, %s, %s
\n',datestr(now,'ddmmyy-
HHMM'),num2str(height),xs_name,num2str(fc),confinement_type,num2str(load_level),num2str(rho_l),...

sys_pl_names{q,1},xs_pl_names{r,1},num2str(ca_disp),num2str(no_of_iteration/2),num2str(parkang_list(co
unter3,1)),num2str(parkang),num2str(dissipated_energy));
            counter3=counter3+1;
         end
         counter2=counter2+1;
      % şimdi bir dur diyelim bu işe
         if parkang>=.4
            break
         end
         % characteristics
      no_of_iteration ;
      fprintf('%f %.0f \n',parkang,no_of_iteration);
      delta_no_of_iteration=10 ; % bu rakam fine-tune edilebilir
      no_of_iteration=delta_no_of_iteration+no_of_iteration;  % hocam işte bu artarrrrrrrr
      %  counter1=counter1+1 ;
   end % while end
% ---------- CA BITTI ----------
copyfile('COL_001.prn',[pwd,'\RESULTS\',analysis_name_1,'\',analysis_name_qs,'-ca.prn']);
movefile([xs_name,'*.dat'],[pwd,'\RESULTS\',analysis_name_1]);
if  no_of_iteration>=600
    no_of_iteration=no_of_iteration-delta_no_of_iteration;  % hocam işte bu artarrrrrrrr
end
% let's plot the force-displacement value
figure (2)
   plot(column_drift_ca,column_shear_ca),grid
   title(['Force-Disp of ',analysis_name_qs]),
   xlabel('Displacement (mm)'),ylabel('Force (kN)'),
   text(min(column_drift_ca),max(column_shear_ca),{['EH= ',num2str(dissipated_energy),' kNmm'];...
      [num2str(ceil(no_of_iteration/2)),' cycles','Height ',num2str(height)];...
      ['PARK-ANG değeri ',num2str(parkang)]}),
   saveas(gcf,[pwd,'\RESULTS\',analysis_name_1,'\',analysis_name_qs,'-CA.png'])
   close(figure(2))
% let's save into the right place
fprintf(fid_log_failure,'%s, %s, %s, %s, %s, %s, %s, %s, %s, %s, %s, %s, %s \n',datestr(now,'ddmmyy-
HHMM'),num2str(height),xs_name,num2str(fc),confinement_type,num2str(load_level),num2str(rho_l),...

sys_pl_names{q,1},xs_pl_names{r,1},num2str(ca_disp),num2str(no_of_iteration/2),num2str(parkang),num2
str(dissipated_energy));
%        mail gönderme
   mail_report2(['PR025-END-',analysis_name_qs,' on '],datestr(now,'ddmmyy-HHMM')) ;
clear  parkang  time_ca  phibot_ca  momentbot_ca  phitop_ca  momenttop_ca  axialforce_ca
column_drift_ca column_shear_ca rotbot_ca plasrotbot_ca rottop_ca plastrotbot_ca no_of_iteration
clc
end
```

```
end
                end
              end
            end
          end
       end
    end
end
%% ftp push: START------
            comp_name=getenv('COMPUTERNAME');
            comp_name2=comp_name(5:end);
            ftp_remote=ftp('10.254.10.90',comp_name2,comp_name2) ;
            mput(ftp_remote,[pwd,'RESULTS']);
%% ftp push: END---------
mail_report2('PR025-BITTI-CA on ',datestr(now,'ddmmyy-HHMM')) ;
fclose(fid_log_failure);
fclose(fid_log_performance);
catch
   s = lasterror ;
   rethrow(s);
mail_report2('PR025-FAIL-CA on ',datestr(now,'ddmmyy-HHMM')) ;
end
fclose all
%% ŞİMDİ BİR FTP PUSH KOYALIM.
comp_name=getenv('COMPUTERNAME') ;
comp_name2=comp_name(5:end) ;
ftp_remote=ftp('10.254.10.90',comp_name2,comp_name2) ;
mput(ftp_remote,[pwd,'\LOG\',log_name,'-LOG-failure.txt'])
mput(ftp_remote,[pwd,'\LOG\',log_name,'-LOG-performance.txt'])
close(ftp_remote);
toc
```

APPENDIX D: THE CAPACITY TABLE OF THE EXAMINED CASES

Axial Load	Section	Shear Span	rl %1			rl %2			rl %3			rl %4		
			%1-IO-MN	%1-LS-SF	%1- CP-CO	%2-IO-MN	%2-LS-SF	%2- CP-CO	%3-IO-MN	%3-LS-SF	%3- CP-CO	%4-IO-MN	%4-LS-SF	%4- CP-CO
fc 20MPa,P/P0 %0	30x30	3	0.53	0.89	0.97	1.15	1.69	2.10	1.97	2.30	2.75	2.32	3.00	3.50
		4	0.56	1.10	1.22	1.12	2.05	2.50	1.86	2.30	3.33	2.20	3.56	4.08
		5	0.60	1.30	1.47	1.09	2.41	2.90	1.76	2.30	3.92	2.07	4.12	4.72
		6	0.63	1.51	1.72	1.07	2.77	3.30	1.65	2.30	4.50	1.94	4.68	5.39
		7	0.66	1.71	1.97	1.04	3.14	3.70	1.54	2.30	5.09	1.81	5.24	6.06
		8	0.69	1.92	2.22	1.01	3.50	4.10	1.44	2.30	5.67	1.68	5.80	6.74
		9	0.72	2.13	2.47	0.98	3.86	4.50	1.33	2.30	6.26	1.55	6.36	7.41
		10	0.76	2.33	2.71	0.96	4.22	4.90	1.22	2.30	6.85	1.42	6.92	8.08
	40x40	3	1.35	2.64	2.83	2.91	5.68	4.77	4.61	8.32	7.42	5.90	9.46	10.74
		4	1.45	3.09	3.28	2.90	6.50	6.11	4.39	9.41	9.33	5.62	11.08	12.20
		5	1.56	3.55	3.79	2.89	7.32	7.45	4.17	10.49	11.24	5.33	12.70	13.83
		6	1.66	4.00	4.42	2.88	8.13	8.78	3.95	11.58	13.14	5.04	14.32	15.77
		7	1.76	4.46	5.05	2.87	8.95	10.12	3.74	12.67	15.05	4.75	15.94	17.72
		8	1.86	4.91	5.68	2.86	9.77	11.46	3.52	13.75	16.96	4.46	17.56	19.67
		9	1.96	5.37	6.30	2.85	10.58	12.79	3.30	14.84	18.86	4.17	19.18	21.61
		10	2.06	5.82	6.93	2.85	11.40	14.13	3.08	15.93	20.77	3.88	20.80	23.56
	50x50	3	2.59	4.81	5.02	4.98	10.43	11.53	8.57	15.95	16.47	11.59	19.37	20.49
		4	2.85	5.73	6.12	5.33	12.20	13.98	8.42	18.36	19.97	11.07	22.72	24.43
		5	3.12	6.65	7.21	5.68	13.97	16.43	8.28	20.76	23.47	10.55	26.08	28.38
		6	3.39	7.57	8.36	6.03	15.74	18.88	8.13	23.17	26.97	10.03	29.43	32.32
		7	3.65	8.49	9.55	6.38	17.51	21.33	7.98	25.57	30.47	9.52	32.78	36.26
		8	3.92	9.41	10.73	6.73	19.28	23.77	7.84	27.98	33.96	9.00	36.14	40.20
		9	4.19	10.34	11.92	7.08	21.04	26.22	7.69	30.38	37.46	8.48	39.49	44.14
		10	4.45	11.26	13.11	7.43	22.81	28.67	7.55	32.79	40.96	7.96	42.85	48.09

Axial Load	Section	Shear Span	rl %1			rl %2			rl %3			rl %4		
			%1-IO-MN	%1-LS-SF	%1- CP-CO	%2-IO-MN	%2-LS-SF	%2- CP-CO	%3-IO-MN	%3-LS-SF	%3- CP-CO	%4-IO-MN	%4-LS-SF	%4- CP-CO
fc 20MPa,P/P0 %5	30x30	3	0.52	0.67	0.71	1.11	1.34	1.52	1.90	2.29	2.44	1.98	2.79	2.94
		4	0.58	0.76	0.90	1.15	1.72	1.89	1.90	2.86	3.03	2.00	3.40	3.71
		5	0.64	0.94	1.10	1.18	2.10	2.26	1.89	3.43	3.62	2.01	4.01	4.02
		6	0.70	1.13	1.29	1.22	2.49	2.64	1.89	4.00	4.22	2.03	4.63	4.71
		7	0.76	1.32	1.48	1.26	2.87	3.01	1.89	4.56	4.81	2.04	5.24	5.40
		8	0.82	1.51	1.68	1.29	3.25	3.38	1.89	5.13	5.41	2.06	5.85	6.09
		9	0.88	1.70	1.87	1.33	3.63	3.75	1.89	5.70	6.00	2.07	6.47	6.78
		10	0.94	1.89	2.07	1.37	4.01	4.13	1.88	6.27	6.59	2.09	7.08	7.47
	40x40	3	1.22	1.93	2.97	2.85	4.55	4.56	4.47	6.32	6.43	5.72	8.12	9.44
		4	1.48	2.33	3.42	2.96	5.40	5.54	4.48	7.77	7.97	5.64	9.71	11.03
		5	1.74	2.74	3.87	3.08	6.25	6.59	4.50	9.22	9.51	5.56	11.31	12.63
		6	2.00	3.15	4.32	3.20	7.10	7.94	4.51	10.67	11.05	5.49	12.90	14.36
		7	2.26	3.55	4.77	3.31	7.95	9.30	4.53	12.12	12.59	5.41	14.50	16.09
		8	2.51	3.96	5.22	3.43	8.80	10.65	4.54	13.57	14.13	5.33	16.09	17.82
		9	2.77	4.37	5.67	3.54	9.65	12.00	4.56	15.02	15.67	5.25	17.69	19.55
		10	3.03	4.77	6.12	3.66	10.49	13.36	4.57	16.47	17.21	5.18	19.28	21.28
	50x50	3	2.49	3.70	4.84	5.46	6.81	9.11	9.21	13.32	16.32	12.28	17.10	18.67
		4	3.03	4.57	5.89	5.73	8.98	11.42	9.21	16.12	18.92	12.03	20.43	22.42
		5	3.57	5.44	6.95	6.01	11.16	13.73	9.21	18.93	21.55	11.77	23.76	26.18
		6	4.11	6.31	8.01	6.28	13.33	16.03	9.22	21.73	24.30	11.51	27.08	29.93
		7	4.65	7.18	9.07	6.55	15.51	18.34	9.22	24.53	27.05	11.26	30.41	33.69
		8	5.19	8.06	10.12	6.83	17.68	20.65	9.22	27.33	29.81	11.00	33.73	37.44
		9	5.73	8.93	11.18	7.10	19.86	22.96	9.23	30.13	32.56	10.75	37.06	41.20
		10	6.27	9.80	12.24	7.37	22.04	25.26	9.23	32.94	35.31	10.49	40.39	44.95

Axial Load	Section	Shear Span	rl %1			rl %2			rl %3			rl %4		
			%1-IO-MN	%1-LS-SF	%1- CP-CO	%2-IO-MN	%2-LS-SF	%2- CP-CO	%3-IO-MN	%3-LS-SF	%3- CP-CO	%4-IO-MN	%4-LS-SF	%4- CP-CO
fc 20MPa,P/P0 %10	30x30	3	0.54	0.54	0.44	1.07	1.23	1.53	1.70	1.79	1.76	1.93	2.33	2.41
		4	0.62	0.72	0.70	1.13	1.51	1.85	1.76	2.27	2.35	1.98	2.91	3.05
		5	0.70	0.90	0.95	1.20	1.80	2.16	1.83	2.75	2.94	2.04	3.48	3.69
		6	0.79	1.08	1.20	1.27	2.09	2.48	1.90	3.24	3.53	2.10	4.06	4.33
		7	0.87	1.26	1.45	1.33	2.37	2.79	1.96	3.72	4.12	2.15	4.63	4.97
		8	0.96	1.44	1.70	1.40	2.66	3.10	2.03	4.20	4.72	2.21	5.21	5.61
		9	1.04	1.63	1.95	1.47	2.95	3.42	2.09	4.69	5.31	2.26	5.78	6.25
		10	1.12	1.81	2.20	1.53	3.23	3.73	2.16	5.17	5.90	2.32	6.36	6.89
	40x40	3	1.33	1.83	2.57	2.86	3.57	4.22	4.39	5.43	5.72	5.20	7.32	7.57
		4	1.53	2.31	3.06	3.06	4.45	5.03	4.52	6.79	6.64	5.37	8.56	9.00
		5	1.73	2.79	3.56	3.26	5.33	5.85	4.64	8.15	8.08	5.54	9.80	10.43
		6	1.92	3.27	4.05	3.46	6.21	6.66	4.76	9.51	9.53	5.71	11.04	11.86
		7	2.12	3.75	4.54	3.66	7.09	7.48	4.88	10.87	10.98	5.88	12.28	13.29
		8	2.31	4.23	5.04	3.86	7.97	8.29	5.01	12.24	12.42	6.05	13.52	14.73
		9	2.51	4.71	5.53	4.06	8.85	9.10	5.13	13.60	13.87	6.22	14.76	16.16
		10	2.71	5.19	6.03	4.26	9.73	9.92	5.25	14.96	15.31	6.39	16.00	17.59
	50x50	3	2.53	4.05	5.73	5.53	7.59	8.28	9.11	11.03	11.53	10.76	13.51	16.11
		4	2.97	4.94	6.74	5.90	9.16	10.05	9.32	14.01	14.56	11.09	16.53	19.19
		5	3.42	5.83	7.74	6.28	10.72	11.81	9.53	17.00	17.60	11.42	19.56	22.27
		6	3.87	6.73	8.74	6.65	12.29	13.57	9.74	19.98	20.64	11.75	22.58	25.35
		7	4.31	7.62	9.74	7.03	13.86	15.34	9.95	22.96	23.67	12.08	25.61	28.42
		8	4.76	8.51	10.74	7.40	15.42	17.10	10.16	25.94	26.71	12.41	28.63	31.50
		9	5.21	9.40	11.75	7.78	16.99	18.87	10.38	28.93	29.75	12.74	31.65	34.58
		10	5.65	10.29	12.75	8.15	18.56	20.63	10.59	31.91	32.78	13.07	34.68	37.66

Axial Load	Section	Shear Span	rl %1			rl %2			rl %3			rl %4		
			%1-IO-MN	%1-LS-SF	%1- CP-CO	%2-IO-MN	%2-LS-SF	%2- CP-CO	%3-IO-MN	%3-LS-SF	%3- CP-CO	%4-IO-MN	%4-LS-SF	%4- CP-CO
fc 20MPa,P/P0 %20	30x30	3	0.81	0.84	0.92	1.06	1.15	1.12	1.61	2.02	2.17	1.81	2.42	2.51
		4	0.86	1.02	1.13	1.14	1.50	1.52	1.69	2.56	2.74	1.88	3.00	3.16
		5	0.92	1.20	1.34	1.22	1.84	1.92	1.76	3.10	3.31	1.96	3.59	3.81
		6	0.97	1.39	1.55	1.30	2.19	2.32	1.83	3.65	3.88	2.04	4.17	4.46
		7	1.03	1.57	1.76	1.38	2.53	2.72	1.90	4.19	4.45	2.12	4.76	5.11
		8	1.09	1.75	1.97	1.46	2.88	3.12	1.97	4.73	5.02	2.19	5.34	5.76
		9	1.14	1.93	2.18	1.54	3.22	3.52	2.05	5.27	5.59	2.27	5.92	6.42
		10	1.20	2.12	2.40	1.62	3.57	3.92	2.12	5.81	6.16	2.35	6.51	7.07
	40x40	3	1.71	1.81	2.10	2.79	2.34	3.50	3.67	4.54	4.72	4.93	6.33	6.54
		4	1.93	2.39	2.65	3.07	3.44	4.32	4.00	5.79	6.03	5.20	7.83	9.10
		5	2.15	2.97	3.21	3.35	4.54	5.15	4.34	7.04	7.34	5.47	9.33	9.61
		6	2.36	3.55	3.77	3.62	5.64	5.97	4.67	8.28	8.66	5.74	10.84	11.49
		7	2.58	4.13	4.33	3.90	6.74	6.79	5.00	9.53	9.97	6.00	12.34	13.36
		8	2.79	4.71	4.88	4.18	7.84	7.61	5.33	10.77	11.29	6.27	13.84	15.24
		9	3.01	5.29	5.44	4.45	8.94	8.43	5.67	12.02	12.60	6.54	15.34	17.11
		10	3.23	5.87	6.00	4.73	10.04	9.25	6.00	13.26	13.91	6.81	16.84	18.99
	50x50	3	3.68	4.57	4.69	5.93	6.61	6.64	8.67	9.81	9.62	10.48	13.94	15.18
		4	4.07	5.50	5.89	6.45	8.23	8.30	9.12	12.21	12.32	10.94	16.83	18.63
		5	4.46	6.44	7.09	6.97	9.86	9.96	9.58	14.61	15.02	11.39	19.71	22.08
		6	4.84	7.38	8.30	7.49	11.48	11.61	10.03	17.02	17.72	11.85	22.59	25.53
		7	5.23	8.31	9.50	8.00	13.11	13.27	10.48	19.42	20.43	12.31	25.47	28.98
		8	5.61	9.25	10.70	8.52	14.73	14.92	10.93	21.82	23.13	12.77	28.35	32.43
		9	6.00	10.19	11.91	9.04	16.36	16.58	11.38	24.22	25.83	13.23	31.23	35.88
		10	6.38	11.13	13.11	9.55	17.98	18.24	11.83	26.63	28.53	13.69	34.11	36.96

Axial Load	Section	Shear Span	rl %1			rl %2			rl %3			rl %4		
			%1-IO-MN	%1-LS-SF	%1- CP-CO	%2-IO-MN	%2-LS-SF	%2- CP-CO	%3-IO-MN	%3-LS-SF	%3- CP-CO	%4-IO-MN	%4-LS-SF	%4- CP-CO
fc 25MPa,P/P0 %0	30x30	3	0.64	0.91	1.16	1.16	1.67	3.61	1.91	2.30	2.70	2.33	3.00	3.50
		4	0.62	1.11	1.35	1.14	2.06	3.88	1.81	2.30	3.43	2.18	3.56	4.23
		5	0.60	1.31	1.55	1.11	2.45	4.16	1.72	2.30	4.15	2.03	4.12	4.95
		6	0.58	1.51	1.74	1.09	2.84	4.44	1.62	2.30	4.88	1.88	4.68	5.68
		7	0.55	1.71	1.93	1.07	3.22	4.71	1.53	2.30	5.60	1.73	5.24	6.40
		8	0.53	1.90	2.13	1.05	3.61	4.99	1.43	2.30	6.33	1.58	5.80	7.13
		9	0.51	2.10	2.32	1.03	4.00	5.27	1.34	2.30	7.05	1.43	6.36	7.85
		10	0.49	2.30	2.52	1.01	4.39	5.55	1.25	2.30	7.78	1.28	6.92	8.57
	40x40	3	1.37	2.69	2.83	2.68	5.47	5.21	4.50	8.38	8.82	5.71	10.51	9.93
		4	1.48	3.08	3.34	2.83	6.36	6.64	4.29	9.59	10.64	5.46	11.99	12.09
		5	1.58	3.48	3.85	2.98	7.25	8.06	4.09	10.79	12.45	5.20	13.47	14.26
		6	1.69	3.88	4.36	3.14	8.15	9.49	3.88	11.99	14.27	4.94	14.94	16.42
		7	1.79	4.27	4.87	3.29	9.04	10.92	3.68	13.20	16.08	4.69	16.42	18.58
		8	1.89	4.67	5.38	3.44	9.93	12.34	3.47	14.40	17.90	4.43	17.90	20.74
		9	2.00	5.06	5.88	3.59	10.82	13.77	3.27	15.61	19.71	4.18	19.38	22.90
		10	2.10	5.46	6.39	3.74	11.72	15.19	3.06	16.81	21.53	3.92	20.86	25.06
	50x50	3	2.76	4.58	5.73	5.23	10.56	10.75	8.50	16.09	17.53	11.71	23.84	21.36
		4	2.96	5.56	6.56	5.54	12.32	13.24	8.36	18.69	21.46	11.15	26.76	25.88
		5	3.16	6.55	7.38	5.84	14.08	15.73	8.21	21.29	25.40	10.60	29.67	30.41
		6	3.36	7.53	8.21	6.14	15.84	18.22	8.07	23.89	29.33	10.04	32.59	34.94
		7	3.56	8.51	9.04	6.44	17.60	20.71	7.93	26.49	33.26	9.48	35.51	39.47
		8	3.76	9.49	9.86	6.74	19.36	23.20	7.79	29.09	37.19	8.92	38.42	44.00
		9	3.96	10.47	10.69	7.05	21.12	25.69	7.65	31.69	41.12	8.36	41.34	48.53
		10	4.16	11.45	11.52	7.35	22.88	28.18	7.51	34.29	45.05	7.80	44.25	53.05

Axial Load	Section	Shear Span	rl %1			rl %2			rl %3			rl %4		
			%1-IO-MN	%1-LS-SF	%1- CP-CO	%2-IO-MN	%2-LS-SF	%2- CP-CO	%3-IO-MN	%3-LS-SF	%3- CP-CO	%4-IO-MN	%4-LS-SF	%4- CP-CO
fc 25MPa,P/P0 %5	30x30	3	0.54	0.62	0.81	1.20	1.27	1.20	1.92	2.49	2.18	2.20	2.53	2.86
		4	0.60	0.78	1.02	1.24	1.69	1.67	1.94	3.07	2.84	2.20	3.28	3.56
		5	0.66	0.95	1.24	1.27	2.12	2.13	1.95	3.65	3.50	2.21	4.03	4.25
		6	0.72	1.11	1.46	1.30	2.54	2.60	1.96	4.23	4.16	2.21	4.78	4.94
		7	0.78	1.28	1.68	1.33	2.96	3.06	1.97	4.81	4.82	2.21	5.53	5.64
		8	0.84	1.44	1.89	1.37	3.38	3.52	1.98	5.39	5.48	2.22	6.28	6.33
		9	0.90	1.61	2.11	1.40	3.80	3.99	1.99	5.97	6.13	2.22	7.03	7.02
		10	0.96	1.77	2.33	1.43	4.22	4.45	2.00	6.55	6.79	2.22	7.78	7.72
	40x40	3	1.14	1.86	2.24	3.23	3.91	5.00	4.30	6.45	6.57	5.67	8.52	8.68
		4	1.45	2.24	2.89	3.31	5.03	6.34	4.39	7.95	8.31	5.66	10.35	10.55
		5	1.76	2.62	3.55	3.38	6.16	7.67	4.48	9.45	10.06	5.64	12.19	12.43
		6	2.07	3.01	4.20	3.46	7.28	9.01	4.57	10.95	11.80	5.62	14.03	14.30
		7	2.38	3.39	4.86	3.54	8.40	10.34	4.66	12.45	13.55	5.60	15.86	16.18
		8	2.69	3.78	5.51	3.61	9.53	11.68	4.75	13.95	15.29	5.58	17.70	18.05
		9	3.00	4.16	6.17	3.69	10.65	13.01	4.85	15.45	17.04	5.56	19.53	19.92
		10	3.31	4.54	6.82	3.77	11.78	14.35	4.94	16.95	18.78	5.54	21.37	21.80
	50x50	3	2.09	3.97	4.51	5.64	7.22	10.38	9.51	16.76	16.97	12.14	17.23	18.85
		4	2.82	4.84	5.61	5.96	9.18	12.79	9.55	19.18	19.71	12.00	20.86	22.85
		5	3.55	5.71	6.72	6.27	11.15	15.19	9.59	21.59	22.45	11.87	24.48	26.85
		6	4.28	6.58	7.83	6.59	13.12	17.59	9.63	24.00	25.19	11.73	28.10	30.85
		7	5.01	7.45	8.93	6.90	15.08	20.00	9.67	26.42	27.93	11.59	31.73	34.85
		8	5.74	8.32	10.04	7.21	17.05	22.40	9.71	28.83	30.67	11.45	35.35	38.85
		9	6.47	9.19	11.15	7.53	19.01	24.81	9.75	31.24	33.41	11.32	38.97	42.85
		10	7.20	10.05	12.26	7.84	20.98	27.21	9.79	33.66	36.15	11.18	42.60	46.85

Axial Load	Section	Shear Span	rl %1			rl %2			rl %3			rl %4		
			%1-IO-MN	%1-LS-SF	%1- CP-CO	%2-IO-MN	%2-LS-SF	%2- CP-CO	%3-IO-MN	%3-LS-SF	%3- CP-CO	%4-IO-MN	%4-LS-SF	%4- CP-CO
fc 25MPa,P/P0 %10	30x30	3	0.56	0.62	0.60	1.01	1.25	1.18	1.77	2.09	2.32	2.02	2.60	2.40
		4	0.64	0.81	0.81	1.11	1.52	1.51	1.84	2.55	2.97	2.07	3.17	3.05
		5	0.73	1.00	1.02	1.21	1.79	1.84	1.91	3.02	3.62	2.13	3.73	3.70
		6	0.81	1.19	1.23	1.31	2.06	2.17	1.98	3.49	4.28	2.19	4.30	4.36
		7	0.89	1.38	1.44	1.41	2.33	2.50	2.05	3.96	4.93	2.24	4.86	5.01
		8	0.97	1.56	1.65	1.52	2.61	2.83	2.12	4.43	5.59	2.30	5.42	5.66
		9	1.05	1.75	1.87	1.62	2.88	3.16	2.19	4.90	6.24	2.36	5.99	6.31
		10	1.13	1.94	2.08	1.72	3.15	3.49	2.25	5.36	6.89	2.41	6.55	6.97
	40x40	3	1.41	1.72	2.41	3.06	3.83	4.21	4.95	5.17	5.32	5.35	6.85	7.81
		4	1.63	2.21	3.06	3.27	4.68	5.20	5.03	6.61	6.86	5.56	8.48	9.30
		5	1.85	2.71	3.71	3.49	5.54	6.19	5.10	8.05	8.40	5.77	10.11	10.79
		6	2.08	3.21	4.36	3.70	6.40	7.18	5.17	9.49	9.93	5.97	11.73	12.29
		7	2.30	3.71	5.01	3.91	7.25	8.17	5.24	10.93	11.47	6.18	13.36	13.78
		8	2.52	4.21	5.65	4.12	8.11	9.16	5.31	12.37	13.01	6.38	14.99	15.27
		9	2.74	4.70	6.30	4.33	8.96	10.15	5.38	13.81	14.55	6.59	16.62	16.76
		10	2.96	5.20	6.95	4.55	9.82	11.14	5.45	15.25	16.08	6.80	18.24	18.25
	50x50	3	2.65	4.24	5.41	6.21	8.08	9.51	9.64	10.82	11.69	11.46	15.86	14.57
		4	3.12	5.18	6.60	6.57	9.73	11.26	9.85	13.95	15.17	11.78	19.05	18.43
		5	3.58	6.12	7.79	6.94	11.37	13.02	10.05	17.08	18.66	12.10	22.24	22.29
		6	4.05	7.07	8.98	7.30	13.02	14.77	10.26	20.21	22.14	12.41	25.44	26.15
		7	4.51	8.01	10.16	7.67	14.67	16.52	10.46	23.34	25.63	12.73	28.63	30.01
		8	4.98	8.96	11.35	8.03	16.31	18.28	10.67	26.47	29.11	13.05	31.82	33.87
		9	5.44	9.90	12.54	8.39	17.96	20.03	10.88	29.59	32.60	13.37	35.01	37.73
		10	5.90	10.84	13.73	8.76	19.60	21.79	11.08	32.72	36.08	13.69	38.21	41.59

Axial Load	Section	Shear Span	rl %1			rl %2			rl %3			rl %4		
			%1-IO-MN	%1-LS-SF	%1- CP-CO	%2-IO-MN	%2-LS-SF	%2- CP-CO	%3-IO-MN	%3-LS-SF	%3- CP-CO	%4-IO-MN	%4-LS-SF	%4- CP-CO
fc 25MPa,P/P0 %20	30x30	3	0.69	0.86	0.83	1.14	1.08	1.02	1.62	1.98	1.94	1.81	2.40	2.54
		4	0.77	1.03	1.03	1.23	1.49	1.44	1.70	2.50	2.53	1.91	3.04	3.19
		5	0.86	1.21	1.24	1.32	1.90	1.85	1.78	3.02	3.12	2.00	3.69	3.85
		6	0.95	1.39	1.44	1.41	2.31	2.27	1.87	3.54	3.70	2.10	4.34	4.50
		7	1.03	1.56	1.65	1.50	2.72	2.68	1.95	4.06	4.29	2.19	4.98	5.16
		8	1.12	1.74	1.85	1.59	3.13	3.10	2.03	4.58	4.87	2.29	5.63	5.82
		9	1.21	1.92	2.06	1.68	3.54	3.51	2.11	5.10	5.46	2.38	6.27	6.47
		10	1.29	2.09	2.26	1.77	3.95	3.93	2.20	5.62	6.04	2.48	6.92	7.13
	40x40	3	1.92	2.23	2.15	3.06	3.11	4.19	4.42	5.62	4.85	5.31	6.55	7.50
		4	2.15	2.83	2.85	3.35	4.20	5.06	4.66	6.85	6.39	5.55	8.28	9.24
		5	2.38	3.42	3.55	3.65	5.28	5.94	4.90	8.08	7.93	5.78	10.01	10.99
		6	2.61	4.01	4.24	3.94	6.37	6.81	5.15	9.31	9.48	6.02	11.74	12.74
		7	2.84	4.60	4.94	4.23	7.46	7.69	5.39	10.55	11.02	6.25	13.47	14.48
		8	3.07	5.19	5.64	4.53	8.54	8.57	5.63	11.78	12.56	6.49	15.20	16.23
		9	3.30	5.79	6.34	4.82	9.63	9.44	5.87	13.01	14.10	6.72	16.93	17.98
		10	3.53	6.38	7.03	5.12	10.72	10.32	6.11	14.25	15.64	6.96	18.66	19.72
	50x50	3	4.13	4.63	4.52	6.37	6.32	6.50	9.12	10.67	11.32	10.34	12.40	14.73
		4	4.59	5.92	5.89	6.89	8.84	9.81	9.55	13.72	14.44	10.98	15.95	18.22
		5	5.04	7.20	7.25	7.41	11.36	13.12	9.99	16.78	17.56	11.63	19.50	21.72
		6	5.39	8.17	8.28	7.80	13.25	15.61	10.32	19.07	19.90	12.11	22.16	24.35
		7	5.73	9.13	9.30	8.19	15.14	18.09	10.64	21.36	22.24	12.59	24.82	26.97
		8	5.96	9.77	9.99	8.45	16.40	19.75	10.86	22.89	23.80	12.92	26.59	28.72
		9	6.42	11.06	11.35	8.97	18.92	23.06	11.30	25.94	26.92	13.56	30.14	32.22
		10	6.87	12.35	12.72	9.49	21.43	26.37	11.73	29.00	30.04	14.21	33.69	35.72

REFERENCES

ACI 318, 2005, *Building Code Requirements for Structural Concrete and Commentary*, American Concrete Institute.

Afet Bölgelerinde Yapılacak Yapılar Hakkında Yönetmelik (ABYYHY), 2008, Bayındırlık ve İskan Bakanlığı, Ankara.

Akbaş, B., 1997, *Energy-Based Earthquake Resistant Design of Steel Moment Resisting Frames*, Ph.D. Thesis, University of Illinois at Urbana-Champaign, Urbana, Illinois.

Akiyama, H., 1985, *Earthquake-Resistant Limit-State Design for Buildings*, University of Tokyo Press.

Anderson, J.C. and F. Naeim, 1984, "*Design Criteria and Ground motion effects in the seismic response of multi-storey buildings",* Proceedings of Applied Technology Council, ATC10-1, Seminar of Earthquake Ground Motion and Building Damage Potential, San Francisco.

Anderson, J.C. and V.V. Bertero, 1987, "*Uncertainties in Establishing Design Earthquakes*, Journal of Structural Engineering, ASCE", Vol. 113, No. 8, pp.1709-1724.

Ang, B.G., M.J.N Priestley and R. Park, 1981, *Ductility of Reinforced Concrete Bridge Piers Under Seismic Loading*, Report 81-3, Department of Civil Engineering, University of Canterbury, Christchurch, New Zealand, 113 pages.

Arias, A., 1970, *A Measure of Earthquake Intensity*, Seismic Design for Nuclear Power Plants, MIT Press, Cambridge, Massachusetts, pp.438-483.

Augusti, G. and M. Ciampoli, 2008, "*Performance-Based Design in Risk Assessment and Reduction",* Probabilistic Engineering Mechanics, Vol. 23, No. 4, pp.496-508.

Banon, H., J.M. Biggs, H.M. Irvine, 1981, "*Seismic Damage in Reinforced Concrete Frames",* Journal of Structural Engineering, ASCE, Vol. 107, No.9, pp. 1713-1729.

Berktay, İ., 2003, *Betonarme 1 (Taşıma Gücü ve Kesit Hesapları),* İMO İstanbul Şubesi.

Bertero, V.V., S.A. Mahin and R.A. Herrera, 1978, "*Aseismic Design Implications of San Fernando Earthquake Records"*, Earthquake Engineering and Structural Dynamics, Vol.6, No.1, pp. 31-42

Bertero, V.V. and C.M. Uang, 1988, *Implications of recorded earthquake ground motions on seismic design of building structures,* Research Report, UCB/EERC-88/13, University of California at Berkeley.

Bertero, V.V. and C.M. Uang, 1992, "*Issues and Future Directions in the Use of An Energy Approach For Seismic-Resistant Design of Structures",* Proceedings of the Nonlinear Seismic Analysis and Design of Reinforced Concrete Buildings, Bled/Ljubljana, pp. 3-22.

Bertero, V.V. and A. Teran-Gilmore, 1994, "*Use of Energy Concepts in Earthquake-Resistant Analysis and Design: Issues and Future Directions*", Advances in Earthquake Engineering Practice, University of California at Berkeley, CA.

Berry, M., M. Perrish, M. Eberhard, 2004, *PEER Structural Performance Database: User's Manual (Version 1.0),* Pacific Engineering Research Center, University of California, Berkeley, CA.

Bozorgnia, Y., K.W. Campbell, 2004, *Engineering Characterization of Ground Motions,* Earthquake Engineering From Engineering Seismology to Performance-Based Engineering, CRC Press,

Bracci, J.M., A.M. Reinhorn and J.B. Mander, 1995, "*Seismic Resistance of Reinforced Concrete Frame Structures Designed for Gravity Loads: Performance of Structural System"*, ACI Structural Journal, Vol. 92, No. 5, Sept-Oct, 1995, pp 597-609

Browning, J, R. L, A. Lynn and J. Moehle, 2000, "*Performance Assessment for a Reinforced Concrete Frame Building",* Earthquake Spectra, Vol. 16, Issue 3, pp. 541-555.

Bruneau, M., Uang, C.M., and Whittaker, A., 1997, *Ductile Design of Steel Structures,* McGraw-Hill.

Büyüköztürk O., A.A. Dindar, H. Özkaynak, C. Yalçın, E. Yüksel, 2008, "*Energy-Based Analysis of RC Structures*", *ACE2008 Proceedings*, Volume 4, page 51.

Calvi G.M. and M.J.N. Priestley, 1997, *Assessment of existing buildings, in: Seismic design of RC structures for controlled inelastic response*, CEB Bulletin 236, Lausanne, pp. 159-204.

Celep, Z., 2007, *Betonarme Taşıyıcı Sistemlerde Doğrusal Olmayan Davranış ve Çözümleme*, Beta Dağıtım, Istanbul.

Chopra, A.K., 2000, *Dynamics of Structures: Theory and Applications to Earthquake Engineering,* Prentice hall, Englewood Cliffs, N.J.

Chai, Y.H., 2004, "*Incorporating Low-Cycle Fatigue Model Into Duration-Dependent Inelastic Design Spectra"*, Earthquake Engineering and Structural Dynamics, Vol.34, No. 1, pp.83-96.

Chou, C. C. and C.M. Uang, 2003. "*A Procedure for Evaluating Seismic Energy Demand of Framed Structures",* Earthquake Engineering and Structural Dynamics, 32, pp. 229-244.

Chung, M., C. Meyer, M. Shinozuka, 1989, "*Modeling of Concrete Damage* Structural" Journal, American Society Institute, Vol. 86, No. 3, pp. 259-271

Clough, R.W. and J. Penzien, 1995, *Dynamics of Structures,* Computers & Structures, Berkeley, CA.

Cosenzai E., G. Manfredi, and K. Ramasco, 1999, *"An Evaluation of the use of damage functionals in Earthquake-Resistant design",* Proceedings of the 9th World Conference on Earthquake Engineering, Moscow, Vol. 9, pp. 303-312.

Decanini, L.D. and F. Mollaioli, 1998, "*Formulation of Elastic Earthquake Input Energy Spectra"*, Earthquake Engineering and Structural Dynamics, Vol. 27, pp. 1503-1522.

Decanini, L.D. and F. Mollaioli, 2001," *An Energy-Based methodology for the Assessment of Seismic Demand,* Soil Dynamic and Earthquake Engineering", Vol. 21, pp. 113-137.

Dimova, S.L. and P. Negro, 2004 , "*Influence of Construction Deficiencies on The Seismic Response of Structures"*, Earthquake Engineering and Structural Dynamics, Vol.34, No. 6, pp.613-635.

Dutta, A. and J.B. Mander, 2001, "*Energy-Based Methodology for Ductile Design of Concrete Columns",* Journal of Structural Engineering, ASCE, Vol. 127, No. 12 ,pp. 1374-1381

Erberik, M.A., 2001, *Energy-Based Seismic Assessment of Degrading Systems,* .D. Thesis, Middle East Technical University, Ankara.

Erberik, A. and H. Sucuoğlu, 2004, "*Seismic Energy Dissipation in Deteriorating Systems through Low-Cycyle Fatigue"*, Earthquake Engineering and Structural Dynamics, Vol. 33, pp. 49-67.

Ersoy, U and G. Özcebe, 2004, *Betonarme,* Evrim Yayınevi

Fajfar, P., T. Vidic and M. Fischinger, 1989, "*Seismic Demand in Medium- and Long-period Structures",* Earthquake Engineering and Structural Dynamics, Vol.18, pp. 1133-1144.

Fajfar, P. and T. Vidic, 1994, "*Consistent Inelastic Design Spectra: Hysteretic and Input Energy",* Earthquake Engineering and Structural Dynamics, Vol. 23, pp. 523-537.

Fischinger, M., M. Kramar and T. Isakovic, 2008, "*Cyclic Response of Slender RC Columns Typicl of Precast Industrial Buildings*", Bulletin of Earthquake Engineering, Volume. 6, pp.519-534.

FEMA 273, *NEHRP Guidelines for the Seismic Rehabilitation of Buildings*, Federal Emergency Management Agency.

FEMA 356, *Prestandard and Commentary for the Seismic Rehabilitation of Buildings*, Federal Emergency Management Agency.

Ferrera, L. and P. Negro, 2004, *Seismic Behavior of Reinforced Concrete Structures: Test on the Precast Prototype*, EU JRC Report , EUR 21096 EN.

Ferrara, L., A. Colombo, P. Negro, G. Toniolo, 2004, "Precast vs. Cast-In_situ RC Indutrial Buildings Under Earthquake Loaing: An Assessment Via PSD Tests", Proceedings of 13th World Conference on Earthquake Engineering, Vancouver, Canada, Paper No.743.

Ghobarah, A., N.M. Aly, and M. El-Attar, 1997, "*Performance Level Criteria and Evaluation",* Proceedings of Seismic Design Methodologies for the Next Generation of Codes, Bled/Ljubljana, pp. 207-215.

Gosain, N.K., R.H. Brown, and J.O. Jirsa, 1977, *Shear Requirements for load Reversals on RC Members*, Journal of Structural Engineering, ASCE, Vol. 103, No. 7, 1605-1622.

Gupta, A.K., 1990, *Response Spectrum Method*, CRC Press Inc.

Gupta, A., and H. Krawinkler, 2000, "*Estimation of Seismic Drift Demands for Frame Structures",* International Journal for Earthquake Engineering and Structural Dynamics, Vol. 29, No. 10.

Gülkan,P., and A.M. Sözen, 1974, "*Inelastic responses of reinforced concrete structures to earthquake motions"*, ACI Journal 71,pp. 604-610

Housner, G.W., 1947, "*Characteristics of Strong-Motion Earthquakes"*, Bulletin of the Seismological Society of America, Vol. 37, No.1, pp.19-31.

Housner, G.W., 1956, *"Limit Design of Structures to Resist Earthquakes"*, Proceedings of First World Conference on Earthquake Engineering, Berkeley, CA, pp.5-1 to 5.13.

Jeong, G.D. and W.D. IWan, 1988, "*Effect of Earthquake Duration on the Damage of Structrues",* Earthquake Engineering and Structural Dynamics, Vol. 16, No.8, pp. 1201-1211.

Kappos, A.J., 1997, "*Partial Inelastic Analysis Procedure for Optimum Capacity Design of RC buildings",* Proceedings of Seismic Design Methodologies for the Next Generation of Codes, Bled/Ljubljana, pp. 229-240.

Kasiraj, I. and J.T.P. Yao, 1968, *Low-cycle Fatigue Failure of Seismic Structures,* Technical Report CE-11(68)NSF-065, University of New Mexico.

Kawashima, K, 1997, "*The 1996 Japanese Seismic Design Specifications of Highway Bridges and the Performanced Based Design",* Proceedings of Seismic Design Methodologies for the Next Generation of Codes, Bled/Ljubljana, pp. 371-382.

Kramer, S.L., 1996, *Geotechnical Earthquake Engineering*, Prentice Hall.

Krawinkler, H. and M. Zohrei, 1983, "*Cumulative Damage in Steel Structures Subjected to Earthquake Ground Motions"*, Computers and Structures, Vol. 16, No.1-4, pp. 531-541.

Krawinkler, H. and A.A. Nassar, 1992,*"Seismic Design Based On Ductility and Cumulative Damage Demands and Capacities"*, Proceedings of the Nonlinear Seismic Analysis and Design of Reinforced Concrete Buildings, Bled/Ljubljana, pp23-40.

Krawinkler, H., 1997, "*Research Issues in Performance Based Seismic Engineering"*, Proceedings of Seismic Design Methodologies for the Next Generation of Codes, Bled/Ljubljana, pp. 47-58.

Kratzig, W.B., I.F. Meyter and K. Meskouris, 1989, "*Damage Evaluation in Reinforced Concrete Members under Cyclic Loading"*, Proceedings of 5th International Conference on Structural Safety and Reliability, San Francisco, Vol. 2, pp. 795-802.

Kuwamura, H., and T.V. Galambos, 1989, "Earthquake Load for Structural Reliability", Journal of Structural Engineering, ASCE, Vol.115, No. 6.

Kunnath, S.K. , J.B. Mander and F. Lee, 1997, "*Parameter Identification for Degrading and Pinched Hysteretic Structural Concrete Systems"*, Engineering Structures, Vol.19, No.3, pp.224-232.

Kunnath, S.K, A. El-Bahy, A.W. Taylor and W.C. Stone, 1997, *Cumulative Seismic Damage of Reinforced Concrete Bridge Piers*, Test Report, Building and Fire Research Laboratory, Gaithersburg, Maryland.

Kunnath,S.K. and Y. H. Chai, 2004, "*Cumulative Damage-Based Inelastic Cyclic Demand Spectrum"*, Earthquake Engineering and Structural Dynamics, Vol. 33, pp. 499-520.

Kunnath, S.K. and Q. Hu, 2004. "*Evaluation of Cyclic Demand in Ductile RC Structures*", Proceedings of 13th World Conference on Earthquake Engineering, Vancouver, Canada, Paper No.290.

Kunnath, S.K., 2003, Personal Communication.

Leelataviwat, S., S.C. Goel and B. Stojadinovic, 2002, "*Energy-Based Seismic Design of Structures using Yield Mechanism and Target Displacement"*, Journal of Structural Engineering, ASCE, Vol. 128, No.8, pp. 1046-1054.

Lehman, D.E. and J.P. Moehle, 2000, "*Seismic Performance of Well-Confined Concrete Bridge Columns"*, Pacific Earthquake Engineering Research Center, PEER 1998/01.

Mahin, S.A. and V.V. Bertero, 1981, "*An Evaluation of Inelastic Seismic Design Spectra",* Journal of Structural Division, ASCE, Vol. 107, No. 9, pp. 1777-1795.

Malhotra, P.K., 1999, "*Response of Buildings to Near-Field Pulse-Like Ground Motions"*, Earthquake Engineering and Structural Dynamics, Vol. 28, pp. 1309-1236.

Malhotra, P.K., 2002, "*Cyclic-Demand Spectrum",* Earthquake Engineering and Structural Dynamics, Vol.33, pp. 1441-1457.

McCabe, S.L. and W.J. Hall, 1989, "*Assessment of Seismic Structural Damage",* Journal of Structural Engineering, ASCE, Vol. 115, No. 9, pp. 2166-2183.

Nakashima, M, 1997, "*Uncertainties associated with ductility performance of steel building structures",* Proceedings of Seismic Design Methodologies for the Next Generation of Codes, Bled/Ljubljana, pp. 111-118.

Nassar, A.A. and H. Krawinkler, 1991, *Seismic Demands for SDOF and MDOF Systems*, Report No.95, The John Blume Earthquake Engineering Center, Stanford University.

Newmark, N.M. and W.J. Hall, 1982, *Earthquake Spectra and Design*, Earthquake Engineering Research Institute, Oakland.

Park, R. and T. Paulay, 1975, *Reinforced Concrete Structures*, John Wiley & Sons, New York.

Park, R. and A.H-S. Ang, 1985, "*Mechanistic Seismic Damage Model For Reinforced Concrete",* Journal of Structural Engineering, ASCE Vol.111, No.ST4, pp. 740-757.

Park, R., 1986, "*Ductile Design Approach for Reinforced Concrete Frames",* Earthquake Spectra, Vo. 2, No. 3, pp. 565-619.

Paulay, T. and M.J.N. Priestley, 1992, *Seismic Design of Reinforced Concrete and Masonry Buildings,* John Wiley & Sons, New York.

PEER Strong Ground Motion Database 2000, Pacific Earthquake Engineering Research Center, California, *http://peer.berkeley.edu/smcat*.

Priestley, M.J.N., F. Siebel, G.M. Calvi, 1996, *Seismic Design and Retrofit of Bridges*, John Wiley & Sons, New York.

Priestley, M.J.N., 2000, "*Performance Based Seismic Design"*, Proceedings of 12th World Conference on Earthquake Engineering, paper 2831.

Priestley, M.J.N, G.M. Calvi, M.J. Kowalsky, 2007, *Displacement-Based Seismic Design of Structures*, IUSS PRESS, Pavia, Italy

Poljansek, K., I. Perus, P. Fajfar, 2009, "*Hysteretic Energy Dissipation Capacity And Cyclic To Monotonic Drift Ratio For Rectangular RC Columns In Flexure*", Earthquake Engineering and Structural Dynamics, Vol.38, No. 7, pp.907-928.

Razvi, S.R. and M. Saatçioğlu, 1994, "*Strength and Deformability of Confined high-Strength Concrete Columns",* ACI Structural Journal, Vol. 91, pp. 678-687.

Reinhorn, A.M., S.K. Kunnath and R.E. Valles, 1994, IDARC2D: *A Program for the Inelastic Damage Analysis of Buildings,* National Center for Earthquake Engineering Research, N.Y.

Reinhorn, A.M., 1997, "*Inelastic Analysis Techniques in Seismic Evaluations",* Proceedings of Seismic Design Methodologies for the Next Generation of Codes, Bled/Ljubljana, pp. 277-288.

Reinhorn, A.M. and M. Sivaselvan, 1999, *Hysteretic Models For Cyclic Behavior of Deteriorating Inelastic Structures*, Report MCEER-99-0018, MCEER/SUNY/Buffalo 1999.

Rothe, D.H. and M.A. Sözen, 1983, *A SDOF Model to Study Nonlinear Dynamic Response of Large- and Small-Scale R/C Test Structures*, Civil Engineering Studies, SRS No.512, University of Illinois at Urbana-Champaign, Urbana, Illinois.

SEAOC's Vision 2000 Committee, *Performance Based Seismic Engineering of Buildings*. Report.

Sivaselvan M., and A.M. Reinhorn, 2001, "*Hysteretic Models for Deteriorating Inelastic Structures"*, ASCE/Journal of Engineering Mechanics, Vol. 126, No. 6, pp. 633-640.

Stephens, J.E. and J.T.P. Yao, 1987, "*Damage Assessment Using Response Measurement",* Journal of Structural Engineering, ASCE, Vol.113, No.4, pp.787-801.

Surahman, A., "2007, *Earthquake-Resistant Structural Design through Energy Demand and Capacity",* Earthquake Engineering and Structural Dynamics, Vol. 36, pp. 2099-2117.

Sürmeli, M., 2008, *Performance Evaluation of Precast Columns under Seismic Excitation*, M.Sc. Thesis, Istanbul Technical University, Istanbul.

Teran-Gilmore, A., 1996, *Performance-Based Earthquake-Resistant Design of Framed Buildings Using Energy Concepts,* Ph.D. thesis, University of California at Berkeley.

Toniolo, G., 2007, *Final report of the EU research project: Behavior of precast concrete structures with respect to Eurocode 8*, Contract No. G6RD-CT-2002-00857.

Trifunac, M.D. and A.G. Brady, 1975, "*A study of the duration of Strong Earthquake Ground Motion",* Bulletin of The seismic Society of America, Vol. 65, pp.581-626.

Toussi, S. and J.T.P. Yao, 1983, "*Hysteresis Identification of Existing Structures",* Journal of Engineering Mechanics, ASCE, Vol. 109, No. 5, pp. 1189-1203.

Uang, C.M. and V.V. Bertero, 1990, "*Evaluation of Seismic Energy in Structures",* Earthquake Engineering and Structural Dynamics, Vol.19, pp. 77-90.

Uang, C.M., 1990, "*Comparison of Seismic Force Reduction Factors Used in USA and Japan"*, Earthquake Engineering and Structural Dynamics, Vol.20, No. 4, pp.389-397.

Veletsos, A. and N.M. Newmark, 1960, "*Effect of Inelasit Behavior on Response of Simple System to Earthquake Motion"*, Proceedings of Second World Conference on Earthquake Engineering, pp. 895-901.

Vidic, T., P. Fajfar and M. Fischinger, 1994, "*Consistent Inelastic Design Spectra: Strength and Displacement*", Earthquake Engineering and Structural Dynamics, Vol.23, No. 5, pp.507-521.

Wang, M.L. and S.P. Shah, 1987, "*Reinforced Concrete Hysteresis Model Based in the Damage Concept",* Earthquake Engineering and Structural Dynamics, Vol. 15, No.8, pp. 993-1003.

Whittaker, A., A. Gilani and V.V. Bertero, 1997, "*Evaluation of Pre-Northridge Steel Moment-Resisting Frame Joints",* The Structural Design Of Tall Buildings, Vol. 7, pp. 263-283.

Wong, K.F. and R. Yang, 2002, "*Earthquake Response and Energy Evaluation of Inelastic Structures"*, Journal of Engineering Mechanics, ASCE, Vol. 128, No. 3, 308-317.

Zahrah T.F., 1982, *Seismic Energy Absorption in Simple Structures*, Ph.D. Thesis, University of Illinois at Urbana-Champaign, Urbana, Illinois.

Zahrah, T.F. and W.J. Hall, 1984, "*Earthquake Energy Absorption in SDOF Structures"*, Journal of Structural Engineering, ASCE, Vol.110, No. 8, pp.1757-1773.